U.PORTO

FACULDADE DE CIÊNCIAS
UNIVERSIDADE DO PORTO

MSc

2.º CICLO

FCUP
2021

U.PORTO

Drosophila melanogaster as a model for the identification of the ataxin-3 interaction regions

Rita Azevedo Sousa e Silva

FC

U.PORTO

FACULDADE DE CIÊNCIAS
UNIVERSIDADE DO PORTO

MSc

Drosophila melanogaster as a model for the identification of the ataxin-3 interaction regions

Rita Azevedo Sousa e Silva

Dissertação de Mestrado apresentada à
Faculdade de Ciências da Universidade do Porto em
Ciências da Vida

2021

MSc

U.PORTO
FACULDADE DE CIÊNCIAS
UNIVERSIDADE DO PORTO

INSTITUTO DE INVESTIGAÇÃO
E INOVAÇÃO EM SAÚDE
UNIVERSIDADE DO PORTO

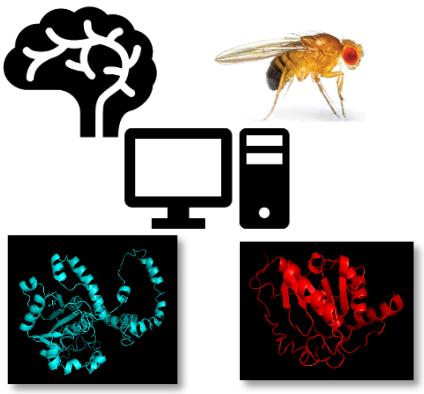

Drosophila melanogaster as a model for the identification of the ataxin-3 interaction regions

Rita Azevedo Sousa e Silva

Master's degree in Cellular and Molecular biology,

Biology Department, Faculdade de Ciências da Universidade do Porto (FCUP)

2020-2021

Supervisors

Cristina Vieira, Assistant Researcher, Instituto de Investigação e Inovação em Saúde (I3S)

Jorge Vieira, Principal Researcher, I3S

U.PORTO
FACULDADE DE CIÊNCIAS
UNIVERSIDADE DO PORTO

Todas as correções determinadas

pelo júri, e só essas, foram efetuadas.

O Presidente do Júri,

Porto, _____/_____/_____

Author: Rita Azevedo Sousa e Silva

Institution Address: Faculdade de Ciências da Universidade do Porto (FCUP), Rua do Campo Alegre, s/n, 4169-007 Porto, Portugal

E-mail: ritassilva@i3s.up.pt

Telephone: 963126977

Supervisor: Cristina Alexandra Gonçalves Paula Vieira; Assistant Researcher

Supervisor: Jorge Manuel de Sousa Basto Vieira; Principal Researcher

Institution Address: Instituto de Investigação e Inovação em Saúde (I3S), Rua Alfredo Allen, 208 4200-135 Porto, Portugal

E-mail: cgvieira@ibmc.up.pt

Telephone: +351 220 408 800

Plagiarism declaration:

I, Rita Azevedo Sousa e Silva, student number 201605875, currently undertaking a Cell and Molecular Master's Degree, edition 2020/2021, hereby declare that this thesis was written by myself and using my own words, not contemplating quotations from published and unpublished sources indicated and acknowledged as such. I am aware of any consequence as a result of plagiarism.

Porto, 30 September 2021

Agradecimentos

Em primeiro lugar tenho que agradecer à minha orientadora, Professora Doutora Cristina Vieira, pelo convite para participar neste projecto e por acreditar que era capaz. Agradeço-lhe também, bem como ao meu orientador Professor Doutor Jorge Vieira todo o empenho dedicado na concretização deste trabalho bem como aos ensinamentos adquiridos no decorrer deste ano. Agradeço também a todos os elementos do grupo Phenotypic Evolution a disponibilidade com que me acolheram, com um especial agradecimento ao André Sousa e à Catarina Vandervoordt, sem os quais este trabalho não teria sido possível.

Agradeço ainda aos “Jamigos” pelos dias de descompressão e aos desabafos ouvidos e a TODOS os amigos envolvidos nas minhas várias etapas de formação.

Um especial agradecimento aos meus pais por acreditarem em mim, e a possibilitarem todas as valências obtidas neste percurso académico. Como é preciso uma Vila, também agradeço a todos os membros da família pelo apoio.

Divirtam-se, e

MUITO OBRIGADA,

Resumo

Ataxia espinocerebelosa tipo 3 (SCA3, ou doença Machado-Joseph MJD) é uma doença neurodegenerativa incapacitante e incurável que, embora rara, apresenta uma elevada prevalência nos Açores (1:239, Ilha da Flores). A SCA3 é causada pela expansão do tracto poliglutamina (polyQ) na proteína ataxina-3, que é codificada pelo gene *ATXN3*. A ataxina-3 é capaz de remover ubiquitina dos substratos e como tal pertence á família das deubiquitinases (DUB). Em humanos, esta família é composta por três outras proteínas, denominadas ataxina-3L, josephin 1 (JosD1), e josephin 2 (JosD2). Estas proteínas partilham o domínio Josephina (JD). De acordo com a filogenia dos genes que codificam estas proteínas, existem duas linhagens distintas, a linhagem josephin 1/josephin 2 e a linhagem ataxina-3/ataxina-3L. Uma das alterações mais significativas resultante da expansão do tracto polyQ é a formação de agregados proteicos, uma característica observada em mutantes de *Drosophila melanogaster* (que expressam no olho o gene humano que codifica para a ataxina-3, levando á formação de agregados proteicos facilmente visíveis). Contudo, no genoma de *Drosophila* existe apenas um gene, que codifica a proteína JOSL-DROME, que pertence á linhagem josephin 1/josephin 2. Esta observação levanta questões como: a rede de interações da ataxina-3 e da JOSL- DROME são semelhantes?, as interações proteicas de mutantes de *Drosophila* são equivalentes às observadas em humanos?, todas as interações proteicas com a ataxina-3 são semelhantes?. Para responder a estas questões, neste estudo comparamos as redes de interações proteicas da ataxina-3 e da JOSL-DROME, utilizando o EvoPPI (uma aplicação web que compara interações proteicas de 12 bases de dados), que complementamos com dados de espectrometria de massa reportados na literatura, bem como os genes modificadores descritos em *Drosophila,* como responsáveis pela alteração de fenótipo do olho, em moscas que expressam ataxina-3. Utilizamos a *metodologia in-silico*, descrita por Rocha e colaboradores [2], para inferir as regiões de interação entre a ataxina-3 e as proteínas que interagem com a mesma, bem como entre JOSL-DROME e as proteínas descrita e previstas como interagindo com esta. Embora identificássemos apenas uma sobreposição de 37% entre as duas redes de interação, as interações com a ataxina-3 são semelhantes quer se utilize as proteínas humanas quer as de mosca. Verificou-se ainda, que o padrão de interação é semelhante para a maioria das proteínas humanas (89%) que interagem com a ataxin-3. Neste trabalho, destaca-se o papel do JD nas interações proteicas com a ataxina-3.

O tracto polyQ está envolvido na modulação e estabilização das interações proteicas. A sua expansão causa a patologia através da modulação das interações das

proteínas nativas, e não da formação de novos complexos. O que implica alterações nas interações das proteínas nativas, devido a diferenças na acessibilidade de resíduos específicos de interação, que podem traduzir-se em modificações pós-traducionais, acesso a regiões de ligação de RNA ou regiões de ligação a proteínas "chaperone", que são necessárias para a atividade normal da proteína. Para perceber como as interações proteicas da ataxina-3 se alteram na presença de uma expansão de 50 polyQs (EXP), usamos a metodologia *in-silico* para todas as proteínas estudadas no ponto anterior. Apesar do JD continuar a ser relevante nas interações com a EXP ataxina-3, os resíduos de interação diferem nas duas formas da ataxina-3. Uma região entre o JD e o primeiro motivo de interação com a ubiquitina parece ser importante nas interações com a EXP ataxina-3. O mesmo padrão de interação com a EXP ataxina-3 é observado em proteínas de *Drosophila* com parálogos em humano. Assim, podemos concluir que *Drosophila* é um bom modelo para estudar a SCA3. Para 17 proteínas (das 86 estudadas) foi observado um aumento superior a 10% na percentagem do número de resíduos de interação com a EXP ataxina-3, quando comparada com a forma não expandida, sugerindo o seu envolvimento na SCA3.

Palavras chave:

SCA3, ataxina-3, tracto polyQ, *in-silico*, interações proteína-proteína, *Drosophila melanogaster*

Abstract

Spinocerebellar ataxia type 3 (SCA3, or Machado-Joseph disease, MJD) is a disabling and incurable neurodegenerative disease that, although rare, is highly prevalent in the Azores (Island of Flores, 1:239). SCA3 is caused by the expansion of the polyglutamine (polyQ) tract in the ataxin-3 protein, encoded by the *ATXN3* gene. Ataxin-3 belongs to the deubiquitinase protein (DUB) family, and as such is capable of removing ubiquitin from substrates. In humans there are three other proteins in this family, ataxin-3L, josephin 1 (JosD1), and josephin 2 (JosD2). These proteins share the Josephin (JD) domain. The phylogenetic relationship of the genes encoding these proteins revealed two distinct lineages, the josephin 1/josephin 2 lineage and the ataxin-3/ataxin-3L lineage. One of the most significant changes in polyQ tract expansion is the formation of protein aggregates, a characteristic observed in *Drosophila melanogaster* mutants (flies that have the human gene encoding ataxin-3, which when expressed in the fly's eye, leads easily visible protein aggregates). However, in the *Drosophila* genome there is only one gene that belongs to josephin 1/josephin 2 lineage, which encodes the protein JOSL-DROME, raising questions such as: is the network of protein interactions of ataxin-3 and JOSL-DROME similar? are *Drosophila* mutants equivalent to those observed in humans?, are all protein interactions with ataxin-3 similar? To answer these questions, in this study we compared the protein networks of ataxin-3 and JOSL-DROME, using EvoPPI (a web application for comparing protein interactions in 12 databases) together with those reported using mass spectrometry, and the genes described in *Drosophila* as phenotype modifiers of ataxin-3. We use the *in-silico* methodology, reported in Rocha *et al.* [2], to infer regions of interaction between proteins that interact with ataxin-3, for which it was possible to identify paralogs in humans, as well as all other human proteins that interact with ataxin-3. Although we identified an overlap of 37% between the two networks, the interactions with ataxin-3 are similar in human proteins and fly proteins. It was also found that the pattern of protein interactions of ataxin-3 is the same for most (89%) human proteins that interact with ataxin-3. From this work, the role of the JD region in protein interactions with ataxin-3 becomes evident.

The polyQ tract is involved in the modulation and stabilization of protein interactions. Its expansion mediates the pathology by modulating the interactions of native proteins, not by forming new complexes. This implies alteration of native protein interactions, due to differences in accessibility of specific interaction residues, which can translate into post-translational modifications, access to RNA binding regions or “chaperone” protein binding regions, which are necessary for the normal activity of the

protein. To infer how ataxin-3 protein interactions change in the presence of an expanded tract of 50 polyQs (EXP), we used the *in-silico* methodology for all proteins studied in the previous point. Although the JD region remains relevant in the interaction with EXP ataxin-3, the protein interaction residues are different in the two forms. Another region between JD and the first ubiquitin interaction motif appears to be important in the interaction with EXP ataxin-3. The same pattern of interaction with EXP ataxin-3 is observed in *Drosophila* proteins that have a paralog in humans. Thus, we can conclude that *Drosophila* is a good model for studying SCA3. For 17 proteins (out of 86 studied) we observed an increase greater than 10% in the percentage of the number of protein interaction residues with EXP ataxin-3, when compared to the non-expanded form, suggesting their involvement in SCA3.

Key words

SCA3, ataxin-3, polyQ tract, *in-silico*, protein-protein interactions, *Drosophila melanogaster*

Contents

Figures List

Tables List

Supplementary material

Supplementary Table 1: Identification of the human selected UniProt sequences. * represent the human proteins common with fly.

Supplementary Table 2: Paralogous human genes of the L1 fly genes identified in EvoPPI as interactors of *Drosophila* Josephin-like protein (CG3781, Gene ID 31560).

Supplementary Table 3: Paralogous human genes of the fly modifiers ataxin-3 genes identified by Vobfeldt according to DIOPT. Stars indicate the genes assigned as suppressors, cardinal those assigned as enhancers, and plus those that are deleterious in flies. &Represent the genes that we used the gene name (instead of CG number) to search human orthologs.

Supplementary Table 4: Paralogous human genes of the fly modifiers ataxin-3 genes identified by Zhang, according to DIOPT.

Supplementary Table 5: Paralogous human genes of the fly modifiers ataxin-3 genes identified by Bilen and Bonine according to DIOPT. * are reported in Vobfeldt ; # are reported in Zhang. & represent the genes where gene name were used to search human orthologs.

Supplementary Table 6: Level 2 ataxin-3 interactors that interact with level 1 ataxin-3 interactors.

Supplementary Table 7: Identification of the *Drosophila* selected UniProt sequences (all common with human).

Supplementary Table 8: Identification of JosD1 network. * represent the proteins common with ataxin-3 network.

Supplementary Table 9: Identification of JosD2 network. * represent the proteins common with ataxin-3 network.

Supplementary Table 10: Identification of interactors more prone to interact with WT or EXP ataxin-3. The polyQ tract were excluded from comparations. * represent the proteins common with *Drosophila*, & represent proteins that interact at an equal amount with WT and EXP ataxin-3, and bold represent proteins that interact more with EXP form.

Abbreviation list

ATM: Ataxia telangiectasia mutated

ATXN1: Ataxin-1

Ataxin-3L: Ataxin-3 like

BRCA1: BRCA1 DNA repair associated

CAG: cytosine-adenine-guanine

Ca^{2+}: calcium ion

CBP: CREB binding protein

CHIP: E3 ubiquitin-protein ligase CHIP

Chk1: checkpoint kinase 1

CK2: casein kinase 2

CNS: central nervous system

DSB: DNA double-strand breaks

DUB: deubiquitinating enzyme

E1: ubiquitin-activating enzyme

E2: ubiquitin-conjugating enzyme

E3: ubiquitin-protein ligase

ERAD: endoplasmic reticulum – associated degradation

ER: endoplasmic reticulum

EXP ataxin-3: ataxin-3 expanded

FOXO4: forkhead box class O (FOXO) transcription factor 4

gp78: E3 ubiquitin-protein ligase AMFR

GSK3β: glycogen synthase kinase 3β

HDAC3: histone deacetylase

HDAC6: histone deacetylase 6

HRD1: E3 ubiquitin-protein ligase synoviolin

JD: Josephin domain

JosD1: Josephin 1

JosD2: Josephin 2

JOLS-DROME: Josephin-like protein

MDC1: mediator of DNA damage checkpoint 1

MJD: Machado-Joseph disease

MMP-2: matrix metalloproteinase-2

NDUFA4: NDUFA4 mitochondrial complex associated

NEDD8: NEDD8 ubiquitin like modifier

NES: nuclear export signals

NLS: nuclear localization signal

Parkin: E3 ubiquitin-protein ligase parkin

Plk: polo-like kinase

PNKP: polynucleotide kinase 3´-phosphatase

polyQ: a group of consecutive glutamines (Q)

polyUb: a group of ubiquitin proteins

PPI: Protein-protein interactions

p62: Sequestosome 1

p53: Cellular tumor antigen p53

P300: E1A binding protein p300

RAD23A: RAD23 homolog A, nucleotide excision repair

RAD23B: RAD23 homolog B, nucleotide excision repair

ROS: reactive oxygen species

SCA3: Spinocerebellar ataxia 3

SIM: small ubiquitin-like modifier [SUMO]-interacting motive

SUMO: small ubiquitin-like modifier

Ub: ubiquitin

UBL: N-terminal ubiquitin-like domain

UIM: ubiquitin interacting motive

VBM: VCP-binding motif

VCP: Vasolin-containig protein

WT ataxin-3: ataxin-3 wild-type

53BP1: p53-binding protein 1

Amino acid abbreviations:

Alanine – Ala – A

Asparagine – Asn – N

Aspartic acid – Asp – D

Cysteine – Cys – C

Glycine – Gly – G

Glutamine – Gln – Q

Histidine – His – H

Lysine – Lys – K

Phenylalanine – Phe – F

Serine – Ser – S

Threonine – Thr – T

Tryptophane – Trp – W

Tyrosine – Tyr – Y

Introduction

In the human genome there are 65 genes containing a stretch with a minimum of 10 consecutive glutamines (cytosine-adenine-guanine-CAG), called polyQ tract, in coding regions [2]. More than 73% of the genes encoding polyQ proteins are associated with diseases [2]. Nevertheless, only for nine polyQ proteins, namely Androgen receptor, Atrophin 1, Ataxin- 1, 2, 3, 7, calcium voltage-gated channel subunit alpha 1A, Huntingtin, and TATA-binding protein, an expansion of the polyQ region over its physiological length has been associated with neurodegenerative disorders (spinal bulbar muscular atrophy (SBMA), dentatorubral-pallidoluysian atrophy (DRPLA), spinocerebellar ataxia types 1 (SCA1), 2 (SCA2), 3 (SCA3 or Machado-Joseph), 7 (SCA7), 6 (SCA6), Huntington´s disease (HD), and spinocerebellar ataxia 17 (SCA17), respectively) [1, 4]. These neurodegenerative disorders present protein aggregates, affect muscle tissues and the nervous system with more incidence in the central nervous system (CNS). These diseases appear in the adulthood, and show slow progression, that culminates in death. There is no successful treatment to prevent the course of action of these diseases. Except for SBMA, that is located on the X chromosome leading to X-linked inheritance pattern, all these neurodegenerative disorders are autosomal dominant [1].

The polyQ diseases are associated with abnormal protein interactions that induce neurotoxicity [5-12]. This is caused by altered natural protein interactions, induced by polyQ expansions, and not by new interactions formed in misfold or aggregating protein complexes [6, 7, 13]. PolyQ diseases identification is a comparative process where in healthy individuals proteins show transient and stable protein – protein interactions (PPI), but in pathological forms not. So, more proteins are retrieved in PPI detection methodologies, for expanded protein forms, when comparing with non-expanded protein forms [5-9]. Nevertheless, a loss of function can cause toxicity in these diseases [14]. Indeed, a polyQ tract expansion could perturb the protein conformation inducing protein loss of function. Therefore, the knowledge of how polyQ expansions alters the protein interactions is essential to understand polyQ disorders. It is hypothesized that polyQ modulates the PPI by expanding the adjacent coiled-coil domain (that is made of antiparallel or parallel α-helices folded as strands of a rope) upon interaction with a coiled-coil domain of an interactor [15, 16]. More interactions have been reported at the polyQ region in EXP ataxin-3 than WT ataxin-3 [15, 16]. However, other regions besides those closer to the polyQ tract could affect the PPIs in expanded polyQ proteins [17]. Consequently, polyQ tract seems to stabilize PPI and/or spacer elements between individually folded domains present in molecules that mediate PPI [16, 18].

This study is focused on the SCA3, also known as Machado-Joseph disease (MJD), the most common spinocerebellar ataxia worldwide [19, 20] affecting 1 in 50.000 or 100.000 people, and the second most common polyQ pathology after non-ataxia neurological disease HD [1]. SCA3 has a higher prevalence in Brazil, Portugal (showing more incidence in Azores Islands, particularly in Flores, where 1 person out of 239 shows the disease), Singapore, China, Germany, Netherlands, and Japan [19, 20]. But it, is also present in other countries such as Canada, USA, Mexico, Australia, and India [19].

1. SCA3 features

SCA3 patients have a life expectancy of 21 years (ranging from 7 to 29 years) after the beginning of symptoms, that appears around the fourth decade of life but can range between five and 75 years [19]. This variation reflects differences in the CAG repeat size, with longer CAG repeat expansion being associated to an early disease beginning and a higher MJD severity [1]. The size of the polyQ region also affects the phenotype of the MJD [21], and based on the variability of this region four clinical subtypes have been described [22, 23], highlighting the MJD heterogeneity. A wide range of symptoms (motor and non-motor) are associated with SCA3 [4, 19]. Motor symptoms are characterized by cerebellar ataxia, that induces alterations in gait (the first symptom to appears, in most cases), balance, speech, and promotes limb incoordination and oculomotor abnormalities (such as nystagmus, progressive external ophthalmoplegia and bulging eyes) [1, 4, 19, 20]. Along with dystonia, that is associated with larger CAG repeat expansion and is observed in early disease stages, pyramidal signs (such as spasticity and hyperreflexia), dysarthria, dysphagia, and facial and lingual fasciculations were also observed in SCA3 individuals [1, 19, 20]. Non-motor symptoms are characterized by psychiatric dysfunction (particularly depressive signs), olfactory alterations (an early ataxias symptom), cognitive deficits (predominantly in memory and executive functions) and sleep disorders (the most common) such as restless legs syndrome (RLS) and rapid eye movement (REM) [1, 19, 20]. In peripherical nervous system (PNS) SCA3 patients have peripherical neuropathy that affected mainly sensory fibers and induce muscle atrophy and impairment stimuli response (areflexia) [1, 19]. In patients with short polyQ repeat expansions and late onset, peripherical neuropathy is often found [19]. Parkinsonism, particularly an akinetic-rigid syndrome, that resembles Parkinson disease is a symptom of SCA3 [4, 19, 20]. Other MJD symptoms are nocturia, urinary incontinence, compromised temperature discrimination (such as cold intolerance and sweeting disorders), gastrointestinal abnormalities, and sexual anomalies [19, 20].

At anatomical level, cell degeneration, provoked by neuronal dysfunction and loss of somatosensory and motor neurons, is present in several CNS structures of SCA3 individuals [1, 4, 24]. In MJD the loss of vestibular, pontine, and motor nuclei affects the brainstem, while loss of dorsal root ganglia, dorsal nuclei and anterior horn affect spinal cord [1, 4, 24]. In other SCA3 patients the affected neurons are the nerve motor nuclei, Clarke´s column nuclei and red nucleus [1, 4, 24]. In basal ganglia, the striatum, the subregion *globus pallidus* and subthalamic nuclei are affected along with degeneration of dopaminergic neurons of the *substantia nigra* [1, 4, 24]. In cerebellum dentate nucleus are affected but in cerebellar cortex Purkinje cells and the inferior olive are relatively conserved, while in cerebellar vermis occurs Purkinje cells and granule loss in SCA3 brain patients [1, 4, 24]. The fourth ventricle is increased due to neuron atrophy in the basilar pons and deep cerebellar nuclei, and loss of pontocerebellar fibers and spinocerebellar tracts are observed in SCA3 brains [1]. Moreover, in thalamus the thalamic nuclei neurons suffer cell degeneration in SCA3 patients [1, 4, 24].

At cellular level, protein intraneuronal inclusions are observed in affected and not affected areas of SCA3 brains [4, 24]. These inclusions appear in nucleus, cytoplasm or even in axons of neurons [1, 4, 24]. These aggregates are composed by expanded and non-expanded SCA3 proteins along with ubiquitin and heat shock proteins, transcription factors, autophagy-associated chaperones (Sequestosome 1 (p62) for example), proteases subunits and other polyQ proteins [1, 24]. Other inclusions affect brain cells such as astrocytes, microglia, and oligodendrocytes [1]. Astrocytes are activated in affected SCA3 brain regions and could lead to massive release of the chemocytokine eotaxin that would be recognized by microglia cells and will enhance production of reactive oxygen species that could culminate in cell death [1]. Transcription dysregulation in oligodendrocytes, observed in a SCA3 mouse model, alters myelination, axon ensheathment and cholesterol biogenesis (also performed by astrocytes) [1]. Cholesterol biogenesis increases the cholesterol levels in brain that is essential for myelin membrane growth, axon growth and synapse remodelling [1]. A SCA3 animal model phenotype could be rescued by overexpression of cholesterol efflux in brain [1].

2. *ATXN3* gene

SCA3 results from a CAG repeat expansion of *ATXN3* gene (also known as *MJD1*), that will encode the ataxin-3 protein [4, 25]. *ATXN3* gene is localized in chromosome 14q32.1 and it is composed by 11 exons (**Figure 1**) [1, 25]. The consecutive CAG repeats are in exon 10 and have a single lysine residue in the

beginning of it [1, 25]. The CAG repeat is located at the 5'-end of exon 10 and has a single lysine residue in the beginning of it [1, 25]. These repeats are unstable and thus, their number differs among individuals (even if they are from the same family), and between tissues [26]. In healthy individuals the size varies between 10 to 44 CAG repeats [4, 24], while in SCA3 patients the repeat size has, at least 87, CAG repeats [1, 4, 24, 25].

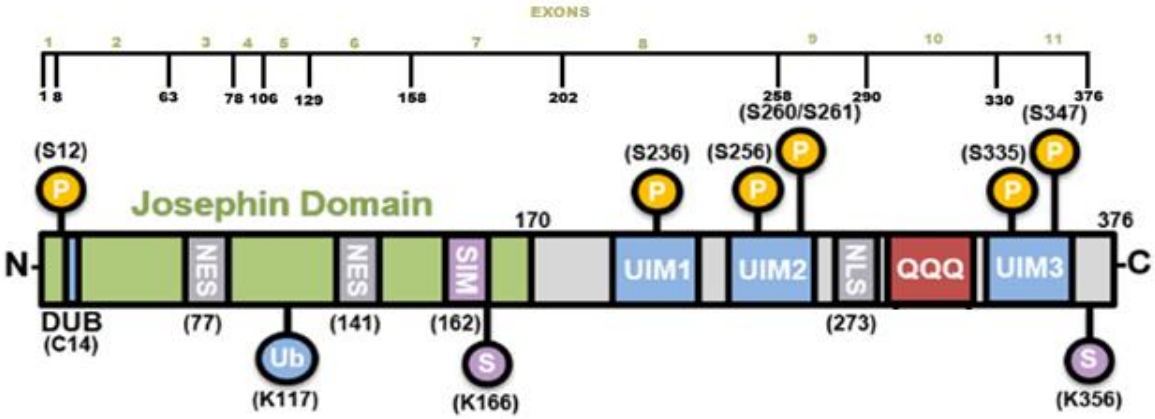

Figure 1: Exon structure of the *ATXN3* gene, and the ataxin-3 product highlighting the functional domains, and post-translational modification sites, modified from McLoughlin *et al.* [1]. DUB stands for deubiquitinase catalytic site (C14), NES nuclear export site, SIM small ubiquitin-like modifier [SUMO]-interacting motif, UIM ubiquitin-interacting motif, QQQ the polyQ region, NLS putative nuclear localization signal, Ub ubiquitin at K117, S SUMOylating at K166 and K356, and P phosphorylation at S12, S236, S256, S260, S261, S335, and S347.

ATXN3 undergoes four types of alternative splicing (exon skipping, novel exons, usage of alternative 5' splice sites, and usage of alternative 3' splice sites) that results in 56 splicing blood variants [27]. Some of them are targeted for degradation by the nonsense-mediated decay, special if they have a premature stop codon [27]. Other splice variants instead of being translated as a polyQ protein will be translated as a polyalanine (polyA) protein due to frameshift alterations [27]. In the human brain three splicing variants, namely ataxin-3aL, ataxin-3aS and ataxin-3c, were found that differ in their translated C-terminal region [28]. Ataxin-3aS results from the ataxin-3aL, because of a SNP in exon 10 that generates a premature stop codon [28]. The isoforms ataxin-3aL and ataxin-3c are generated by alternative splicing of *ATXN3* [28]. The isoform ataxin-3c is the most common in the human brain and has a hydrophilic C-terminal tail, while the other two have a hydrophobic tail [28]. The expanded ataxin-3a isoforms shown a quicker protein aggregation than the expanded ataxin-3c [28]. Furthermore, expansion of CAG repeats in *ATXN3* induce the transcription of hydrophobic tail isoforms [28]. Since

this type of isoforms is more prone to aggregate, this may explain a step in SCA3 development.

3. The ataxin-3 protein

Ataxin-3 is composed by a N-terminal region where the globular Josephin domain (JD) is located, while in the flexible C-terminal tail there are at least three ubiquitin interacting motives (UIMs), depending on isoform, and the polyQ tract (**Figure 1**) [25, 26, 29]. In this study, I used the most common ataxin-3 in brain that has 3 UIMs [28]. Their domains and motives are distributed, according to UniProt sequence P54252, in the following amino acid regions 1-180, 224-243, 244-263, 292-305 and 335-354, that correspond to JD, UIM1, UIM2, polyQ tract (composed of 14Q) and the UIM3, respectively. Also, two nuclear export signals (NES), NES77 (range from residues 77-99) and NES141 (ranging from residues 141-158) and a small ubiquitin-like modifier [SUMO]-interacting motive (SIM, ranging between residues 162-166) where identified in N-terminal region and a nuclear localization signal (NLS), ranging from residues 273-286, was found in the C-terminal tail of ataxin-3 [1, 30].

Ataxin-3 is ubiquitously expressed through the body, and it is present in nucleus, cytoplasm, and mitochondria of cells [25]. This protein rapidly alters between nucleus and cytoplasm due the two NES and the NLS [25]. But normal ataxin-3 is considered a cytoplasmatic protein, that under polyQ tract expansion goes to nucleus to form aggregates [31]. This localization turnover may be due to conformational alteration provoked by the expanded glutamine tract [31].

Ataxin-3 is a deubiquitinating enzyme (DUB), capable of recognizing polyubiquitin (polyUb) chains with four or more ubiquitins (Ub) [32]. Ataxin-3 DUB activity is important to rescue proteins from proteasome degradation, since Ub targets for this major type of degradation, and for ubiquitin recycling that is essential for cell homeostasis [32]. Ataxin-3 catalytic activity is centered in JD [33]. The JD is constituted by six antiparallel β-sheets (β1-β6) flanked by seven α-helices (α1-α7) that are rearranged in a similar way as papain-like cysteine(Cys)-protease family proteins [33]. Thus, it is composed by two lobes, one without β-sheets, composed by the α-helices 1, 2, 3, 4 and 7, while the other lobe has all the six β-sheets and the remaining α-helices (α5 and α6) [33]. Two conformational dynamic states of ataxin-3 ubiquitin recognition and binding have been described [29, 33]. This is caused by the loop formed by α3, α4 and C-terminal portion of α2 that allows the Ub binding site above the catalytic site [33]. The catalytic site is composed by residues Q9, C14, H119 and N134, characteristic of Cys-proteases

[25, 33, 34]. The helical hairpin (formed by α2 and α3) conformational arrangements allow an open or a close conformational state of ataxin-3 [29]. Additionally, two ubiquitin binding sites were found in JD [33, 35]. The first, located above the catalytic site, is the most important, while the second site is not essential for ubiquitin cleavage [33, 34]. But it could be important for JD polyUb preference [34]. Site 2 is composed by the aromatic cluster Y27, F28 and W87 [35]. Besides Ub binding, site 2 could interact with RAD23A and RAD23B proteins, through their UBL (N-terminal ubiquitin-like) domain [35, 36]. These proteins have a role in substrate degradation via proteasome pathway [37].

UIMs induce a polyUb preference in JD [25, 34]. For example, ataxin-3 cleaves both K48 and K63-linked Ub chains but preferably cleaves K63-linked in a UIM dependent manner, since JD alone preferably cleaves K48-linked Ub chains [34, 38]. Also, UIMs would help in ataxin-3 binding conformation, by correcting the position of polyUb chains, and allowing interactions with site 2 [33, 34]. Burnett and collaborators showed that UIM are required for polyUb (having four or more Ub) substrate binding sites to ataxin-3 [32]. UIM2 is the crucial one, since mutation in it inhibits Ub trapping, while UIM1 and UIM3 mutations ineffective inhibit Ub binding [33]. The UIM1 and UIM2 are α-helices associated by a short linker that upon ubiquitin addition form a more compact structure [29].

PolyQ tracts are flexible but have influence on their flanking residues [26]. It forms a coiled-coil structure, that could stabilize protein interactions [26], in this case, between ataxin-3 and their interactors. The expanded polyQ tract undergoes a structure conformation of β-rich amyloid-like protein inclusions [26]. Expanded polyQ could induce toxicity as a result from the novel conformation adopted, that could be a precursor of toxic species or could induce protein interactions which are pathogenic [26]. But seems not influence the ataxin-3 catalytic activity, the polyUb binding and the hydrolysis [29, 38]. However, catalytic activity was inferred in *in vitro* studies, so the cellular context could lead to a different outcome [38]. It has been shown that wild type ataxin-3 (WT ataxin-3) is prone to aggregation, under stress conditions, by JD self-association that forms SDS sensitive protofibrils [29]. This is the first step of protein aggregation and is common with expanded ataxin-3 (EXP ataxin-3) [29]. But an expanded polyQ tract increases self-assembly events and promotes protofibrils maturation that are SDS resistant [29]. These maturated fibrils are stabilized due to hydrogen bonds via expanded glutamine residues [29]. It was observed a loss of ataxin-3 DUB function in protofibrils, probably due to JD structure modification that alters α-helices to β-sheet under aggregation [25].

3.1 Post-translation modifications

Ataxin-3 after translation undergoes several modifications such as phosphorylation, ubiquitination, SUMOylation and proteolytic cleavage, that could have influence in ataxin-3 localization and functions.

3.1.1 Phosphorylation

Ataxin-3 phosphorylation is mediated by phosphorylated enzymes such as casein kinase 2 (CK2), glycogen synthase kinase 3β (GSK3β) or polo-like kinases (Plk). The phosphorylated residues are S12, S29, S55, T60, S111, S219, S236, S256, S260, S261, S265, S278, S340 and S352 [29, 39-42]. S12 is close to the ataxin-3 catalytic site, and its phosphorylation reduces the deubiquitinase activity of the protein [29]. In EXP ataxin-3, phosphorylation at S12 decreases protein aggregation and ameliorates dendritic tract and synapse (excitatory and inhibitor) loss that is caused by expanded protein form [29]. S29 phosphorylation is mediated by CK2 and GSK3β and promotes ataxin-3 nuclear localization [41]. S55 phosphorylation is increased in EXP ataxin-3 [42]. The phosphorylation at S55 and T60 may modulate ataxin-3 catalytic activity [41]. S111 phosphorylation promotes nuclear localization of ataxin-3, upon heat shock, since residue mutation (change of S111 for A111) impairs this action (in JD fragments), although some alanine mutated ataxin-3 full-length is found in the nucleus [43]. This phosphorylation may be mediated by Plk1 or other polo-like kinases proteins since Plk1 is not present in the brain, but neurons have polo-like kinase 2 and 3 [43]. For both WT and EXP ataxin-3, it has been shown that phosphorylation, mediated by CK2 (under basal conditions [43]) at residues S236, S340 and S352 increase ataxin-3 nuclear localization, while phosphorylation at residues S256, S260 and S261 had minor influence in ataxin-3 localization [39]. S256 is phosphorylated by GSK3β in both ataxin-3 forms, but in EXP ataxin-3, mutation at this residue (change of S to A) caused aggregation [40]. So, it is possible that S256 phosphorylation impairs EXP ataxin-3 aggregation [40]. Also, it was found that S256 phosphorylation is increased in EXP ataxin-3 [42].

3.1.2 Ubiquitination

Ubiquitination is mediated by three enzymes: E1 (ubiquitin-activating enzyme), E2 (ubiquitin-conjugating enzyme) and E3 (ubiquitin-protein ligase) [41, 44, 45]. E1 enzymes transform ubiquitin for substrate binding and this step is ATP dependent. Next, ubiquitin is transferred to the cysteine (that is the E2 active site) residue of E2. Finally,

E3 enzyme transfers ubiquitin to a lysine residue in substrate [44]. Ubiquitination will endorse substrates for a specify pathway depending on the ubiquitin attached site of the next ubiquitin to form polyUb linked chains [44]. For example, K48-linked proteins are targeted for proteasome degradation, while K63-linked proteins play a role in autophagy, DNA damage and transcription activity, and K11 linked proteins could have a role in targeting cell cycle regulatory proteins and endoplasmic reticulum (ER) substrates for proteasomal degradation [42, 44].

Ataxin-3 (both WT and EXP) prefers to be ubiquitinated by K48-linkaged ubiquitin chains [42]. Ataxin-3 ubiquitination happened at K8, K29, K117, K190, K200, K206 and K291 [29, 41, 42, 46]. All these residues are ubiquitinated independently of polyQ expansion, except for K8 that is enhanced in EXP ataxin-3 and therefore, could influence the catalytic ataxin-3 activity, and K200 where polyQ expansion abolishes ubiquitination in this residue [41, 42, 46]. K117 ubiquitination alters the conformal state of ataxin-3 that improves its deubiquitinating activity [29, 41, 46]. It is the preferred residue for ataxin-3 (either WT or EXP) ubiquitination [46]. If K117 is mutated K200 becomes the preferred residue of WT ataxin-3 ubiquitination [46]. If ataxin-3 is ubiquitinated is should be degraded via proteasome, however, ataxin-3 degradation doesn´t depend on ubiquitination but rather on RAD23 homolog A, nucleotide excision repair (RAD23A) and/or RAD23 homolog B, nucleotide excision repair (RAD23B) binding to site 2 [37]. If site 2 or RAD23 proteins are mutated ataxin-3 cellular levels are decreased [37]. Also, UIM mutations increase ataxin-3 levels [37]. So, Blount *et al.* proposed that ataxin-3 goes to proteasome due to its UIMs interactions with ubiquitinated substrates, but in proteasome RAD23 proteins binding to ataxin-3 site 2 rescue ataxin-3 from degradation [37]. Because of ataxin-3 polyQ tract RAD23A and/or RAD23B should have higher affinity to ataxin-3 than to the proteasome [37]. Consequently, ataxin-3 can only be degraded if it didn´t bind to RAD23 [37].

3.1.3 SUMOylation

SUMOylation, mediated by SUMO (small ubiquitin-like modifier) proteins, could influence the substrate function, activity, and localization [47]. Ataxin-3 has a SUMO-interacting motif (SIM) located in residues 162-165 and mutation in it abolishes SUMO1 interaction [48]. In ataxin-3 two residues (K166 and K356) suffer SUMOylation [47, 49]. SUMOylation at residue 166 is mediate by SUMO1 and is independent of polyQ tract length [47]. But this modification in EXP ataxin-3 seems to stabilize the protein [47]. Also, SUMO1, along with SUMO2, are capable of SUMOylation *in vitro*, residue 356 in both

pathogenic and non-pathogenic ataxin-3 forms [49]. This change decreases ataxin-3 self-assembly, and promotes a faster association with VCP, probably due to conformational changes of ataxin-3 [49]. Also, ataxin-3 SUMOylation has a role in the recruiting of ataxin-3 for DNA double-strand breaks, where this protein will influence the DNA damage signalling and DNA repair [48].

3.1.4 Proteolysis

Ataxin-3 protein cleavage is a very important post-translation modification since nuclear aggregates are formed by EXP ataxin-3 fragments [41]. Ataxin-3 could be cleaved by the protease's caspases (caspase 1 and 3) and/or calpains (calpain 1 and 2) [41]. EXP ataxin-3 protein cleavage between NES and NLS sites promotes C-terminal fragments translocation to the nucleus and consequently aggregation and neurotoxicity [31]. The fragments have 37 kDa or 50 kDa [50]. Disturbances at mitochondrial (increased membrane fission and reactive oxygen species formation, while decreasing mitochondrial membrane potential) level are also seen because of polyQ fragments [50]. Ataxin-3 caspases cleavage sites (close to aspartate residues) are residues 241, 244, 248, where their mutation impairs proteolysis [50]. In *Drosophila* expressing human EXP ataxin-3, proteolysis is suppressed when changing to aspartate residues 171, 208, 217, 223, 225 and 228, which eliminates the 37 kDa fragment in cells [50]. Calpains cleave ataxin-3 at the residues H187, D208, S256 and T277 [50, 51]. Calpains 1 and 2, *in vitro*, induce proteolysis at a similar way in both ataxin-3 proteins (WT and EXP forms) [51]. It should be noted that, calpains are expressed in the brain [50].

3.2 Ataxin-3 is involved in multiple pathways

Ataxin-3 seems not to be an essential protein, since mouse and *Caenorhabditis elegans* knockout models of *ATXN3* orthologues reveal a little phenotypic changes [25]. Nevertheless, in humans, EXP ataxin-3 pathogenesis is associated with an ataxin-3 toxic gain of function [31]. So, in here, I will summarize the biological pathways where ataxin-3 seems to be involved.

3.2.1 DNA repair mechanism:

Aging of neurons enhances DNA damage accumulation, but this is a normal process, although it is associated with neurodegenerative diseases [1]. DNA damage is characterized by single or double strand breaks that are very toxic genome alterations,

because they impair the DNA polymerase and DNA ligases actions [52]. Consequently, their repair is very important. Several enzymes were shown to mediate this process and two of them are associated with ataxin-3, they are the mediator of Mediator of DNA damage checkpoint 1 (MDC1) and polynucleotide kinase 3´-phosphatase (PNKP) [48, 52, 53].

MDC1, under DNA double-strand breaks (DSBs), is recruited to DNA damage regions and marks with ubiquitin the chromatin associated proteins in the affected region, facilitating the DNA damage response (provided by proteins such as p53-binding protein 1 (53BP1) and BRCA1 DNA repair associated (BRCA1)) [48]. SUMO proteins are also important in this type of response, probably because they enhance DNA damage response proteins affinity towards ubiquitin, as was observed for BRCA1/BARD1 (BRCA1 associated RING domain 1) complex or by recruiting proteins for DNA damage sites, for example ring finger protein 4 (RNF4) that improves ubiquitin removal from chromatin associated MDC1 [48]. Both MDC1 and RNF4 promotes DNA repair through non-homologous end-joining (NHEJ) or homologous recombination (HR) [48]. The ataxin-3 recruitment to DNA damage sites is independent of their catalytic activity, their UIMs or even VCP (that is also present in DNA damage sites) binding but is dependent of SUMO1 interactions that happened due to the SIM motif present in JD [29]. An interaction between MDC1 and ataxin-3 is constitutive and independent of MDC1 SUMOylation [48]. Ataxin-3 knockdown leads to a faster exchange of MDC1, indicating that ataxin-3 might stabilize MDC1 chromatin binding [48]. Also, ataxin-3 depletion leads to increase polyUb MDC1 proteins along with a decreased accumulation of BRCA1 and 53BPI, both downstream in DNA repair mechanisms [48]. 53BPI levels are restored by expressing WT ataxin-3 but not by expressing an inactive DUB ataxin-3 [48]. Suggesting that MDC1 is deubiquitinated by ataxin-3 [48]. Taken together, these data, suggest that ubiquitylation of MDC1 regulates MDC1 release from chromatin [48]. Likewise, during DNA repair ataxin-3 does not remove ubiquitin from MDC1, and thus the latter is maintained bound to chromatin. Nevertheless, when the signalling cascade downstream of 53BPI and BRCA1 effector proteins is initiated, ataxin-3 will deubiquitinate MDC1 that is then released, leading to DNA damage sites being repaired by NHEJ or HR [48]. Therefore, polyQ tract expansion could impair this regulation of MDC1 that would increase the levels of DNA damage in cells, that might enhance SCA3 pathology.

The single or double strand breaks creates 3´- P groups and 5´-OH termini [52]. PNKP is capable of restoring the 3´-OH (hydroxy) and 5´-P (phosphate) DNA ends necessary for DNA polymerase and DNA ligases action that repair the damage DNA [52]. PNKP is composed by 3 domains: forkhead-associated (FHA) domain (residues 1-

119), phosphatase domain (residues 120-339) and Kinase domain (residues 340-521) [52]. PNKP interacts with ataxin-3 (both WT and EXP versions), but the used domains differ [52]. For WT ataxin-3, PNKP interacts through phosphatase and kinase domains, while for EXP ataxin-3 PNKP only interacts with the latter [52]. WT ataxin-3 stimulates PNKP 3´-phosphatase activity, while EXP ataxin-3 inhibits PNKP activity leading to accumulation of DNA strand breaks [52, 53]. Gao and co-workers observed that PNKP is present in EXP ataxin-3 aggregates located in and out of nucleus, and this is an additional way to prevent PNKP activity [53]. The PNKP inhibition by EXP ataxin-3 could explain the age related SCA3 pathology, since this inhibition is slow and progressive, in heterozygote SCA3 individuals (that have a normal ataxin-3 allele and one mutant ataxin-3 allele) [52]. So, as the years go by, more DNA strand breaks accumulate that would induce dysregulation of gene expression that impairs neuronal function, leading to neurodegeneration and ataxia (showing the SCA3 phenotype) [52].

Ataxia telangiectasia mutated (ATM) is a DNA damage-response kinase that is autophosphorylated under oxidative DNA-damage or double-strand breaks that regulates the DNA damage response such as PNKP phosphorylation (DNA-PK also can do this) [52, 53]. PNKP phosphorylation allows its maintenance levels in cell, because inhibits ubiquitination and consequently degradation [52]. Other proteins such as histone H2AX and 53BP1 are phosphorylated in cases of DNA damage and are recruited to injury sites [53]. It was observed that EXP ataxin-3 induces ATM and H2AX phosphorylation, along with checkpoint kinase 2 (Chk2) and cellular tumor antigen p53 (p53) (downstream effectors of ATM pathway) [53]. But ATM signalling is impaired with WT ataxin-3 expression [53]. So, these authors propose that EXP ataxin-3 is capable of activating DNA damage signalling and that polyQ tract is important for ATM activation [53]. Under inactivation of oxidative stress (by an antioxidant enzyme), EXP ataxin-3 were capable of activating ATM pathway, suggesting that this activation in independent of oxidative cell state [53]. EXP ataxin-3 were found to induce p53-dependent apoptosis [53]. Authors observed p53 mediated apoptosis was inhibited in cells with EXP ataxin-3 but overexpressing PNKP [53]. In sum, PNKP inactivation by mutant ataxin-3 will impair DNA repair which increases the DNA damage inducing ATM signalling activation, in particularly p53, that promotes apoptosis that culminates in neuronal death in SCA3 patients [53].

Checkpoint kinase 1 (Chk1) is a kinase that is activated by DNA damage or replication stress [54]. Consequently, it is involved in DNA repair or cell death if the damage is too high [54]. Also, Chk1 is involved in cell cycle [54]. Ataxin-3 (WT and EXP forms) interacts with Chk1, trough JD [54]. Moreover, ataxin-3 stabilizes Chk1 by

inhibition of proteasome Chk1 degradation during the DNA repair period [54]. The final step in DNA repair, is ataxin-3 dissociation from Chk1 and the Chk1 endorsement for proteasome degradation [54].

3.2.2 Transcription regulation:

PolyQ proteins can repress transcription because they recruit transcription regulators into aggregates [55]. For instance, CREB binding protein (CBP), E1A binding protein p300 (P300), and Lysine acetyltransferase 2B (KAT2B/PCAF) are transcriptional coactivators regulated by ataxin-3. They have histone acetyltransferase activity (HAT) and are predominant in the nucleus [55]. These coactivators are stimulated by cAMP response element (CRE) binding protein (CREB) that in response to cAMP, binds CRE enhancer, promoting its phosphorylation, histone acetylase function and transcription [55]. A more efficient binding to these coactivators were noticed with EXP ataxin-3 [55]. The CBP, P300 and PCAF transcription repression is mediated by C-terminal tail that allows their interaction in WT and EXP ataxin-3 [55]. Moreover, N-terminal WT and EXP ataxin-3 interacts with histone 3 (H3) and 4 (H4) where it would decrease their acetylation, inhibiting transcription [55].

Another transcription factor identified as an interactor of ataxin-3 is the forkhead box class O (FOXO) transcription factor 4 (FOXO4) [56]. FOXO family is involved in multicellular processes such as cell death and resistance to cellular oxidative stress [56]. Ataxin-3 polyQ tract length doesn´t play a role in FOXO4 binding, and the interaction happens in residues 19-39, 70-87, 88-111 and 139-165 of ataxin-3 JD [56]. Noteworthy is the fact that FOXO4 does not colocalize with nuclear inclusions of pons SCA3 patients [56]. Additionally, ataxin-3 (both WT and EXP) seems not to deubiquitinate the FOXO4 ubiquitinated protein (mediated by Mdm2 E3 ligase that promotes FOXO4 translocation to nucleus, while E3 ligase Skp2 inhibits it) [56]. Under stress, FOXO4 is translocated from cytoplasm to nucleus [56], that happens when ataxin-3 is under oxidative stress [43]. Consequently, reactive oxygen species (ROS) production increases along with the expression of antioxidant enzyme SOD2 (responsible for ROS removal) [56]. *In vivo,* both ataxin-3 and FOXO4 interact with human *SOD2* gene promoter [56]. Only WT ataxin-3 activates the FOXO4 dependent expression of *SOD2* gene promotor [56]. Suggesting that normal ataxin-3 functions as a redox-sensitive protein [56].

Additionally, matrix metalloproteinase-2 (MMP-2) promotor is another player in ataxin-3 transcription regulation [57]. Upon WT ataxin-3 MMP-2 is downregulated, while upon EXP ataxin-3 is upregulated [57]. This could be mediated by different properties of

ataxin-3 forms [57]. Furthermore, it was observed that ataxin-3 binds to NCoR (nuclear receptor corepressor) and histone deacetylase (HDAC3) mediates its biding to MMP-2 promotor and promoting histone deacetylation [57], inhibiting MMP-2 transcription. Ataxin-3 (WT and EXP forms) interacts with HDAC3, since ataxin-3 overexpression upregulate HDAC3 levels, and enriches HDAC3 stability and levels [57, 58]. Further, ataxin-3 promotes HDAC3 deubiquitination [58]. WT ataxin-3 represses the MMP-2 gene transcription, while EXP ataxin-3, activates MMP-2 gene transcription [57]. WT ataxin-3 increase the deacetylase activity that deacetylates H3, promoting transcription repression [57]. But EXP ataxin-3 allows target genes transcription activity since it does not allow the deacetylation of H3 [57].

Additionally, ataxin-3 also interacts with TATA-binding protein-associated factor TAFII130, another component of the transcription machinery [56].

3.2.3 Autophagy

Autophagy is a mechanism involved in cell survival and degradation of misfolded proteins, such as EXP ataxin-3 [59, 60]. This process begins with the formation and elongation of the autophagosomal membrane, mediated by phosphatidylethanolamine (PE) and autophagosomal anchoring of six Atg8 family members [60]. The Atg8 family are ubiquitin-like modifiers localized in luminal side of autophagic vesicle and it is composed by 6 members: LC3A, LC3B, LC3C, GABARAP, GABARAPL1 and GABARAPL2 that are responsible for the recruitment of autophagy proteins and receptors to autophagosome [60]. This process is mediated by LC3-interacting regions (LIR) present in the Atg8 family members [60]. The next step is the autophagosome fusion with lysosomes [60], forming the autolysosome that is capable of degrading the misfolded proteins promoting the cell survival. During this step LC3 and GABARAP proteins are destroyed [60]. Ashkenazi *et al.* propose that ataxin-3 impairs autophagosome synthesis, since ataxin-3 knockdown in neurons decreases the LC3 and beclin-1 levels [59]. Next, Herzog *et al.* observed that ataxin-3 interacts with Atg8 proteins through multiple LIR motifs in JD, the first (LIR1) comprising residues 74-77, while the second (LIR2) is localized in residues 130-133 [60]. Both LIR motifs interact with LC3C, while only the last one interacts with GABARAP [60]. LIR1 is very close to ubiquitin binding site 1 (responsible for DUB ataxin-3 catalytic activity), so ataxin-3 binding to Atg8 proteins could affect ubiquitin binding and ataxin-3 activity [60]. For LIR2 interactions ataxin-3 needs to alter significatively the JD structure [60]. Beclin-1 inhibits autophagy under starvation [59]. Neurons where ataxin-3 has been knockdown show a

decrease of beclin-1 levels, that rapidly increase when the proteasome is inhibited or when WT ataxin-3 (but not mutant DUB ataxin-3) is expressed in these cells [59]. So, it was proposed that ataxin-3 interacts with beclin-1 and deubiquitinate it, impairing beclin-1 degradation by proteasome [59]. Thereby, under starvation conditions autophagy will be inhibited. Additionally, ataxin-3 interacts with beclin-1 trough polyQ tract since depletion of it decreases beclin-1 levels [59]. Longer polyQ repeats are associated with a stronger interaction between ataxin-3 and beclin-1 [59]. Consequently, the ataxin-3 polyQ region mediates deubiquitylation of beclin-1, inhibiting its degradation by proteasome [59].

Another protein that has a role in autophagy and interacts with ataxin-3 is the p62 [61]. But studies report that p62 has a predominant role in EXP ataxin-3 aggresomes formation instead of on the autophagy pathway [61], see in the section 3.2.5.

3.2.4 Proteasome:

Ataxin-3 is being associated with proteasome because of its capability to remove ubiquitin from substrates, allowing their rescue from proteasome mediated degradation [32]. As expected, ataxin-3 was shown to interact with several proteasome related proteins (E3 enzymes, for example). Also, ataxin-3 through its N-terminal region is capable to interact with 26S proteasome (composed by the subunits 20S and 19S) [62].

Ubiquitination is a major cell signalling pathway involved in a wide range of biological processes ranging from protein degradation (by the proteasome or autophagy) to DNA damage and transcription activity [42, 44]. Ubiquitination is mediated by three enzymes where the last one, E3 enzyme, is responsible to transfer ubiquitin to lysine residues in substrates [44]. E3 enzymes can be subdivided in HECT and RING-domain [63]. Ataxin-3 was found to interact with the E3 enzymes E3 ubiquitin-protein ligase CHIP (CHIP), E3 ubiquitin-protein ligase parkin (parkin), E3 ubiquitin-protein ligase AMFR (gp78) and E3 ubiquitin-protein ligase synoviolin (HRD1) [45, 64-67].

CHIP is composed by the TPR (tetratricopeptide repeat) domain, that allows chaperone interaction, and a U-box domain, responsible for recruiting E2 enzymes [64]. Consequently, CHIP ubiquitinates and promotes degradation of misfolded proteins, such as polyQ proteins [64, 68]. CHIP can be found in the cytosol, under normal conditions [68]. But it is present in WT and EXP ataxin-3 aggregates [68]. CHIP is capable of ubiquitinating WT and EXP ataxin-3 at K117 (but not other ataxin-3 lysine's), that enhances DUB ataxin-3 activity [46] that would help Ub edition [69]. But interacts more with EXP ataxin-3 [3, 64, 68]. Another CHIP function is the endorsement of ataxin-3 for

degradation, a process that will be mediated by Hsp70 [3]. CHIP Hsp70 interaction is mediated by TPR CHIP domain [70]. If Hsp70 is missing, CHIP ataxin-3 ubiquitination reveals, *in vitro*, a lower efficiency [70]. Additionally, CHIP or Hsp70 overexpression leads to the same phenotype, an increase in ataxin-3 ubiquitination [70]. Moreover, TPR mutations impair CHIP Hsp70 interaction, and ubiquitination of ataxin-3 is lost [70]. So, Hsp70 modulates ataxin-3 ubiquitination and therefore plays a role in polyQ protein degradation through proteasome [70]. Moreover, WT ataxin-3 under basal and stress conditions activates the Hsp70 promotor [71].

In another perspective ataxin-3 controls the CHIP substrates polyUb length, through JD and UIM1 and UIM2 [64]. Moreover, ataxin-3 deubiquitinate Ub from CHIP, after polyubiquitinated substrates are formed [64]. This action could regulate the rate of CHIP substrate degradation by proteasome or diminish the proteins targeted for proteasome [64].

Parkin is a RING-inBetweenRING-RING protein composed by six domains: the ubiquitin-like domain (UBL), unique-parkin domain (UPD), RING0, RING1 (necessary for E2 recruitment), IBR (inBetweenRING) and RING2 (important for transfers Ub) [45, 65]. Parkin interacts with ataxin-3, probably by C-terminal ataxin-3 region since different isoforms (that differ in the C-terminal tail) shown distinct parkin affinities [28]. For example, short ataxin-3 isoforms (lacking the UIM3) shown a strong parkin interaction [28]. Further studies identified that UBL domain weakly binds to the three UIM in ataxin-3, suggesting a multi or polyvalent ligand mode, where all UIM recognize parkin UBL but only one will bind it [45]. A conserved serine (236, 256 and 347) in each UIM (UIM1, UIM2 and UIM3, respectively) is essential for UBL-UIM ataxin-3 interaction, since their mutation impairs UBL binding [45, 72]. Moreover, the length of polyQ tract does not influence the parkin-ataxin-3 interaction [72]. Additionally, ataxin-3 JD interacts with Parkin through Parkin IBR-RING2 domains [72]. Ataxin-3 was shown to exert DUB activity in parkin, independent of E2 enzyme used [72]. EXP ataxin-3 has an increased DUB activity for parkin, and targets parkin for degradation by autophagy [72]. This could be linked to SCA3 pathology if protein degradation becomes a disadvantage instead of having a protective role towards misfolded proteins [72]. WT ataxin-3 stabilizes parkin in brain, by stabilizing the E2 (particularly, UBC7) interactions with parkin and this could alter the normal association/dissociation (therefore, decreases the efficiency of E2 recharging by the E1) of ubiquitination proteins [63, 72]. This stabilization may arise because of a complex interaction between ataxin-3-parkin-E3 [63]. EXP ataxin-3 does not stabilize the previous interaction [63]. Parkin UBL domain can be phosphorylated

and alters the ataxin-3 interaction, by decreasing UBL affinity for ataxin-3 UIMs [65]. Therefore, ataxin-3 inhibits parkin deubiquitination [65].

HRD1 and gp78 are two E3 enzymes involved in ERAD pathway [66, 67]. HRD1 is composed by 6 transmembrane domains and a C-terminal cytosolic domain that has the catalytic site [66]. HRD1 interacts with ataxin-3 [73]. Gp78 has a RING finger-type ubiquitin ligase activity site located on ER surface localised towards the cytoplasmic site [67]. Gp78 (N-terminal region, with 340 amino acids length) interacts with ataxin-3 and mediates WT and EXP ataxin-3 degradation, by enhancing ataxin-3 ubiquitination [67]. Furthermore, gp78 is recruited for ataxin-3 aggregates [67]. The presence of misfolding proteins increase ER stress that upregulates gp78 and HRD1 proteins [67]. Additionally, C-terminal EXP ataxin-3 fragments were seen to induce ER stress, since Bip (an ER stress marker) and gp78 increase [67]. The accumulation of misfolded proteins, that leads to ER stress, is caused by EXP ataxin-3 inhibitions of endoplasmic reticulum – associated degradation (ERAD) pathway [67].

Vasolin-containing protein (VCP) interacts with ataxin-3, but this interaction decreases with the reduction of polyQ tract, consequently EXP ataxin-3 interacts more strongly with VCP comparing with WT ataxin-3 [62, 74-76]. Further, the ataxin-3 motif responsible for VCP binding was identified. This motif is the VCP-binding motif (VBM) located in residues 281-289 of ataxin-3, where the region composed by residues 282 to 285 is sufficient for VCP binding [76-78]. Mutations in this region abolish WT and EXP ataxin-3 interaction with VCP, but arginine residues 282 and 285 can´t be altered (are essential residues), while the other ones have a little range for change [76]. VBM was described as overlapping with the ataxin-3 NLS [76], but in another study it was shown that this is not true [77]. Since mutations in VBM showed the same distribution as non-mutant VBM ataxin-3 (for WT and EXP forms) [77]. VCP is an AAA-ATPase, located in brain, and involved in ERAD pathway [75, 76]. The ERAD pathway is responsible for degradation of unassembled protein complexes and misfolded proteins [75]. In the first step the damage components are removed from ER, using VCP [75]. Next occurs proteasome degradation, that happens in cytosol [75]. Ataxin-3 was observed to inhibit VCP action in ERAD mechanism, suggesting a competition with Ufd1 (enhances VCP binding to ER ubiquitinated proteins) for VCP binding [73, 75]. So, ataxin-3 will impair the extraction of misfolded proteins from the ER, thus allowing more folding cycles or the use of other quality controls pathways [75]. This could be a mechanism for control of the homeostatic ERAD process [75]. VCP is present in SCA3 brain aggregates [76], and VBM disruptions abolish VCP recruitment into aggregates [77]. The interaction between ataxin-3 and VCP damages in response to cell stressors (inhibition of proteasome,

activating the unfold protein response or heat shock), but only heat shock stress causes ataxin-3 accumulation in nucleus [43]. VCP is recruited for DNA damage sites (double strand breaks), independent of ataxin-3, and ataxin-3 recruitment is independent of VCP [48]. So, these proteins are partners for protein degradation but not for DNA repair. This shown that VCP interacts with several other protein besides ataxin-3. One of them is E4B protein, an additional enzyme required for ubiquitination of some substrates [74]. The VCP-E4B interaction mediates ataxin-3-E4B interaction, forming a ternary complex [74]. E4B is associated to ataxin-3 endorsement for degradation, that would be mediated by VCP (promotes ataxin-3 dissociation from E4B) [74]. As a consequence of an expanded polyQ tract in ataxin-3, the ataxin-3-VCP affinity increases, inhibiting the EXP ataxin-3 dissociation of the ternary complex thus delaying the EXP ataxin-3 proteasome degradation [74]. E4B is found in neurons of mice and *C. elegans*, suggesting a E4B role in human neurons and SCA3 [74]. Moreover, VCP could deliver substrates for ataxin-3, since RAD23 proteins only bind ataxin-3 when VCP is also bound [62]. Other VCP interacting proteins are gp78 and BRCA1, for example [76]. Furthermore, VCP performs neddylation and EXP ataxin-3 downregulates this process [77].

NEDD8 ubiquitin like modifier (NEDD8) is present in SCA3 inclusions [79]. NEDD8 is a ubiquitin-like protein (UBL) very similar to Ub and is capable of conjugation with p53 and cullin family members in a process named neddylation [79]. Also, NEDD8 is vital for the activity of SCF-like ubiquitin ligase complexes that are responsible for substrate degradation [79]. NEDD8 is present in nucleus and cytoplasm and authors observed that ataxin-3 interacts with NEDD8 through JD [79]. This was achieved by GST pull down assays using the following WT ataxin-3 fragments: only the JD, full-length ataxin-3 with UIM1 and UIM2 or only C-terminal tail, where only for the first two an interaction was reported [79]. But ataxin-3 seems not suffer neddylation, since the JD fragments have a size incompatible with this modification [79]. For ataxin-3 to accommodate NEDD8, JD rearrangement are needed, as it happens for Ub binding [79]. Also, it was observed that ataxin-3 has deneddylase activity with residue 14 being essential for it (similar to what happens with DUB activity) [79]. Therefore, ataxin-3 is capable of removing NEDD8 from substrates.

The UBL domain of RAD23 proteins (RAD23A and RAD23B) interacts with ubiquitin binding site 2 (present in JD) of ataxin-3 (both WT and EXP form) and prevents ataxin-3 proteasome degradation [36, 37]. RAD23 proteins are homologs of yeast RAD23 protein that plays a role in DNA repair and nucleotide excision repair [36]. It is composed by four domains: the UBL, responsible for nucleotide excision repair, XPC-binding domain, responsible for DNA repair and two ubiquitin associated (UBA) domains,

capable of interacting with ubiquitin and polyUb proteins [36, 80]. RAD23 proteins are involved in different biological process (such as proteasome degradation, proteolytic cleavage, and regulation of cell cycle), because it interacts with different interactors such as proteasome subunits, heat shock proteins and elongation factors, while RAD23B (one of the RAD23 proteins) interacts with VCP (that mediates substrates delivery from RAD23B to ataxin-3 for proteasome degradation [62]), BRCA1 fragments and vimentin [36, 80]. It was observed that UBL domain is important for RAD23 proteins proteasome interaction, promoting ubiquitinated proteins to degradation in proteasome [36, 78, 80]. RAD23A is capable of interacting with ataxin-3 and ubiquitin simultaneously, and does not impair ataxin-3 DUB activity but decrease this reaction, probably because of RAD23A and ataxin-3 competition for Ub proteins [78]. RAD23A prefers K48-linked Ub chains, and upon ataxin-3 DUB activity (that cleaves K63-linkage chains and form 48-linked Ub chains) K48-linkage Ub chains are available for RAD23A binding, endorsing substrates for proteasome degradation, for example [78]. Under cell stress (such as inhibition of proteasome, activity or heat shock stress) dynamic alteration between RAD23B and ataxin-3 interaction was observed, but only heat shock causes ataxin-3 localization to the nucleus [43]. RAD23A colocalizes with EXP ataxin-3 aggregates [36, 78]. Even though JD is necessary for interaction, C-terminal ataxin-3 fragments (composed by amino acids 249 to 341) with 130Q maintain the capability to recruit RAD23A for aggregates [36]. Impairment of EXP ataxin-3 DUB activity, probably caused by its inability to interact with VCP [78], blocks K48-linked chains formation and available RAD23A proteins won´t be capable to endorse proteasome misfolded proteins for degradation, causing toxic cell effects.

In sum, all the above mentioned proteins play a role in protein degradation mediated by ubiquitin proteasome system (UPS). Consequently, any alteration in ataxin-3 binding to them, induced by the polyQ tract expansion, negatively influence this pathway (abolishes protein degradation), allowing or enhancing SCA3 pathology.

3.2.5 Aggresomes formation:

Proteasome is the predominant mechanism for misfold protein degradation, however under an excess of misfolded proteins or proteasomal dysfunction perinuclear aggresomes are formed [81, 82]. Consequently, aggresomes are an alternative way of misfolding protein clearance. To do that chaperones, proteasome and autophagic components are recruited to them [24, 81]. Aggresomes formation is mediated by microtubules and dynein (a microtubule-associated motor, responsible for the transport

of proteins across microtubules), thus aggresomes are in the vicinity of the microtubule-organization centre (MTOC) [81]. It is proposed that histone deacetylase 6 (HDAC6) binds to polyUb proteins (marked for degradation) and dynein [81]. That way misfolded proteins could be translocated to aggresomes [81]. It was observed that WT ataxin-3 is important for aggresomes formation because interacts with dynein and HDAC6, in the initial steps of aggresomes formation [83]. Ataxin-3 DUB activity and UIM are essential for these ataxin-3 interactions since mutations in ataxin-3 catalytic site and in UIM1 and UIM2 abolish these interactions [83]. The HDCA6 and ataxin-3 interaction is mediated by ataxin-3 C-terminal tail (more specifically residues 319-344) [81]. Burnett and Pitman proposed that DUB ataxin-3 activity would stabilize dynein and HDAC6 proteins [83]. Therefore, conformational alteration, imposed by the polyQ tract expansion, could abolish EXP ataxin-3 activity that would impair protein misfolding proteins trafficking to aggresomes thus culminating in neurodegeneration.

Microtubules are polymers, composed by tubulin alpha (*TUBA1A*) and beta (*TUBB*, for example) subunits, responsible for cell support, intracellular trafficking (such as transport of misfolding proteins to aggresomes), cell division and other functions [82, 84]. Tubulin beta can be encoded by five genes, one of them being *TUBB* [84]. Tubulin can interact with microtubule-associated proteins (MAPs) and motor proteins (such as dynein) that allows the dynamic behaviour of microtubules [84]. It was shown that WT ataxin-3 is capable of interacting with tubulin alpha and beta, probably through ataxin-3 JD (since a construct containing only JD or full-length ataxin-3 binds to these subunits), along with MAP2 and β-actin [85]. Bonanomi *et al.* observed that WT ataxin-3 interacts with tubulin by two additional regions, named as tubulin binding regions (TBR) located before (TBR2, range from amino acids 244-291) and after (TBR3, range from amino acids 319-362) the polyQ tract [82]. The presence of the TBR3 is supported by the fact that ataxin-3 with UIM3 shown less affinity for tubulin interactions, probably due the absence or inactivation of TBR3 [82]. Weishäupl *et al.* observed a preference of tubulin beta interaction with shorter ataxin-3 version (lacking the UIM3) [28], supporting the inferences observed by Bonanomi and colleagues. Consequently, TBR3 seems not to be an essential region for tubulin binding. Additionally, the length of polyQ tract influences the binding affinity with TBR3 where ataxin-3 with 24Q show more affinity than ataxin-3 with 6Q [82]. Co-localization assays, performed by overexpression of murine ataxin-3 (that has higher homology with human ataxin-3 and, also interacts with tubulin subunits), to avoid aggregation of WT ataxin-3 version (that at higher concentrations promotes aggregation), shown that WT murine ataxin-3 colocalizes with tubulin subunits, while mutant murine ataxin-3 did not, probably due to their nuclear aggregate's formation

[85]. So, the inability of EXP ataxin-3 to interact with tubulin could have a role in aggresomes formation [82, 85].

In other human diseases, such as amyotrophic lateral sclerosis (ALS), aggresomes formation mediated by ataxin-3 has been shown to be an essential mechanism to prevent cytotoxicity of misfolded proteins [86]. This becomes a clue into how ataxin-3 mutation could affect the cell and could induce SCA3 [86]. In the ALS case, copper-zinc superoxide dismutase (SOD1) is mutated and is more prone to aggregate, inducing cytotoxicity in cells, but the presence of ataxin-3 (either WT or EXP forms) is capable of cleaving K63-linked SOD1 chains and allows aggresomes formation, hence protecting cells from cytotoxicity effects [86]. This ataxin-3 mediated mechanism seems to be independent of polyQ tract length [86], but with other misfolded proteins this may be different and SCA3 could then arise.

In sum, EXP ataxin-3 might prevent aggresomes formation leading to cytotoxic effects of misfolded proteins that ultimate could induce or enhance SCA3 pathology. But there are mechanisms to prevent EXP ataxin-3 cell toxicity, such as the case of p62. P62 interacts with poly-ubiquitinated proteins and LC3, and plays a role in autophagy-lysosome pathway, protein aggregation and aggresomes formation [61]. It was observed that p62 interacts only with EXP ataxin-3 inducing aggresomes formation [61]. Mutation of p62 in cells expressing EXP ataxin-3 increases cell death, while cells expressing WT ataxin-3 are not affected [61]. This reinforces the importance of p62 in the protection of cells under polyQ tract expansions [61].

3.2.6 Mitochondrial dysfunction:

Mitochondria participates in ATP production, production of ROS, apoptosis, and calcium homeostasis [87]. Consequently, mitochondrial dysfunction is a hallmark in some diseases such as the neurodegenerative disorders [87]. Mitochondrial alterations, such as the swollen and “bean shaped” types, were observed in *in vitro* SCA3 model [31]. It is possible that these alterations are characterized by a reduced mitochondrial DNA copy number and increased oxidative stress, that allows mitochondria-mediated cell death, since the radial swelling does not happen due to mitochondria fusion [31].

Both WT and EXP ataxin-3 were found in the mitochondria, and a few ataxin-3 mitochondria interactors have been identified [3], such as mitochondrial genome maintenance exonuclease 1 (MGME1), dynamic related protein-1 (DRP-1/DNM1L) and MARCH5/MITOL. In general, they are implicated in mitochondrial DNA repair and regulation of mitochondrial fission/fusion, that is associated with mitochondria

fragmentation, and thus, regulating cellular senescence and neuronal death [3, 88]. MARCH5/MITOL protein, an E3 mitochondria ligase associated with removal of SCA3 proteins, regulates DRP-1 [3], and thus, is critical for mitochondria quality control [87, 88]. Additionally, MARCH5 ubiquitinates mitofusin Mfn2 and therefore, plays a role in regulation of the endoplasmic reticulum-mitochondrial tethering [88].

Moreover, succinate dehydrogenase subunit B (SDHB), NDUFA4 mitochondrial complex associated (NDUFA4) and Cytochrome c oxidase assembly factor 7 (COA7) mitochondrial proteins show more interactions with EXP ataxin-3 [3]. Furthermore, NDUFA4 interacts preferentially with shorter ataxin-3 isoforms (without the UIM3) [28]. These three proteins are constituents of mitochondrial respiratory chain [3, 89, 90]. ATP production is obtained by oxidative phosphorylation that happens because of respiratory chain that is composed by complex I, II, III, IV and the ATP synthetase (complex V) [90].

Succinate dehydrogenase (also known as mitochondrial respiratory complex II) has four subunits SDHA, SDHB, SDHC and SDHD [89]. Complex II dysfunction impairs electron transfer to oxygen that increase the ROS formation directing for a redox cell imbalance [89].

NDUFA4, previously identified as a complex I subunit, is a complex IV subunit [90, 91]. Complex IV (also known as cythorome c oxidase) forms water (H_2O) by transferring electrons from cythorome c to oxygen (O_2) [90]. NDUFA4 is expressed in higher amounts in brain and liver [90, 91]. NDUFA4 is present in these supercomplexes, where it interacts with complex I and IV, which led to the hypothesis that NDUFA4 could be an assembly factor of supercomplexes [90]. Supercomplexes, known as respirasome, are composed by complexes I, III and IV and constitutively express ubiquinone and cythorome c, but does not use the electron carriers, consequently, reduce the ROS production [90]. Additionally, NDUFA4 protects neurons from death, since its overexpression increases Blc-2 expression and decrease cythorome c expression. Both are mitochondrial apoptosis markers, leading to a decrease in apoptosis [91]. NDUFA4 depletion has the opposite effect [91]. Moreover, NDUFA4 enhance growth factors (nerve growth factor (NGF), brain derived neurotrophic factor (BDNF) and brain fibroblast growth factor (bFGF)) expression that induces neuron growth [91].

In sum, ataxin-3 expansion interactions with these proteins might lead to mitochondrial dysfunction that culminate in cell apoptosis, particularly in neurons, contributing for SCA3.

3.2.7 Calcium signalling

Calcium (Ca^{2+}) is an ion essential in neurons, because is involved in neurite outgrowth, neurotransmitter release and synaptic plasticity [31]. This ion is stored in ER [31]. A type 1 inositol 1,4,5-triphosphate receptor (IP3R1), an intracellular Ca^{2+} channel present in ER, interacts with EXP ataxin-3, activating Ca^{2+} release [24, 31]. As result, EXP ataxin-3 induces Ca^{2+} ER release to cytosol. The excess of free Ca^{2+} in cell induces cell death through oxidative stress, mitochondrial permeabilization, disruption of cytoskeleton and calpain activation [4, 24]. Calpains are proteolytic enzymes induced by higher intracellular Ca^{2+} levels in the cell [50]. Therefore, calpains cleave mutant ataxin-3 [50], allowing C-terminal fragments formation contributing to SCA3 pathology.

4. Ataxin-3 pathogenesis

The polyQ tract expansion is associated with a gain of ataxin-3 function [31], since for some interactors (such as ATM, CBP, P300, PCAF, MMP-2, CHIP, VCP, SDHB, NDUFA4, and Ca^{2+} signalling) the expanded polyQ enhances ataxin-3 binding, thus causing dysfunction. Nevertheless, function loss is also associated with ataxin-3 expansion. For example, the impairment of expanded ataxin-3 inactivates PNKP [52, 53] or FOXO4 dependent *SOD2* expression [56].

Although protein aggregates are a SCA3 hallmark [1], the pathology happens at different cellular levels and at different cell sites. In the nucleus DNA repair and transcription dysfunctions are seen, as illustrated by EXP ataxin-3 inhibition of PNKP activity [52, 53] and the deubiquitination of MDC1 [48], and the stimulation of cell apoptosis mediated by ATM pathway activation by EXP ataxin-3 in response to DNA damage [53]. This is a very strong alteration imposed by polyQ tract expansion that should be decisive for the SCA3 appearance. At transcription level, depending on the gene, there is a stimulation of transcription (case of MMP-2) or an inhibition of transcription (case of *SOD2* gene) mediated by EXP ataxin-3 [56, 57]. These alterations could affect the transcription of essential enzymes that maintain the homeostasis in cell. Consequently, it could be a further step in SCA3 appearance. The second site is in cytosol, where different protein degradation machinery (proteasome, autophagy and aggresomes) is altered. For example, EXP ataxin-3 induces Parkin autophagic degradation [72] and inhibits ERAD pathway [67]. Also, EXP ataxin-3 interaction with VCP prolongs the time necessary for expanded ataxin-3 degradation [74]. Additionally, EXP ataxin-3 seems not to interact with tubulin proteins, that are essential for aggresomes formation [82, 85]. Consequently, all these induced expanded ataxin-3

alterations must be important for SCA3 progress, since they alter the protective misfolding degradation mechanism. Moreover, an excess of Ca^{2+}-signalling induce EXP ataxin-3 cleavage by calpains [50], and C-terminal fragments are involved in aggregates formation [41]. Despite all the negative cell alterations imposed by EXP ataxin-3 the presence of p62 protein protects cells from death by inducing aggresomes formation [61]. Although, this wouldn´t be sufficient to avoid SCA3.

However, EXP ataxin-3 phosphorylation at residues S12 and S256 could prevent EXP ataxin-3 aggregates [29, 40], while other protein modifications would affect the EXP ataxin-3 activity or facilitate EXP ataxin-3 localization (nucleus or cytosol) [39, 41, 42, 46] that probably would enhance SCA3 pathology. In sum, EXP ataxin-3 inducing pathology is a dynamic process that involves several components and modifications that trough time disrupt cell homeostasis and induce cell death, particularly neurodegeneration, culminating in SCA3 phenotype.

In conclusion, alterations imposed by EXP ataxin-3 in the DNA repair mechanism and in the misfolding protein degradation mechanism seems be the most important for inducing SCA3. This will further investigate in here.

5. Ataxin-3 related proteins evolution

Ataxin-3 belongs to MJD family, one of the six groups of DUBs [92]. In mammals, MJD family is composed by ataxin-3, ataxin-3-like (ataxin-3L), Josephin-1 (JosD1) and Josephin-2 (JosD2) [92, 93]. The four proteins have in common the catalytic domain [92, 93]. Because of that, it was hypothesized that these proteins would be capable of performing a compensatory mechanism in animals lacking *ATXN3* [25]. Due to the fact that these animals are relatively normal [25]. JosD1 and JosD2 are the smallest proteins, containing not much more than the catalytic domain [92, 93]. Since ataxin-3L shows conservation at JD level as well as at C-terminal tail (UIMs and the polyQ tract), it is the most related protein with ataxin-3, sharing 85% identity between the two [92]. JosD2 catalytic domain differs from ataxin-3 in the last triad residue, instead of an asparagine has an aspartate [92]. So, JosD2 catalytic triad is composed by residues C24, H25 and D140 [92]. Probably JosD1 would has a catalytic triad like JosD2, since it shares 51% identity with and this value drops below 30% when compared to ataxin-3 for both proteins [92].

These four MDJ family proteins represent distinct lineages of MJD family proteins [94]. The ataxin-3/ataxin-3-like lineage and the josephin 1/josephin 2 lineage [94] are old

and are present even in basal animals. Ataxin-3L results from a gene duplication that happened in Catarrhini lineage (belongs to Cercopithecidae, Hominidae, and Hylobidae primate orders) at 40 million years ago [92, 94, 95]. While josephin 1 and josephin 2 duplication happens in the vertebrate's base [94]. Almost all animals show at least one protein of each lineage [93, 94]. Nevertheless, in insects such as *Drosophila* there is only one Josephin-like protein (JOSL-DROME) that according to phylogenetic analyses belongs to the josephin 1/josephin 2 lineage [94].

6. *Drosophila melanogaster* as a SCA3 model

Drosophila melanogaster (also known as fruit fly) is an animal model for diverse human diseases, in particular for neurological disorders [96]. Indeed, *Homo sapiens* and *D. melanogaster* share about 75% of human genes associated with diseases [97]. The fact that in *Drosophila* there is a large number of transgenic flies, where gene transcription could be mediated by UAS/GAL4 system, allowing to target expression of the desired transgene in a tissue such as the fly eye, (not essential for flies' survival and with a phenotype easy to study [98]), together with rapidly reproduction rate, makes *Drosophila* an animal model for human pathologies [96]. Moreover, for polyQ disorder, flies expressing human disease proteins in the eye are capable of mimicking some features of human diseases [96, 99, 100]. For instance, flies expressing expanded ataxin-3 generate adult-onset degeneration, since it induces progressive blindness from the birth and over time [100]. Also, nuclear inclusions were observed [100] with ubiquitin in them [99]. Large-scale genetic screens use these hallmarks to identify modifiers of polyQ disorders, as those for SCA3 [101, 102]. Vobfeldt and collaborators identified 502 ataxin-3 modifiers, by using trangenic flies with a polyQ transgene expressing ataxin-3 (with 78Q) and RNA interference (RNAi) flies for those genes that present human orthologs [101]. Many of the modifiers are enriched in proteasomal components, protein turnover/quality control, nuclear import/export or mRNA transport/editing/translation, suggesting that these pathways can lead to SCA3 [101]. Billen *et al.* (2007) identified 18 modifiers by performing genetic screens using transgenic flies and P-element insertion lines (each carrying a transposon engineered to direct expression of the downstream gene in the presence of the yeast GAL4 protein) [99]. Zhang *et al.* [102] identified 126 candidates by performing genetic screens using *Drosophila* cell lines obtained from transgenic fly lines that express enhanced-GFP-tagged mutant Huntingtin fragments to identify modifiers of polyQ aggregation). It should be noted that only DnaJ-1 (DnaJ protein homolog 1 (Gene ID 38643); details in **Table 1**, in Results section) is common in

these studies, suggesting that candidates for toxicity and aggregation can be different [101].

It should be noted that *Drosophila* as SCA3 model presents disadvantages due to the fact that human and flies have some biological differences (such as their brain structures, physiology, genome coding proteins and others). Furthermore, the information provided using this model species results from disease protein overexpression (where biological findings need to be validated), and *Drosophila* lost the ataxin gene lineage [94, 96]. Since the *Drosophila* gene (JOSL-DROME) that shows similarity with *ATXN3* belongs to josephin 1/josephin 2 lineage, it is not known if the human orthologs of the fly interactors interact differently with ataxin-3, as here addressed. If the interactions are found to be similar, *Drosophila* is an ideal system to address the importance of the JD (the only region in common with the ataxin-3) in SCA3.

7. The *in-silico* approach

This approach allows the prediction of interactions between two query proteins through several steps [2]. To summarize, four steps are needed to obtain the predicted PPI [2]. The first is the obtention of the 3D structure of the protein (performed by I-TASSER), followed by the obtention of active (interact directly) and passive (interact indirectly) residues in CPORT [2]. The third step is the proper prediction of the docking of the two proteins (performed in HADDOCK) and the analysis of the results using PDBePISA [2].

This methodology presents three main disadvantages: first proteins larger than 1500 amino acids, cannot be used due to I-TASSER restrictions [2], second is the impossibility of analysing protein complex interactions [2], and third is the fact that, when a polyQ protein is used the number of interactions at the polyQ tract need to be less than six to have an accurate model prediction [2]. Due to the fact that I-TASSER uses the data of PDB library to identify template proteins that are similar to the query protein (in a process call threading), and the more accurate templates are used to start the protein prediction [103], because the polyQ tract has a reduced number of residues, the template threading identification will be less confident [2]. Nevertheless, using this methodology and the WT and EXP ataxin 1 (ATXN1) forms, Rocha *et al.* inferred that the EXP ATXN1 shows larger number of interactors than the WT form, that the number of interface residues is larger in the EXP ATXN1, as observed in *in vitro* experiments performed using yeast two-hybrid screens and DNA microarrays for high-throughput quantitative

PPI detection [2]. Therefore, this *in-silico* methodology seems to be a good tool to infer differences regarding the consequences of ataxin-3 polyQ tract expansion.

Objectives

In this study, through an *in-silico* approach we aim to:

- ♣ determine the overlap of the ataxin-3/JOSL-DROME interactors network
- ♣ identify the regions of interaction between the wild-type ataxin-3 and JOSL-DROME for the common *D. melanogaster* and *H. sapiens* interactors.
- ♣ assess the generality of the ataxin-3 interfacing regions, by analysing the proteins that do not present a *Drosophila* paralogous gene.
- ♣ identify the interactors that behave differently in the presence of an expanded polyQ, and thus identify those proteins that contribute for SCA3 pathology.
- ♣ address if *D. melanogaster* is a good model to study PPI in SCA3 pathology.
- ♣ address the putative role of JosD1 in SCA3 pathology.

Material and Methods

Ataxin-3, JosD1, and JOSL-DROME interactors database

Ataxin-3 full-length with three UIMs (Gene ID 4287; UniProt ID P54252), JosD1 (Gene ID 9929; UniProt ID Q15040), and JOSL-DROME (Gene ID 31560, UniProt ID Q9W422) interactors were obtained from EvoPPI (http://evoppi.i3s.up.pt/dashboard) [104], using the same species search, level 1 interactions (proteins that interact directly with query protein), and all databases available in this web platform. Using EvoPPI, for ataxin-3 and JOSL-DROME, we also identified level 2 interactors (proteins that interact with level 1 proteins), by searching all level 1 interactors. In addition, ataxin-3 interactors identified by Kristensen and colleagues [3] were used in our analysis. Moreover, fly genes reported as ataxin-3 modifiers (521 genes of Vobfeldt *et al.* [101], 126 of Zhang *et al.* [102] and 18 genes of Bilen and Bonini [99]) were also considered in this study.

To identify the human paralogs genes of the fly genes we used DIOPT (DRSC Integrative Ortholog Prediction Tool, https://www.flyrnai.org/diopt) [105] without filters and with all the available algorithms. In case of Vobfeldt *et al.* data the results were manually verified by looking at the transformant ID provided by Vienna Drosophila Resource Centre (VDRC). When multiple fly gene were retrieved, the Ensembl [106] orthologues database was used to select those to be studied. To identify the common genes between human ataxin-3 interactome and fly paralogs, Venn diagrams (http://bioinformatics.psb.ugent.be/webtools/Venn/) were used.

In-silico interaction predictions

The interaction regions between ataxin-3 and the selected interactors were predicted using the *in-silico* methodology, described by Rocha *et al.* [2]. The protein sequence of the selected 150 human and 45 fly proteins was retrieved from UniProt (https://www.uniprot.org/). We also used two ataxin-3 sequences, the WT with 14Q and the EXP form with 50Q. The 3D structure of these proteins was predicted using by I-TASSER [103, 107, 108]. Due to I-TASSER size limitation (https://zhanglab.ccmb.med.umich.edu/I-TASSER/) [103, 107, 108], six proteins longer than 1500 residues were excluded from the analyses (CREB binding protein (CBP, Gene ID 1387, UniProt ID Q92793), E1A binding protein p300 (P300, Gene ID 2033, UniProt ID Q09472), Mitogen-activated protein kinase kinase kinase 1 (Gene ID 4214, UniProt ID Q13233), Mediator of DNA damage checkpoint 1 (MDC1, Gene ID 9656, UniProt ID Q14676) and Nuclear receptor corepressor 1 (Gene ID 9611, UniProt ID O75376) and

the fly proteins Histone acetyltransferase (gene ID 43856, UniProt ID M9MS40)). To select the best prediction model for the WT and EXP ataxin-3 forms, the five models obtained for each form were compared using the TM-align tool (with TM-score normalized by WT ataxin-3 size), to infer the folding similarity between two query proteins [109]. It should be noted that TM-score range from zero to 1, with a score of 0,5 representing the same fold between the query proteins (whereas 1 represents a full match between them), while a TM-score below than 0,2 represents random similarity between the two proteins [109]. We selected model 1 and model 5, respectively, since they present the highest *C*-score.

For each protein, the interacting residues (actives and passives) were predicted using CPORT (http://milou.science.uu.nl/services/CPORT/) [110]. For two proteins (Ubiquitination factor E4B (Gene ID 10277, UniProt ID O95155) and Remodeling and spacing factor 1 (Gene ID 51773, UniProt ID Q96T23) this software was unable to produce results.

Docking predictions for WT and EXP ataxin-3, as well as JOSL-DROME, with the human and/or *Drosophila* interactors were obtained using HADDOCK (http://milou.science.uu.nl/services/HADDOCK2.2/) [111]. Only the clusters with the *z*-score ≤ 0 were used [111]. The docking predictions failed for three proteins (two human proteins – E3 ubiquitin-protein ligase Itchy homolog (Gene ID 83737, UniProt ID Q96J02) and Calmodulin regulated spectrin associated protein family member 3 (Gene ID 57662, UniProt ID Q9P1Y5), and one fly protein MPN domain-containing protein CG4751 (Gene ID 34551, UniProt ID Q9VKJ1).) The identification of the best cluster and the best structure representation of the interaction, according to the number of interface residues, was performed using PDBePISA (https://www.ebi.ac.uk/pdbe/pisa/) [112] docker image pisa_xml_extract, provided at pegi3S https://pegi3s.github.io/dockerfiles/, under utilities. The highest number of interactions in the reference protein (structure 1) represent the best docking structure. In case of tie, we use the highest number of interactions in the interactor (structure 2). If the tie still holds, we use the solvent-accessible area (Å) interface to choose the best cluster.

The same methodology was used to infer interacting residues of JosD1 and those proteins that interact with ataxin-3.

The protein structure was visualized with Pymol docker image accessible at https://pegi3s.github.io/dockerfiles/.

Additional, WT ataxin-3 motives were accessed using ELMs (Eukaryotic Linear Motif) tool [113].

PPI analysis

The PPI interactions obtained for WT and EXP ataxin-3, JosD1 and JOSL-DROME proteins were manually curated by the following criteria: a protein region was considered to be a major point of interaction if it shows half or more of possible interactions (therefore report 50% or more on interactions), needs to be a minimum of 2 consecutive highly interacting residues and terminates when exist two consecutive residues with 10% or less of interactions. Middle point of interactions were obtained using the same criteria, but their residues report between 11% and 49% of interactions. Note that polyQ tract region was excluded from this analysis, due to *in-silico* methodology limitations to predict PPI in this region [2].

The greater affinity was represented by a higher level of interface residues for the specific PPI, as was described by Rocha and co-workers [2].

Protein alignment

The alignment between WT ataxin-3 and JOSL-DROME protein sequences, as well as the WT and EXP ataxin-3 Josephin domain and JosD1 protein was performed in MEGA X [114] using Muscle alignment algorithm.

Interactor's characterization

The interactors (*Homo* and *Drosophila*) were characterized for enriched molecular function using the Gene Ontology enrichment analysis power by PANTHER [115-117]. For human interactors the tissue expression was, first, accessed in Expression Atlas (https://www.ebi.ac.uk/gxa/home) under the GTEx (Genotype-Tissue Expression) project. Then, the interactors tissue expression was rechecked using BrainSpan: Atlas of the Developing Human Brain (http://www.brainspan.org/rnaseq/search/index.html) [118] in order to obtain a detailed brain region expression through the human life (range from 8 years to 40 years). For *Drosophila* interactors, tissue expression was reified in FlyAtlas 2: the *Drosophila* expression atlas (http://flyatlas.gla.ac.uk/FlyAtlas2/index.html) [119].

Statistical analysis

Statistical analyses were performed using SPSS, version 27.0 [120] using non-parametric tests. If the data is paired we used a Sign test, while if the two samples are

independent, a Mann-Whitney U test was used. The statistics were considered significative if $p<0,05$. Note that, in the comparisons performed, all the protein region was considered with exception of polyQ tract.

Results

1. *Drosophila* as a good SCA3 model

To get insight into SCA3 disease, transgenic *Drosophila* has been used, with both WT and EXP human ataxin-3. Expression of the WT ataxin-3, in levels similar to the EXP form, caused no detectable anatomical or behavioural phenotype. In contrast, EXP ataxin-3 expressed in the *Drosophila* eye, causes progressive adult-onset neural degeneration and accumulation in ubiquitinated inclusions, like observed in humans [99, 100]. Furthermore, *Drosophila* WT ataxin-3 protects against neurodegeneration, that occurs through ubiquitin pathways associated with protein quality control [100]. Despite of the insights obtained using ataxin-3 transgenic flies, in *Drosophila* there is only one JOSL-DROME protein, that belongs to a different lineage than that of human ataxin-3 [94]. The two proteins share the catalytic domain only, the Josephin domain [92, 93], and therefore it is possible that the two interaction networks are different. Furthermore, for the paralogous interactors, it is possible that the regions of interaction observed in human PPI show only a partial overlap with those observed in flies. To address these questions, in this section, we compare the ataxin-3 and JOSL-DROME interactors network, and characterize the interaction regions in human and fly for paralogous interactors.

1.1 Overlap between human and fly ataxin-3/JOSL-DROME networks

The collection of human ataxin-3 interactors, obtained from EvoPPI, retrieved 99 proteins (**Supplementary Table 1**). This network is incomplete since 51 proteins (out of 53) related with protein quality control and mitochondrial biology, reported in Kristensen *et al.* [3], used to identify enriched EXP ataxin-3 interactions, are not included. Therefore, in total we have considered 150 ataxin-3 interactors (**Supplementary Table 1**). In *Drosophila* only four proteins are reported in EvoPPI as JOSL-DROME interactors (**Supplementary Table 2**). Although, all present human orthologous genes, these are not described as ataxin-3 interactors. To complete the fly network, we used the 521, 126, and 18 modifier genes reported in mutant ataxin-3 flies reported by Vobfeldt *et al.* [101] (**Supplementary Table 3**), Zhang *et al.* [102] (**Supplementary Table 4**) and Billen and Bonini [99] (**Supplementary Table 5**), respectively. Using DIOPT and Ensembl (Material and Methods) we obtained the 3090, 692, and 172 paralogous human genes, respectively (**Supplementary Table 3-5**). By comparing the two lists, we identified 56 interactors in common (**Table 1**). Therefore, we could find only 37% of the human ataxin-3 network present in *Drosophila*. To further address overlap of the two networks, we also used the interactors level 2 (i. e. the interactors of the proteins interacting with ataxin-3),

since 144 (out of 4909) human interactors level 2 are also ataxin-3 interactors (**Supplementary Table 6**). This is because, none of the 4909 interactors are, however reported in the fly network here considered.

The interactors present in human and flies are, according to Gene Ontology enrichment analysis power by PANTHER [115-117], involved in the ubiquitination pathways, transport, binding, transcription activity, protein cleavage, phosphorylation, among others (**Table 1**). As expected all these proteins are expressed in human brain, according to BrainSpan [118]. *Drosophila* interactors are also expressed in brain and eye, except for seven proteins (Serpin 28Db (Gene ID 326261), GEO10511p1 (Gene ID 41285), Pickpocket 14 (Gene ID 33887), Maltase A3 (Gene ID 35826), Uncharacterized protein, isoform B (Gene ID 33318), AT19485p (Gene ID 31978), and Regulatory particle triple-A ATPase 6-related (Gene ID 43635)) that present very low or inexistent expression.

Table 1: Ataxin-3 interactors presenting *Drosophila* paralogs gene reported as a modifier of polyQ toxicity in mutant flies. The description of the ataxin-3 interactor, as well as the methodology used to identify these interactors is presented.

Ataxin-3 interactor (Gene synonyms; GeneID)	Paralogous *Drosophila* gene	Interactor description and ataxin-3 interaction	Methodology
Heat shock 70 kDa protein 1A (HSPA1A; 3303+)	39557 (CG6603)	Heat shock 70 kDa protein 1A/HSPA1A belongs to heat shock 70 kDa family that is responsible for protein folding, transport, regulation of apoptosis, cell proliferation and inactivation [71]. HSPA1A endogenous protein immunoprecipitated with WT and EXP ataxin-3 [3].	affinity chromatography
Heat shock cognate 71 kDa protein (HSPA8; 3312+)	39557 (CG6603)	Heat shock cognate 71 kDa protein interacts with WT and EXP ataxin-3 [3, 28].	affinity chromatography
Heat shock 70 kDa protein 4L (HSPA4L, 22824+)	39557 (CG6603)	Heat shock 70 kDa protein 4L interacts with WT and EXP ataxin-3 [3, 28].	affinity chromatography
Heat shock 70 kDa protein 4 (HSPA4; 3308+)	39557 (CG6603)	Heat shock 70 kDa protein 4 interacts with ataxin-3 [28].	affinity chromatography
Heat shock protein 105 kDa (HSPH1; 10808+)	39557 (CG6603)	Heat shock protein 105 kDa/HSPH1 is a member of heat shock protein 110 family, involved in protein fold [121]. HSPH1 interacts with WT and EXP ataxin-3 [3]. Authors observed that HSPH1 interacts with ataxin-3 [28].	affinity chromatography
Heat shock protein HSP 90-alpha (HSP90AA1; 3320+)	38389 (CG1242)	Hsp90 family is involved in apoptosis, cell cycle control, cell viability, protein degradation and signalling events [122]. Authors observed that HSP90AA1 interacts with ataxin-3 [28].	affinity chromatography
Serpin H1 (SERPINH1; 871#)	49803 (CG10913); 326261 (CG12318/CG33121)	SERPINH1 gene belongs to serpin (serine protease inhibitor) superfamily, that encodes Hsp47, that is an ER- molecular chaperone that specifically binds to procollagens, allowing it correct fold [3, 123]. SERPINH1 was shown to be enriched in EXP ataxin-3 samples comparing with WT ataxin-3 samples [3].	Two hybrid pooling; two hybrid array; affinity chromatography

Table 1 - Continuation

DnaJ homolog subfamily B member 2 (DNAJB2; 3300+)	38643 (CG10578); 31978 (CG2887)	UIMs of DnaJ homolog subfamily B member 2/HSJ1 protect ubiquitinated ataxin-3 from proteasomal degradation [70]. HSJ1 regulates the ATPase activity of Hsp70. To prevents ataxin-3 degradation HSJ1 UIM domains binds to ubiquitinated chains on ataxin-3 [70]. Mutations of HPD to QPN removes the ability of HSJ1a to reduce WT ataxin-3. Mutation in UIMs HSJ1 decrease the levels of WT ataxin-3 [70].	affinity chromatography
4F2 cell-surface antigen heavy chain (SLC3A2; 6520+)	35826 (CG8695)	4F2 cell-surface antigen heavy chain/SLC3A2 is important for Cystine activity, a major antioxidant import. A lower expression of cysthationine-γ-lyase (CSE), that is transform in cystine, is possible mediated by aggregation with EXP ataxin-3. Overexpression of CSE in EXP ataxin-3 reverse abnormalities [124]. Other works report SLC3A2 interaction with ataxin-3 [28, 125].	coimmunoprecipitation; affinity chromatography
CREB binding protein (CREBBP; 1387$)	43856 (CG15319)	CBP, a transcriptional coactivator with histone acetyltransferase (HAT) activity, is recruited for promoters by interacting with DNA-binding transcriptional factors such as CREB. EXP ataxin-3 binds more effectively to CBP than the WT ataxin-3, at the C-terminal region [55]. Authors shown that WT huntingtin forms a transcription-coupled DNA repair (TCR) complex with ataxin-3, HAP-1, CREB binding protein, PNKP and other proteins [126]. TCR complex monitors and edits DNA strand beaks/damage during transcriptional elongation, preserving genome integrity and neuronal survival [126]. Mutant huntingtin impairs the normal TCR complex function and leads to pro-apoptotic signal that ultimate amplified the neurodegeneration in brain [126]. EXP ataxin-3 C-terminal tail is capable of binding to CBP in nucleus as well in cytosol, but WT C-terminal ataxin-3 tail didn´t interact with CBP in cytosol [127].	Pull down; imaging technique; affinity chromatography
Histone acetyltransferase p300 (EP300; 2033$)	43856 (CG15319)	P300 is a transcriptional coactivator with histone acetyltransferase activity [55]. EXP ataxin-3 binds more effectively to P300 than WT ataxin-3, at the C-terminal region [55].	Pull down; affinity chromatography
Histone deacetylase 3 (HDAC3; 8841$)	38565 (CG7471)	HDAC3 promotes histone deacetylation and inhibits transcription. HDAC3 binds to WT and EXP ataxin-3 [57]. Particularly WT ataxin-3 recruit this protein, along with others, for the chromatin regions of metalloproteinase-2 (MMP-2) gene promoter, inhibiting MMP-2 transcription [57]. N-terminal ataxin-3 region inhibits histone 4 acetylation [55]. It was found that ataxin-3 is a positive regulator of HDAC3, that enhances the stabilization of HDAC3 protein [58].	Pull down; affinity chromatography
Histone deacetylase 6 (HDAC6; 10013$)	38565 (CG7471)	HDAC6 is a microtubule-associated deacetylase involved in regulation of microtubule acetylation and chemotactic cell motility [81]. HDAC6 binds to C-terminal region of WT ataxin-3, between residues 319-344 [82].	pull down
Caspase 1 (CASP1; 834&)	39173 (CG8091)	Caspases are involved in apoptotic cell death, signal transduction pathways and dismantling of proteins. Caspase 1 is involved in ataxin-3 cleavage. Mutant aspartates 241, 244 and 248 inhibits ataxin-3 cleavage. In contrast mutations in aspartates 145, 171, 208, 217, 225 and 228 allows ataxin-3 cleave [50]. Caspase 1 interacts with ataxin-3 [128]. Ataxin-3 is cleaved by caspase 1, with low efficiency, and forms a fragment with 14 kDa (in case of WT ataxin-3) or 18 kDa (in case of EXP ataxin-3) [129].	two hybrid pooling approach; two hybrid array; *in vitro*
Caspase 3 (CASP3; 836&)	43514 (CG7788)	Caspase 3 as ataxin-3 interactor has been reported using two approaches [128].	two hybrid pooling approach; two hybrid array
DnaJ homolog subfamily A member 1 (DNAJA1; 3301+)	41646 (CG8863); 31978 (CG2887); 34984 (CG4599); 38643 (CG10578); 36797 (CG8448)	DNAJA proteins belongs to chaperone DNAJ family responsible for regulation the HSP70 chaperone though ATP hydrolysis [130]. DNAJA1 interacts with WT and EXP ataxin-3 [3]. This interaction has been also reported by Weishaupl *et al.* [28].	affinity chromatography
ADP/ATP translocase 2 (SLC25A5; 292+)	32007 (CG16944)	ADP/ATP translocase 2/SLC25A5 exchange the ATP produced in mitochondria, by ATP synthase, with ADP produced in cytosol by several dependent energetic reactions. This protein also maintains the mitochondria membrane potential and prevents apoptosis [131]. SLC25A5 interacts with WT and EXP ataxin-3 [3]. SLC25A5 interacts predominantly with shorter isoforms of ataxin-3, caused by a stop SPN in exon 10 that culminates in a premature stop codon that create two versions of this short isoform (ataxin-3aL and ataxin-3aS) [28].	affinity chromatography
ADP/ATP translocase 3 (SLC25A6; 293+)	32007 (CG16944)	See SLC25A5. ADP/ATP translocase 3/SLC25A6 interacts with WT and EXP ataxin-3 [3]. SLC25A6 interacts predominantly with shorter isoforms of ataxin-3, caused by a stop SPN in exon 10 that culminates in a premature stop codon that create two versions of this short isoform (ataxin-3aL and ataxin-3aS) [28].	affinity chromatography
ATP-dependent RNA helicase DDX39A (DDX39A; 10212#)	33781 (CG7269)	DExD-box helicase 39A belongs to DEAD-box RNA helicase, more precise the DDX39, and is important in RNA nuclear export. DDX39 is responsible for cell growth and tumorigenesis [132]. DDX39A interacts with WT and EXP ataxin-3 [3].	affinity chromatography

Table 1 - Continuation

Monocarboxylate transporter 1 (SLC16A1; 6566+)	38062 (CG6905)	Solute carrier family 16 member 1/MCT1 transports monocarboxylic acids, such as pyruvate, lactate, and ketone bodies, that are necessary, in particularly the lactate, to maintain the neurons in glucose absence [133]. MCT1 interacts with WT and EXP ataxin-3 samples [3].	affinity chromatography
Sideroflexin 4 (SFXN4; 119559+)	40552 (CG11739)	Sideroflexin 4/SFXN4 is essential for Fe-S cluster biogenesis, mitochondrial respiration and the function of Fe-S cluster proteins involved in cellular iron homeostasis and the synthesis of haemoglobin in erythroid cells [134]. SFXN4 interacts with WT and EXP ataxin-3 [3].	affinity chromatography
Dynamin-1-like protein (DNM1L; 10059+)	31581 (CG3869)	Dynamin-1-like protein/DNM1L is a GTPase capable of outer mitochondrial membrane cleavage, and therefore, is necessary for mitochondrial fission and peroxisome division [135]. DNM1L interacts with WT and EXP ataxin-3 [3].	affinity chromatography
2-amino-3-ketobutyrate coenzyme A ligase (GCAT; 23464$)	36448 (CG4016)	2-amino-3-ketobutyrate coenzyme A ligase/GCAT, along with L-threonine dehydrogenase, converts L-threonine in glycine and acetyl-CoA [136]. GCAT interacts with WT and EXP ataxin-3 [3].	affinity chromatography
Acid-sensing ion channel 1 (ASIC1; 41+)	33887 (CG9501)	ASIC are proton-gated sodium channels sensitive to amiloride [137]. It was shown that ataxin-3 interacts with ASIC1 [138].	two hybrid
BAG family molecular chaperone regulator 3 (BAG3; 9531#)	38151 (CG9153); 37851 (CG4005)	BAG cochaperone 3 (also, known as Bcl2-associated athanogene 3) is involved in apoptosis, development, cytoskeleton organization, autophagy, and stress. The C-terminal BAG domain allows interaction with Hsp70 [139]. It was observed that BAG3 interacts with ataxin-3 [139].	affinity chromatography
E3 ubiquitin-protein ligase SMURF1 (SMURF1; 57154*)	38151 (CG9153); 37851 (CG4005)	SMURF1 is a HECT domain ubiquitin ligase, involved in cell differentiation, cell shape and polarity, cell adhesion and migration, autophagy, embryonic pattern formation, morphogenesis and others [140]. I*n vitro* it is reported that ataxin-3 is ubiquitinated by SMURF1 [141].	enzymatic study
E3 ubiquitin-protein ligase Itchy homolog (ITCH; 83737*)	38151 (CG9153); 37851 (CG4005)	ITCH is a member of E3 ubiquitin ligase, a member of Nedd4 family of HECT domain E3 ligases, that recruits misfold proteins and EXP polyQ proteins in the cytoplasmic compartment [142]. It was shown an interaction between ataxin-3 and ITCH and that an overexpression of ITCH decrease EXP ataxin-3. Thus, it has been proposed that ITCH could have a cytoprotection role against misfold protein stress [142].	affinity chromatography
Ubiquitin carboxyl-terminal hydrolase 21 (USP21; 27005&)	33132 (CG14619)	USP21 belongs to DUB family and is able of deubiquitinating histone H2A and receptor-interacting protein 1. Interacts with protein kinases and phosphatases, suggesting a role in cell signalling [143]. UPS21 show the capability of deubiquitinate ubiquitinated ataxin-3 [144].	enzymatic study
Ubiquitin-like modifier-activating enzyme 1 (UBA1; 7317*)	35998 (CG1782); 41532 (CG12276); 44496 (CG7528)	UBA1 has functions in the UPS, selective autophagy, cell cycle progression, DNA damage repair, transcription, translation, vesicle transport, and apoptosis [145]. UBA1 acts as an important modifier of polyQ protein toxicity, and thus inhibition of UBA1 led to an increase in levels of mutant protein aggregates [146]. Authors observed that UBA1 interacts with ataxin-3 [28].	affinity chromatography
Polynucleotide kinase 3´-phosphatase (PNKP; 11284«)	40994 (CG9601)	PNKP has a function in DNA strand break repair that is composed by 3 domains: forkhead-associated (FHA) domain (residues 1-119), phosphatase (P) domain (residues 120-339) and Kinase (K) domain (residues 340-521) [52]. EXP ataxin-3 inactivates PNKP and possible traps it in polyQ aggregates, thus decreasing PNKP activity [53]. It has been showed that WT huntingtin forms a transcription-coupled DNA repair (TCR) complex with ataxin-3, HAP-1, CREB binding protein, PNKP and other proteins [126]. TCR complex monitors and edits DNA strand breaks/damage during transcriptional elongation, preserving genome integrity and neuronal survival [126]. Mutant huntingtin impairs the normal TCR complex function and leads to pro-apoptotic signal that ultimate amplified the neurodegeneration in brain [126]. WT and EXP ataxin-3 interact with PNKP full-length or kinase domain of PNKP [52]. The phosphatase domain only interacts with WT ataxin-3 and FHA domain didn´t interact with ataxin-3 [52]. WT ataxin-3 stimulates PNKP 3´-phosphatase activity, while EXP ataxin-3 inhibits PNKP activity leading to accumulation of DNA strand breaks [52]. Heterozygote SCA3 individual (that have a normal ataxin-3 allele and one mutant ataxin-3 allele) show an inhibition of PNKP activity (mediated by EXP ataxin-3) that is slow and progressive (could explain why SCA3 pathology is related with age), that leads to DNA strand breaks accumulation that activate intrinsic signalling that leads to dysregulation gene expression that impairs neuronal function, leading to neurodegeneration and ataxia [52].	protein complementation assay; imaging technique; affinity chromatography
Calnexin (CANX; 821#)	44643 (CG11958)	Calnexin is a glycoprotein involved in protein fold [147]. Calnexin interacts with ataxin-3 [28, 125].	coimmunoprecipitation; affinity chromatography
Alpha-parvin (PARVA; 55742#)	3772007 (CG33931)	Alpha-parvin is part of the integrin-linked kinase signalling complex and plays a role in cell adhesion, motility, and survival. Alpha-parvin interacts of ataxin-3 [128].	two hybrid pooling approach; two hybrid array

Table 1 - Continuation

TNF receptor associated factor 6 (TRAF6; 7189*)	31746 (CG10961)	TRAF6 has a role in cross talk between the ubiquitin proteasomal system (UPS) and autophagy [148]. Authors shown that TRAF6-polyUbiquitin (Lys63) was deubiquitinated by ataxin-3, proposing an interaction between the two proteins [149].	enzymatic study
TOMM20-like protein 1 (TOMM20L; 387990+)	41285 (CG14690)	TOMM20-like protein 1/TOMM20L was identified as mitochondrial membrane protein responsible for recognizing and translocating preproteins into the mitochondria [150]. TOMM20L interacts with ataxin-3 [151, 152].	coimmunoprecipitation; affinity chromatography technology
Calpain 2 (CAPN2; 824&)	39165 (CG8107)	Calpain are cysteine protease that are activated when the levels of calcium increase in cell. Ataxin-3 cleave for calpain 2 is around the residues 60, 200 and 260 [50]. Calpains were capable of cleavage ataxin-3 in four calpain residues: H187, D208, S256 and T277 [51]. Calpain 2 interacts with ataxin-3 even though ataxin-3 lack 88 residues (coded by exon 8 and 9), that where hypothesize to be the calpain 2 cleavage sites LERVLE (comprehends the residues 210) and MQGSSRNI (that comprehends the residue 260) [153].	enzymatic study
Sorcin (SRI; 6717#)	39165 (CG8107)	Sorcin binds directly to calcium or can interact with proteins and calcium channels. High levels of sorcin expression increases the levels of calcium in endoplasmic reticulum, prevents endoplasmic stress, unfolded protein response and increases the escape from apoptosis [154]. Author found that sorcin interacts with ataxin-3 [125].	affinity chromatography
Tubulin beta chain (TUBB; 203068§)	37238 (CG9277)	TUBB is one of the five tubulin beta genes, that is important for cell support, intracellular trafficking, and cell division [84]. WT ataxin-3 binds to alpha and beta tubulin at the JD, but not the EXP ataxin-3 [85]. TUBB can interact with ataxin-3 through tree regions: the JD, before the polyQ tract (range from 244-291) and after the polyQ tract (range from residues 319-362) [82]. Also found that polyQ tract length influence the affinity for tubulin interaction, where 6Q shown less affinity than 24Q of WT ataxin-3 [82]. It was observed that TUBB interacts predominantly with shorter isoforms of ataxin-3, caused by a stop SPN in exon 10 (ataxin-3aL and ataxin-3aS) [28].	pull down; affinity chromatography
Tubulin alpha-1A chain (TUBA1A; 7846§)	37238 (CG9277)	TUBA1A is involved in cell support, intracellular trafficking, and cell division [84]. WT ataxin-3 binds to alpha and beta tubulin at the JD, but not EXP ataxin-3 form [85]. It is found that tubulin alpha could interact with ataxin-3 through tree regions: the JD, before the polyQ tract (range from 244-291) and after the polyQ tract (range from residues 319-362) [82]. Also found that polyQ tract length influence the affinity for tubulin interaction, where 6Q shown less affinity than 24Q WT ataxin-3 [82].	pull down
Casein kinase 2 beta (CSNK2B; 1460«)	32132 (CG15224)	CK2 regulates transcription, translation, stability, signal transduction, cell survival, circadian rhythm and embryonic development [155]. CK2 could phosphorylate ataxin-3 at S29 inducing ataxin-3 nuclear localization [156]. Additionally, CK2 is capable of phosphorylated WT and EXP ataxin-3 at S236, S340 and S352, that increase the protein nuclear localization, while CK2 phosphorylation at residues 256, 260 and 261 as a minimal influence [157].	enzymatic study; affinity chromatography
NF-kappa-B inhibitor alpha (NFKBIA; 4792«)	39375 (CG17153)	NFKB is a transcription factor that regulates inflammatory, cell adhesion, differentiation, oxidative stress, and apoptosis [158]. NFKBIA interacts with ataxin-3 [125].	affinity chromatography
26S proteasome regulatory subunit 8 (PSMC5; 5705*)	43635 (CG2241)	26S proteasome degrade unfold protein but needs ubiquitin and ATP [62]. Proteasome 26S regulatory subunit 8 (ATPase 5)/p45 degrades both WT and EXP ataxin-3 [159]. The interaction between the two proteins happens by the ataxin-3 N-terminal region [159]. If exist 20ng or more of p45 EXP ataxin-3 degradation is higher than WT ataxin-3 [159]. P45 interacts with ataxin-3 [28].	affinity chromatography
26S proteasome non-ATPase regulatory subunit 4 (PSMD4; 5710*)	40388 (CG7619)	See PSMC5. PSMD4 interacts with ataxin-3 [28].	affinity chromatography
26S proteasome non-ATPase regulatory subunit 7 (PSMD7; 5713*)	34551 (CG4751)	WT and EXP ataxin-3 are capable to interact with the proteasome, at residues 1-150 [62]. PSMD7 interacts with ataxin-3 [28, 128].	two hybrid pooling approach; two hybrid array; pull down; *in vitro*; co-sedimentation through density gradient; affinity chromatography
Small ubiquitin like modifier 1 (SUMO1; 7341*)	33981 (CG4494)	SUMO proteins are ubiquitin-like proteins and share 20% of identity with ubiquitin [47]. Ubiquitination of ataxin-3 was not significantly different in WT and EXP ataxin-3 [47]. SUMOylation of ataxin-3 promotes faster association with VCP, probably by orient ataxin-3 in optimal position for VCP binding or VCP can has a second binding site that can be used in ataxin-3 SUMOylation [49]. It was observed that SUMO1 interacts with N-terminal ataxin-3 region [138] and mutation at SIM (SUMO-interacting motif) unable SUMO1 interaction with ataxin-3 [48].	two hybrid; pull down
Lysine acetyltransferase 2B (KAT2B; 8850$)	43460 (CG14514);43856 (CG15319)	Lysine acetyltransferase 2B/PCAF is a transcriptional coactivator with histone acetyltransferase (HAT) activity. EXP ataxin-3 binds more effectively to PCAF than WT ataxin-3, at the C-terminal region [55].	pull down; affinity chromatography
Ubiquilin 1 (UBQLN1; 29979*)	31564 (CG11700)	Ubiquilin 1 is involved in degradation of misfold proteins [160]. UBQLN1 is an ataxin-3 interactor [128].	two hybrid pooling approach; two hybrid array; pull down; *in vitro*; imaging technique

Table 1 - Continuation

Ubiquitin conjugating enzyme E2 L3 (UBE2L3; 7332*)	37035 (CG5788); 33226 (CG3018); 33318 (CG5440)	Ubiquitin conjugating enzyme E2 L3 interacts with Parkin cysteine active-site and plays an important role in ubiquitin-ester formation [161]. Ataxin-3 stabilizes, in cells, the interaction between parkin and E2 enzyme [162]. This decreases the efficiency of E2 recharging by the E1 [162].	pull down
Ubiquitin conjugating enzyme E2 G1 (UBE2G1; 7326*)	33226 (CG3018); 33318 (CG5440); 37035 (CG5788)	WT ataxin-3 was shown to interact with Ubc7 (E2 enzyme used in this study) protein (but only after use a cross-linking agent DTSSP for detected the complex ataxin-3-Ubc7 sensitive to DTT), while mutant ataxin-3 (at C14) do not, showing that the active site cysteine is necessary for interaction [162]. Ataxin-3 stabilizes the interaction between Ubc7 and parkin, therefore E2 didn´t dissociated from parkin and decrease the efficiency of E2 recharging by E1 [162]. Ataxin-3 is capable of deubiquitinated parkin independently of E2 used (UBEG1 were one E2 used for this assay) [72].	pull down
Ubiquitin conjugating enzyme E2 S (UBE2S; 27338*)	37035 (CG5788); 33226 (CG3018); 33318 (CG5440)	E2 enzymes normally determine the type of chain linkage [149].	enzymatic study
Ubiquitin conjugating enzyme E2 N (UBE2N; 7334*)	37035 (CG5788);33226 (CG3018);33318 (CG5440)	Combination between Ubiquitin conjugating enzyme E2 N/UBC13 and TRAF6 mediates K63-polyubiquitin linkages on substrates that can be recognized by autophagy receptors like p62 [148].	
Polyubiquitin-B (UBB; 7314*)	31564 (CG11700)	The addition of ubiquitin to substrates is an important post-translate modification that endorse the substrate recognition for proteasome degradation and membrane trafficking [163]. UBB interacts with WT and EXP ataxin-3 [3]. Ubiquitin localizes in neuronal inclusions, along with ataxin-3 and VCP [76].	*in vitro*; fluorescence microscopy; affinity chromatography
Polyubiquitin-C (UBC; 7316*)	31564 (CG11700)	The addition of ubiquitin to substrates is an important post-translate modification that endorse the substrate recognition for proteasome degradation or membrane trafficking. Ubiquitin can be single attached to lysine residues of substrates or can form polyubiquitin chains, through ubiquitin ligases [163]. UBC interacts with ataxin-3 [28]. Ubiquitin enhances ataxin-3 activity through expose the catalytic site or by altering the conformation of catalytic site, that increase it ability of cleave isopeptide bonds [69]. EXP ataxin-3 C-terminal tail recruits more Ub forms to insoluble aggregates than WT ataxin-3 C-terminal tail, where UIM is responsible of this recruitment [77]. It was shown that Ub could interact with the two ubiquitin binding sites of ataxin-3 JD, and that site 1 is essential for cleavage, while site 2 could interact with other Ub-like domains of other proteins or modulate the characteristics of site 1 [164].	x-ray crystallography; pull down; imaging technique; anti tag coimmunoprecipitation; anti bait coimmunoprecipitation; affinity chromatography
RAD23 homolog B, nucleotide excision repair (RAD23B; 5887*)	31564 (CG11700)	RAD23B is important in nucleotide excision repair, in cases where DNA damage is induced by UV [80]. RAD23B interact in N-terminal region of ataxin-3 [36]. Amino acid 87 located in the second ataxin-3 ubiquitin binding site is essential for this interaction [37]. RAD23B interacts with ataxin-3 [165], and this interaction is dynamic, and is altered according to the stress type (inhibition of proteasome, activating the unfold protein response or proteotoxic stress) [43]. Only the proteatoxic stress causes the accumulation of ataxin-3 in the nucleus [43].	two hybrid array; two hybrid; pull down; *in vivo*; affinity chromatography
RAD23 homolog A, nucleotide excision repair (RAD23A; 5886*)	31564 (CG11700)	RAD23A is important in nucleotide excision repair, in cases where DNA damage is induced by UV [80]. RAD23A interacts with ataxin-3 [28, 128, 165]. Wang *et al.* reported that RAD23A interacts in N-terminal region of WT and EXP ataxin-3 by the UBL (ubiquitin-like) domain present in RAD23 protein [36]. C-terminal region (249-341 aa) of EXP ataxin-3 is responsible for recruit RAD23A to aggregates [36]. N-terminal region of mutant ataxin-3 is colocalized in inclusions formed by C-terminal region of EXP ataxin-3. Wang and collaborators propose that the N-terminal region may interact with C-terminal region of ataxin-3, and thus full-length ataxin-3 may be necessary for interaction [36]. Other authors also shown that ataxin-3 interacts with RAD23A [78, 166, 167].	validated two hybrid; two hybrid pooling approach; two hybrid array; pull down; *in vivo*; affinity chromatography
NEDD8 ubiquitin like modifier (NEDD8; 4738*)	31564 (CG11700)	NEDD8 activates SCF-like ubiquitin ligase complexes, responsible of substrate degradation [79]. WT ataxin-3 interacts with NEDD8 at the JD [79]. Furthermore, the *C.elegans* (atx-3) ataxin-3 homolog is capable of binding to human NEDD8, that suggests conservation at the JD, although amino acid identity is only 36% [79].	two hybrid; pull down
Dynamin 2 (DNM2; 1785§)	31581 (CG3869)	Dynamin 2/DNM2 is involved with endocytosis, formation of new vesicles by Golgi, regulation of microtubules and actin cytoskeleton dynamics [168]. DNM2 is a ataxin-3 interactor [128]. [169].	two hybrid pooling approach; two hybrid

* ubiquitination pathways, + transport, #binding, $transcription activity, &protein cleavage, «phosphorylation and §tubulin related

1.2 Regions of interaction of the paralogs ataxin-3 and JOSL-DROME interactors

The 56 human ataxin-3 interactors that show paralogs in flies, that could interact with ataxin-3 in mutant flies, correspond to 5 fly interactors, since 15 fly proteins are paralogs of different human proteins (**Table 1**; see **Supplementary Table 7** for fly

UniProt codes). This is due to the two round of whole genome duplication in vertebrates [170]. For the fly interactors we first address if they are able to interact with JOSL-DROME, using the *in-silico* methodology described in Rocha *et al.* [2] (see Material and Methods for details). Because of the protein size (only interactors smaller than 1500 amino acids can be analysed, and protein Histone acetyltransferase (Gene ID 43856) is larger), as well as in HADDOCK inferences (for protein MPN domain-containing protein CG4751 (Gene ID 34551) interacting residues with JOSL-DROME could not be predicted), only 43 fly interactors were considered. The interaction regions of the all fly interactors with JOSL-DROME are represented in **Figure 2**. They are located in four main regions located in the JD. The JD is highly conserved between JOSL-DROME and ataxin-3 (**Figure 3**), and thus, this result sugests that the JD region maybe also be, important for ataxin-3 PPIs.

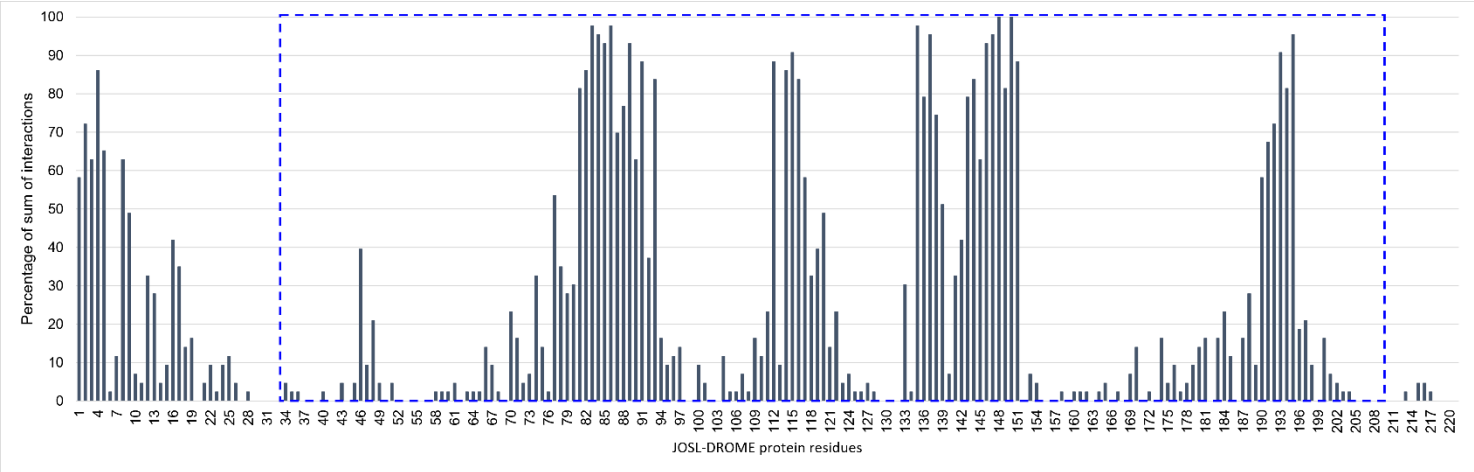

Figure 2: Predicted interaction sites at JOSL-DROME for 43 fly interactors. The Josephin domain (JD) is marked with a blue square.

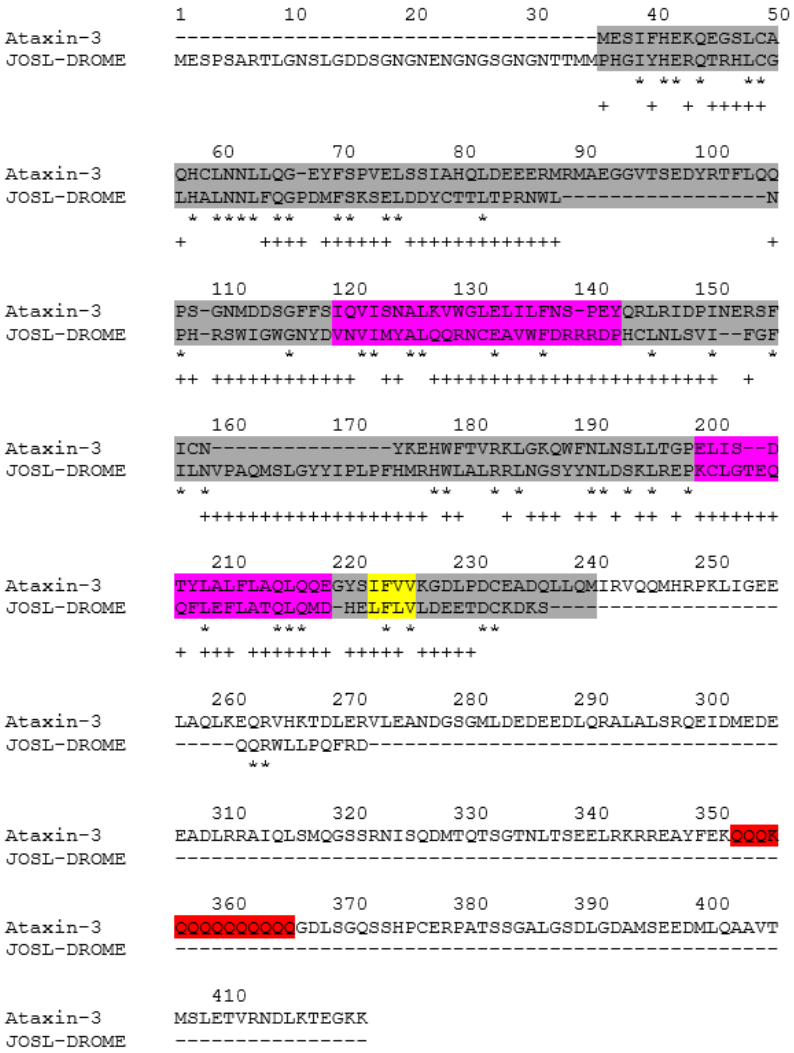

Figure 3: Alignment between WT ataxin-3 and JOSL-DROME. * represents conserved residues. Colours represent: grey the JD, magenta the two nuclear export signals, yellow the [SUMO]-interacting motif, in red the polyQ tract. + represents the JOSL-DROME predicted interacting residues.

To address the role of the JD in ataxin-3 protein interactions, we have predicted the interface residues of human and orthologous fly interactors with ataxin-3. Once again, due to the *in-silico* methodology limitations (see Material and Methods), only 52 humans (CBP (Gene ID 1387) and P300 (Gene ID 2033), E3 ubiquitin-protein ligase Itchy homolog (Gene ID 83737) and 26S proteasome non-ATPase regulatory subunit 7 (Gene ID 5713) were excluded because they are larger than 1500 residues or HADDOCK is unable to predict interactions, respectively) could be analysed.

Moreover, we also excluded four JOSL-DROME (Calnexin 99A, isoform A (Gene ID 44643), DnaJ-like-2, isoform A (Gene ID 41646), Tetratricopeptide repeat protein 2 (Gene ID 34984), and Mrj, isoform E (Gene ID 36797)) and four ataxin-3 (RAD23B

(Gene ID 5887), DnaJ homolog subfamily A member 1 (Gene ID 3301), Heat shock 70 kDa protein 4L (Gene ID 22824), and Calnexin (Gene ID 821)) interactors that show more than six or more interactions, at ataxin-3 polyQ tract, since this interaction degree at this region is associated with low confident prediction of PPI [2]. As shown in **Figure 4**, there is an overlap of ataxin-3 regions used in the protein interactions with human and the paralogous fly proteins (N=39; *p*=0,522; Sign test). Although a large number of interacting residues are located at the JD, the region in the vicinity of the JD, as well as the C-terminal region, also show a large number of interfacing residues. A similar interaction pattern is observed when considering the ataxin-3 interactors and the human paralogous of the fly interactors (**Figure 5**). The obervation that fly paralogous genes behave as human interactors with WT ataxin-3, sugests that *Drosophila* is an excelant SCA3 model species. Nevertheless, the gererality of the observed ataxin-3 interactions need to be address using interactors that do not present a paralogous fly gene.

Furthermore, similarities need also to be addess with EXP ataxin-3.

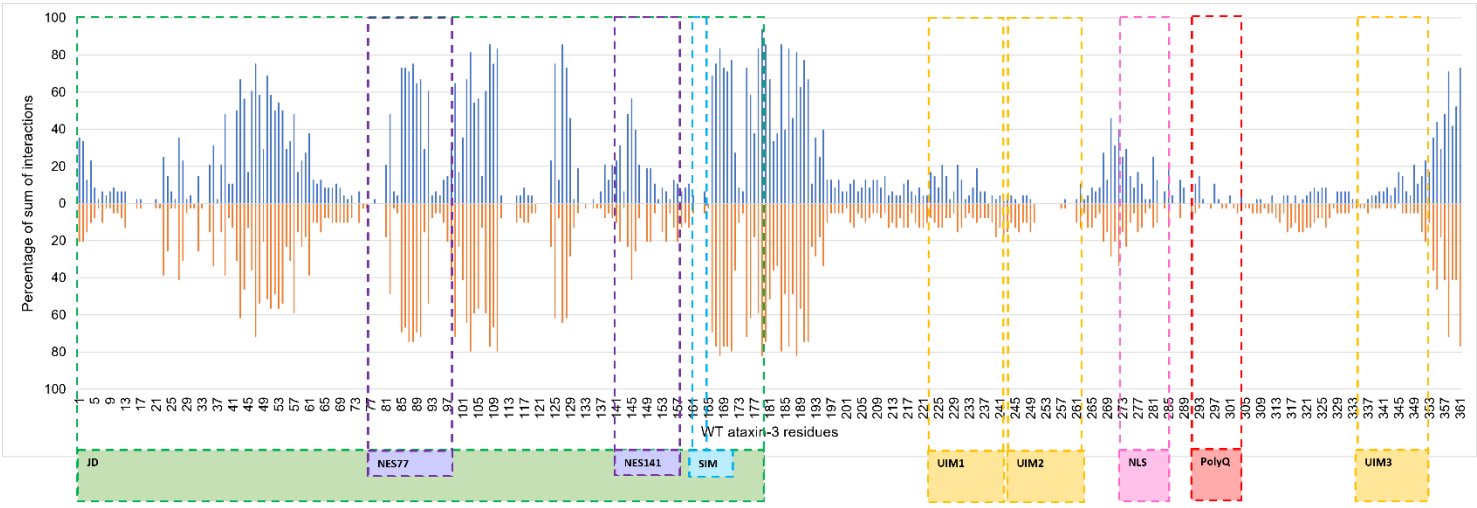

Figure 4: Predicted WT ataxin-3 interactions with *Homo sapiens* interactors (blue) and their respective *D. melanogaster* paralogs (orange). The Josephin domain (JD, 1-180 aa) is marked in green, nuclear export signal (NES) 77 (77-99 aa) and 141 (141-158 aa) are marked in purple, [SUMO]-interacting motive (SIM, 162-165 aa), ubiquitin interacting motif (UIM) 1 (224-243 aa), 2 (244-263 aa) and 3 (335-354 aa), nuclear localization signal (NLS, 273-286 aa) and the polyQ tract (292-305 aa, 14Q).

1.3 The JD is a major interaction region in ataxin-3 PPIs

To address if the ataxin-3 interacting regions observed in **Figure 4** are general to other ataxin-3 interactors that do not present a fly paralogous gene, we performed the *in-silico* approach [2] using 94 ataxin-3 interactors (**Table 2;** see **Supplementary Table 1** for UniProt codes). Of this set, only 88 proteins were successfully analysed mitogen-activated protein kinase kinase kinase 1 (Gene ID 4214), mediator of DNA damage

checkpoint protein 1 (Gene ID 9656) and nuclear receptor corepressor 1 (Gene ID 9611) were excluded because are larger than 1500 amino acids; ubiquitin conjugation factor E4B (Gene ID 10277) and Remodeling and spacing factor 1 (Gene ID 51773) were removed due to CPORT failing; and calmodulin-regulated spectrin-associated protein 3 (Gene ID 57662) was removed since no docking was obtained. Moreover, six proteins (Amyloid beta precursor protein (Gene ID 351), BCL2 like 1 (Gene ID 598), Proline/serine-rich coiled-coil protein 1 (Gene ID 84722), Rho GTPase-activating protein 19 (Gene ID 84986), Ribosomal protein S6 kinase alpha-1 (Gene ID 6195), and Dihydroxyacetone phosphate acyltransferase (Gene ID 8443)) were excluded from analyses since they present six or more interactions at ataxin-3 polyQ tract, that is associated with low predicted confidence [2]. The interacting pattern between human proteins without a fly paralog (**Figure 5**), agrees well with that observed in **Figure 4**. No statistical significant differences (p=0,657; Mann-Whitney U test) were observed using the two data sets (N=82 and N=48, respectively). In the JD there are six regions where interactions are enriched (**Figure 5**). The region between the JD and the polyQ seems to be also relevant for binding with WT ataxin-3.

The presence of interacting regions in the JD does not imply that all proteins show interacting residues in all these regions. As mentioned in the introduction most proteins interact with ataxin-3 in the JD region. Indeed, when all (N= 130 (48 plus 82)) ataxin-3 interactors are considered, 89% interact mostly at JD region (**Figure 5**). For the 14 proteins that show a different pattern (BAG3 (Gene ID 9531), PARVA (Gene ID 55742), HSP90AA1 (Gene ID 3320), PCAF (Gene ID 8850), DNM2 (Gene ID 1785), CDKN1A (Gene ID 1026), VCP (Gene ID 7415), SPRTN (Gene ID 83932), EWSR1 (Gene ID 2130), Praja1 (Gene ID 64219), SLC27A4 (Gene ID 10999), HSDL2 (Gene ID 84263), MARCH5 (Gene ID 54708), and MCU (Gene ID 90550)) VCP and PCAF are described as interacting with ataxin-3 outside of the JD (**Table 2** and **Table 1**). The observation that interactions are established mostly in six specific ataxin-3 JD regions, as here shown, could not be, however, inferred from the literature. Furthermore, here we report that all interactors, show interacting residues in the region after the JD and before the polyQ with WT ataxin-3.

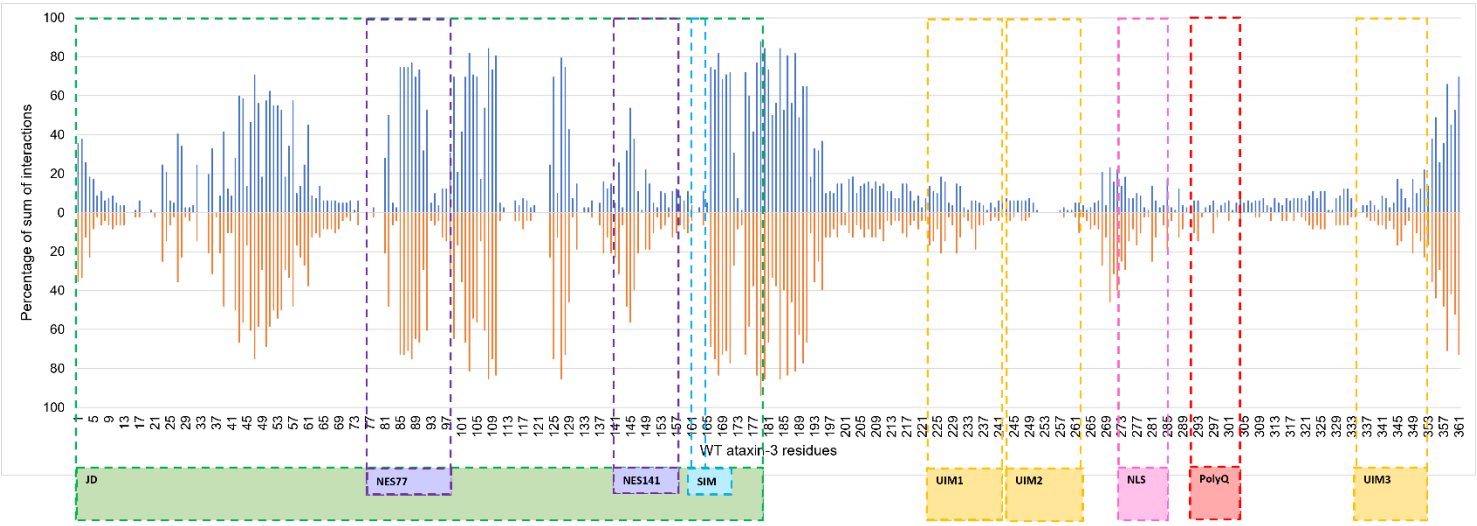

Figure 5: Predicted WT ataxin-3 interactions not presenting a fly paralogs (blue) versus the interactors presenting a paralogous fly gene (orange). The JD (1-180 aa) is marked in green, nuclear export signals (NES) 77 (77-99 aa) and 141 (141-158 aa) are marked in purple, [SUMO]-interacting motive (SIM, 162-165 aa), ubiquitin interacting motifs (UIM) 1 (224-243 aa), 2 (244-263 aa) and 3 (335-354 aa), nuclear localization signal (NLS, 273-286 aa) and the polyQ tract (292-305 aa, 14Q).

Table 2: The 94 ataxin-3 interactors, from EvoPPI and Kristensen *et al*.[3], not presenting *Drosophila* paralogs, reported as ataxin-3 fly modifiers. A short description of the ataxin-3 interactors, as well as the methodology used to identify these interactors is presented.

Ataxin-3 interactor description (Gene synonyms; GeneID)	Interactor description in the context of ataxin-3 interaction	Used technique
DNA-dependent metalloprotease SPRTN (SPRTN; 83932*)	SprT-like N-terminal domain is involved in impairs DNA damage upon replication stress [171]. It is a DNA damage-targeting VCP [171].	affinity chromatography
Ubiquitin carboxyl-terminal hydrolase 13 (USP13; 8975*)	Ubiquitin specific peptidase 13 is a deubiquitinating enzyme possible involved in the deubiquitination of histones [172]. Also, may have a role in ERAD pathway [172]. UPS13 is an interactor of ataxin-3 [128].	two hybrid pooling approach; two hybrid array; anti tag coimmunoprecipitation; affinity chromatography
Sequestosome 1 (SQSTM1; 8878*)	Sequestosome 1/p62 interacts with poly-ubiquitinated proteins and LC3 (microtubule-associated protein 1 light chain 3) [61]. Therefore, p62 plays a role in autophagy-lysosome pathway, protein aggregation and aggresomes formation [61]. P62 interacts with EXP ataxin-3 but not WT ataxin-3 and regulates the aggresomes formation in a microtubule dependent manner [61].	pull down; affinity chromatography
Ubiquitin thioesterase OTUB2 (OTUB2; 78990*)	Ubiquitin thioesterase OTUB2 is a protease with deubiquitinating activity [173]. It seems be involved in the choice of DNA repair pathways and in the turnover of TRAF3/6 [173]. This protein is highly expressed in the brain [173]. OTUB2 interacts with the DUB site of ataxin-3 [172].	two hybrid pooling approach; two hybrid array; anti tag coimmunoprecipitation; affinity chromatography
E3 ubiquitin-protein ligase parkin (PRKN; 5071*)	Parkin binds to WT and EXP ataxin-3 by UIMs (with UBL domain) or by JD (by IBR-RING2) [72]. Mutation in UIM (S to alanine) impairs parkin binding, S236, S256 and S347 are important for these interaction [45]. Also interaction through UIMs is weakly, suggesting that parkin binds to ataxin-3 through multi- or polyvalent ligand binding mode, where different UIM could recognize a single site of parkin but only one will bind [45]. EXP ataxin-3 reduces parkin levels in HEK293 cells and inhibition of autophagy pathway annuls this effect [72] So, it has been proposed that removing parkin contributes for SCA3 pathology [72]. Ataxin-3 stabilizes the interaction between parkin and E2 enzyme [162]. This decreases the efficiency of E2 recharging by the E1 [162]. Phosphorylation of UBL modulates the ubiquitin-editing function of ataxin-3, through decrease parkin affinity to UIM (necessary for ataxin-3 deubiquitinating activity with parkin) [65]. Parkin interacts with several ataxin-3 isoforms [28].	x-ray crystallography; pull down; nuclear magnetic resonance; enzymatic study; affinity chromatography
E3 ubiquitin-protein ligase synoviolin (SYVN1; 84447*)	E3 ubiquitin-protein ligase synoviolin/HRD1 is a membrane-bound E3 ubiquitin ligase that is involved in ERAD pathway [66]. HRD1 interacts with ataxin-3 [73].	affinity chromatography

Table 2 - Continuation

Vasolin containing protein (VCP; 7415*)	VCP, is an ATPase protein involved in ERAD pathway [75]. VCP transfers ubiquitinated proteins from ER to cytosol [75]. VCP binds to ataxin-3 by polyQ region, but more strongly with EXP ataxin-3 [74]. Boeddrich *et al.* Identified the VBM (VCP-binding motif) motif in residues 281-289 of ataxin-3 [76]. Also, Matsumoto *et al*. reported that VCP binds to E4B (ubiquitin chain assembly factor, an ortholog of yeast Ufd2, capable of adding polyubiquitin chains in some substrates, particularly to ataxin-3) and ataxin-3 simultaneously [74]. Thus, VCP would mediate delivery of ataxin-3 to proteasome [74]. EXP ataxin-3 binds strongly to VCP and inhibits it release from VCP-E4B, delaying it degradation by proteasome [28, 74]. It was shown that VCP ataxin-3 interaction is a dynamic interaction, that is altered according to the stress type (inhibition of proteasome, activating the unfold protein response or proteotoxic stress) [174]. Only the proteatoxic stress causes the accumulation of ataxin-3 in the nucleus [174].	x-ray crystallography; unspecified method; two hybrid pooling approach; two hybrid array; pull down; proximity labelling ; peptide array; *in vitro*; fluorescence microscopy; cosedimentation through density gradient; competition binding; biochemical; anti tag coimmunoprecipitation; anti bait coimmunoprecipitation; affinity chromatography
E3 ubiquitin-protein ligase AMFR (AMFR; 267*)	E3 ubiquitin-protein ligase AMFR/gp78 has a RING finger-type ubiquitin ligase activity site located on ER surface toward to cytoplasmic site [67]. Therefore, it has a role in ERAD pathway [67]. The degradation of WT and EXP ataxin-3 is dependent of gp78 level, where higher level leads to a higher degradation level [67]. N-terminal (1-340) of gp78 is the cause of her interactions with EXP ataxin-3 [67]. Cells expressing EXP ataxin-3 increase the levels of Bip (an ER stress marker protein) and gp78. Therefore, EXP ataxin-3 causes ER stress that culminates the higher levels of gp78 [67].	imaging technique; affinity chromatography
Ubiquitin conjugation factor E4B (UBE4B; 10277*)	E4 enzymes are necessary for assembly polyubiquitin chains in some substrates [74]. The U-box domain is essential for polyubiquitination mediated by U-box proteins [74]. E4B is abundant the neurons of mice and *C.elegans*, suggesting a role of E4B in clearance of damage proteins in nervous system [74]. E4B has four residues (RRRR) in N-terminal region (start at residue 10) that are important for E4B interaction with VCP [76]. E4B interacts with ataxin-3, and this interaction is mediated by VCP, since when it is present the interaction E4B-ataxin-3 increase [74]. Co-expression of recombinant E4B decrease the levels of WT and EXP ataxin-3 in HEK293T cells, and the mRNA levels of ataxin-3 are not affected [74]. Mutant E4B, lacking the U-box domain was co-expressed with EXP ataxin-3, and a delay degradation was observed [74]. Also, was shown that E4B is a limiting factor for ataxin-3 degradation [74].	pull down; competition binding
E3 ubiquitin-protein ligase CHIP (STUB1; 10273*)	E3 ubiquitin-protein ligase CHIP is a E3 (ubiquitin ligase) enzyme that interacts with chaperones and mediates ubiquitination and degradation of misfold proteins [64, 68]. CHIP interacts with WT and EXP ataxin-3 [3]. But interacts more with EXP ataxin-3 [3, 64, 68]. Without HSP70, CHIP can ubiquitinate ataxin-3 *in vitro* but with a low efficiency [70]. Silencing of CHIP gene in HEK293T cells increases the amount of ataxin-3, suggesting that CHIP down-regulate ataxin-3 levels [70]. It has been proposed that CHIP-ataxin-3 interaction is a form of up-regulating ataxin-3 DUB activity, since ataxin-3 is ubiquitinated by CHIP during the ubiquitination cycles of model substrates, that facilitates Ub chain editing when Ub is conjugated in proteins [69]. Moreover, CHIP promotes the ubiquitination of residue K117 on both ataxin-3 forms that enhances DUB catalytic activity [46].	pull down; enzymatic study; affinity chromatography
E3 ubiquitin-protein ligase rififylin (RFFL; 117584*)	E3 ubiquitin-protein ligase rififylin/CARP2 belongs to CARPs family of apoptosis inhibitors particularly targeting death effector domain-containing caspases for degradation (caspases 8 and 10) [175]. CARP2 shows the capacity to ubiquitinate ataxin-3 [144].	enzymatic study
Cyclin dependent kinase inhibitor 1 (CDKN1A; 1026*)	Cyclin dependent kinase inhibitor 1A is involved in DNA repair, transcription regulation and apoptosis [176]. This is mediated by capability of cyclin dependent kinase inhibitor 1A inhibited cyclin-dependent kinase activity such as CDK1 and CDK2 [176]. Ataxin-3 interacts with CDKN1A [169].	two hybrid
Protein PML (PML; 5371*)	PML is a major component of the PML nuclear body, a protein-based sub-nuclear structure associated with the nuclear matrix [177]. Within PML nuclear bodies, PML protein is immobile, indicating that it may play a structural role [177]. PML is a major component of PML nuclear bodies and are present in all nuclear inclusions (NI) caused by EXP ataxin-3 [177]. Co-immunoprecipitation assays reveal that PML precipitate with WT and EXP ataxin-3 [177].	affinity chromatography
Glycogen synthase kinase 3 beta (GSK3B; 2932*)	Glycogen synthase kinase 3 beta is serine/threonine kinase widely expressed in mammal's tissues, where is involved in several biological process [40]. This isoform is the most abundant in central nervous system with neuronal specificity [40]. Both WT and EXP ataxin-3 are phosphorylated by GSK3β [40]. Although there are 5 potential sites for GSK3β phosphorylation in ataxin-3, S256 is the only one were change to alanine impairs phosphorylation using WT ataxin-3 mutant (S256A) [40]. EXP ataxin-3 mutated at S256, put an alanine (A) instead of a serine (S), revel aggregation of ataxin-3, but phosphorylation at S256 (not mutated) did not show aggregation, so it is possible that phosphorylation at S256 may play a critical role in EXP ataxin-3 aggregation process [40]. The S256 phosphorylation inhibits ataxin-3 aggregation [156]. Authors report interaction between ataxin-3 and GSK3β [169].	two hybrid; pull down; enzymatic study; affinity chromatography
Cellular tumor antigen p53 (TP53; 7157*)	Cellular tumor antigen p53/p53 is important for control cancer-suppressive and age-promoting functions, so regulation of p53 allows normal cellular functions [178]. Co-immunoprecipitation assays (provided from extracts of 293T cells, expressing ataxin-3, treat or not with H_2O_2) revels that p53 interacts with ataxin-3 *in vitro* and *in vivo* [178]. N-terminal region of WT ataxin-3, (range from 1 to 223 amino acid) were enough for promote interaction with p53 [178]. UIMs facilitate the binding to ubiquitinated p53 [178]. Full-length ataxin-3 were capable of deubiquitinated ubiquitinated p53 [178]. GST pull down assays with EXP ataxin-3 shows a strong interaction with native and ubiquitinated p53 than WT ataxin-3 [178]. EXP ataxin-3 stabilizes p53, since DUB activity is more strongly than WT ataxin-3 and degradation of p53 is slower, also levels of p53 were higher in cells with EXP ataxin-3 [178]. Aberrant activation of p53 pathways was find in SCA3 patients and mice [178]. P53 stabilization is important for cell arrest and apoptosis [178].	pull down; enzymatic study; affinity chromatography
Telomere length regulation protein TEL2 homolog (TELO2; 9894+)	Authors identified telomerase maintenance 2 to be an interactor of ataxin-3 [128].	validated two hybrid; two hybrid pooling approach; two hybrid array
Rho GDP-dissociation inhibitor 1 (ARHGDIA; 396+)	This protein extract Rho family GTPases from membranes and solubilize them in cytosol [179]. Rho GTPases act as a molecular switch cycling between inactive (GDP-bound) and active (GTP-bound) forms [179]. It was found that Rho GDP-dissociation inhibitor 1 interacts with N-terminal region of ataxin-3 [138].	two hybrid
Amyloid beta precursor protein (APP; 351+)	Amyloid beta precursor protein under proteolytic action form Aβ [180]. Several proteins are capable of interact with Aβ, and one of these proteins is ataxin-3 [180].	pull down

Table 2 - Continuation

BCL2 like 1 (BCL2L1; 598+)	BCL2 like 1 is an anti-apoptotic protein present in mitochondria and involved in oxidative stress, by form a heterodimer complex with Bax protein (pro-apoptotic protein) that will lead to inhibition of apoptosis induced by mitochondrial oxidative stress [181]. Oxidative stress is involved in SCA3 [181]. It was observed by GST pulldown assays that BCL2 like 1 interacts trough residues 196-233 (C-terminal region) with residues 1-133 of WT ataxin-3 but not with UIM domains of WT ataxin-3 [181]. Also, was shown that *in vivo* EXP ataxin-3 interacts more with BCL2 like 1 but *in vitro* is WT ataxin-3 that interacts more [181]. In conclusion polyQ length doesn´t influence the interaction between the two proteins [181]. Besides that, it was reported that ataxin-3 can enhance the interaction between BCL2 like 1 and Bax, probably by change the conformation of BCL2 like 1 that enhancing the interaction with Bax [181].	affinity chromatography
PRKCA-binding protein (PICK1; 9463+)	PRKCA-binding protein/PICK1 acts a transport protein that traffics the ASIC to the plasm membrane that increase the influx of ions, and under conditions of traumatic neuronal injury and ischemia, this leads to an increase in cell death [182]. By yeast two-hybrid screens revels that ataxin-3 interacts with PICK1 [165]. PICK1 connects ataxin-3 with the mitochondrial protein Frataxin (responsible for Friedreich´s ataxia, FA) [182]. Using fly expressing human EXP ataxin-3 in eye tissue and show that when PICK1 is knockdown occurs suppression the external eye degeneration of mutant fly [182]. This also, was confirmed by a downregulation of PICK1 gene that supress the degeneration of photoreceptor neurons [182]. All this indicate that reduction of PICK1 act as a neuroprotective in SCA3 flies [182].	two hybrid
E3 ubiquitin-protein ligase TRIM63 (TRIM63; 84676+)	Tripartite motif containing 63/Murf1 when it is translocated for nucleus is capable of regulates the gene expression and degradation of transcriptional factors [183]. Through a microarrays approach was identified substrates of DUBs, where microarrays were ubiquitylated by a cocktail contain Murf1 or Murf1 alone [144]. The substrates used involved proteins such ataxin-3, were Murf1 show their capability of ubiquitinated ataxin-3, proposing an interaction between the two [144].	enzymatic study
Tripartite motif containing 55 (TRIM55; 84675+)	Tripartite motif containing 55/MURF2 was capable of ubiquitylate ataxin-3 [144].	enzymatic study
Thymidine kinase 1 (TK1; 7083+)	Thymidine kinase 1 is a DNA salvage pathway enzyme involved in regeneration of thymidine for DNA synthesis and damage [184]. It was reported that thymidine kinase 1 interacts with ataxin-3 [169].	two hybrid
Tripartite motif containing 54 (TRIM54; 57159+)	Authors show that tripartite motif containing 54/MURF3 was capable of ubiquitylate ataxin-3 [144]	enzymatic study
Syndecan 2 (SDC2; 6383+)	Syndecan 2 is a member of the syndecan family of cell surface transmembrane heparan sulfate (HS) proteoglycans and allows the communication between the external environment and the organization of the cortical cytoplasm [185]. Syndecan can bind to extracellular matrix molecules and/or soluble ligands [185]. This allows the signal transduce that influence the cell adhesion, motility, proliferation, differentiation, and morphogenesis [185]. It was found that SDC2 interacts with ataxin-3 [125].	affinity chromatography
Forkhead box class O transcription factor 4 (FOXO4; 4303+)	FOXO4 belongs to FOXO family transcription factors that are involved in cell cycle arrest, differentiation, cell death and resistance to cellular oxidative stress [56]. It was observed that N-terminal region of ataxin-3 interacts with FOXO4 and this interaction is independent of polyQ tract length [56]. Besides that, by peptide assays with WT ataxin-3 and His-tagged FOXO4, authors prove that residues 19-39, 70-87, 88-111 and 139-165 interacts with FOXO4 [56]. Only WT ataxin-3 activates FOXO4 dependent expression of SOD2 gene promoter [56].	imaging technique; affinity chromatography
cAMP responsive element binding protein 1 (CREB1; 1385+)	cAMP responsive element binding protein 1 is a transcriptional factor that is activated by CBP (a coactivator) [177].	affinity chromatography
RNA-binding protein EWS (EWSR1; 2130+)	EWS RNA binding protein 1 is an RNA/DNA binding protein involved in transcription, RNA splicing and is proposed to have a role in genetic and epigenetic aspects [186]. It was identified that EWSR1 is an interactor of ataxin-3 [128]. It was shown that EWSR1 interacts with ataxin-3 [165].	validated two hybrid; two hybrid pooling approach; two hybrid array; two hybrid
BTB/POZ domain-containing adapter for CUL3-mediated RhoA degradation protein 3 (KCTD10; 83892+)	BTB/POZ domain-containing adapter for CUL3-mediated RhoA degradation protein 3/KCTD10 is a member of KCTD family that share a similarity with the cytoplasmatic domain of voltage-gated K+ channels (Kv channels) [187]. KCTD family has a BTB domain that may be involved in transcriptional repression, cytoskeleton regulation, tetramerization and gating ion channels, and interacting with Cullin E3 (Cul3) ubiquitin ligase complex [187]. DUB ataxin-3 interacts with KCTD10 [172].	anti tag coimmunoprecipitation; affinity chromatography
Mitogen-activated protein kinase kinase kinase 1 (MAP3K1; 4214+)	Mitogen-activated protein kinase kinase kinase 1/MAP3K1 is a member of MAP kinase kinase (MAPK3) family that regulates c-Jun N-terminal kinase (JNK) and p38 by phosphorylation of their MAP kinase (MAPK2) upstream activating loop [188]. MAP3K1 shown E3 Ub ligase activity, mediated by PHD (plant homeodomain) motif present in MAP3K1 N-terminal regulatory region [188]. Using a microarray profiling of pluripotent *Map3K1*^{mPHD} (representing a PHD mutation in MAP3K1 that would disrupt of PHD activity as E3 Ub ligase) it was seen that ataxin-3 is present and has positive Z-score values for MAP3K1 PHD-GST assays [188].	enzymatic study
Mediator of DNA damage checkpoint 1 (MDC1; 9656+)	Mediator of DNA damage checkpoint 1 marks chromatin-associated proteins in the vicinity of sites of DNA damage with ubiquitin [48]. Ataxin-3 is recruited for DSB, so it is possible that this recruitment is caused by UIM in presence of ubiquitylated chromatin, but mutations in ataxin-3 UIM reveal that ataxin-3 continued be recruited for the DSB [48]. Also, mutation in C14 (inactivation of JD) reveal that ataxin-3 is localized to sites of DNA damage [48]. Without SUMO (SUMO conjugate Ubc9 or SUMO ligase PIAS4) ataxin-3 is not recruited for DNA damage sites, showing that SUMOylation is important for ataxin-3 recruitment [48]. SUMO1 mutation on residues 162-IFVV to 162-AFAA reveal that ataxin-3 does not interact with SUMO1 nor able to accumulate at DNA damage sites, therefore SUMOylating is important for recruitment of ataxin-3 for DSB as was previous accessed [48]. Knockdown of ataxin-3 result in a faster exchange kinetics of MDC1, suggesting that ataxin-3 contribute for a more stable retention of MDC1 on DSB-containing chromatin [48]. Co-immunoprecipitation reveal that ataxin-3 and MDC1 have an interaction that was not enhanced by DNA damage [48]. Depletion of ataxin-3 reveal an increase in polyubiquitinated MDC1 and this could not be rescued by mutant, at C14, ataxin-3, revealing that MDC1 is deubiquitinated by ataxin-3 [48]. Ataxin-3 presence in DNA damage seems prevent de premature remove MDC1 and therefore reenforces the DNA damage signalling and DNA repair [48]. Ubiquitination of MDC1 seems to be the regulated of MDC1 release from chromatin, and ataxin-3 control this (depletion of ataxin-3 increase the MDC1 ubiquitinated levels) [48].	affinity chromatography
Annexin A7 (ANXA7; 310#)	Annexin A7 is a member of annexin family of Ca^{2+}-dependent phospholipids binding proteins and codes for Ca^{2+}-dependent GTPases [189]. Annexin A7 is involved in carcinogenesis by signalling tumour suppressor genes, DNA-repair genes, and apoptosis-related genes [189]. Also, annexin A7 is involved in autophagy [189]. It was found that annexin A7 interacts with ataxin-3 [169].	two hybrid

Table 2 - Continuation

X-ray repair cross-complementing protein 6 (XRCC6; 2547#)	X-ray repair cross complementing 6/Ku70 is a Bax-inhibiting peptides (BIPs) and were named from Bax binding domain of Ku70 [127]. Ku70 is a multifunctional protein playing roles in DNA repair and cell survival [127]. Ku70 is a Bax-inhibiting peptides (BIPs) that inhibit BAX, a proapoptotic member of Bcl-2 family proteins that plays a key role in programmed cell death in neurons [127]. C-terminal ataxin-3 region decreases the interaction between Bax and Ku70 [127]. Also found that expanded C-terminal region induce acetylation of Ku70, that is known to dissociate Bax and Ku70 [127]. Ku70 bind to WT and EXP C-terminal truncated ataxin-3, in the cytosol [127]. CBP was showed to acetylate cytosolic Ku70 in response to apoptotic stimuli [127]. EXP ataxin-3 binds to CBP, by C-terminal region since it was co-immunoprecipitation with CBP but WT C-terminal region not [127]. Also, results suggest that expanded C-terminal tail stimulate Ku70 acetylation by bridging Ku70 and CBP [127]. Ku70 interacts with ataxin-3 [28].	affinity chromatography
HLA class I histocompatibility antigen, A alpha chain (HLA-A; 3105#)	HLA class I histocompatibility antigen, A alpha chain interacts with ataxin-3 [125].	affinity chromatography
60S ribosomal protein L6 (RPL6; 6128#)	60S ribosomal protein L6/RPL6 is the building blocks of ribosome [190]. It is involved in DNA damage response, facilitating the interaction between MDC1 and H2A that promotes da DNA repair cascade [190]. RPL6 is an interactor of ataxin-3 [128].	validated two hybrid; two hybrid pooling approach; two hybrid array
Ribosomal protein S6 kinase alpha-1 (RPS6KA1; 6195#)	Ribosomal protein S6 kinase alpha-1 interacts with ataxin-3 [169].	two hybrid
MAPK interacting serine/threonine kinase 1 (MKNK1; 8569#)	MAPK interacting serine/threonine kinase 1 interacts with ataxin-3 [169].	two hybrid
Huntingtin associated protein 1 (HAP1; 9001#)	Huntingtin associated protein 1 interacts with huntingtin in polyQ-dependent manner and has protective effect on neurons against apoptosis induced by polyQ-expanded huntingtin [191]. Also was found to interact with STB (stigmoid body), a type of inclusions without aggresomes characteristics (such as being ubiquitinated and surrounded by vimentin) [191]. Cotransfection of expressed vectors of HAP1 and WT ataxin-3 induce cytoplasmatic aggregations [191]. Next analysis using truncated ataxin-3 (only with JD, lacking the JD or lacking the JD and the UIMs) reveals that the first mutants have ambiguous expression in nucleus and cytoplasm, and the third reveal diffuse expression [191]. Only the JD mutant reveal aggregate formation in cytoplasm with HAP1 [191].Coimmunoprecipitation assays reveal that HAP1 precipitates with WT ataxin-3 or the mutant containing only the JD but not with mutant lacking the JD [191]. Therefore, JD is essential for HAP1 interactions [191]. Cells expressing EXP ataxin-3 have a diffuse expression in cytoplasm and nuclei [191]. Also, EXP ataxin-3 aggregates with HAP1, but no statistical difference were seen in aggregation rate between WT or EXP ataxin-3 [191]. WT huntingtin forms a transcription-coupled DNA repair (TCR) complex with ataxin-3, HAP1, CREB binding protein, PNKP and other proteins [126]. TCR complex monitors and edits DNA strand beaks/damage during transcriptional elongation, preserving genome integrity and neuronal survival [126]. Mutant huntingtin impairs the normal TCR complex function and leads to pro-apoptotic signal that ultimate amplified the neurodegeneration in brain [126].	fluorescence microscopy; anti tag coimmunoprecipitation; affinity chromatography
B-cell CLL/lymphoma 7 protein family member C (BCL7C; 9274#)	B-cell CLL/lymphoma 7 protein family member C interacts with ataxin-3 [125].	anti tag coimmunoprecipitation; affinity chromatography
Nuclear receptor corepressor 1 (NCOR1; 9611#)		pull down; affinity chromatography
E3 ubiquitin-protein ligase MGRN1 (MGRN1; 23295#)	E3 ubiquitin-protein ligase MGRN1/MGRN1 is a E3 protein ligase involved in recognition and clearance of ubiquitin-positive intracellular aggregates [192]. In this study was investigate the effects of MGRN1 in aggregates caused by polyQ proteins, such as WT and EXP ataxin-3 [192]. The levels of MGRN1 mRNA decrease in cells expressing EXP ataxin-3 [192]. MGRN1 associates more with aggregates caused by expanded polyQ proteins [191]. Also, EXP ataxin-3 were ubiquitinated in cells having positive aggregates, while WT ataxin-3 didn´t show ubiquitination [192]. MGRN1 is strongly immunoprecipitated with EXP ataxin-3 but not with WT ataxin-3 and the interacting region is the N-terminal region [192].	affinity chromatography
Remodeling and spacing factor 1 (RSF1; 51773#)	Remodeling and spacing factor 1 is a chromatin remodelling factor and is recruited for sites of DNA damage [193]. Remodeling and spacing factor 1 interacts with ataxin-3 [125].	anti tag coimmunoprecipitation; affinity chromatography
Calcium load-activated calcium channel (TMCO1; 54499#)	Calcium load-activated calcium channel/TMCO1 is in the endoplasmic reticulum [194]. TMCO1 seems has a role in lipid-droplet formation, acts on Ca^{2+} load-activation Ca^{2+} channels (realising the Ca^{2+} excess from ER), and may has some effect on mitochondria, since mutation in TMCO1 impairs mitochondria function [192]. TMCO1 interacts with ataxin-3 [125].	anti tag coimmunoprecipitation; affinity chromatography
Testis-expressed protein 11 (TEX11; 56159#)	Testis-expressed protein 11/TEX11 is highly or exclusive expressed in testis [195]. TEX11 is expressed in mouse cytoplasmic and nuclei of type B spermatogonia and early spermatocytes, suggesting its role in early stages of germ cell development [195]. Also, TEX11 is a present in meiotic nodules involved in recombination and interacts with Sycp2 (a component of synaptonemal complex) [195]. TEX11 interacts with ataxin-3 [128, 165].	validated two hybrid; two hybrid pooling approach; two hybrid array; two hybrid
Calmodulin-regulated spectrin-associated protein 3 (CAMSAP3; 57662#)	Calmodulin-regulated spectrin-associated protein 3/CAMSAP3 belongs to CAMSAP family that recognize and decorate free microtubule minus ends and protect non-centrossomal microtubules from depolymerization [196]. CAMSAP3 was shown to interact with components of adherent's junctions and to anchor microtubule minus ends at these sites [196]. CAMSAP3 interacts with ataxin-3 [125].	anti tag coimmunoprecipitation; affinity chromatography
E3 ubiquitin-protein ligase Praja-1 (PJA1; 64219#)	Loch and Strickler used a microarrays approach to identify substrates of DUBs, where microarrays were ubiquitylated by a cocktail contain E3 ubiquitin-protein ligase Praja-1/Praja1 or Praja1 alone [144]. The substrates used involved proteins such ataxin-3, were Praja1 show their capability of ubiquitinated ataxin-3, propose an interaction between the two [144].	enzymatic study
Phagosome assembly factor 1 (PHAF1; 80262#)	Phagosome assembly factor 1 interact s with ataxin-3 [128, 165].	validated two hybrid; two hybrid pooling approach; two hybrid array; two hybrid; pull down; affinity chromatography
Proline/serine-rich coiled-coil protein 1 (PSRC1; 84722#)	Proline/serine-rich coiled-coil protein 1 interacts with ataxin-3 [125].	anti tag coimmunoprecipitation; affinity chromatography
Rho GTPase-activating protein 19 (ARHGAP19; 84986#)	Rho GTPase-activating protein 19 is involved in cell shape changes during lymphocyte mitosis by regulation of RhoA activity and subsequent ROCK (Rho effector kinases proteins)-mediates phosphorylation of myosin and vimentin [197]. Rho GTPase-activating protein 19 interacts with ataxin-3 [128, 165].	validated two hybrid; two hybrid pooling approach; two hybrid array; two hybrid
NADH dehydrogenase [ubiquinone] 1 alpha subcomplex assembly factor 2 (NDUFAF2; 91942#)	NADH dehydrogenase [ubiquinone] 1 alpha subcomplex assembly factor 2/NDUFAF2 is one of 7 assemble factors necessary for NADH dehydrogenase enzyme formation [198]. It is not required for enzyme formation but plays important role in it [198]. NDUFAF2 interacts with ataxin-3 [125].	anti tag coimmunoprecipitation; affinity chromatography technolog

Table 2 - Continuation

Zinc finger protein AEBP2 (AEBP2; 121536#)	Zinc finger protein AEBP2 interacts with ataxin-3 [151, 152].	anti tag coimmunoprecipitation; affinity chromatography
Dead end protein homolog 1 (DND1; 373863#)	Dead end protein homolog 1/DND1 binds to mRNA and prohibits miRNA interaction, likewise, prevents miRNA-mediated repression [199]. DND1 expression is restricted to germ cells and certain neural tissues [199]. DND1 interacts with ataxin-3 [151, 152].	anti tag coimmunoprecipitation; affinity chromatography
Plasmanylethanolamine desaturase (PEDS1; 387522#)		
Ubiquitin-conjugating enzyme E2 variant 1 (UBE2V1; 7335#)		
Mitochondrial import inner membrane translocase subunit Tim23 (TIMM23; 100287932#)	Mitochondrial import inner membrane translocase subunit Tim23 interacts with ataxin-3 [125].	anti tag coimmunoprecipitation; affinity chromatography
CCR4-NOT transcription complex subunit 6 (CNOT6; 57472#)	CCR4-NOT transcription complex subunit 6 interacts with ataxin-3 [125].	anti tag coimmunoprecipitation; affinity chromatography
Succinate dehydrogenase [ubiquinone] iron-sulfur subunit (SDHB; 6390+)	Succinate dehydrogenase (SDH, also known as mitochondrial respiratory complex II) has four subunits SDHA, SDHB, SDHC and SDHD [89]. Therefore, loss of function in SDH subunits leads to reprogramming cellular metabolic pathways, disruption of electron transfer to oxygen, that increase the ROS levels, and redox imbalance [89]. SDHB were enriched in EXP ataxin-3 samples comparing with WT ataxin-3 samples [3].	affinity chromatography
Cytochrome c oxidase assembly factor 7 (COA7; 65260#)	COA7 were enriched in EXP ataxin-3 samples comparing with WT ataxin-3 samples [3]. COA7 is present in complexes of respiratory chain [3].	affinity chromatography
Cytochrome c oxidase subunit NDUFA4 (NDUFA4; 4697+)	Cytochrome c oxidase subunit NDUFA4/NDUFA4 is a transmembrane subunit, previous identified as complex I subunit, but later identified as complex IV (cythorome c oxidase) subunit [90]. It is possible that NDUFA4 is a complex I subunit since binds to complex IV like other proteins [90]. Also was found that NDUFA4 can form supercomplexes that could connect difference respiratory chain complexes, such as complex I and complex IV [90]. The formation of supercomplexes need of several assembly factors that differ in growing, postmitotic, hypoxic and cancer cells [90]. Therefore, is proposed that NDUFA4 is an assembly factor [90]. Complex IV is responsible for H_2O formation, because transfers two electrons to O_2 [90]. NDUFA4 seems to have a higher expression in the liver and the brain [90]. It was shown that NDUFA4 over-expression decrease the neuron apoptosis rate, along with caspase-3 expression, but increase the Bcl-2 expression [91]. Also was found that NDUFA4 enhances the neuron growth by triggering growth factors (NGF, BDNF and bFGF) expression [91]. NDUFA4 were enriched in EXP ataxin-3 samples comparing with WT ataxin-3 samples [3]. It was observed that NDUFA4 interacts predominantly with shorter isoforms of ataxin-3, caused by a stop SPN in exon 10 that culminates in a premature stop codon that create two versions of this short isoform (ataxin-3aL and ataxin-3aS) [28].	affinity chromatography
ATP-citrate synthase (ACLY; 47+)	ATP citrate synthase is important in *de novo* lipid synthesis and could be involved in biosynthesis of acetylcholine in nervous tissue [3]. ACLY were enriched in EXP ataxin-3 samples comparing with WT ataxin-3 samples [3]. ACLY interacts with ataxin-3 [28].	affinity chromatography
Protein FAM184B (FAM184B; 27146#)	Protein FAM184B interacts with WT and EXP ataxin-3 samples [3].	affinity chromatography
Dihydroxyacetone phosphate acyltransferase (GNPAT; 8443+)	Dihydroxyacetone phosphate acyltransferase interacts with WT and EXP ataxin-3 samples [3].	affinity chromatography
Cyclin dependent kinase 4 (CDK4; 1019+)	Cyclin dependent kinase 4 interacts with WT and EXP ataxin-3 samples [3].	affinity chromatography
Hydroxysteroid dehydrogenase-like protein 2 (HSDL2; 84263+)	Hydroxysteroid dehydrogenase-like protein 2 interacts with WT and EXP ataxin-3 samples [3].	affinity chromatography
Retinol dehydrogenase 13 (RDH13; 112724+)	Retinol dehydrogenase 13/RDH13 is a member of short-chain dehydrogenases/reductases (SDRs) family, composed by different proteins involved in metabolism of steroids, prostaglandins, retinoids, aliphatic alcohols and xenobiotics [200]. RDH13 seems to be a peripherical mitochondrial membrane protein, facing the intermembrane space [200]. RDH13 as a oxidoreductase activity towards to retinoids, prefers NADPH over NADH as a cofactor, and has more catalytic efficiency as reductase over dehydrogenase [200]. RDH13 interacts with WT and EXP ataxin-3 samples [3]	affinity chromatography
Mitochondrial glutamate carrier 1 (SLC25A22; 79751+)	Mitochondrial glutamate carrier 1/SLC25A22 interacts with WT and EXP ataxin-3 samples [3]. It was observed that SLC25A22 interacts with ataxin-3 [28].	affinity chromatography
Succinate dehydrogenase [ubiquinone] flavoprotein subunit (SDHA; 6389+)	Succinate dehydrogenase (SDH, also known as mitochondrial respiratory complex II) has four subunits SDHA, SDHB, SDHC and SDHD [89]. Therefore, loss of function in SDH subunits leads to reprogramming cellular metabolic pathways, disruption of electron transfer to oxygen, that increase the ROS levels, and redox imbalance [89]. SDHA interacts with WT and EXP ataxin-3 samples [3]. SDHA interacts with ataxin-3 [28].	affinity chromatography
Rho-related GTP-binding protein RhoG (RHOG; 391+)	Rho-related GTP-binding protein RhoG interacts with WT and EXP ataxin-3 samples [3].	affinity chromatography
Mucosa-associated lymphoid tissue lymphoma translocation protein 1 (MALT1; 10892+)	Mucosa-associated lymphoid tissue lymphoma translocation protein 1/MALT1 has a major role in scaffolding protein because it binds to E3 ubiquitin ligase TRAF6 (which polyubiquitinates itself), itself (MALT1) and Bcl-10 [201]. This recruit IKK gamma (that activates IKK complex) that leads to NF-kB inhibitor release, allowing the translocation of NF-kB to the nucleus [201]. Also, MALT1 acts as a protease that activates NF-kB independent of IKK complex [201]. MALT1 interacts with WT and EXP ataxin-3 samples [3]. MALT1 interacts with ataxin-3 [128].	validated two hybrid; two hybrid pooling approach; two hybrid array; affinity chromatography
Acyl-CoA thioesterase 9 (ACOT9; 23597+)	Acyl-CoA thioesterase 9/ACOT9 interacts with WT and EXP ataxin-3 samples [3]. ACOT9 interacts with ataxin-3 [28].	affinity chromatography
Long-chain fatty acid transport protein 4 (SLC27A4; 10999+)	Long-chain fatty acid transport protein 4 interacts with WT and EXP ataxin-3 samples [3].	affinity chromatography
Tricarboxylate transport protein (SLC25A1; 6576+)	Tricarboxylate transport protein interacts with WT and EXP ataxin-3 samples [3].	affinity chromatography
Nucleoporin SEH1 (SEH1L; 81929)	Nucleoporin SEH1 interacts with WT and EXP ataxin-3 samples [3].	affinity chromatography
Mitochondrial dicarboxylate carrier (SLC25A10; 1468+)	Mitochondrial dicarboxylate carrier interacts with WT and EXP ataxin-3 samples [3].	affinity chromatography

Table 2 - Continuation

Iron-sulfur cluster assembly factor IBA57 (IBA57; 200205+)	Iron-sulfur cluster assembly factor IBA57 interacts with WT and EXP ataxin-3 samples [3].	affinity chromatography
Bifunctional methylenetetrahydrofolate dehydrogenase/cyclohydrolase (MTHFD2;10797+)	Bifunctional methylenetetrahydrofolate dehydrogenase/cyclohydrolase/MTHFD2 has a role in mitochondrial folate-mediated metabolism, where MTHFD2 produces formate from methylenetetrahydrofolate [202]. The MTHFD2 has the dehydrogenase and cyclohydrolase activity in embryonic and transformed cells [202]. MTHFD2 interacts with WT and EXP ataxin-3 samples [3].	affinity chromatography
Phosphate carrier protein (SLC25A3; 5250+)	Phosphate carrier protein/SLC25A3 has two isoforms caused by alternative splicing of exon 3 [203]. The isoform A is expressed in heart and skeletal muscle, while isoform B is expressed in the rest of tissues [203]. Isoform B (SLS25A3-B) as a higher rate of phosphate transport than isoform A (SLC25A3-A) [203]. SLC25A3 interacts with WT and EXP ataxin-3 samples [3]. SLC25A3 interacts with ataxin-3 [28].	affinity chromatography
Ubiquitin-associated domain-containing protein 2 (UBAC2; 337867#)	Ubiquitin-associated domain-containing protein 2 interacts with WT and EXP ataxin-3 samples [3].	affinity chromatography
Mitochondrial genome maintenance exonuclease 1 (MGME1; 92667+)	Mitochondrial genome maintenance exonuclease 1/MGME1 is linked to mitochondrial DNA repair [24]. MGME1 interacts with WT and EXP ataxin-3 samples [3].	affinity chromatography
Very-long-chain enoyl-CoA reductase (TECR; 9524+)	Very-long-chain enoyl-CoA reductase/TECR interacts with WT and EXP ataxin-3 samples [3]. TECR interacts with ataxin-3 [28].	affinity chromatography
Arfaptin-2 (ARFIP2; 23647#)	Arfaptin-2 probably promotes huntingtin aggregation by negatively regulating UPS system [204]. It was found that Arfaptin-2 blocks 26S proteasome activity [204]. Arfaptin-2 can interact with Ras-related GTPases ARF6 and Rac1 and may regulate cytoskeletal remodelling mediated by these GTPases [204]. Arfaptin-2 interacts with WT and EXP ataxin-3 samples [3].	affinity chromatography
Regulator of microtubule dynamics protein 1 (RMDN1; 51115#)	Regulator of microtubule dynamics protein 1 interacts with WT and EXP ataxin-3 samples [3].	affinity chromatography
UPF0598 protein C8orf82 (C8orf82; 414919#)	UPF0598 protein C8orf82 interacts with WT and EXP ataxin-3 samples [3].	affinity chromatography
Lysophosphatidylcholine acyltransferase 1 (LPCAT1; 79888+)	LPCATs are important in lipid metabolism and homeostasis, by regulation of several phosphatidylcholine in tissue and cells [205]. Lysophosphatidylcholine acyltransferase 1/LPCAT1 is a member of acylglycerophosphate acyltransferase family, composed of 4 conserved LPA acyltransferase motif and an endoplasmic reticulum localization sequence [205]. LPCAT1 prefers palmitoyl-CoA as the course of acyl-CoA [205]. LPCAT1 localize in the surface of lipid droplets in several mammal cells [205]. The lipid droplets are intracellular organelles that store neutral lipids for use as energy source in membrane synthesis and in production of signalling lipids [205]. Some pathway involving these organelles are lipid storage, fatty acid trafficking and activation of transcription factors [205]. Also LPCAT1 (is the most abundant LPCAT in alveolar type II cells) is responsible for DPPC biosynthesis [205]. DPPC compose 50% of lipid fraction of pulmonary surfactant [205]. LPCAT1 interacts with WT and EXP ataxin-3 samples [3].	affinity chromatography
Isocitrate dehydrogenase [NAD] subunit beta (IDH3B; 3420+)	Isocitrate dehydrogenase [NAD] subunit beta interacts with WT and EXP ataxin-3 samples [3].	affinity chromatography
ALG1 Chitobiosyldiphosphodolichol beta-mannosyltransferase (ALG1; 56052+)	ALG1 Chitobiosyldiphosphodolichol beta-mannosyltransferase interacts with WT and EXP ataxin-3 samples [3].	affinity chromatography
60S acidic ribosomal protein P0 (RPLP0; 6175#)	60S acidic ribosomal protein P0 interacts with WT and EXP ataxin-3 samples [3].	affinity chromatography
E3 ubiquitin-protein ligase MARCHF5 (MARCHF5; 54708+)	E3 ubiquitin-protein ligase MARCHF5/(MARCH5 or MITOL) removes misfold proteins and is responsible for mitochondrial dynamics, that culminate in control the mitochondrial integrity [87]. MARCH5 regulates Drp1 activity and, therefore impact the cellular senescence and modulating neuronal death [88]. Also, was proposed that MARCH5 regulates ER - mitochondrial tethering through ubiquitination of mitofusion Mfn2 [88]. MARCH5 interacts with WT and EXP ataxin-3 samples [3].	affinity chromatography
Ribose-phosphate pyrophosphokinase 1 (PRPS1; 5631+)	Ribose-phosphate pyrophosphokinase 1 interacts with WT and EXP ataxin-3 samples [3].	affinity chromatography
Ras-related protein Rab-21 (RAB21; 23011+)	Ras-related protein Rab-21/RAB21 belongs to RABs family that are important regulators of several biological processes such as: cell growth, development, cellular behaviour, membrane tracking, membrane fusion and transport of organelles and cytoskeleton frameworks [206]. RAB21 is ubiquitous expressed and mediates endosomal trafficking of integrins, gamma-secretases and other signalling proteins [206]. Authors shown that RAB21 regulates LPS-induce pro-inflammatory responses in macrophages and monocytes, probably by promoting TLR4 endosomal traffic and downstream signalling events [206]. In another study, was found that RAB21 interacts indirectly with TMED10 [207]. Both TMED10 and RAB21 were found in Golgi, but RAB21 is mainly an endosomal protein [207]. TMED10, also, can be found in endoplasmic reticulum, secretory vesicles and at the plasma membrane [207]. RAB21 interacts with WT and EXP ataxin-3 samples [3].	affinity chromatography
NADH dehydrogenase [ubiquinone] 1 alpha subcomplex subunit 8 (NDUFA8; 4702+)	NADH dehydrogenase [ubiquinone] 1 alpha subcomplex subunit 8 interacts with WT and EXP ataxin-3 samples [3].	affinity chromatography
CDGSH iron-sulfur domain-containing protein 2 (CISD2; 493856#)	CDGSH iron-sulfur domain-containing protein 2/CISD2 mediates lipid synthesis, protein folding, and as a transport conduit redox calcium between the endoplasmic reticulum, mitochondria and cytosol and mitochodria-associated ER membranes [208]. Redox reactions are important for modulating mitochondria in neurodegenerative disorder [208]. CISD2 protects cells from calcium excitotoxicity, apoptosis, and mitochondrial abnormality [208]. CISD2 interacts with WT and EXP ataxin-3 samples [3].	affinity chromatography
Estradiol 17-beta-dehydrogenase 11 (HSD17B11; 51170+)	Estradiol 17-beta-dehydrogenase 11 interacts with WT and EXP ataxin-3 samples [3].	affinity chromatography
Calcium uniporter protein (MCU; 90550+)	Calcium uniporter protein/MCU mediates calcium influx into the organelle matrix [209]. MCU complex expression is mediated by CREB, a dependent calcium transcription factor, that binds to MCU promoter [209]. An increase of calcium in mitochondria impair ATP synthesis and iron-induced mitochondrial swelling and structural modifications [209]. Also, was shown that mitochondria calcium accumulation favour permeability transition and cell death [209]. Bcl-2 proteins control the Calcium export from endoplasmic reticulum [209]. MCU overexpression leads to cell death [209]. MCU interacts with WT and EXP ataxin-3 samples) [3].	affinity chromatography

*represent ubiquitination, + represent non-ubiquitination, # represent non-enriched,

Since the sample used could be biased towards a given function, to exclude any relationship between function and regions of interaction, we subdivided the ataxin-3 network (N= 130) in three major groups (according to PANTHER Gene Ontology enrichment analysis [115-117]): there involved in the ubiquitination pathway (29 in total), there not involved (incorporates the remaining molecular functions, 73 in total), and the ones involved in functions that are not-enriched (contains proteins with many molecular functions, 28 in total). No differences were observed between ubiquitination and non-ubiquitination groups, (N=29, N=73; *p*=0,156; Mann-Whitney U Test), ubiquitination and non-enriched groups (N=29, N=28; *p*=0,119; Mann-Whitney U Test), and in non-ubiquitination and non-enriched groups (N=73, N=28; *p*=0,622; Mann-Whitney U Test), confirming that the interaction region is independent of function.

1.4 Interaction regions at ataxin-3 are affected by the presence of an EXP polyQ

SCA3 pathology only appears in the presence of an expanded polyQ tract in ataxin-3 protein [1, 4]. The expanded polyQ tract alters the conformational state of ataxin-3 that enhances the formation of β-rich amyloid-like protein inclusions [26]. This is a step, possibly, mediated by expansion of coiled-coil domains in adjacent regions of polyQ tract, upon interaction with a coiled-coil domain of an interactor [15, 16]. Suggesting, that polyQ tract expansion will interfere with ataxin-3 binding or create precursors of toxic species [26] inducing alterations in ataxin-3 biological functions. Moreover, as reported in **Table 2**, interactors show a higher affinity for EXP ataxin-3, affecting biological processes. For instance, VCP delays EXP ataxin-3 for proteasome degradation, because EXP ataxin-3 is not dissociated from E4B protein (that endorses ataxin-3 for degradation) [74]. It is thus possible that proteins show different interaction regions with EXP ataxin-3. To address this question, we used the predicted interacting residues of 86 proteins with WT and EXP ataxin-3, after removing the interactors presenting six or more interactions at the polyQ region (54 in total). The excluded proteins (represented by name and Gene ID), are Heat shock 70 kDa protein 4L (22824), DnaJ homolog subfamily A member 1 (3301), Heat shock 70 kDa protein 4 (3308), HDAC3 (8841), PCAF (8850), CK2 (1460), NF-kappa-B inhibitor alpha (4792), Calpain 2 (824), Caspase 1 (834), Acid-sensing ion channel 1 (41), Dynamin 2 (1785), Tubulin beta chain (203068), TNF receptor associated factor 6 (7189), E3 ubiquitin-protein ligase SMURF1 (57154), 26S proteasome regulatory subunit 8 (5705), Dynamin-1-like protein (10059), Heat shock protein 105 kDa (10808), Heat shock 70 kDa protein 1A (3303), RAD23B (5887), Ubiquitin-like modifier-activating enzyme 1 (7317), parkin (5071), p53 (7157), VCP

(7415), Sequestosome 1 (8878), HRD1 (84447), Amyloid beta precursor protein (351), BCL2 like 1 (598), cAMP responsive element binding protein 1 (1385), FOXO4 (4303), Tripartite motif containing protein 54 (57159), Syndecan 2 (6383), BTB/POZ domain-containing adapter for CUL3-mediated RhoA degradation protein 3 (83892), E3 ubiquitin-protein ligase TRIM63 (84676), PRKCA-binding protein (9463), Telomere length regulation protein TEL2 homolog (9894), Proline/serine-rich coiled-coil protein 1 (84722), Rho GTPase-activating protein 19 (84986), Ribosomal protein S6 kinase alpha-1 (6195), X-ray repair cross-complementing protein 6 (2547), 60S ribosomal protein L6 (6128), Huntingtin associated protein 1 (9001), E3 ubiquitin-protein ligase MGRN1 (23295), CCR4-NOT transcription complex subunit 6 (57472), E3 ubiquitin-protein ligase Praja-1 (64219), Testis-expressed protein 11 (56159), Dihydroxyacetone phosphate acyltransferase (8443), Mucosa-associated lymphoid tissue lymphoma translocation protein 1 (10892), Iron-sulfur cluster assembly factor IBA57 (200205), Protein FAM184B (27146), Succinate dehydrogenase [ubiquinone] flavoprotein subunit (6389), Mitochondrial glutamate carrier 1 (79751), Regulator of microtubule dynamics protein 1 (51115), Ribose-phosphate pyrophosphokinase 1 (5631) and Calcium uniporter protein (90550), that include most of the proteins known to interact with EXP ataxin-3, as reported in **Table 1** and **2**. Nevertheless, being conservative we discard the possible effect of the presence of six or more interactions in the polyQ. As shown in **Figure 6**, the binding pattern is distinct between the two ataxin-3 forms. For instance, in the JD, interaction regions largely used in the WT ataxin-3 interaction are rarely used in the interaction with the EXP ataxin-3. Indeed, statistical analyses for this domain were performed, revealing significant differences between WT and EXP ataxin-3 (N=86; p<0,001; Sign test). Furthermore, in the 5' region of UIM1 there is an increase in the number of interactions with EXP ataxin-3 compared with the WT form. Nevertheless, regarding the total number of interactions in the two ataxin-3 forms statistical analysis reveals no significant differences (N=86; p=0,822; Sign test). JD is the region with more binding interactions (81%) in the EXP ataxin-3 form, as observed for the WT ataxin-3 interactions.

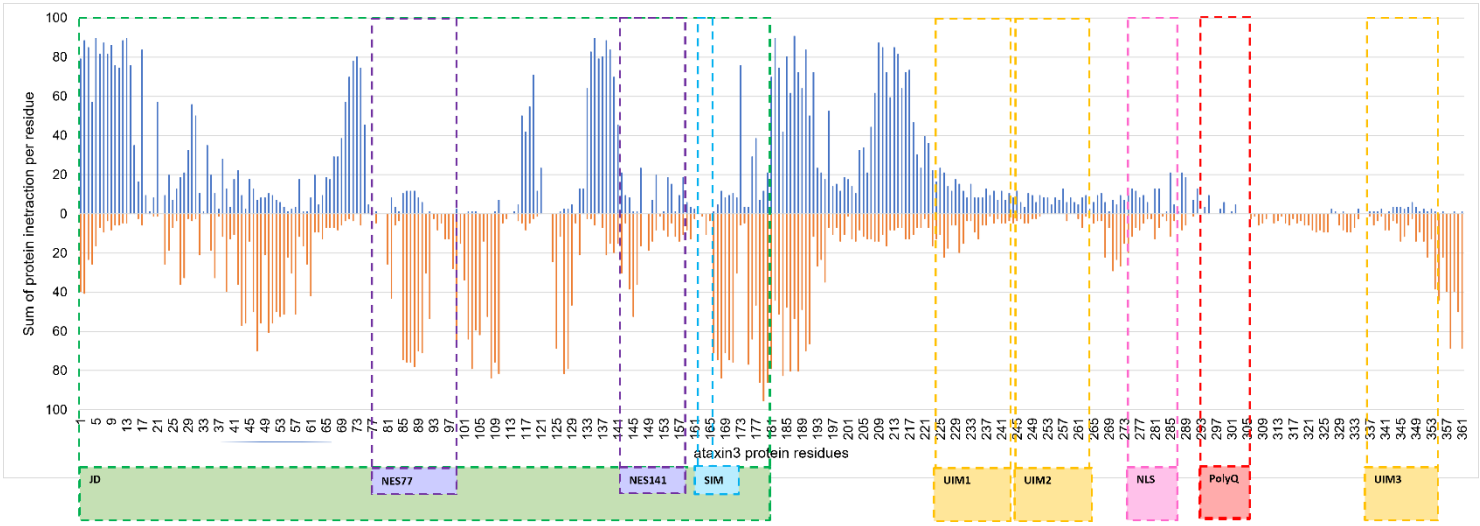

Figure 6: Predicted EXP (blue) versus WT (orange) ataxin-3 interacting regions. Note that comparation is performed at residue level. The JD (1-180 aa), nuclear export signals (NES) 77 (77-99 aa) and 141 (141-158 aa), [SUMO]-interacting motive (SIM, 162-165 aa), ubiquitin interacting motifs (UIM) 1 (224-243 aa), 2 (244-263 aa) and 3 (335-354 aa), nuclear localization signal (NLS, 273-286 aa) and the polyQ tract are assigned.

As observed for WT ataxin-3 the interaction regions are similar between EXP ataxin-3 interactors and those that have a fly paralog (**Figure 7**), making *Drosophila* a good animal model to study SCA3 pathology. In this analyses in order to erase possible effects of wrong inferences due to the presence of six or more interactions in the polyQ region, only 20 human proteins (Serpin H1 (Gene ID 871), ATP-dependent RNA helicase DDX39A (Gene ID 10212), Sideroflexin 4 (Gene ID 119559), 2-amino-3-ketobutyrate coenzyme A ligase (Gene ID 23464), ADP/ATP translocase 2 (Gene ID 292), ADP/ATP translocase 3 (Gene ID 293), Calnexin (Gene ID 821), Alpha-parvin (Gene ID 55742), DnaJ homolog subfamily B member 2 (Gene ID 3300), HDCA3 (Gene ID 10013), Caspase 3 (Gene ID 836), Ubiquitin carboxyl-terminal hydrolase 21 (Gene ID 27005), TOMM20-like protein 1 (Gene ID 387990), Tubulin alpha-1A chain (Gene ID 7846), SUMO1 (Gene ID 7341), 26S proteasome non-ATPase regulatory subunit 4 (Gene ID 5710), Ubiquitin conjugating enzyme E2 G1 (Gene ID 7326), Ubiquitin conjugating enzyme E2 L3 (Gene ID 7332), Ubiquitin conjugating enzyme E2 N (Gene ID 7334), Ubiquitin conjugating enzyme E2 S (Gene ID 27338)) and 19 fly proteins (AT19485p (Gene ID 31978), Ubiquitin carboxyl-terminal hydrolase Usp2 (Gene ID 33132), Small ubiquitin-related modifier (Gene ID 33981), Ubiquitin-conjugating enzyme E2-18 kDa (Gene ID 37035), Uncharacterized protein, isoform B (Gene ID 33318), Dorsal interacting protein 4 (Gene ID 33226), Calnexin 99A, isoform A (Gene ID 44643), Caspase (Gene ID 43514), Tubulin beta-1 chain (Gene ID 37238), Histone deacetylase HDAC1 (Gene ID 38565), GEO10511p1 (Gene ID 41285), Ribonuclease P protein subunit p20 (Gene ID 3772007), 26S proteasome non-ATPase regulatory subunit 4

(Gene ID 40388), Serpin 28Db (Gene ID 326261), SD11922p (Gene ID 49803), ADP,ATP carrier protein (Gene ID 32007), ATP-dependent RNA helicase WM6 (Gene ID 33781), RE58623p (Gene ID 36448), Sideroflexin-1-3 (Gene ID 40552)) were analysed.

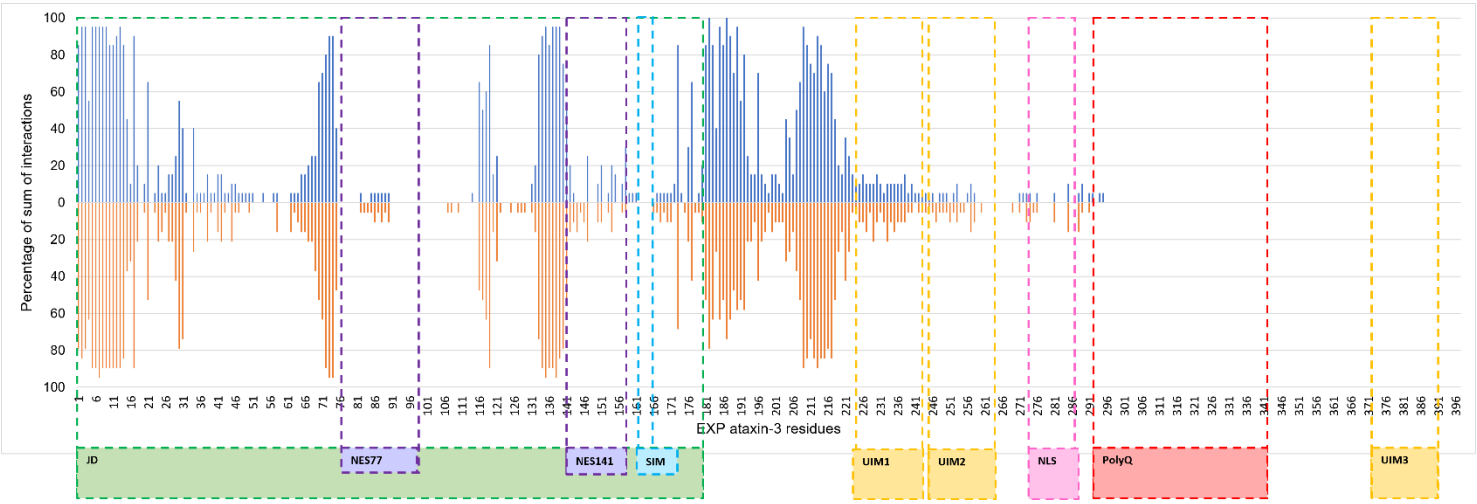

Figure 7: Predicted EXP ataxin-3 interactions with *Homo sapiens* interactors (blue) and their respective paralogs in *D. melanogaster* (orange). The Josephin domain (JD, 1-180 aa) is marked in green, nuclear export signal (NES) 77 (77-99 aa) and 141 (141-158 aa) are marked in purple, [SUMO]-interacting motive (SIM, 162-165 aa), ubiquitin interacting motif (UIM) 1 (224-243 aa), 2 (244-263 aa) and 3 (371-390 aa), nuclear localization signal (NLS, 273-286 aa) and the polyQ tract (292-341 aa, 50Q), are highlighted.

2. Ataxin-3 structural differences are associated with WT and EXP interacting behaviour

The polyQ tract expansion is associated with ataxin-3 protein structural changes [26]. In order to see if our inferences support this finding, a structural alignment was performed using the TM-align tool [109], and the inferred WT and EXP ataxin-3 proteins. A TM-score of 0,58 (normalized by WT ataxin-3 length) illustrate the presence of same fold amongst the two ataxin-3 forms. The JD between the two forms aligns well (**Figure 8**), and the C-terminal flexible tail is the major region that undergoes conformational alterations in the presence of an expanded polyQ tract. Despite having the same fold (**Figure 8**), the predominant interacting regions are different for WT and EXP ataxin-3 (**Figure 6**, see Material and Methods section for details). For WT ataxin-3, the main interacting regions (report 50% or more of interactions) are 35 – 61, 85 – 92, 96 – 110, 124 – 131, 166 – 172, 175 – 195, and 349 – 361, while for EXP ataxin-3 are 1 – 17, 24 – 31, 65 – 75, 116 – 121, 131 – 142, and 176 – 233; **Figure 6**). Only one region (176 – 195) is in both protein structures. The fold of that region is conserved (**Figure 8** and **9;** 5,6Å and 5,8Å, for WT and EXP ataxin-3, respectively), so the similar interactions between WT and EXP ataxin-3 at this region (**Figure 6**) is expected. Furthermore, the WT ataxin-3 residues 202 – 211, 216 – 217, 223 – 227, and 230 – 231 (report a percentage of interaction between 11 and 49, so are named as middle interacting regions) are in common with EXP ataxin-3 binding regions adjacent to the conserved region 181 – 209 (**Figure 8**), and both regions present few interaction residues with the ataxin-3 forms (**Figure 6**). This region is located in the region of the catalytic site in WT and EXP ataxin-3, suggesting that substrates access to DUB ataxin-3 site involved residues located in this region. The fold of residues 258 – 281 is conserved between the two ataxin-3 forms, but at this region the two ataxin-3 forms present little overlap for number of interactions (**Figure 6**). This region is slightly far away from JD (14,3Å in WT and 9,2Å in EXP ataxin-3 forms; **Figure 10**).

Taking a closer look to JD of WT ataxin-3 it is possible to observe that besides the conserved 181 – 209 amino acid regions there is another region nearby (9,2Å), the end of C-terminal tail (**Figure 11**). Moreover, there are interacting residues at the end of C-terminal tail (349 – 361 residues). So, it is possible that interactions in this region stabilize and promote JD interactions in the correct way. In EXP ataxin-3, these interactions are not observed possibly due to the fact that the end of protein shifts apart from JD (**Figure 8B**).

Overlapping the high and middle interacting residues region in WT and EXP ataxin-3 structure, reveals that in WT almost all the interactions are located in the opposite side of DUB catalytic site (**Figure 12A**), as was proposed by Mao *et al.* using ubiquitin as the interactor partner of ataxin-3. In these experiments a chemical shift perturbation was observed in the ataxin-3 residues located in the loop formed by α3, α4 and the end of α2 [33]. Suggesting that ubiquitin will be located above the catalytic site (composed by residues Q9, C14, H119 and N134) [25, 33, 164]. Moreover, a second site for ubiquitin binding is reported, the aromatic cluster Y27, F28 and W87 [35]. So, it is possible that these regions accommodate other proteins besides Ub. Looking for EXP ataxin-3 interaction (**figure 12B**), all are in the same side as the catalytic site. So, ataxin-3 DUB site will be inactive. Nevertheless, prior to this work polyQ expansion was considered not to influence the catalytic site [29, 38]. This could happen because the adopted polyQ expansion induced conformation changes that exposed the catalytic site. Possible facilitating the interaction in this region instead of being in ubiquitin interacting site 1 and others in opposite catalytic site.

Also, it has been suggested that the expanded polyQ tract will interact with a coiled-coil domain of an interactor modulating the interactions [15, 16]. There are few interactions adjacent to polyQ tract, supporting this view.

Additionally, ataxin-3 motives (retrieved from ELMs [113]) were identified and are specific for a protein or for related proteins. So, they do not seem to influence EXP ataxin-3 interactions. Although, the N-degron motive (residues 1–3) that may be recognized by ubiquitin ligases and thus, endorse proteins for degradation [210, 211], could justify the higher numbers of interactions reported for EXP ataxin-3 in region 1 – 17. Nevertheless, the ataxin-3 network has a vast variety of functions (besides ubiquitination), and all of them interact in this region. Some confirmed motives are the CK2 phosphorylation site (range from 26 – 32 and 233 – 239 amino acids), the LIR motif (necessary for Atg8 proteins binding, located in residues 72 – 77), the Plk1 kinase site (residues 108 – 114), caspases 3 and 7 cleavage site (residues 214 – 218), the GSK3β phosphorylation site (residues 253 – 260), di-Arginine retention/retrieving signal (282 – 285 amino acids) and SUMO1 site (inverted – 349 to 357 amino acids, and 355 – 358). None of the confirmed motives are the glycosaminoglycan attachment sites, SH2 (Src homology 2) domain sites (in humans are present in kinases, phosphatases, cytoskeletal proteins, regulators of small GTPases, E3 ubiquitin ligases and others [212]) phosphorylation proteins sites, Pin1 WW domain site (Pin1 is expressed in the brain and prevents age-related neurodegeneration [213]), and others. The last three, in the future may be found to be

associated with ataxin-3 since the proteins in which they are found share functions with other ataxin-3 interacting proteins or are present in the brain.

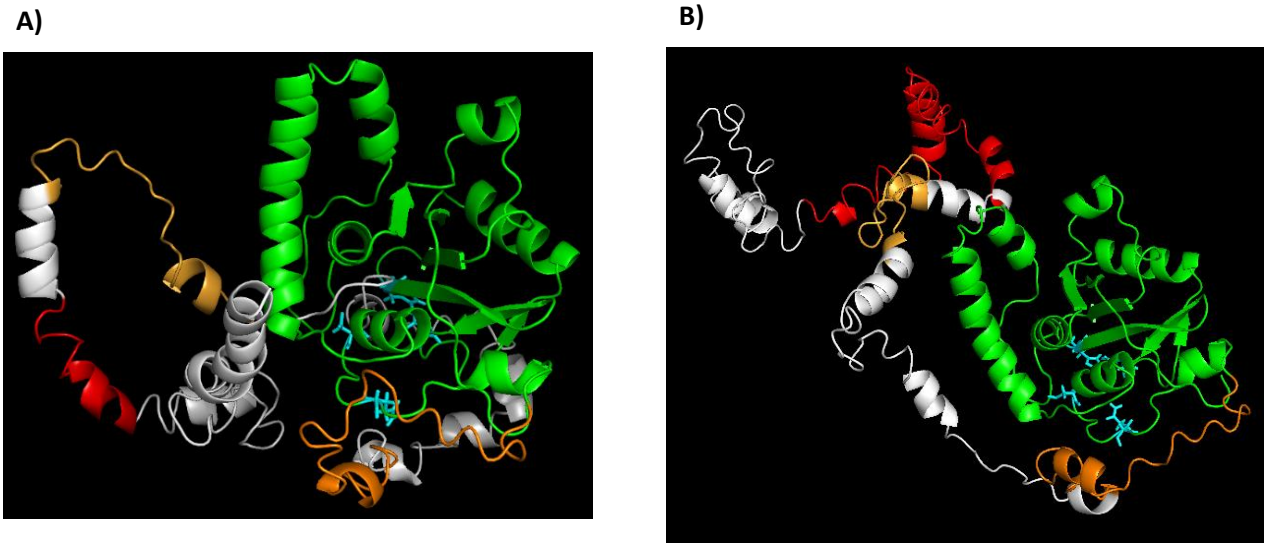

Figure 8: WT (**A**) and EXP (**B**) ataxin-3 conserved region. The conserved regions are the JD (green), the residues 181 – 209 (orange) and 258 – 281 (bright orange). The polyQ is represented in red. The protein catalytic site is represented as cyan sticks.

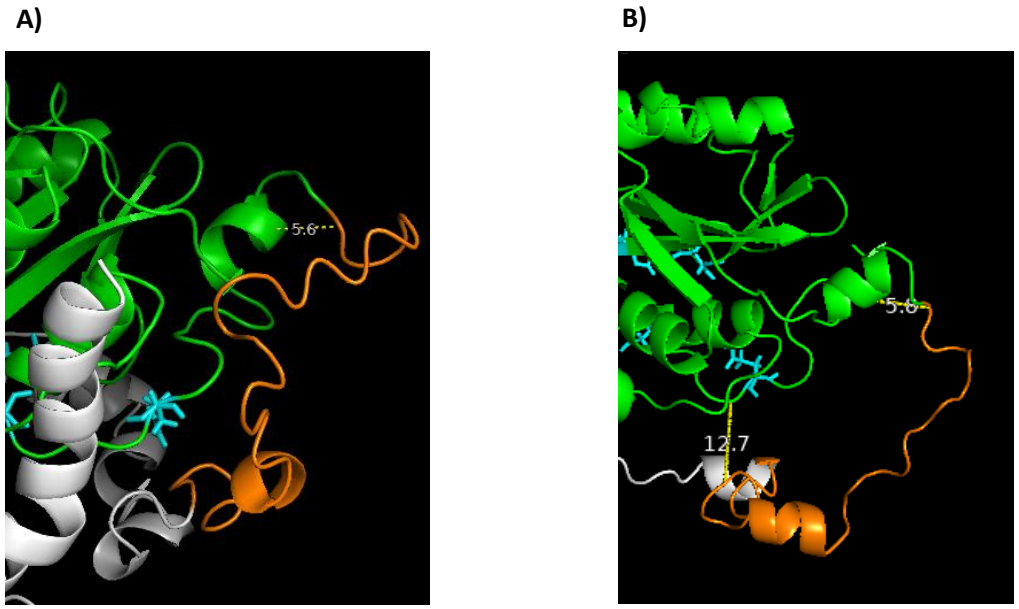

Figure 9: Proximity of 181 – 209 amino acids region (orange) in both WT (**A**) and EXP (**B**) ataxin-3 to Josephin domain (green). A) Closer proximity of 5,6 Å. B) Closer proximity of 5,8 Å.

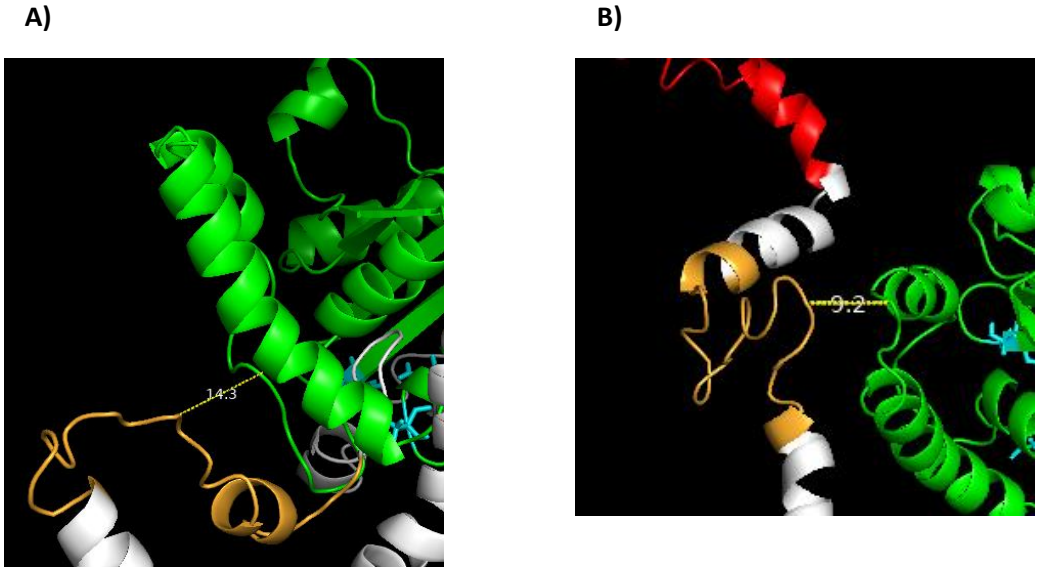

Figure 10: Proximity of 258 – 281 amino acids region (bright orange) in both WT (**A**) and EXP (**B**) ataxin-3 to Josephin domain (green). A) Closer proximity of 14,3Å. B) Closer proximity of 9,2Å.

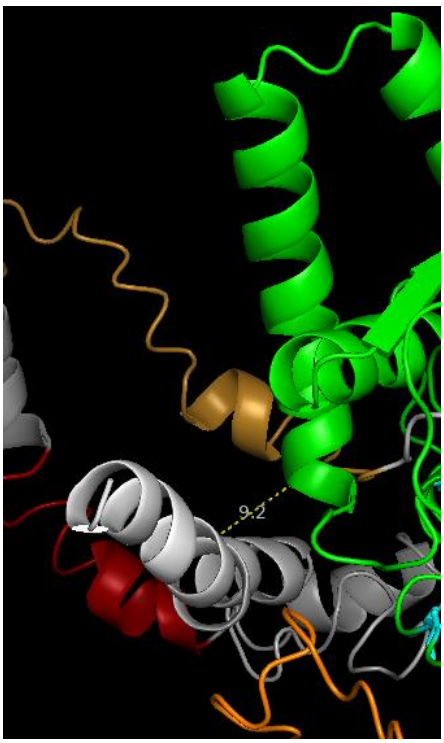

Figure 11: Proximity representation, in WT ataxin-3, of the protein C-terminal end to JD.

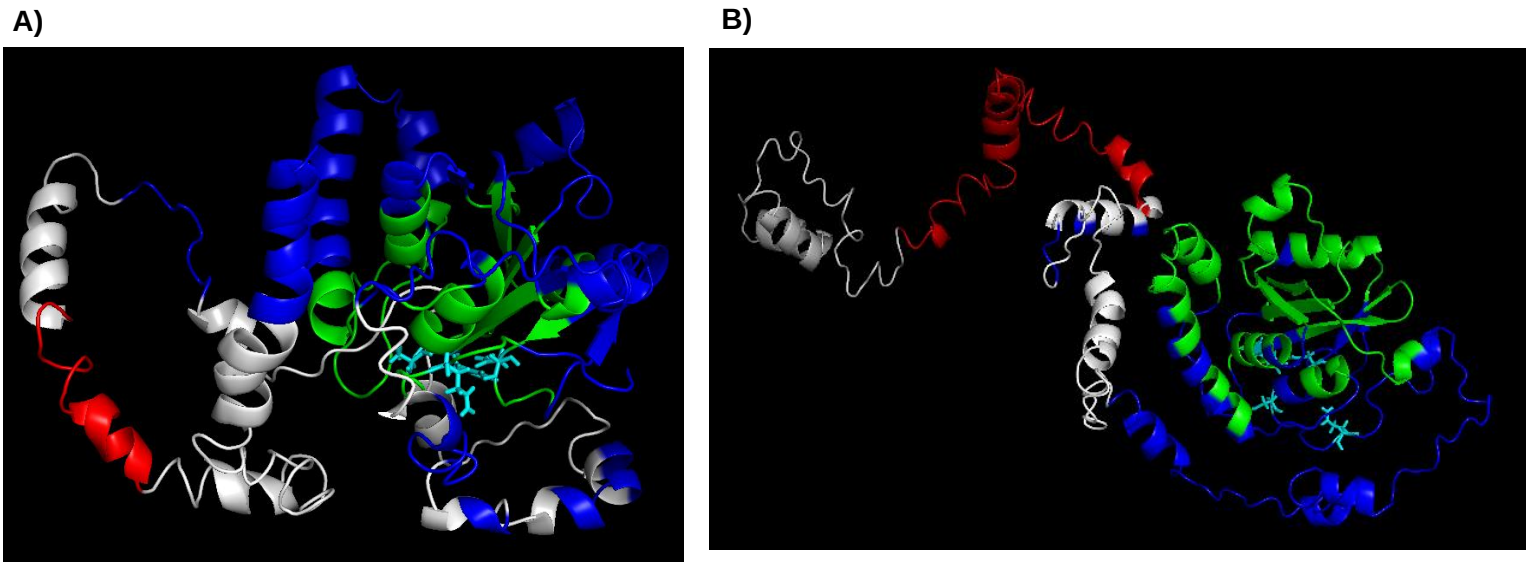

Figure 12: Representation of the predicted interacting regions in ataxin-3 structure. **A**) represents the WT ataxin-3. **B**) represents the EXP ataxin-3. The highlighted regions are the Josephin domain (green), the polyQ tract (red), the interacting regions (blue) and the protein catalytic site (sticks and cyan).

2.1 Interactors with increased affinity to EXP ataxin-3

Interaction differences were previous by (section 1.4) observed between WT and EXP ataxin-3. To infer binding preference between WT and EXP ataxin-3, here we analysed separately the sum of the number of interface residues of 86 interactors with WT and EXP ataxin-3 considering the whole protein, in the JD region, the region between the JD and the polyQ, and after the C-terminal region after the polyQ. For the first and third regions considered there is an excess of cases for which the number of interactions is higher in WT than EXP (number of interactors that show more interacting residues with EXP form (M-EXP)= 20, number of interactors that show more interacting residues with the WT form (M-WT)= 63, number of interactors presenting equal number of interacting residues in both forms (EXP-WT) = 3, Sign test p<0,001); and M-EXP=4, M-WT=72, EXP-WT=10, Sign test p<0,001; respectively). For the smaller middle region there is, however, a higher number of interactions in EXP than in WT (M-EXP=73, M-WT=11, EXP-WT=2, Sign test p<0,001; respectively).

There are 17 ataxin-3 interactors that show an increase higher than 10% in the percentage of the number of interacting residues with the EXP form compared with the WT form, when considering the entire ataxin-3 protein (**Table 3**). This increase is mainly due to an increase in the region between the JD and the polyQ region (**Figure 13**). Indeed, for all 17 interactors there is an increase in this region that is always higher than

19%, while for the JD there are only four such cases and the value is always below 15% (**Table 3**).

The comparison of the number of binding residues between these 17 proteins with the other 69 with WT ataxin-3 we find a significant difference only at the region between the JD and the polyQ region in the two groups (Mann-Whitney U test *p*=0,010; mean ranks: 46,9 (N= 69), 29,53 (N=17); **Figure 14**). When performing a similar analysis with the number of residues of the EXP ataxin-3 form we also observed a significant difference in this region (Mann-Whitney U test *p*=0,014; mean ranks: 46,8 (N= 69), 30,09 (N=17); **Figure 15**). These results show that these 17 interactors interact more in the region between the JD and before the polyQ region than the remaining network, even with the WT ataxin-3 form. These 17 interactors are not enriched in any protein function, according to Panther classification system [115-117]. Furthermore, 23% of these interactors have paralogs in *Drosophila,* described as modifiers of mutant flies [99, 101, 102]. These proteins could play a role in SCA3 pathology.

Table 3: Interactors that show an increase in the number of interacting residues higher than 10% in EXP ataxin-3 compared to WT, when using the entire protein. We also show these differences considering only the JD, region between the JD and the polyQ, and the region after the polyQ. Stars indicate the proteins that present a *Drosophila* paralogue.

Protein name	Gene name	Gene ID	Percentage of interaction differences (EXP-WT ataxin-3)			
			Entire protein	JD	Between the JD and the polyQ region	After polyQ region
60S acidic ribosomal protein P0	RPLP0	6175	18,6	0,0	57,7	-100,0
Mitochondrial genome maintenance exonuclease 1	MGME1	92667	16,9	14,7	19,4	0,0
B-cell CLL/lymphoma 7 protein family member C	BCL7C	9274	16,8	7,8	56,5	0,0
Chitobiosyldiphosphodolichol beta-mannosyltransferase	ALG1	56052	15,4	-1,4	54,2	-100,0
Very-long-chain enoyl-CoA reductase	TECR	9524	11,8	-11,7	60,9	-100,0
Histone deacetylase 6*	HDAC6	10013	11,3	-8,0	61,9	-100,0
Cyclin-dependent kinase 4	CDK4	1019	10,8	-31,0	80,8	0,0
Mitochondrial dicarboxylate carrier	SLC25A10	1468	10,7	-10,9	62,1	-100,0
Acyl-coenzyme A thioesterase 9, mitochondrial	ACOT9	23597	9,9	2,8	44,7	-100,0
HLA class I histocompatibility antigen, A alpha chain	HLA-A	3105	9,5	-7,2	65,5	0,0
Sideroflexin-4*	SFXN4	119559	9,4	-15,4	58,1	-100,0
Rho GDP-dissociation inhibitor 1	ARHGDIA	396	9,1	1,3	44,8	-100,0
Ubiquitin-conjugating enzyme E2 variant 1	UBE2V1	7335	8,1	-16,9	54,7	-100,0
Polyubiquitin-B*	UBB	7314	7,9	-2,1	55,6	-100,0
Polyubiquitin-C*	UBC	7316	7,6	-31,6	53,2	-100,0

E3 ubiquitin-protein ligase AMFR	AMFR	267	7,1	-2,9	24,1	33,3
Estradiol 17-beta-dehydrogenase 11	HSD17B11	51170	4,8	-16,7	54,7	-100,0

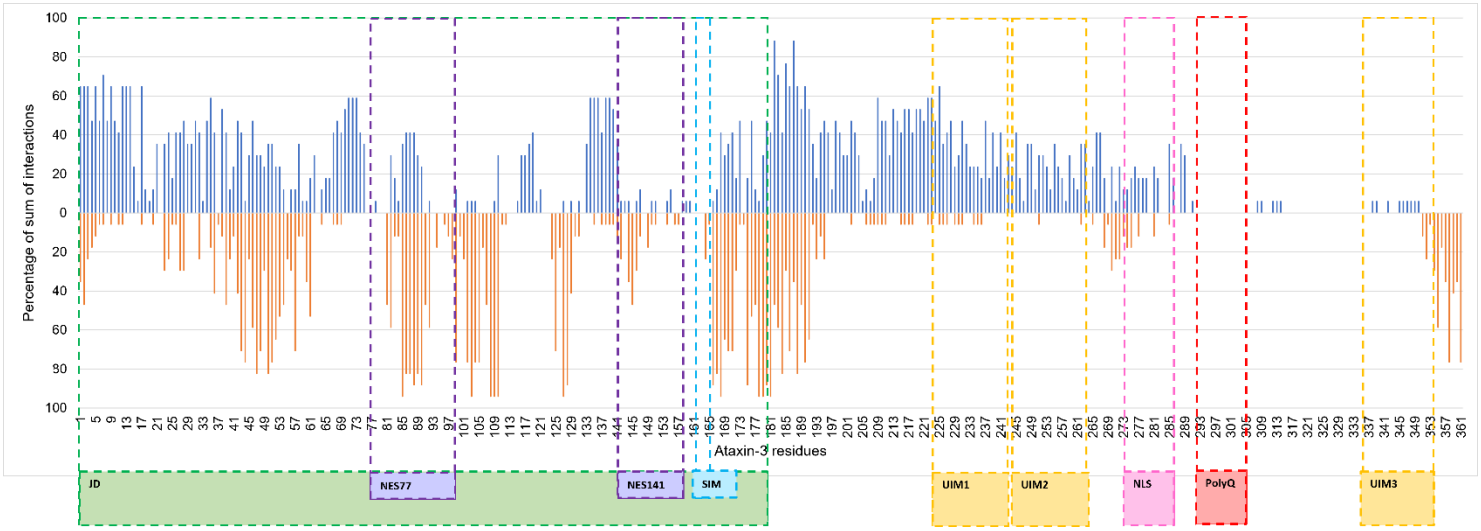

Figure 13: Predicted representation of 17 proteins that interact more with EXP ataxin-3 (blue) versus their interaction with WT ataxin-3 (orange). The JD represents the Josephin domain (1 – 180 residues), NES77 and NES141 represent the nuclear export signal 77 (77 – 99 residues) and 141 (141 – 158 residues), SIM represents the [SUMO]-interacting motif (162 – 165 residues), UIM represents the ubiquitin interacting motif 1 (224 – 243 residues) 2 (244 – 263 residues) and 3 (335 – 354 residues) and the polyQ tract (292 – 305 residues).

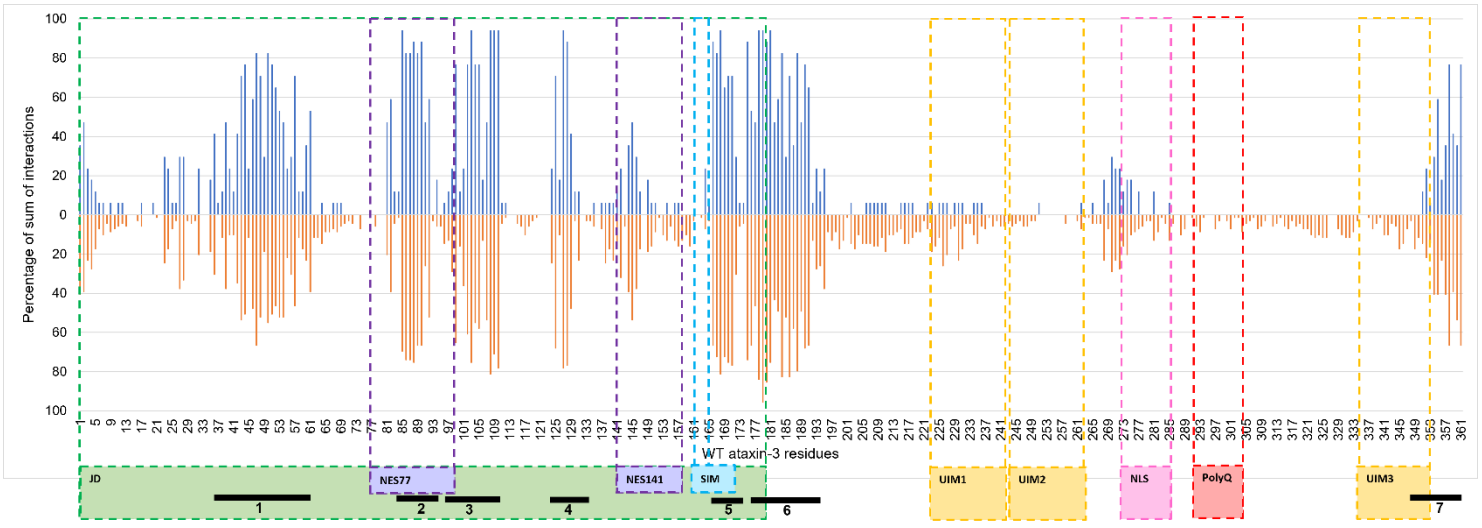

Figure 14: Predicted representation of 17 proteins (blue) versus the rest of analysed network (orange) for WT ataxin-3. The JD represents the Josephin domain (1 – 180 residues), NES77 and NES141 represent the nuclear export signal 77 (77 – 99 residues) and 141 (141 – 158 residues), SIM represents the [SUMO]-interacting motif (162 – 165 residues), UIM represents the ubiquitin interacting motif 1 (224 – 243 residues) 2 (244 – 263 residues) and 3 (335 – 354 residues) and the polyQ tract (292 – 305 residues). The main interacting regions (black bars) are also represented 1 (35 – 61 residues), 2 (85 – 92 residues), 3 (96 – 110 residues), 4 (124 – 131 residues), 5 (166 – 172 residues), 6 (175 – 195 residues) and 7 (349 – 361 residues).

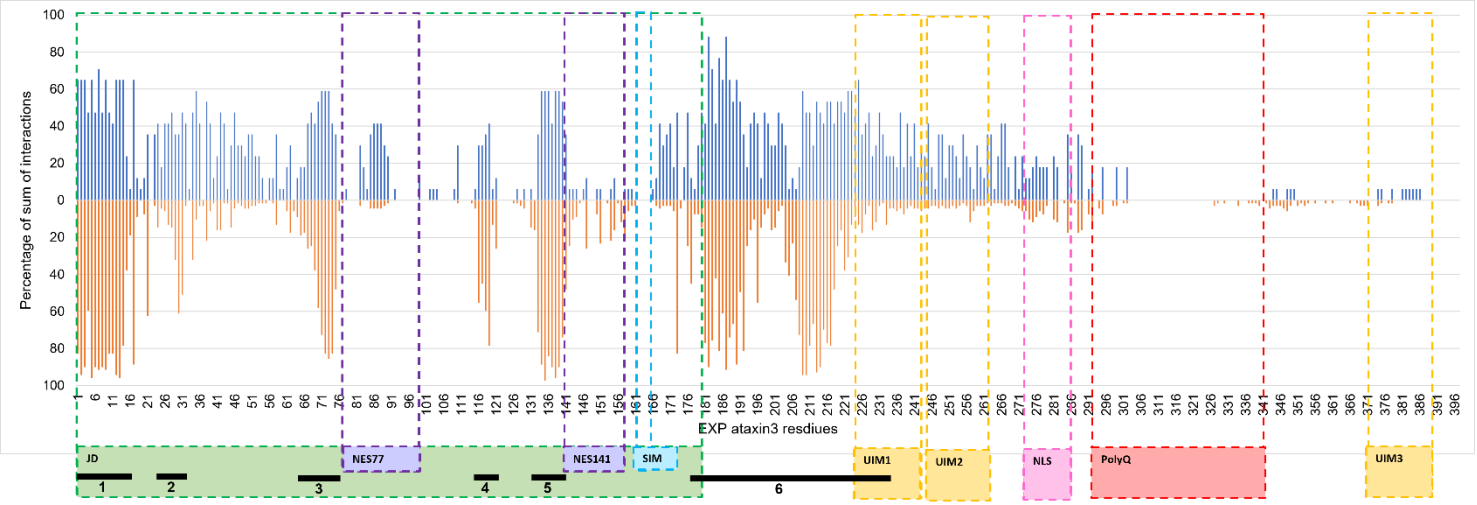

Figure 15: Predicted representation of 17 proteins (blue) versus the rest of analysed network (orange) for EXP ataxin-3. The JD represents the Josephin domain (1 – 180 residues), NES77 and NES141 represent the nuclear export signal 77 (77 – 99 residues) and 141 (141 – 158 residues), SIM represents the [SUMO]-interacting motif (162 – 165 residues), UIM represents the ubiquitin interacting motif 1 (224 – 243 residues) 2 (244 – 263 residues) and 3 (371 – 390 residues) and the polyQ tract (292 – 341 residues). The main interacting regions (black bars) are also represented 1 (1 – 17 residues), 2 (24 – 31 residues), 3 (65 – 75 residues), 4 (116 – 121 residues), 5 (131 – 142 residues) and 6 (176- 233 residues).

It should be noted that by using such a high threshold, we discard the five proteins (SDHB, COA7, serpin H1, NDUFA4 and ATP-citrate synthase) identified as interacting more with EXP ataxin-3, using mass spectrometry analysis [3]. These results agree with those reported for polyubiquitin-C (UBC), since it has been described that this protein is recruited into aggregates formed by C-terminal EXP ataxin-3 [77].

3. Changes in gene expression of the proteins that could be relevant in SCA3 are not associated with the disease

Individuals having the *ATXN3* with an expanded polyQ region express the gene during its life but they only show the disease phenotype late in life (around 40 years of age). One known fact that contributes for an early disease appearance is the polyQ tract length [1]. As we show here (section 2) the polyQ tract expansion alters the C-terminal tail conformation that impairs substrates interactions with ataxin-3, allowing the catalytic site inactivation. So, it is possible that larger polyQ tract expansions destabilize even more the ataxin-3 structure and that cellular perturbation would be more severe. But this does not explain why the disease appears late in life. It should also be noted that SCA3 is an autosomal hereditary disease [1], where one mutated *ATXN3* allele is sufficient to cause the disease. But why the disease is latte onset? It is possible that during the lifetime the expression of the genes associated with the disease changes drastically, causing the appearance of the disease.

To address this hypothesis we looked at the expression of genes of the ataxin-3 interactors reported in **Table 3**, during life time of SCA3 appearance (8 years (the earliest age associated with SCA3), to 40 years (the oldest available age associated with SCA3), using data from BrainSpan: Atlas of the Developing Human Brain, for the CNS structures that matter in SCA3, namely the basal ganglia (striatum), and the thalamus (mediodorsal nucleus of thalamus) [1, 4, 24]. As shown in **Figure 16**, none of the 17 genes that show a marked increase in the number of interactions with the EXP ataxin-3 shows suppressed expression at late ages. Therefore, the cause of the disease seems not to be related with expression of the gene during lifetime.

A)

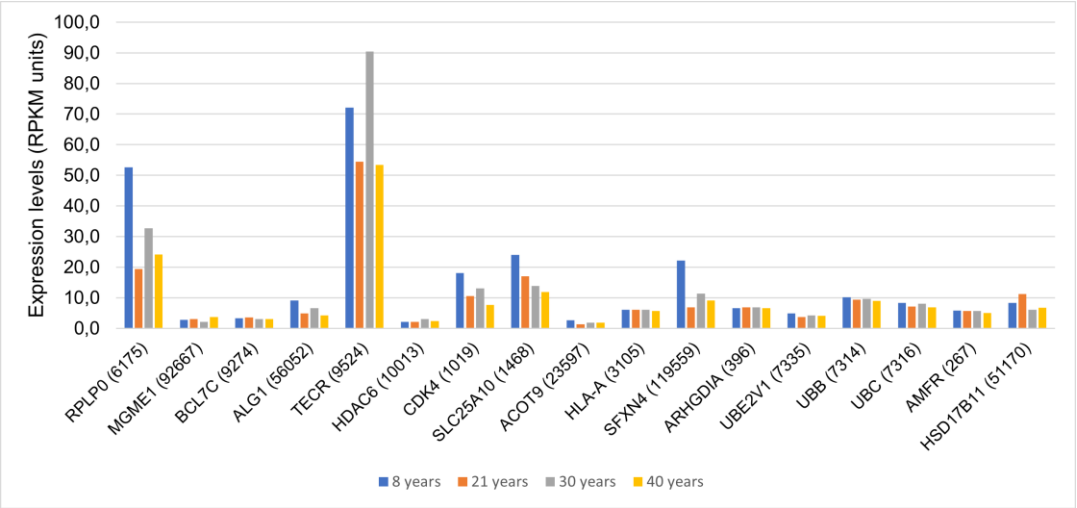

B)

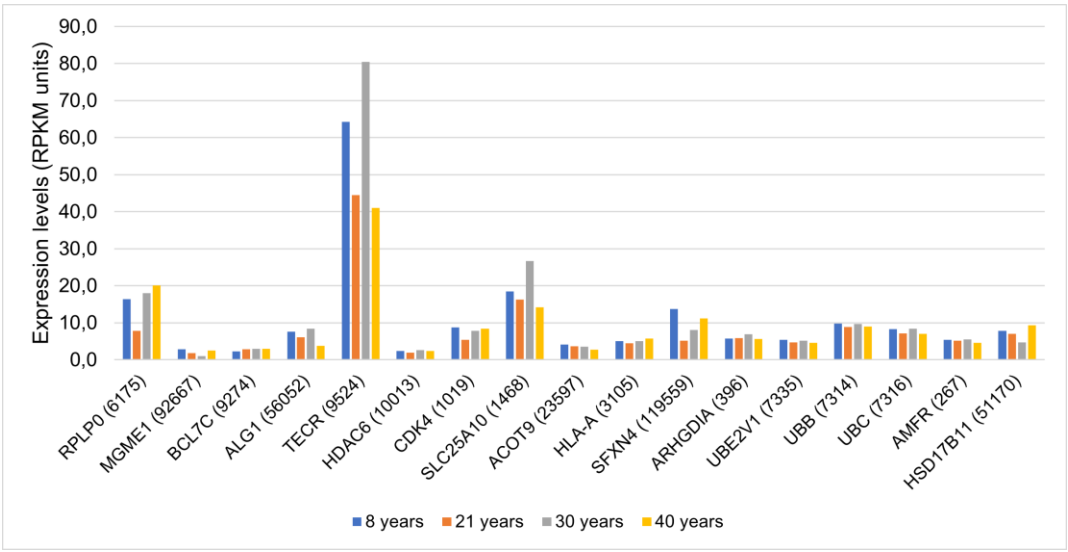

Figure 16: Expression of 17 proteins that interacts more with EXP ataxin-3 for the ages of 8 years (blue), 21 years (orange), 30 years (grey) and 40 years (yellow) in striatum (**A**) and mediodorsal nucleus of thalamus (**B**).

4. JosD1 can interact with ataxin-3 interactors

It is known that inactivation of the *ATXN3* in mouse does not lead to gross abnormalities compared with WT animals, although morphological examination revealed increased levels of ubiquitinated proteins in tissues [214]. A similar result has been reported for *C. elegans* [215]. One hypothesis to explain this observation is that other elements of the MJD DUB family could compensate for the lack of *ATXN3*. It should be noted that in mouse there is only JosD1 and JosD2, since the duplication that gave rise to ataxin-3L occurred only about 40 million years ago in Catarrhini (Cercopithecidae, Hominidae, e Hylobidae) [92, 94, 95].

Levels of expression, according to Brainspain [118], for the human JosD1 and JosD2 in striatum (belongs to basal ganglia) and mediodorsal nucleus of thalamus, two brain tissues that matter to SCA3, are shown in **Figure 17**. JosD1 and JosD2 are expressed in these tissues, and they present higher expression levels than ataxin-3. It should also be noted that ataxin-3L is not expressed in these tissues and is mainly expressed in testis.

A)

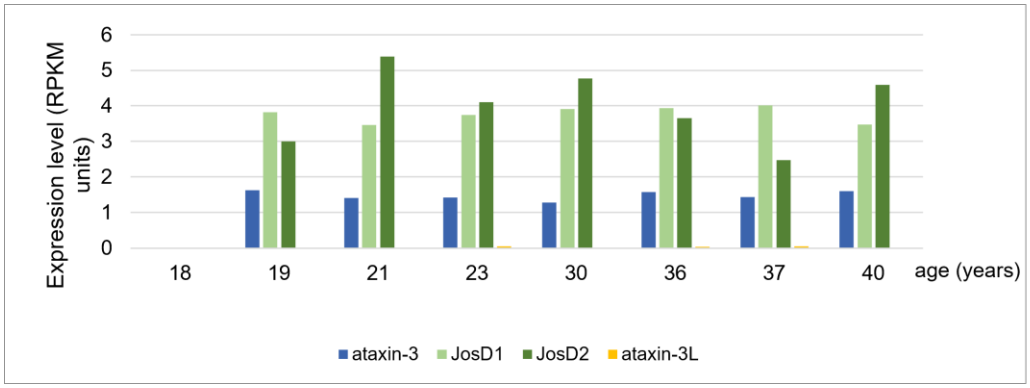

B

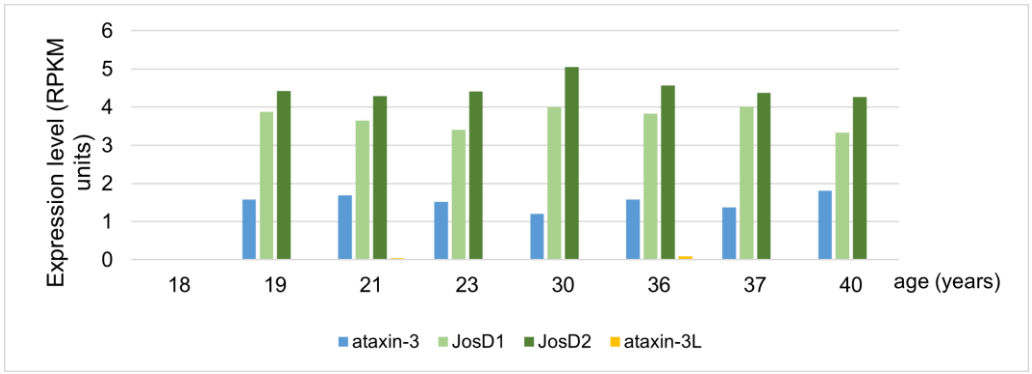

Figure 17: Expression of the four MJD DUB family (ataxin-3, JosD1, JosD2 and ataxin-3L), through lifetime in the affected SCA3 tissues: striatum (**A**) and mediodorsal nucleus of thalamus (**B**).

The JosD1 and JosD2 network (considering only the proteins that interact directly with these proteins (L1 level)), obtained from EvoPPI, revealed 39 interactors for JosD1 (**Supplementary Table 8**), and 17 interactors for JosD2 (**Supplementary Table 9**). Only two proteins are in common in the two PPI networks (CHIP and UBC), suggesting that either the two networks are incomplete or that, they are performing different functions, in spite of having a JD. Comparing these networks with that of the ataxin-3 only 15% of JosD1 network (E3 ubiquitin-protein ligase TRIM63 (Gene ID 84676), E3 ubiquitin-protein ligase Praja-1 (Gene ID 64219), Ubiquitin carboxyl-terminal hydrolase 21 (Gene ID 27005), Tripartite motif containing protein 54 (Gene ID 57159), CHIP (Gene ID 10273) and UBC (Gene ID 7316)) and 12% of JosD2 network (NADH dehydrogenase [ubiquinone] 1 alpha subcomplex subunit 8 (Gene ID 4702), CHIP and UBC) are in common. Since we have shown that most of the ataxin-3 interactors are predicted to interact in the JD, this result suggests that the JosD1 and JosD2 networks are incomplete. Here, we address for JosD1, using the *in-silico* methodology and 81 (out of the 86) ataxin-3 interactors analysed in the previous section, the overlap of the two networks.

The results reveal that all 81 ataxin-3 interactors can also interact with JosD1, and that most of the predicted interacting residues are located in the C-terminal region of the JD (**Figure 18**). Although only three proteins (CHIP, UBC and Ubiquitin carboxyl-terminal hydrolase 21) of the JosD1 network were here analysed, the interaction pattern is similar to that observed for the 78 proteins here predicted as JosD1 interactors (**Figure 19**). This result is in agreement due to the high structural similarity of JosD1 and ataxin-3 in their catalytic domain [216]. When the predicted interacting regions of the JosD1 are compared with those of WT and EXP ataxin-3, we observe that two of the JD regions (124 – 131 that correspond to 99 – 106 in ataxin-3 and 107 – 114 in JosD1, and near to the 166 – 172 that correspond to 127 – 133 in ataxin-3 and 147 – 153 in JosD1) important for WT ataxin-3 binding, are in common with the predicted JosD1 interaction regions (**Figure 20**). Binding in these regions could explain the phenotype rescue in mutant mouse without ataxin-3. Indeed, at these regions, 52% and 84% of proteins report, at least, one interacting residue in 107 – 114 and 147 – 153 of JosD1 regions respectively. These JD regions are not predicted as binding regions of EXP ataxin-3 (**Figure 20**), and thus, JosD1 seems not to play a role in SCA3.

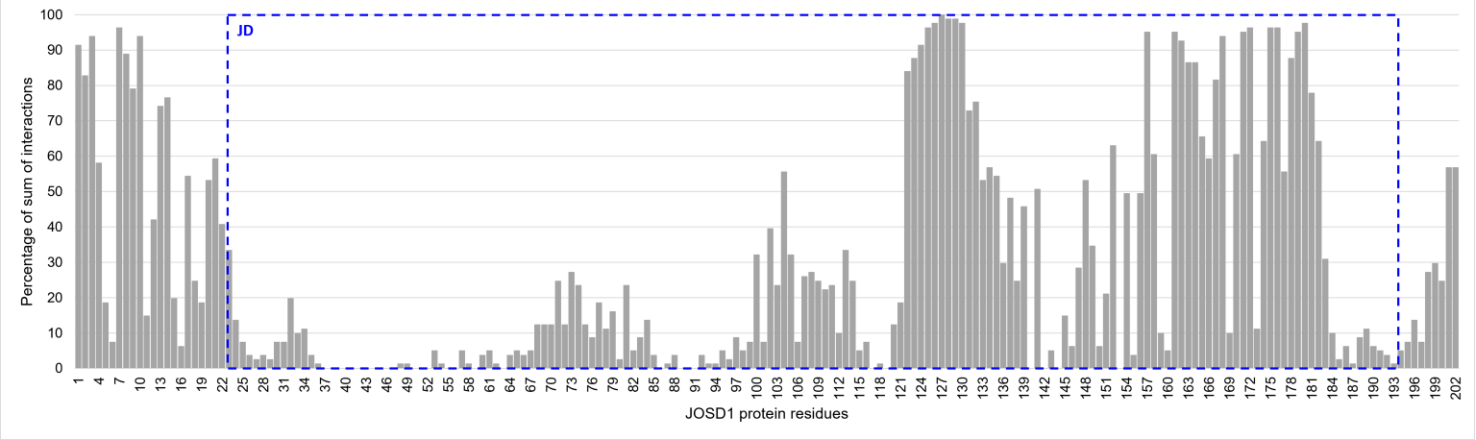

Figure 18: Predict JosD1 interactions regions with the 81 ataxin-3 interactors analysed in this study. The blue square represents the JD (range from 23 to 194 amino acids).

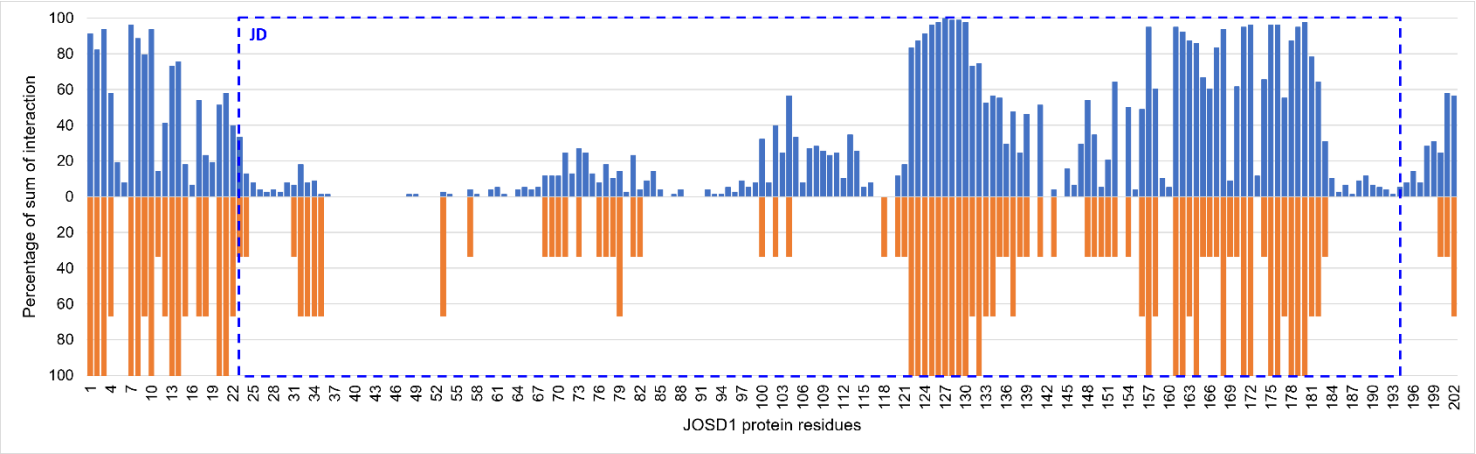

Figure 19: Predicted JosD1 interactions of three JosD1 network (orange) versus the remaining 78 proteins of ataxin-3 network (blue). The JD is represented by the blue square.

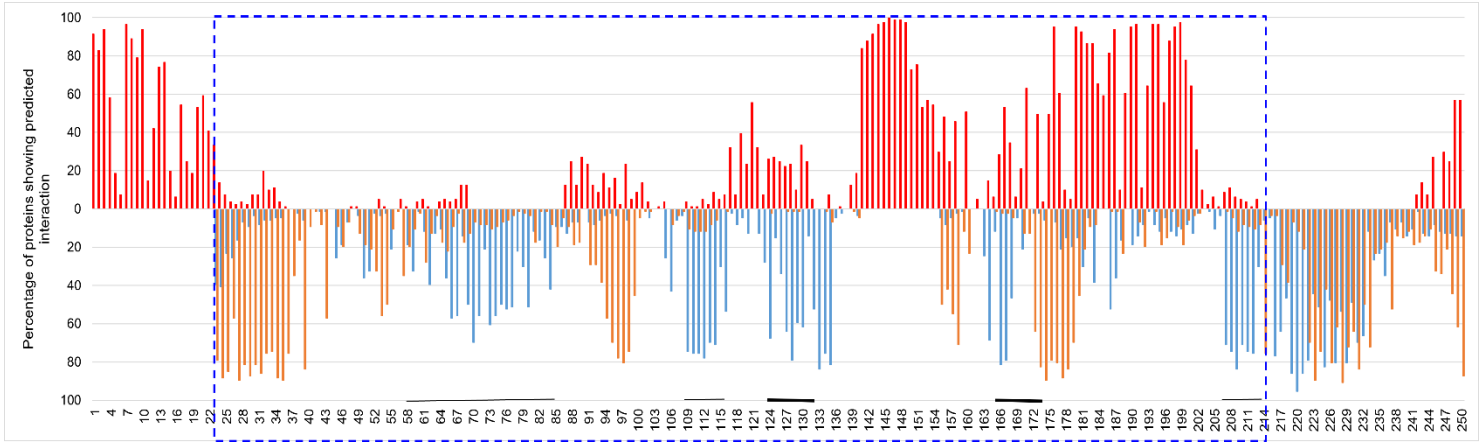

Figure 20: Percentage of proteins showing interaction with JosD1 (in red) and WT (in blue) and EXP (orange) ataxin-3 forms with evidence for JD (blue square). The lines represent the most interacting regions in WT ataxin-3, the ticked lines represent the regions that are common with JosD1.

Discussion

1. *Drosophila melanogaster* is an important SCA3 model

Drosophila overexpressing human EXP ataxin-3 in the eye has been used as a model for SCA3 research [96]. Nevertheless, the suitability of such model is not obvious. Ataxin-3 is composed of a JD and a C-terminal region that is larger than the JD. In *Drosophila*, there is only one gene (JOSL-DROME), that encodes for a protein that is mainly the JD. Furthermore, the human and fly genes belong to different gene linages [93, 94, 96]. Therefore, the JOSL-DROME interactome could be different from that of ataxin-3. Here we show that fly paralogs have been found for only 56 out of 150 ataxin-3 interactors, even when large modifier data sets are used (521 [101], 126 [102] and 18 [99]) as well as EvoPPI web tool [104]. This observation suggests that the fly model offers an incomplete picture of the interactions observed in humans. The discrepancy between the number of reported ataxin-3 interactions in humans (150) and the large number of modifier fly genes (more than 521) could either mean that the human ataxin-3 interactome is very incomplete, or that, the genes identified as modifiers genes in flies, are related with toxicity and not the aggregation phenotype characteristic of the SCA3.

Another limitation is that not all ataxin-3 interactors have fly paralogous genes that are expressed in the fly eye. Expression studies (by RNA-seq) of male and female flies reveal that seven proteins (Serpin 28Db Gene ID 326261, GEO10511p1 Gene ID 41285, Pickpocket 14 Gene ID 33887, Maltase A3 Gene ID 35826, Uncharacterized protein, isoform B Gene ID 33318, AT19485p Gene ID 31978, and Regulatory particle triple-A ATPase 6-related Gene ID 43635) have a low or are even non-expressed in the fly brain and eye. Their identification as ataxin-3 modifiers could be an indication of the weaknesses of the RNAi methodology used [101], but the same argument applies to RNA-seq experiments [119]. Moreover, RNA-Seq experiments may not be able to detect the expression of genes with low expression levels [119]. Here, it has been noticed that genes (Gene IDs) 326261, 33318 and 31978 have paralogs other than the ones considered before, that are expressed in the fly eye. In this study, interactions are inferred between all seven proteins and ataxin-3 or JOSL-DROME, suggesting that they are true interactors of JOSL-DROME, although not necessarily in the eye. Indeed, the gene encoding JOSL-DROME (CG3781) is expressed through fly body. For two human proteins (Caspase 1 and TOMM20-like protein 1) that show little expression in human brain**,** the same argument could apply since ataxin-3 is ubiquitously expressed through the human body [25]. For both the human protein TOMM20-like protein 1 and its fly paralog (GEO10511p1, CG14690), low or non-existent expression in brain or eye is observed, meaning that this is likely the case.

In this study, it is also shown that the JOSL-DROME proteins reported as ataxin-3 modifiers is fly mutants that have a paralogous ataxin-3 interactor, can interact with JOSL-DROME, and that, the predicted interaction regions in the JD region are observed in regions conserved with ataxin-3 (**Figure 2** and **3**). Indeed, the ataxin-3 predicted interaction residues are the same for human interactors and their *Drosophila* paralogs (**Figure 4** and **Figure 7**). Moreover, the interaction residues are similar in other proteins that do not present a fly paralogs (**Figure 5**). These results support *Drosophila* as a good model to study ataxin-3 interactions, and that, the absence of ataxin-3/ataxin-3L lineage is not a major disadvantage of the model. Inferences made in *Drosophila* for genes with human paralogs can likely be extended to fly genes without human paralogs. The common ground to the ataxin-3 interactome groups is the ubiquitination pathway. This is not surprising, since ataxin-3 is capable of removing ubiquitin (the major endorsement for proteins degradation, in particularly by the proteasome) from substrates [32].

2. JD as a major interacting region of ataxin-3 that is influenced by the polyQ tract expansion

Since most of the ataxin-3 interactome proteins denote the same binding behaviour (**Figure 5**), which implies that the *in-silico* method works well, further studies were conducted to evaluate the impact of the presence of an expanded polyQ tract in ataxin-3. The expanded polyQ tract likely promotes coiled-coil domain formation in its vicinity, which can modulate ataxin-3 PPI [15, 16]. Comparison of WT and EXP ataxin-3 interacting residues was performed revealing a distinct behaviour between the two (**Figure 6**). The most affected area seems to be the JD (**Figure 6**), and as expected, since SUMO1 [48, 138], NEDD8 [79], HDAC6 [83], tubulin alpha [85] and RAD23A [36, 37] are reported to interact with this domain, this likely implies loss of ataxin-3 function. This is likely true even for some of the proteins that could not be studied because they show more than six interacting residues at the polyQ tract, which has been associated with poor predictions [2]. Indeed, tubulin beta [85], p53 [178], Rho GDP dissociation inhibitor alpha [138], BCL2 like [181] and HAP-1 [191], FOXO4 [56], 26S proteasome [62, 159], parkin [72], RAD23B [36, 37] and E3 ubiquitin-protein ligase MGRN1 [192] also mainly interact with JD. FOXO4 [56], 26S proteasome [62, 159], parkin [72], RAD23A and RAD23B [36, 37] proteins have also been reported to interact at the JD in the presence of an expanded polyQ tract. There is thus no doubt that JD is the major ataxin-3 interacting region. 89% of the proteins here analysed interact in this region when considering the WT ataxin-3. Nevertheless, 11% of the interactors here studied, show a preference for interacting with the C-terminal ataxin-3 region, mainly in the region

between the JD and the polyQ. Some proteins, such as VCP, CBP, P300 and PCAF have been reported to interact predominantly with C-terminal ataxin-3 with a higher affinity for expanded forms. VCP forms a ternary complex with ataxin-3 and E4B [74], so it is possible that proteins that interact at C-terminal ataxin-3 free the JD for interaction with other proteins.

In this study five major interacting regions of WT ataxin-3 were identified, at the JD (35 – 61, 85 – 92, 96 – 110, 124 – 131 and 166 – 172 residues). The other two main interacting regions are the residues 175 – 195 and 349 – 361, both located close to JD (**Figure 12A**), suggesting their involvement in ataxin-3 interactions, possibly by stabilizing them. However, in EXP ataxin-3 there are five main interacting regions in JD, namely 1 – 17, 24 – 31, 65 – 75, 116 – 121 and 131 – 142, all different from WT ataxin-3, and only one (176 – 233) is in common with WT ataxin-3. But further studies are needed to better understand this implication in SCA3 pathology and how it could help in a novel therapy development.

JD interactions in WT ataxin-3 are located above the ataxin-3 catalytic site (**Figure 12A**), while in EXP ataxin-3 are not (**Figure 12B**). As a consequence, EXP ataxin-3 catalytic site could be inactive, and although *in vitro* studies do not report catalytic activity, polyUb binding and hydrolysis alterations are observed in the presence of an expanded polyQ [29, 38]. The fact that the DNA repair pathway becomes inactive under polyQ tract expansion (inactivation of PNKP [52, 53]), offers support to the predicted catalytic site inactivation. Moreover, the JD predicted binding regions of WT ataxin-3, for most of the used interactors, are located in ubiquitin binding site 1 (above the catalytic site) and 2 (aromatic cluster Y27, F28 and W87), suggesting that these regions will shelter more than ubiquitin and RAD23 proteins (in case of site 2) [33, 35, 36]. Another two regions are conserved between the two proteins (**figure 8**), but since region 181 – 209 is closer to JD, it may be the most important one (**Figure 9**), even because there is a high number of interactions in this region. JD proximity could stabilize substrates interaction and because of that increase the interface binding.

In sum, the ataxin-3 binding alterations are imposed by an expanded polyQ tract that perturbs the native conformational state, allowing DUB activity inactivation. As a result, biological pathways are dysregulated, culminating in SCA3 pathology.

Interaction affinities are also here inferred, since in some cases, such as VCP binding with ataxin-3, a more stable interaction could delay EXP ataxin-3 degradation by proteasome [74]. For 38 out of 86 interactors (**Supplementary Table 10**), distributed by ubiquitination, non-ubiquitination, non-enriched and with fly paralogs, higher affinity is

inferred with EXP ataxin-3 than with WT ataxin-3. A subset of 17 proteins (**Table 3**) shown a high increase in the number of interacting residues and those are the most likely to contribute to SCA3 pathology. Kristensen and co-workers identified five proteins (SDHB, COA7, serpin H1, NDUFA4 and ATP-citrate synthase) as interacting more with EXP ataxin-3. There are also 16 proteins (SLC25A5, SFXN4, UBB, CHIP, CDK4, ACOT9, SLC25A1, SLC25A10, MGME1, TERC, C8orf82, ALG1, RPL10, NDUFA8, CISD2 and HSD17B11) that are here inferred as having more interaction sites with EXP ataxin-3 that weren´t reported by these authors [3]. At first this seems a bit odd, but the authors also report that, when performing Western blot analysis, SDHB and NDUF4A do not show binding differences between the two ataxin-3 forms but that when performing immunoprecipitation assays differences are observed [3]. Therefore, further confirmation needs to be done for these proteins. Nevertheless, for two proteins (CHIP, and UBC that is in the short list of proteins with the higher number of interactors with the EXP ataxin-3) predicted affinities are increased in EXP ataxin-3, as previously reported. CHIP interacts more with EXP ataxin-3 than with WT ataxin-3 [64, 68], and UBC is more recruited into aggregates formed by C-terminal EXP ataxin-3 than by WT ataxin-3 [77]. These observations raise doubts on whether the available large scale techniques used to infer binding affinities have the needed accuracy to detect such differences. Therefore, the 38 proteins here identified as binding more with EXP ataxin-3 than with WT ataxin-3, and in particular the subset of 17 that show large differences between the two protein forms, may have an important role in SCA3. Experimental evidence supporting the role of these proteins is, however, unavailable.

3. Evaluation of the SCA3 late onset appearance

SCA3 is a dominant autosomal hereditary disease [1], so affected individuals can have one mutated *ATXN3* allele and one normal allele, and this is associated with a late onset (appearing around the fourth decade of life) [19]. In this work we address if expression during lifetime of ataxin-3 interactors could be associated with SCA3 pathology. We found no major expression variation through lifetime for those proteins that interact with ataxin-3 (**Figure 16**), and thus their expression seems not to be associated with SCA3 development.

4. JosD1 and SCA3 pathology

It is known that in mice and nematodes *ATXN3* knockouts do not report significant abnormalities, suggesting that other MDJ DUB family members could be performing

similar functions and compensate for its absence [25]. Because of the high structural similarity of JosD1 and ataxin-3 in their catalytic domain [216], in this work, we predicted the interaction of 81 (out 86) interactors of ataxin-3 with JosD1 protein (**Figure 18**). The results also revealed that JosD1 and WT ataxin-3 share two binding regions (107 – 144 and 147 – 153 in JosD1 that correspond to 99 – 106 and 127 – 133 in ataxin-3; **Figure 20**), suggesting that JosD1 is able to replace, at least partially, WT ataxin-3 function. This result is in agreement with the observation that DUB activity of JosD1, that is positively regulated by its own ubiquitination, is similar to that of ataxin-3 [216]. The binding preferences of JosD1 with the ataxin-3 interactors seem to be different from those observed with EXP ataxin-3 (**Figure 20**), questioning the involvement of JosD1 in SCA3 pathology.

5. Validation of predicted ataxin-3 interactions

The *in-silico* methodology here used was proven to be an important tool for predicting protein interactions, even when an expanded polyQ tract is present [2]. However, there are limitations. For instance, PPI with six or more interactions in the polyQ region have been associated with low confidence [2]. Nevertheless, the I-TASSER limitation [103], could be in principle be overcome using a novel prediction tool, such as the recently published AlphaFold [217].

Alphafold is a new protein structure prediction algorithm based on artificial intelligence, that in CASP14 event performed better than the other tools (including I-TASSER), even when predicting proteins together with their cofactors (without the cofactors prediction) [218]. Additionally, sequences with 2700 amino acids were predicted by AlphaFold, but isn´t the limit of it [217]. This is an advantage, since six human proteins and one fly protein were here not studied due to the length limitation of I-TASSER. Moreover, I-TASSER builds its structure from PDB templates and only if they are not present in the reference database, it starts from scratch [103, 108], but AlphaFold uses PDB to learn and not to predict [218]. That is, AlphaFold uses the limited data available in PBD to understand the relationship between protein sequences and protein structures, and then predict structures [218]. AlphaFold is at present the most accurate prediction tool, but further work is, however, needed to understand possible limitations of this tool. For instance, AlphaFold only retrieves, in most cases, one protein structure, and thus proteins with multiple conformations are left out, while in I-TASSER a maximum of five can be obtained [2]. Other AlphaFold limitations are the fact that protein ligands are not predicted but their sites are (in a similar way as in I-TASSER [108]), does not

validate the effect of mutations in a predicted structure, and for unstructured or disorganized regions the predictions are not as accurate.

The *in-silico* approach here applied is validated using earlier publication data but, although very useful predictions must be validated using experimental data.

Conclusion:

The *in-silico* approach described by Rocha *et al.* for ATXN1 [2] was successfully applied to predict interactions for WT and EXP ataxin-3, JOSL-DROME, and JosD1 proteins. Here it is shown that *Drosophila* is a good model to study SCA3, even though there is no ataxin-3/ataxin-3L orthologs in flies. Moreover, we identified regions that seem to be essential for ataxin-3 binding. We also show that these regions change with the conformational alterations imposed by polyQ tract expansion, that are the cause of SCA3 pathology. We postulate a major role for 17 ataxin-3 interactors in SCA3 pathology, based on the binding differences with the two ataxin-3 forms.

Future Work

In the future we aim to understand the importance of the main interacting regions of WT and EXP ataxin-3, as well as validate the involvement of the 17 proteins (that have a higher affinity to EXP ataxin-3) in SCA3, using *in vitro* and/or *in vivo* assays. Furthermore, mass spectrometry analyses of mutant flies will be performed, to identify further ataxin-3 interactors. Moreover, validation of the *in-silico* analyses will be performed using the AlphaFold predicted protein structures, as well as a strategy to overcome I-TASSER limitations.

Bibliography

1. McLoughlin, H.S., L.R. Moore, and H.L. Paulson, *Pathogenesis of SCA3 and implications for other polyglutamine diseases.* Neurobiol Dis, 2020. **134**: p. 104635.
2. Rocha, S., et al., *ATXN1 N-terminal region explains the binding differences of wild-type and expanded forms.* BMC Med Genomics, 2019. **12**(1): p. 145.
3. Kristensen, L.V., et al., *Mass spectrometry analyses of normal and polyglutamine expanded ataxin-3 reveal novel interaction partners involved in mitochondrial function.* Neurochem Int, 2018. **112**: p. 5-17.
4. Matos, C.A., L.P.d. Almeida, and C. Nóbrega, *Machado-Joseph disease/spinocerebellar ataxia type 3: lessons from disease pathogenesis and clues into therapy.* Journal of Neurochemistry, 2019. **148**(1): p. 8-28.
5. Hosp, F., et al., *Quantitative interaction proteomics of neurodegenerative disease proteins.* Cell Rep, 2015. **11**(7): p. 1134-46.
6. Suter, B., et al., *Development and application of a DNA microarray-based yeast two-hybrid system.* Nucleic Acids Res, 2013. **41**(3): p. 1496-507.
7. Ratovitski, T., et al., *Huntingtin protein interactions altered by polyglutamine expansion as determined by quantitative proteomic analysis.* Cell Cycle, 2012. **11**(10): p. 2006-2021.
8. Nedelsky, N.B., et al., *Native functions of the androgen receptor are essential to pathogenesis in a Drosophila model of spinobulbar muscular atrophy.* Neuron, 2010. **67**(6): p. 936-52.
9. Lim, J., et al., *A Protein–Protein Interaction Network for Human Inherited Ataxias and Disorders of Purkinje Cell Degeneration.* Cell, 2006. **125**(4): p. 801-814.
10. Lam, Y.C., et al., *ATAXIN-1 interacts with the repressor Capicua in its native complex to cause SCA1 neuropathology.* Cell, 2006. **127**(7): p. 1335-47.
11. Harjes, P. and E.E. Wanker, *The hunt for huntingtin function: interaction partners tell many different stories.* Trends Biochem Sci, 2003. **28**(8): p. 425-33.
12. MacDonald, M.E., *Huntingtin: Alive and Well and Working in Middle Management.* Science's STKE, 2003. **2003**(207): p. pe48.
13. Takeuchi, T. and Y. Nagai, *Protein Misfolding and Aggregation as a Therapeutic Target for Polyglutamine Diseases.* Brain Sci, 2017. **7**(10).
14. Kratter, I.H. and S. Finkbeiner, *PolyQ disease: too many Qs, too much function?* Neuron, 2010. **67**(6): p. 897-9.
15. Petrakis, S., et al., *Aggregation of polyQ-extended proteins is promoted by interaction with their natural coiled-coil partners.* Bioessays, 2013. **35**(6): p. 503-7.
16. Schaefer, M.H., E.E. Wanker, and M.A. Andrade-Navarro, *Evolution and function of CAG/polyglutamine repeats in protein-protein interaction networks.* Nucleic Acids Res, 2012. **40**(10): p. 4273-87.
17. Lim, J., et al., *Opposing effects of polyglutamine expansion on native protein complexes contribute to SCA1.* Nature, 2008. **452(7188)**: p. 713–718.
18. Karlin, S. and C. Burge, *Trinucleotide repeats and long homopeptides in genes and proteins associated with nervous system disease and development.* Proc. Natl. Acad. Sci., 1996. **93**: p. 1560-1565.
19. Mendonça, N., et al., *Clinical Features of Machado-Joseph Disease.* Adv Exp Med Biol, 2018. **1049**: p. 255-273.
20. Schöls, L., et al., *Autosomal dominant cerebellar ataxias: clinical features, genetics, and pathogenesis.* The Lancet Neurology, 2004. **3**(5): p. 291-304.
21. Subramony, S.H. and R.D. Currier, *Intrafamilial variability in Machado-Joseph disease.* Movement Disorders, 1996. **11**: p. 741-743.

22. Matsumura, R., et al., *The relationship between trinucleotide repeat length and phenotypic variation in Machado-Joseph disease.* J Neurol Sci, 1996a. **139**: p. 52-57.
23. Sequeiros, J. and P. Coutinho, *Epidemiology and clinical aspects of Machado-Joseph disease.* Adv Neurol, 1993. **61**: p. 139-153.
24. Da Silva, J.D., A. Teixeira-Castro, and P. Maciel, *From Pathogenesis to Novel Therapeutics for Spinocerebellar Ataxia Type 3: Evading Potholes on the Way to Translation.* Neurotherapeutics, 2019. **16**(4): p. 1009-1031.
25. Costa Mdo, C. and H.L. Paulson, *Toward understanding Machado-Joseph disease.* Prog Neurobiol, 2012. **97**(2): p. 239-57.
26. Almeida, B., et al., *Trinucleotide repeats: a structural perspective.* Front Neurol, 2013. **4**: p. 76.
27. Bettencourt, C., et al., *Increased transcript diversity: novel splicing variants of Machado-Joseph disease gene (ATXN3).* Neurogenetics, 2010. **11**(2): p. 193-202.
28. Weishaupl, D., et al., *Physiological and pathophysiological characteristics of ataxin-3 isoforms.* J Biol Chem, 2019. **294**(2): p. 644-661.
29. Carvalho, A.L., A. Silva, and S. Macedo-Ribeiro, *Polyglutamine-Independent Features in Ataxin-3 Aggregation and Pathogenesis of Machado-Joseph Disease.* Adv Exp Med Biol, 2018. **1049**: p. 275-288.
30. Antony, P.M., et al., *Identification and functional dissection of localization signals within ataxin-3.* Neurobiol Dis, 2009. **36**(2): p. 280-92.
31. Nobrega, C., et al., *Molecular Mechanisms and Cellular Pathways Implicated in Machado-Joseph Disease Pathogenesis.* Adv Exp Med Biol, 2018. **1049**: p. 349-367.
32. Burnett, B., F. Li, and R.N. Pittman, *The polyglutamine neurodegenerative protein ataxin-3 binds polyubiquitylated proteins and has ubiquitin protease activity.* Hum Mol Genet, 2003. **12**(23): p. 3195-205.
33. Mao, Y., et al., *Deubiquitinating function of ataxin-3: Insights from the solution structure of the Josephin domain.* PNAS, 2005. **102**: p. 12700-12705.
34. Tuite, M.F., et al., *Understanding the Role of the Josephin Domain in the PolyUb Binding and Cleavage Properties of Ataxin-3.* PLoS ONE, 2010. **5**(8).
35. Nicastro, G., et al., *Josephin domain of ataxin-3 contains two distinct ubiquitin-binding sites.* Biopolymers, 2009. **91**(12): p. 1203-14.
36. Wang, G.-h., et al., *Ataxin-3, the MJD1 gene product, interacts with the two human homologs of yeast DNA repair protein RAD23, HHR23A and HHR23B.* Human Molecular Genetics, 2000. **9**: p. 1795-1803.
37. Blount, J.R., et al., *Ubiquitin-binding site 2 of ataxin-3 prevents its proteasomal degradation by interacting with Rad23.* Nat Commun, 2014. **5**: p. 4638.
38. Winborn, B.J., et al., *The deubiquitinating enzyme ataxin-3, a polyglutamine disease protein, edits Lys63 linkages in mixed linkage ubiquitin chains.* J Biol Chem, 2008. **283**(39): p. 26436-43.
39. Mueller, T., et al., *CK2-dependent phosphorylation determines cellular localization and stability of ataxin-3.* Hum Mol Genet, 2009. **18**(17): p. 3334-43.
40. Fei, E., et al., *Phosphorylation of ataxin-3 by glycogen synthase kinase 3beta at serine 256 regulates the aggregation of ataxin-3.* Biochem Biophys Res Commun, 2007. **357**(2): p. 487-92.
41. Wan, L., et al., *Roles of Post-translational Modifications in Spinocerebellar Ataxias.* Frontiers in Cellular Neuroscience, 2018. **12**.
42. Kristensen, L.V., et al., *Polyglutamine expansion of ataxin-3 alters its degree of ubiquitination and phosphorylation at specific sites.* Neurochem Int, 2017. **105**: p. 42-50.
43. Reina, C.P., X. Zhong, and R.N. Pittman, *Proteotoxic stress increases nuclear localization of ataxin-3.* Human Molecular Genetics, 2010. **19**(2): p. 235-249.

44. Amerik, A.Y. and M. Hochstrasser, *Mechanism and function of deubiquitinating enzymes.* Biochim Biophys Acta, 2004. **1695**(1-3): p. 189-207.
45. Bai, J.J., et al., *Ataxin-3 is a multivalent ligand for the parkin Ubl domain.* Biochemistry, 2013. **52**(42): p. 7369-76.
46. Todi, S.V., et al., *Activity and cellular functions of the deubiquitinating enzyme and polyglutamine disease protein ataxin-3 are regulated by ubiquitination at lysine 117.* J Biol Chem, 2010. **285**(50): p. 39303-13.
47. Zhou, Y.F., et al., *SUMO-1 modification on K166 of polyQ-expanded ataxin-3 strengthens its stability and increases its cytotoxicity.* PLoS One, 2013. **8**(1): p. e54214.
48. Pfeiffer, A., et al., *Ataxin-3 consolidates the MDC1-dependent DNA double-strand break response by counteracting the SUMO-targeted ubiquitin ligase RNF4.* EMBO J, 2017. **36**(8): p. 1066-1083.
49. Almeida, B., et al., *SUMOylation of the brain-predominant Ataxin-3 isoform modulates its interaction with p97.* Biochim Biophys Acta, 2015. **1852**(9): p. 1950-9.
50. Matos, C.A., L.P.d. Almeida, and C. Nóbrega, *Proteolytic Cleavage of Polyglutamine Disease-Causing Proteins: Revisiting the Toxic Fragment Hypothesis.* Current Pharmaceutical Design, 2016. **23**: p. 753-775.
51. Weber, J.J., et al., *A combinatorial approach to identify calpain cleavage sites in the Machado-Joseph disease protein ataxin-3.* Brain, 2017. **140**(5): p. 1280-1299.
52. Chatterjee, A., et al., *The role of the mammalian DNA end-processing enzyme polynucleotide kinase 3'-phosphatase in spinocerebellar ataxia type 3 pathogenesis.* PLoS Genet, 2015. **11**(1): p. e1004749.
53. Gao, R., et al., *Inactivation of PNKP by mutant ATXN3 triggers apoptosis by activating the DNA damage-response pathway in SCA3.* PLoS Genet, 2015. **11**(1): p. e1004834.
54. Tu, Y., et al., *Ataxin-3 promotes genome integrity by stabilizing Chk1.* Nucleic Acids Res, 2017. **45**(8): p. 4532-4549.
55. Li, F., et al., *Ataxin-3 is a histone-binding protein with two independent transcriptional corepressor activities.* J Biol Chem, 2002. **277**(47): p. 45004-12.
56. Araujo, J., et al., *FOXO4-dependent upregulation of superoxide dismutase-2 in response to oxidative stress is impaired in spinocerebellar ataxia type 3.* Hum Mol Genet, 2011. **20**(15): p. 2928-41.
57. Evert, B.O., et al., *Ataxin-3 represses transcription via chromatin binding, interaction with histone deacetylase 3, and histone deacetylation.* J Neurosci, 2006. **26**(44): p. 11474-86.
58. Feng, Q., et al., *ATXN3 Positively Regulates Type I IFN Antiviral Response by Deubiquitinating and Stabilizing HDAC3.* J Immunol, 2018. **201**(2): p. 675-687.
59. Ashkenazi, A., et al., *Polyglutamine tracts regulate beclin 1-dependent autophagy.* Nature, 2017. **545**(7652): p. 108-111.
60. Herzog, L.K., et al., *The Machado-Joseph disease deubiquitylase ataxin-3 interacts with LC3C/GABARAP and promotes autophagy.* Aging Cell, 2020. **19**(1): p. e13051.
61. Zhou, L., et al., *p62/sequestosome 1 regulates aggresome formation of pathogenic ataxin-3 with expanded polyglutamine.* Int J Mol Sci, 2014. **15**(9): p. 14997-5010.
62. Doss-Pepe, E.W., et al., *Ataxin-3 interactions with rad23 and valosin-containing protein and its associations with ubiquitin chains and the proteasome are consistent with a role in ubiquitin-mediated proteolysis.* Mol Cell Biol, 2003. **23**(18): p. 6469-83.
63. Durcan, T.M., et al., *Ataxin-3 Deubiquitination Is Coupled to Parkin Ubiquitination via E2 Ubiquitin-conjugating Enzyme.* Journal of Biological Chemistry, 2012. **287**(1): p. 531-541.

64. Scaglione, K.M., et al., *Ube2w and ataxin-3 coordinately regulate the ubiquitin ligase CHIP.* Mol Cell, 2011. **43**(4): p. 599-612.
65. Aguirre, J.D., et al., *Impact of altered phosphorylation on loss of function of juvenile Parkinsonism-associated genetic variants of the E3 ligase parkin.* J Biol Chem, 2018. **293**(17): p. 6337-6348.
66. Bernardi, K.M., et al., *A deubiquitinase negatively regulates retro-translocation of nonubiquitinated substrates.* Mol Biol Cell, 2013. **24**(22): p. 3545-56.
67. Ying, Z., et al., *Gp78, an ER associated E3, promotes SOD1 and ataxin-3 degradation.* Hum Mol Genet, 2009. **18**(22): p. 4268-81.
68. Jana, N.R., et al., *Co-chaperone CHIP associates with expanded polyglutamine protein and promotes their degradation by proteasomes.* J Biol Chem, 2005. **280**(12): p. 11635-40.
69. Todi, S.V., et al., *Ubiquitination directly enhances activity of the deubiquitinating enzyme ataxin-3.* EMBO J, 2009. **28**(4): p. 372-82.
70. Gao, X.C., et al., *Co-chaperone HSJ1a dually regulates the proteasomal degradation of ataxin-3.* PLoS One, 2011. **6**(5): p. e19763.
71. Reina, C.P., et al., *Basal and stress-induced Hsp70 are modulated by ataxin-3.* Cell Stress and Chaperones, 2012. **17**(6): p. 729-742.
72. Durcan, T.M., et al., *The Machado-Joseph disease-associated mutant form of ataxin-3 regulates parkin ubiquitination and stability.* Hum Mol Genet, 2011. **20**(1): p. 141-54.
73. Wang, Q., L. Li, and Y. Ye, *Regulation of retrotranslocation by p97-associated deubiquitinating enzyme ataxin-3.* J Cell Biol, 2006. **174**(7): p. 963-71.
74. Matsumoto, M., et al., *Molecular clearance of ataxin-3 is regulated by a mammalian E4.* EMBO J, 2004. **23**(3): p. 659-69.
75. Zhong, X. and R.N. Pittman, *Ataxin-3 binds VCP/p97 and regulates retrotranslocation of ERAD substrates.* Hum Mol Genet, 2006. **15**(16): p. 2409-20.
76. Boeddrich, A., et al., *An arginine/lysine-rich motif is crucial for VCP/p97-mediated modulation of ataxin-3 fibrillogenesis.* EMBO J, 2006. **25**(7): p. 1547-58.
77. Yang, H., et al., *Aggregation of polyglutamine-expanded ataxin-3 sequesters its specific interacting partners into inclusions: implication in a loss-of-function pathology.* Sci Rep, 2014. **4**: p. 6410.
78. Laco, M.N., et al., *Valosin-containing protein (VCP/p97) is an activator of wild-type ataxin-3.* PLoS One, 2012. **7**(9): p. e43563.
79. Ferro, A., et al., *NEDD8: a new ataxin-3 interactor.* Biochim Biophys Acta, 2007. **1773**(11): p. 1619-27.
80. Chen, L. and K. Madura, *Evidence for distinct functions for human DNA repair factors hHR23A and hHR23B.* FEBS Lett, 2006. **580**(14): p. 3401-8.
81. Kawaguchi, Y., et al., *The Deacetylase HDAC6 Regulates Aggresome Formation and Cell Viability in Response to Misfolded Protein Stress.* Cell, 2003. **115**: p. 727-738.
82. Bonanomi, M., et al., *Interactions of ataxin-3 with its molecular partners in the protein machinery that sorts protein aggregates to the aggresome.* Int J Biochem Cell Biol, 2014. **51**: p. 58-64.
83. Burnett, B.G. and R.N. Pittman, *The polyglutamine neurodegenerative protein ataxin 3 regulates aggresome formation.* PNAS, 2005. **102**: p. 4330-4335.
84. Romaniello, R., et al., *Tubulin genes and malformations of cortical development.* Eur J Med Genet, 2018. **61**(12): p. 744-754.
85. Mazzucchelli, S., et al., *Proteomic and biochemical analyses unveil tight interaction of ataxin-3 with tubulin.* Int J Biochem Cell Biol, 2009. **41**(12): p. 2485-92.
86. Wang, H., Z. Ying, and G. Wang, *Ataxin-3 regulates aggresome formation of copper-zinc superoxide dismutase (SOD1) by editing K63-linked polyubiquitin chains.* J Biol Chem, 2012. **287**(34): p. 28576-85.

87. Kim, S.H., et al., *Self-clearance mechanism of mitochondrial E3 ligase MARCH5 contributes to mitochondria quality control.* FEBS J, 2016. **283**(2): p. 294-304.
88. Fang, L., et al., *MARCH5 inactivation supports mitochondrial function during neurodegenerative stress.* Front Cell Neurosci, 2013. **7**: p. 176.
89. Liu, Y., et al., *Therapeutic Targeting of SDHB-Mutated Pheochromocytoma/Paraganglioma with Pharmacologic Ascorbic Acid.* Clin Cancer Res, 2020. **26**(14): p. 3868-3880.
90. Kadenbach, B., *Regulation of Mammalian 13-Subunit Cytochrome c Oxidase and Binding of other Proteins: Role of NDUFA4.* Trends Endocrinol Metab, 2017. **28**(11): p. 761-770.
91. Fu, F., et al., *NDUFA4 enhances neuron growth by triggering growth factors and inhibiting neuron apoptosis through Bcl-2 and cytochrome C mediated signaling pathway.* Am J Transl Res, 2018. **10**: p. 164-174.
92. Grasty, K.C., S.D. Weeks, and P. J.Loll, *Structural insights into the activity and regulation of human Josephin-2.* Journal of Structural Biology: X, 2019.
93. Scheel, H., S. Tomiuk, and K. Hofman, *Elucidatin of ataxin-3 and ataxin-7 function by integrative bioinformatics.* Human Molecular, 2003. **12**.
94. Marques, I., *Estudos evolutivos dos genes da família da ATXN3 no reino Animalia*. 2020, Faculdade de Ciências.
95. Weeks, S.D., et al., *Crystal structure of a Josephin-ubiquitin complex: evolutionary restraints on ataxin-3 deubiquitinating activity.* J Biol Chem, 2011. **286**(6): p. 4555-65.
96. Xu, Z., et al., *Studying polyglutamine diseases in Drosophila.* Exp Neurol, 2015. **274**(Pt A): p. 25-41.
97. Marsh, J.L. and L.M. Thompson, *Drosophila in the Study of Neurodegenerative Disease.* Neuron, 2006. **52**(1): p. 169-178.
98. Duffy, J.B., *GAL4 system in Drosophila: a fly geneticist's Swiss army knife.* Genesis, 2002. **34**(1-2): p. 1-15.
99. Bilen, J. and N.M. Bonini, *Genome-Wide Screen for Modifiers of Ataxin-3 Neurodegeneration in Drosophila.* PlosGenetics, 2007. **3**(10).
100. Warrick, J.M., et al., *Ataxin-3 suppresses polyglutamine neurodegeneration in Drosophila by a ubiquitin-associated mechanism.* Mol Cell, 2005. **18**(1): p. 37-48.
101. Vobfeldt, H., et al., *Large-Scale Screen for Modifiers of Ataxin-3-Derived Polyglutamine-Induced Toxicity in Drosophila.* Plos One, 2012. **7**(11).
102. Zhang, S., et al., *A genomewide RNA interference screen for modifiers of aggregates formation by mutant Huntingtin in Drosophila.* Genetics, 2010. **184**(4): p. 1165-79.
103. Roy, A., A. Kucukural, and Y. Zhang, *I-TASSER: a unified platform for automated protein structure and function prediction.* Nat Protoc, 2010. **5**(4): p. 725-38.
104. Vazquez, N., et al., *EvoPPI 1.0: a Web Platform for Within- and Between-Species Multiple Interactome Comparisons and Application to Nine PolyQ Proteins Determining Neurodegenerative Diseases.* Interdiscip Sci, 2019. **11**(1): p. 45-56.
105. Hu, Y., et al., *An integrative approach to ortholog prediction for disease-focused and other functional studies.* BMC Bioinformatics, 2011. **12**.
106. Yates, A.D., et al., *Ensembl 2020.* Nucleic Acids Res, 2020. **48**(D1): p. D682-D688.
107. Yang, J., et al., *The I-TASSER Suite: protein structure and function prediction.* Nat Methods, 2015. **12**(1): p. 7-8.
108. Yang, J. and Y. Zhang, *I-TASSER server: new development for protein structure and function predictions.* Nucleic Acids Res, 2015. **43**(W1): p. W174-81.
109. Zhang, Y. and J. Skolnick, *TM-align: a protein structure alignment algorithm based on the TM-score.* Nucleic Acids Res, 2005. **33**(7): p. 2302-9.
110. de Vries, S.J. and A.M. Bonvin, *CPORT: a consensus interface predictor and its performance in prediction-driven docking with HADDOCK.* PLoS One, 2011. **6**(3): p. e17695.

111. van Zundert, G.C.P., et al., *The HADDOCK2.2 Web Server: User-Friendly Integrative Modeling of Biomolecular Complexes.* J Mol Biol, 2016. **428**(4): p. 720-725.
112. Krissinel, E. and K. Henrick, *Inference of macromolecular assemblies from crystalline state.* J Mol Biol, 2007. **372**(3): p. 774-97.
113. Kumar, M., et al., *ELM-the eukaryotic linear motif resource in 2020.* Nucleic Acids Res, 2020. **48**(D1): p. D296-D306.
114. Kumar, S., et al., *MEGA X: Molecular Evolutionary Genetics Analysis across Computing Platforms.* Mol Biol Evol, 2018. **35**(6): p. 1547-1549.
115. Ashburner, M., et al., *Gene ontology: tool for the unification of biology. The Gene Ontology Consortium.* Nat Genet, 2000. **25**(1): p. 25-9.
116. Gene Ontology, C., *The Gene Ontology resource: enriching a GOld mine.* Nucleic Acids Res, 2021. **49**(D1): p. D325-D334.
117. Mi, H., et al., *PANTHER version 14: more genomes, a new PANTHER GO-slim and improvements in enrichment analysis tools.* Nucleic Acids Res, 2019. **47**(D1): p. D419-D426.
118. Hawrylycz, M.J., et al., *An anatomically comprehensive atlas of the adult human brain transcriptome.* Nature, 2012. **489**(7416): p. 391-399.
119. Leader, D.P., et al., *FlyAtlas 2: a new version of the Drosophila melanogaster expression atlas with RNA-Seq, miRNA-Seq and sex-specific data.* Nucleic Acids Res, 2018. **46**(D1): p. D809-D815.
120. IBM, C. *Released 2020*. IBM SPSS Statistics for Windows, Version 27.0.
121. Lyon, M.S. and C. Milligan, *Extracellular heat shock proteins in neurodegenerative diseases: New perspectives.* Neuroscience Letters, 2019. **711**: p. 134462.
122. Hoter, A., M.E. El-Sabban, and H.Y. Naim, *The HSP90 Family: Structure, Regulation, Function, and Implications in Health and Disease.* Int J Mol Sci, 2018. **19**(9).
123. Ito, S. and K. Nagata, *Biology of Hsp47 (Serpin H1), a collagen-specific molecular chaperone.* Semin Cell Dev Biol, 2017. **62**: p. 142-151.
124. Paul, B.D., J.I. Sbodio, and S.H. Snyder, *Cysteine Metabolism in Neuronal Redox Homeostasis.* Trends Pharmacol Sci, 2018. **39**(5): p. 513-524.
125. Hein, M.Y., et al., *A human interactome in three quantitative dimensions organized by stoichiometries and abundances.* Cell, 2015. **163**(3): p. 712-23.
126. Gao, R., et al., *Mutant huntingtin impairs PNKP and ATXN3, disrupting DNA repair and transcription.* Elife, 2019. **8**.
127. Li, Y., et al., *Bax-inhibiting peptide protects cells from polyglutamine toxicity caused by Ku70 acetylation.* Cell Death Differ, 2007. **14**(12): p. 2058-67.
128. Haenig, C., et al., *Interactome Mapping Provides a Network of Neurodegenerative Disease Proteins and Uncovers Widespread Protein Aggregation in Affected Brains.* Cell Rep, 2020. **32**(7): p. 108050.
129. Wellington, C.L., et al., *Caspase cleavage of gene products associated with triplet expansion disorders generates truncated fragments containing the polyglutamine tract.* J Biol Chem, 1998. **273**(15): p. 9158-67.
130. Zarouchlioti, C., et al., *DNAJ Proteins in neurodegeneration: essential and protective factors.* Philos Trans R Soc Lond B Biol Sci, 2018. **373**(1738).
131. Clemencon, B., M. Babot, and V. Trezeguet, *The mitochondrial ADP/ATP carrier (SLC25 family): pathological implications of its dysfunction.* Mol Aspects Med, 2013. **34**(2-3): p. 485-93.
132. Park, S., et al., *The role of RNA helicases in aging and lifespan regulation.* Translational Medicine of Aging, 2017. **1**: p. 24-31.
133. Lee, Y., et al., *Oligodendroglia metabolically support axons and contribute to neurodegeneration.* Nature, 2012. **487**(7408): p. 443-8.

134. Paul, B.T., et al., *Sideroflexin 4 affects Fe-S cluster biogenesis, iron metabolism, mitochondrial respiration and heme biosynthetic enzymes.* Sci Rep, 2019. **9**(1): p. 19634.
135. Vanstone, J.R., et al., *DNM1L-related mitochondrial fission defect presenting as refractory epilepsy.* Eur J Hum Genet, 2016. **24**(7): p. 1084-8.
136. Polak, A.J.E.a.J.M., *Molecular cloning of the human and murine 2-amino-3-ketobutyrate coenzyme A ligase cDNAs.* Eur. J. Biochem., 2000. **267**: p. 1805-1812.
137. Vig, P.J., et al., *Knockdown of acid-sensing ion channel 1a (ASIC1a) suppresses disease phenotype in SCA1 mouse model.* Cerebellum, 2014. **13**(4): p. 479-90.
138. Shen L, T.J., Tang BS, Jiang H, Zhao GH, Xia K, Zhang YH, Cai F, Tan LM, Pan Q, *Research on screening and identification of proteins interacting with ataxin-3.* Journal of Medical Genetics, 2005. **22**: p. 242-247.
139. Chen, Y., et al., *Bcl2-associated athanogene 3 interactome analysis reveals a new role in modulating proteasome activity.* Mol Cell Proteomics, 2013. **12**(10): p. 2804-19.
140. Thomsen, G.H., *Smurf1.* MOLECULE PAGE, 2012. **1**(1): p. 31-43.
141. Andrews, P.S., et al., *Identification of substrates of SMURF1 ubiquitin ligase activity utilizing protein microarrays.* Assay Drug Dev Technol, 2010. **8**(4): p. 471-87.
142. Chhangani, D., et al., *Ubiquitin ligase ITCH recruitment suppresses the aggregation and cellular toxicity of cytoplasmic misfolded proteins.* Sci Rep, 2014. **4**: p. 5077.
143. Ye, Y., et al., *Polyubiquitin binding and cross-reactivity in the USP domain deubiquitinase USP21.* EMBO Rep, 2011. **12**(4): p. 350-7.
144. Loch, C.M. and J.E. Strickler, *A microarray of ubiquitylated proteins for profiling deubiquitylase activity reveals the critical roles of both chain and substrate.* Biochim Biophys Acta, 2012. **1823**(11): p. 2069-78.
145. Lambert-Smith, I.A., D.N. Saunders, and J.J. Yerbury, *The pivotal role of ubiquitin-activating enzyme E1 (UBA1) in neuronal health and neurodegeneration.* Int J Biochem Cell Biol, 2020. **123**: p. 105746.
146. Groen, E.J.N. and T.H. Gillingwater, *UBA1: At the Crossroads of Ubiquitin Homeostasis and Neurodegeneration.* Trends Mol Med, 2015. **21**(10): p. 622-632.
147. Liu, Y. and Y. Ye, *Proteostasis regulation at the endoplasmic reticulum: a new perturbation site for targeted cancer therapy.* Cell Res, 2011. **21**(6): p. 867-83.
148. Liebl, M.P. and T. Hoppe, *It's all about talking: two-way communication between proteasomal and lysosomal degradation pathways via ubiquitin.* Am J Physiol Cell Physiol, 2016. **311**(2): p. C166-78.
149. Bremm, A., S.M. Freund, and D. Komander, *Lys11-linked ubiquitin chains adopt compact conformations and are preferentially hydrolyzed by the deubiquitinase Cezanne.* Nat Struct Mol Biol, 2010. **17**(8): p. 939-47.
150. Yano, M., et al., *Functional analysis of human mitochondrial receptor Tom20 for protein import into mitochondria.* J Biol Chem, 1998. **273**(41): p. 26844-51.
151. Huttlin, E.L., et al., *Architecture of the human interactome defines protein communities and disease networks.* Nature, 2017. **545**(7655): p. 505-509.
152. Huttlin, E.L., et al., *The BioPlex Network: A Systematic Exploration of the Human Interactome.* Cell, 2015. **162**(2): p. 425-440.
153. Toonen, L.J., et al., *Antisense oligonucleotide-mediated exon skipping as a strategy to reduce proteolytic cleavage of ataxin-3.* Sci Rep, 2016. **6**: p. 35200.
154. Colotti, G., et al., *Sorcin, a calcium binding protein involved in the multidrug resistance mechanisms in cancer cells.* Molecules, 2014. **19**(9): p. 13976-89.
155. Tao, R.S., et al., *Casein kinase 2 interacts with and phosphorylates ataxin-3.* Neurosci Bull, 2008. **24**(5): p. 271-7.

156. Wan, L., et al., *Roles of Post-translational Modifications in Spinocerebellar Ataxias.* Front Cell Neurosci, 2018. **12**: p. 290.
157. Mueller, T., et al., *CK2-dependent phosphorylation determines cellular localization and stability of ataxin-3.* Hum Mol Genet, 2009. **18**(17).
158. Gilmore, T.D. and M. Herscovitch, *Inhibitors of NF-kappaB signaling: 785 and counting.* Oncogene, 2006. **25**(51): p. 6887-99.
159. Wang, H., et al., *p45, an ATPase subunit of the 19S proteasome, targets the polyglutamine disease protein ataxin-3 to the proteasome.* J Neurochem, 2007. **101**(6): p. 1651-61.
160. Heir, R., et al., *The UBL domain of PLIC-1 regulates aggresome formation.* EMBO Rep, 2006. **7**(12): p. 1252-8.
161. Geisler, S., et al., *The ubiquitin-conjugating enzymes UBE2N, UBE2L3 and UBE2D2/3 are essential for Parkin-dependent mitophagy.* J Cell Sci, 2014. **127**(Pt 15): p. 3280-93.
162. Durcan, T.M., et al., *Ataxin-3 deubiquitination is coupled to Parkin ubiquitination via E2 ubiquitin-conjugating enzyme.* J Biol Chem, 2012. **287**(1): p. 531-541.
163. Kathryn M. Donaldson, W.L., Keith A. Ching, Serge Batalov, Chih-Cheng Tsai, and Claudio A. P. Joazeiro, *Ubiquitin-mediated sequestration of normal cellular proteins into polyglutamine aggregates.* PNAS, 2003. **100**: p. 8892-8897.
164. Nicastro, G., et al., *Understanding the role of the Josephin domain in the PolyUb binding and cleavage properties of ataxin-3.* PLoS One, 2010. **5**(8): p. e12430.
165. Lim, J., et al., *A protein-protein interaction network for human inherited ataxias and disorders of Purkinje cell degeneration.* Cell, 2006. **125**(4): p. 801-14.
166. Luck, K., et al., *A reference map of the human binary protein interactome.* Nature, 2020. **580**(7803): p. 402-408.
167. Scanlon, T.C., et al., *Isolation of human proteasomes and putative proteasome-interacting proteins using a novel affinity chromatography method.* Exp Cell Res, 2009. **315**(2): p. 176-89.
168. Gonzalez-Jamett, A.M., et al., *Dynamin-2 function and dysfunction along the secretory pathway.* Front Endocrinol (Lausanne), 2013. **4**: p. 126.
169. Vinayagam, A., et al., *A directed protein interaction network for investigating intracellular signal transduction.* Sci Signal, 2011. **4**(189): p. rs8.
170. Friedman, R. and A.L. Hughes, *Pattern and timing of gene duplication in animal genomes.* Genome Res, 2001. **11**(11): p. 1842-7.
171. Mosbech, A., et al., *DVC1 (C1orf124) is a DNA damage-targeting p97 adaptor that promotes ubiquitin-dependent responses to replication blocks.* Nat Struct Mol Biol, 2012. **19**(11): p. 1084-92.
172. Sowa, M.E., et al., *Defining the human deubiquitinating enzyme interaction landscape.* Cell, 2009. **138**(2): p. 389-403.
173. Altun, M., et al., *The human otubain2-ubiquitin structure provides insights into the cleavage specificity of poly-ubiquitin-linkages.* PLoS One, 2015. **10**(1): p. e0115344.
174. Reina, C.P., X. Zhong, and R.N. Pittman, *Proteotoxic stress increases nuclear localization of ataxin-3.* Hum Mol Genet, 2010. **19**(2): p. 235-49.
175. Yang, W., et al., *CARPs are ubiquitin ligases that promote MDM2-independent p53 and phospho-p53ser20 degradation.* J Biol Chem, 2007. **282**(5): p. 3273-81.
176. Al Bitar, S. and H. Gali-Muhtasib, *The Role of the Cyclin Dependent Kinase Inhibitor p21(cip1/waf1) in Targeting Cancer: Molecular Mechanisms and Novel Therapeutics.* Cancers (Basel), 2019. **11**(10).
177. Chai, Y., et al., *The role of protein composition in specifying nuclear inclusion formation in polyglutamine disease.* J Biol Chem, 2001. **276**(48): p. 44889-97.
178. Liu, H., et al., *The Machado-Joseph Disease Deubiquitinase Ataxin-3 Regulates the Stability and Apoptotic Function of p53.* PLoS Biol, 2016. **14**(11): p. e2000733.

179. Dovas, A. and J.R. Couchman, *RhoGDI: multiple functions in the regulation of Rho family GTPase activities.* Biochem J, 2005. **390**(Pt 1): p. 1-9.
180. Olah, J., et al., *Interactions of pathological hallmark proteins: tubulin polymerization promoting protein/p25, beta-amyloid, and alpha-synuclein.* J Biol Chem, 2011. **286**(39): p. 34088-100.
181. Zhou, L., et al., *Ataxin-3 protects cells against H2O2-induced oxidative stress by enhancing the interaction between Bcl-X(L) and Bax.* Neuroscience, 2013. **243**: p. 14-21.
182. McGurk, L. and N.M. Bonini, *Protein interacting with C kinase (PICK1) is a suppressor of spinocerebellar ataxia 3-associated neurodegeneration in Drosophila.* Hum Mol Genet, 2012. **21**(1): p. 76-84.
183. Heras, G., et al., *Muscle RING-finger protein-1 (MuRF1) functions and cellular localization are regulated by SUMO1 post-translational modification.* J Mol Cell Biol, 2019. **11**(5): p. 356-370.
184. Bitter, E.E., et al., *Thymidine kinase 1 through the ages: a comprehensive review.* Cell Biosci, 2020. **10**(1): p. 138.
185. Carolina Meloni Vicente, R.R., Helena Bonciani Nader and Leny Toma, *Syndecan-2 is upregulated in colorectal cancer cells through interactions with extracellular matrix produced by stromal fibroblasts.* BMC Cell Biology, 2013. **14:25**.
186. Lee, J., et al., *EWSR1, a multifunctional protein, regulates cellular function and aging via genetic and epigenetic pathways.* Biochim Biophys Acta Mol Basis Dis, 2019. **1865**(7): p. 1938-1945.
187. Zhepeng Liu, Y.X.a.G.S., *The KCTD family of proteins structure, function, disease relevance.* Cell & Bioscience, 2013. **3:45**.
188. Charlaftis, N., et al., *The MEKK1 PHD ubiquitinates TAB1 to activate MAPKs in response to cytokines.* EMBO J, 2014. **33**(21): p. 2581-96.
189. Li, H., et al., *Identification of a small molecule targeting annexin A7.* Biochim Biophys Acta, 2013. **1833**(9): p. 2092-9.
190. Yang, C., et al., *Ribosomal protein L6 (RPL6) is recruited to DNA damage sites in a poly(ADP-ribose) polymerase-dependent manner and regulates the DNA damage response.* J Biol Chem, 2019. **294**(8): p. 2827-2838.
191. Takeshita, Y., et al., *Interaction of ataxin-3 with huntingtin-associated protein 1 through Josephin domain.* Neuroreport, 2011. **22**(5): p. 232-8.
192. Chhangani, D., et al., *Mahogunin ring finger 1 suppresses misfolded polyglutamine aggregation and cytotoxicity.* Biochim Biophys Acta, 2014. **1842**(9): p. 1472-84.
193. Min, S., et al., *Chromatin-remodeling factor, RSF1, controls p53-mediated transcription in apoptosis upon DNA strand breaks.* Cell Death Dis, 2018. **9**(11): p. 1079.
194. Zhang, N., et al., *Expression, purification and characterization of TMCO1 for structural studies.* Protein Expr Purif, 2021. **179**: p. 105803.
195. Bellil, H., et al., *Human testis-expressed (TEX) genes: a review focused on spermatogenesis and male fertility.* Basic Clin Androl, 2021. **31**(1): p. 9.
196. Noordstra, I., et al., *Control of apico-basal epithelial polarity by the microtubule minus-end-binding protein CAMSAP3 and spectraplakin ACF7.* J Cell Sci, 2016. **129**(22): p. 4278-4288.
197. Marceaux, C., et al., *Phosphorylation of ARHGAP19 by CDK1 and ROCK regulates its subcellular localization and function during mitosis.* J Cell Sci, 2018. **131**(5).
198. Schlehe, J.S., et al., *The mitochondrial disease associated protein Ndufaf2 is dispensable for Complex-1 assembly but critical for the regulation of oxidative stress.* Neurobiol Dis, 2013. **58**: p. 57-67.
199. Kedde, M., et al., *RNA-binding protein Dnd1 inhibits microRNA access to target mRNA.* Cell, 2007. **131**(7): p. 1273-86.

200. Belyaeva, O.V., et al., *Human retinol dehydrogenase 13 (RDH13) is a mitochondrial short-chain dehydrogenase/reductase with a retinaldehyde reductase activity.* FEBS J, 2008. **275**(1): p. 138-47.
201. Pelzer, C., et al., *The protease activity of the paracaspase MALT1 is controlled by monoubiquitination.* Nat Immunol, 2013. **14**(4): p. 337-45.
202. Christensen, K.E. and R.E. MacKenzie, *Chapter 14 Mitochondrial Methylenetetrahydrofolate Dehydrogenase, Methenyltetrahydrofolate Cyclohydrolase, and Formyltetrahydrofolate Synthetases*, in *Folic Acid and Folates*. 2008. p. 393-410.
203. Boulet, A., et al., *The mammalian phosphate carrier SLC25A3 is a mitochondrial copper transporter required for cytochrome c oxidase biogenesis.* J Biol Chem, 2018. **293**(6): p. 1887-1896.
204. Peters, P.J., et al., *Arfaptin 2 regulates the aggregation of mutant huntingtin protein.* Nat Cell Biol, 2002. **4**(3): p. 240-5.
205. Wang, B. and P. Tontonoz, *Phospholipid Remodeling in Physiology and Disease.* Annu Rev Physiol, 2019. **81**: p. 165-188.
206. Li, P., et al., *Requirement of Rab21 in LPS-induced TLR4 signaling and pro-inflammatory responses in macrophages and monocytes.* Biochem Biophys Res Commun, 2019. **508**(1): p. 169-176.
207. Del Olmo, T., et al., *RAB21 interacts with TMED10 and modulates its localization and abundance.* Biol Open, 2019. **8**(9).
208. Kung, W.M. and M.S. Lin, *The NFkappaB Antagonist CDGSH Iron-Sulfur Domain 2 Is a Promising Target for the Treatment of Neurodegenerative Diseases.* Int J Mol Sci, 2021. **22**(2).
209. Penna, E., et al., *The MCU complex in cell death.* Cell Calcium, 2018. **69**: p. 73-80.
210. Tasaki, T., et al., *The N-end rule pathway.* Annu Rev Biochem, 2012. **81**: p. 261-89.
211. Varshavsky, A., *N-degron and C-degron pathways of protein degradation.* Proc Natl Acad Sci U S A, 2019. **116**(2): p. 358-366.
212. Huang, H., et al., *Defining the specificity space of the human SRC homology 2 domain.* Mol Cell Proteomics, 2008. **7**(4): p. 768-84.
213. Agostoni, E., et al., *Effects of Pin1 Loss in Hdh(Q111) Knock-in Mice.* Front Cell Neurosci, 2016. **10**: p. 110.
214. Schmitt, I., et al., *Inactivation of the mouse Atxn3 (ataxin-3) gene increases protein ubiquitination.* Biochem Biophys Res Commun, 2007. **362**(3): p. 734-9.
215. Rodrigues, A.J., et al., *Functional genomics and biochemical characterization of the C. elegans orthologue of the Machado-Joseph disease protein ataxin-3.* FASEB J, 2007. **21**(4): p. 1126-36.
216. Seki, T., et al., *JosD1, a membrane-targeted deubiquitinating enzyme, is activated by ubiquitination and regulates membrane dynamics, cell motility, and endocytosis.* J Biol Chem, 2013. **288**(24): p. 17145-55.
217. Tunyasuvunakool, K., et al., *Highly accurate protein structure prediction for the human proteome.* Nature, 2021. **596**(7873): p. 590-596.
218. Jumper, J., et al., *Highly accurate protein structure prediction with AlphaFold.* Nature, 2021. **596**(7873): p. 583-589.

Appendix

Supplementary Table 1: Identification of the human selected UniProt sequences. * represent the human proteins common with fly.

Protein Name	Gene name	Gene ID	UniProt ID
Heat shock 70 kDa protein 1A*	HSPA1A	3303	P0DMV8
Heat shock cognate 71 kDa protein*	HSPA8	3312	P11142
Heat shock 70 kDa protein 4L*	HSPA4L	22824	O95757
Heat shock 70 kDa protein 4*	HSPA4	3308	P34932
Heat shock protein 105 kDa*	HSPH1	10808	Q92598
Heat shock protein HSP 90-alpha *	HSP90AA1	3320	P07900
Serpin H1*	SERPINH1	871	P50454
DnaJ homolog subfamily B member 2*	DNAJB2	3300	P25686
4F2 cell-surface antigen heavy chain*	SLC3A2	6520	P08195
CREB binding protein*	CREBBP	1387	Q92793
Histone acetyltransferase p300*	EP300	2033	Q09472
Histone deacetylase 3*	HDAC3	8841	O15379
Histone deacetylase 6*	HDAC6	10013	Q9UBN7
Caspase 1*	CASP1	834	P29466
Caspase 3*	CASP3	836	P42574
DnaJ homolog subfamily A member 1*	DNAJA1	3301	P31689
ADP/ATP translocase 2*	SLC25A5	292	P05141
ADP/ATP translocase 3*	SLC25A6	293	P12236
ATP-dependent RNA helicase DDX39A*	DDX39A	10212	O00148
Monocarboxylate transporter 1*	SLC16A1	6566	P53985
Sideroflexin 4*	SFXN4	119559	Q6P4A7
Dynamin-1-like protein*	DNM1L	10059	O00429
2-amino-3-ketobutyrate coenzyme A ligase*	GCAT	23464	O75600
Acid-sensing ion channel 1*	ASIC1	41	P78348
BAG family molecular chaperone regulator 3*	BAG3	9531	O95817
E3 ubiquitin-protein ligase SMURF1*	SMURF1	57154	Q9HCE7
E3 ubiquitin-protein ligase Itchy homolog*	ITCH	83737	Q96J02
Ubiquitin carboxyl-terminal hydrolase 21*	USP21	27005	Q9UK80
Ubiquitin-like modifier-activating enzyme 1*	UBA1	7317	P22314
Polynucleotide kinase 3´-phosphatase *	PNKP	11284	Q96T60
Calnexin*	CANX	821	P27824
Alpha-parvin*	PARVA	55742	Q9NVD7
TNF receptor associated factor 6*	TRAF6	7189	Q9Y4K3
TOMM20-like protein 1*	TOMM20L	387990	Q6UXN7
Calpain 2*	CAPN2	824	P17655
Sorcin*	SRI	6717	P30626
Tubulin beta chain*	TUBB	203068	P07437
Tubulin alpha-1A chain*	TUBA1A	7846	Q71U36
Casein kinase 2 beta*	CSNK2B	1460	P67870
NF-kappa-B inhibitor alpha*	NFKBIA	4792	P25963
26S proteasome regulatory subunit 8*	PSMC5	5705	P62195
26S proteasome non-ATPase regulatory subunit 4*	PSMD4	5710	P55036
26S proteasome non-ATPase regulatory subunit 7*	PSMD7	5713	P51665
Small ubiquitin like modifier 1*	SUMO1	7341	P63165
Lysine acetyltransferase 2B*	KAT2B	8850	Q92831
Ubiquilin 1*	UBQLN1	29979	Q9UMX0
Ubiquitin conjugating enzyme E2 L3*	UBE2L3	7332	P68036
Ubiquitin conjugating enzyme E2 G1*	UBE2G1	7326	P62253
Ubiquitin conjugating enzyme E2 S*	UBE2S	27338	Q16763
Ubiquitin conjugating enzyme E2 N*	UBE2N	7334	P61088
Polyubiquitin-B*	UBB	7314	P0CG47
Polyubiquitin-C*	UBC	7316	P0CG48
RAD23 homolog B, nucleotide excision repair*	RAD23B	5887	P54727
RAD23 homolog A, nucleotide excision repair*	RAD23A	5886	P54725
NEDD8 ubiquitin like modifier*	NEDD8	4738	Q15843
Dynamin 2*	DNM2	1785	P50570
DNA-dependent metalloprotease SPRTN	SPRTN	83932	Q9H040
Ubiquitin carboxyl-terminal hydrolase 13	USP13	8975	Q92995
Sequestosome 1	SQSTM1	8878	Q13501
Ubiquitin thioesterase OTUB2	OTUB2	78990	Q96DC9
E3 ubiquitin-protein ligase parkin	PRKN	5071	O60260
E3 ubiquitin-protein ligase synoviolin	SYVN1	84447	Q86TM6
Vasolin containing protein	VCP	7415	P55072
E3 ubiquitin-protein ligase AMFR	AMFR	267	Q9UKV5
Ubiquitin conjugation factor E4B	UBE4B	10277	O95155
E3 ubiquitin-protein ligase CHIP	STUB1	10273	Q9UNE7
E3 ubiquitin-protein ligase rififylin	RFFL	117584	Q8WZ73
Cyclin dependent kinase inhibitor 1	CDKN1A	1026	P38936
Protein PML	PML	5371	P29590
Glycogen synthase kinase 3 beta	GSK3B	2932	P49841
Cellular tumor antigen p53	TP53	7157	P04637
Telomere length regulation protein TEL2 homolog	TELO2	9894	Q9Y4R8

Rho GDP-dissociation inhibitor 1	ARHGDIA	396	P52565
Amyloid beta precursor protein	APP	351	P05067
BCL2 like 1	BCL2L1	598	Q07817
PRKCA-binding protein	PICK1	9463	Q9NRD5
E3 ubiquitin-protein ligase TRIM63	TRIM63	84676	Q969Q1
Tripartite motif containing protein 55	TRIM55	84675	Q9BYV6
Thymidine kinase 1	TK1	7083	P04183
Tripartite motif containing protein 54	TRIM54	57159	Q9BYV2
Syndecan 2	SDC2	6383	P34741
Forkhead box class O transcription factor 4	FOXO4	4303	P98177
cAMP responsive element binding protein 1	CREB1	1385	P16220
RNA-binding protein EWS	EWSR1	2130	Q01844
BTB/POZ domain-containing adapter for CUL3-mediated RhoA degradation protein 3	KCTD10	83892	Q9H3F6
Mitogen-activated protein kinase kinase kinase 1	MAP3K1	4214	Q13233
Mediator of DNA damage checkpoint 1	MDC1	9656	Q14676
Annexin A7	ANXA7	310	P20073
X-ray repair cross-complementing protein 6	XRCC6	2547	P12956
HLA class I histocompatibility antigen, A alpha chain	HLA-A	3105	P04439
60S ribosomal protein L6	RPL6	6128	Q02878
Ribosomal protein S6 kinase alpha-1	RPS6KA1	6195	Q15418
MAPK interacting serine/threonine kinase 1	MKNK1	8569	Q9BUB5
Huntingtin associated protein 1	HAP1	9001	P54257
B-cell CLL/lymphoma 7 protein family member C	BCL7C	9274	Q8WUZ0
Nuclear receptor corepressor 1	NCOR1	9611	O75376
E3 ubiquitin-protein ligase MGRN1	MGRN1	23295	O60291
Remodeling and spacing factor 1	RSF1	51773	Q96T23
Calcium load-activated calcium channel	TMCO1	54499	Q9UM00
Testis-expressed protein 11	TEX11	56159	Q8IYF3
Calmodulin-regulated spectrin-associated protein 3	CAMSAP3	57662	Q9P1Y5
E3 ubiquitin-protein ligase Praja-1	PJA1	64219	Q8NG27
Phagosome assembly factor 1	PHAF1	80262	Q9BSU1
Proline/serine-rich coiled-coil protein 1	PSRC1	84722	Q6PGN9
Rho GTPase-activating protein 19	ARHGAP19	84986	Q14CB8
NADH dehydrogenase [ubiquinone] 1 alpha subcomplex assembly factor 2	NDUFAF2	91942	Q8N183
Zinc finger protein AEBP2	AEBP2	121536	Q6ZN18
Dead end protein homolog 1	DND1	373863	Q8IYX4
Plasmanylethanolamine desaturase	PEDS1	387522	A5PLL7
Ubiquitin-conjugating enzyme E2 variant 1	UBE2V1	7335	Q13404
Mitochondrial import inner membrane translocase subunit Tim23	TIMM23	100287932	O14925
CCR4-NOT transcription complex subunit 6	CNOT6	57472	Q9ULM6
Succinate dehydrogenase [ubiquinone] iron-sulfur subunit	SDHB	6390	P21912
Cytochrome c oxidase assembly factor 7	COA7	65260	Q96BR5
Cytochrome c oxidase subunit NDUFA4	NDUFA4	4697	O00483
ATP-citrate synthase	ACLY	47	P53396
Protein FAM184B	FAM184B	27146	Q9ULE4
Dihydroxyacetone phosphate acyltransferase	GNPAT	8443	O15228
Cyclin dependent kinase 4	CDK4	1019	P11802
Hydroxysteroid dehydrogenase-like protein 2	HSDL2	84263	Q6YN16
Retinol dehydrogenase 13	RDH13	112724	Q8NBN7
Mitochondrial glutamate carrier 1	SLC25A22	79751	Q9H936
Succinate dehydrogenase [ubiquinone] flavoprotein subunit	SDHA	6389	P31040
Rho-related GTP-binding protein RhoG	RHOG	391	P84095
Mucosa-associated lymphoid tissue lymphoma translocation protein 1	MALT1	10892	Q9UDY8
Acyl-coenzyme A thioesterase 9	ACOT9	23597	Q9Y305
Long-chain fatty acid transport protein 4	SLC27A4	10999	Q6P1M0
Tricarboxylate transport protein	SLC25A1	6576	P53007
Nucleoporin SEH1	SEH1L	81929	Q96EE3
Mitochondrial dicarboxylate carrier	SLC25A10	1468	Q9UBX3
Iron-sulfur cluster assembly factor IBA57	IBA57	200205	Q5T440
Bifunctional methylenetetrahydrofolate dehydrogenase/cyclohydrolase	MTHFD2	10797	P13995
Phosphate carrier protein	SLC25A3	5250	Q00325
Ubiquitin-associated domain-containing protein 2	UBAC2	337867	Q8NBM4
Mitochondrial genome maintenance exonuclease 1	MGME1	92667	Q9BQP7
Very-long-chain enoyl-CoA reductase	TECR	9524	Q9NZ01
Arfaptin-2	ARFIP2	23647	P53365
Regulator of microtubule dynamics protein 1	RMDN1	51115	Q96DB5
UPF0598 protein C8orf82	C8orf82	414919	Q6P1X6
Lysophosphatidylcholine acyltransferase 1	LPCAT1	79888	Q8NF37
Isocitrate dehydrogenase [NAD] subunit beta	IDH3B	3420	O43837
Chitobiosyldiphosphodolichol beta-mannosyltransferase	ALG1	56052	Q9BT22
60S acidic ribosomal protein P0	RPLP0	6175	P05388
E3 ubiquitin-protein ligase MARCHF5	MARCHF5	54708	Q9NX47
Ribose-phosphate pyrophosphokinase 1	PRPS1	5631	P60891
Ras-related protein Rab-21	RAB21	23011	Q9UL25
NADH dehydrogenase [ubiquinone] 1 alpha subcomplex subunit 8	NDUFA8	4702	P51970
CDGSH iron-sulfur domain-containing protein 2	CISD2	493856	Q8N5K1

Estradiol 17-beta-dehydrogenase 11	HSD17B11	51170	Q8NBQ5
Calcium uniporter protein	MCU	90550	Q8NE86

Supplementary Table 2. Paralogous human genes of the L1 fly genes identified in EvoPPI as interactors of *Drosophila* Josephin-like protein (CG3781, Gene ID 31560).

FlyBase Gene ID	Fly Gene ID	Fly gene symbol	Human Gene ID	HGNC ID	Human gene symbol
CG15862	36041	Pka-R2	5576	9391	PRKAR2A
			5577	9392	PRKAR2B
			5575	9390	PRKAR1B
			5573	9388	PRKAR1A
			375775	24768	PNPLA7
			10908	16268	PNPLA6
			5592	9414	PRKG1
			5593	9416	PRKG2
			140894	16145	CNBD2
CG8455	34116	PGAP5	65258	15988	MPPE1
CG42236	36102	RanBPM	10048	13727	RANBP9
			57610	29285	RANBP10
			84926	25920	SPRYD3
CG2830	48572	Hsp60B	3329	5261	HSPD1
			22948	1618	CCT5
			10576	1615	CCT2
			6950	11655	TCP1
			908	1620	CCT6A
			7203	1616	CCT3
			79738	26291	BBS10
			10574	1622	CCT7
			154807	21492	VKORC1L1
			10693	1621	CCT6B
			8195	7108	MKKS
			10575	1617	CCT4

Supplementary Table 3: Paralogous human genes of the fly modifiers ataxin-3 genes identified by Vobfeldt according to DIOPT. Stars indicate the genes assigned as suppressors, cardinal those assigned as enhancers, and plus those that are deleterious in flies. &Represent the genes that we used the gene name (instead of CG number) to search human orthologs.

FlyBase Gene ID	Fly Gene ID	Fly gene symbol	Human Gene ID	HGNC ID	Human gene symbol
CG17048*	36479	CG17048	54941	21150	RNF125
			51283	17613	BFAR
CG9501*	33887	ppk14	41	100	ASIC1
			9311	101	ASIC3
			51802	17537	ASIC5
			55515	21263	ASIC4
			40	99	ASIC2
			6337	10599	SCNN1A
			6339	10601	SCNN1D
			6340	10602	SCNN1G
			6338	10600	SCNN1B
			4882	7944	NPR2
CG7123*	34068	LanB1	3913	6487	LAMB2
			3912	6486	LAMB1
			22798	6491	LAMB4
			59277	13658	NTN4
			3914	6490	LAMB3
			1955	3234	MEGF9
			8577	11866	TMEFF1
			100526694	38838	MSANTD3-TMEFF1
			23671	11867	TMEFF2
			3909	6483	LAMA3
			3908	6482	LAMA2
			284217	6481	LAMA1
			3911	6485	LAMA5
CG9131*	44132	slmo	51012	15892	PRELID3B
			10650	24639	PRELID3A
			100533975		SLMO2-ATP5E
CG9153*	38151	Herc4	26091	24521	HERC4
			8916	4876	HERC3
			51191	24368	HERC5
			55008	26072	HERC6
			143279	26736	HECTD2
			79654	26117	HECTD3
			7337	12496	UBE3A
			8924	4868	HERC2
			101929134	54080	PIGY-DT
			55920	30297	RCC2
			6103	10295	RPGR
			55213	18243	RCBTB1
			284086	13387	NEK8
			26297	17499	SERGEF
			81554	14948	RCC1L
			1102	1914	RCBTB2
			1104	1913	RCC1
			8925	4867	HERC1
			91433	30457	RCCD1
			91754	18591	NEK9
			51008	24268	ASCC1
			8522	4169	GAS7
			9320	12306	TRIP12
			25831	20157	HECTD1
			54477	30036	PLEKHA5
			57520	29853	HECW2
			23327	7728	NEDD4L
			51366	16806	UBR5
			4734	7727	NEDD4
			11060	16804	WWP2
			9531	939	BAG3
			10075	30892	HUWE1
			11059	17004	WWP1
			89910	13478	UBE3B
			80014	24148	WWC2
			9690	16803	UBE3C
			55841	29237	WWC3
			23072	22195	HECW1
			83737	13890	ITCH
			144100	27049	PLEKHA7

			10413	16262	YAP1
			23286	29435	WWC1
			64750	16809	SMURF2
			260425	29647	MAGI3
			79917	30006	MAGIX
			25937	24042	WWTR1
			9223	946	MAGI1
			57154	16807	SMURF1
			9870	20363	AREL1
			9863	18957	MAGI2
			57531	21033	HACE1
CG8696*	35824	Mal-A1	6519	11025	SLC3A1
			6520	11026	SLC3A2
			276	474	AMY1A
			278	476	AMY1C
			280	478	AMY2B
			277	475	AMY1B
CG4264*	41840	Hsc70-4	3312	5241	HSPA8
			3304	5233	HSPA1B
			3306	5235	HSPA2
			3305	5234	HSPA1L
			3310	5239	HSPA6
			3303	5232	HSPA1A
			3309	5238	HSPA5
			3313	5244	HSPA9
			3311	5240	HSPA7
			6782	11375	HSPA13
			137814	32940	NKX2-6
			10808	16969	HSPH1
			259217	19022	HSPA12A
			10525	16931	HYOU1
			284525	28664	SLC9C2
			339416	24786	ANKRD45
			51182	29526	HSPA14
			116835	16193	HSPA12B
			3308	5237	HSPA4
			22824	17041	HSPA4L
			3312	5241	HSPA8
			3304	5233	HSPA1B
			3306	5235	HSPA2
			3305	5234	HSPA1L
			3310	5239	HSPA6
			3303	5232	HSPA1A
			3309	5238	HSPA5
			3313	5244	HSPA9
			3311	5240	HSPA7
			6782	11375	HSPA13
			137814	32940	NKX2-6
			10808	16969	HSPH1
			259217	19022	HSPA12A
			10525	16931	HYOU1
			284525	28664	SLC9C2
			339416	24786	ANKRD45
			51182	29526	HSPA14
			116835	16193	HSPA12B
			3308	5237	HSPA4
			22824	17041	HSPA4L
CG3284*	41741	RpII15	5438	9196	POLR2I
			51728	14121	POLR3K
			6919	11614	TCEA2
			9441	2376	MED26
			6920	11615	TCEA3
			170082	28277	TCEANC
			127428	26494	TCEANC2
			6917	11612	TCEA1
			30834	13182	ZNRD1
CG5799*	37546	dve	6304	10541	SATB1
			23314	21637	SATB2
CG9448*	41179	trbd	54764	18224	ZRANB1
			7128	11896	TNFAIP3
			161725	20718	OTUD7A
			56957	16683	OTUD7B
			80124	30897	VCPIP1

CG15618*	33001	THADA	63892	19217	THADA
CG14514*	43460	Brd8	10902	19874	BRD8
			11177	960	BAZ1A
			2033	3373	EP300
			1387	2348	CREBBP
			29994	963	BAZ2B
			23476	13575	BRD4
			6046	1103	BRD2
			8019	1104	BRD3
			8850	8638	KAT2B
			2648	4201	KAT2A
			11176	962	BAZ2A
			676	1105	BRDT
			2186	3581	BPTF
			9031	961	BAZ1B
			55193	30064	PBRM1
CG8863*	41646	Droj2	55466	14885	DNAJA4
			3301	5229	DNAJA1
			10294	14884	DNAJA2
			11080	14886	DNAJB4
			80331	16235	DNAJC5
			5611	9439	DNAJC3
			3300	5228	DNAJB2
			202052	28429	DNAJC18
			374407	30718	DNAJB13
			120526	26979	DNAJC24
			51726	14889	DNAJB11
			552891	37501	DNAJC25-GNG10
			79982	25881	DNAJB14
			3337	5270	DNAJB1
			79962	25802	DNAJC22
			23341	29157	DNAJC16
			548645	34187	DNAJC25
			4189	6968	DNAJB9
			54431	24637	DNAJC10
			85479	24138	DNAJC5B
			10049	14888	DNAJB6
			9093	11808	DNAJA3
			285126	24844	DNAJC5G
			134218	27030	DNAJC21
			165721	23699	DNAJB8
			150353	24986	DNAJB7
			25822	14887	DNAJB5
			55735	25570	DNAJC11
			54788	14891	DNAJB12
			7266	12392	DNAJC7
CG7108*	38942	DNApol-alpha50	5557	9369	PRIM1
CG8937*	39542	Hsc70-1	3312	5241	HSPA8
			3306	5235	HSPA2
			3304	5233	HSPA1B
			3310	5239	HSPA6
			3305	5234	HSPA1L
			3303	5232	HSPA1A
			3309	5238	HSPA5
			3313	5244	HSPA9
			3311	5240	HSPA7
			6782	11375	HSPA13
			137814	32940	NKX2-6
			10808	16969	HSPH1
			259217	19022	HSPA12A
			10525	16931	HYOU1
			284525	28664	SLC9C2
			339416	24786	ANKRD45
			51182	29526	HSPA14
			116835	16193	HSPA12B
			3308	5237	HSPA4
			22824	17041	HSPA4L
CG2720*	33202	Stip1	10963	11387	STIP1
			54970	23700	TTC12
			10953	15746	TOMM34
			10910	16987	SUGT1
			23331	29179	TTC28
			64427	25759	TTC31

CG16890*	34781	CG16890	118924	1162	FRA10AC1
CG13969*	250736	bwa	340485	23675	ACER2
			125981	18356	ACER1
			55331	16066	ACER3
			126328	20371	NDUFA11
CG6755*	42749	EloA	6924	11620	ELOA
			51224	30771	ELOA2
			100506888	33511	ELOA3D
			728929	31007	ELOA3B
			162699	24617	ELOA3
			107983955	52410	ELOA3C
CG10545*	32544	Gbeta13F	2782	4396	GNB1
			59345	20731	GNB4
			2783	4398	GNB2
			2784	4400	GNB3
			10681	4401	GNB5
			4041	6697	LRP5
CG1658*/CG42320*	43415	Doa	1196	2069	CLK2
			1198	2071	CLK3
			57396	13659	CLK4
			1195	2068	CLK1
			9149	3092	DYRK1B
			1859	3091	DYRK1A
			8444	3094	DYRK3
			28996	14402	HIPK2
			147746	19007	HIPK4
			204851	19006	HIPK1
			8798	3095	DYRK4
			10114	4915	HIPK3
			8899	17346	PRPF4B
			8445	3093	DYRK2
CG5687*	38255	CG5687	6528	11040	SLC5A5
			160728	19119	SLC5A8
			159963	28750	SLC5A12
			8884	11041	SLC5A6
			115584	23091	SLC5A11
			6526	11038	SLC5A3
			200010	22146	SLC5A9
			125206	23155	SLC5A10
			60482	14025	SLC5A7
			6524	11037	SLC5A2
			6527	11039	SLC5A4
			6523	11036	SLC5A1
CG9695*	39866	Dab	1600	2661	DAB1
			1601	2662	DAB2
			112267931		LOC112267931
			9253	8061	NUMBL
			26119	18640	LDLRAP1
			163933	31791	FAM43B
			131583	26888	FAM43A
			400793	34351	C1orf226
			9479	6882	MAPK8IP1
			23542	6883	MAPK8IP2
			731	1352	C8A
			732	1353	C8B
CG1107*	40527	aux	2580	4113	GAK
			9829	15469	DNAJC6
			22848	19679	AAK1
			55589	18041	BMP2K
			7179	12023	TPTE
			64759	21616	TNS3
			7145	11973	TNS1
			93492	17299	TPTE2
			5728	9588	PTEN
			23371	19737	TNS2
CG14619*	33132	Usp2	9099	12618	USP2
			27005	12620	USP21
			9101	12631	USP8
			9100	12608	USP10
			389856	13486	USP27X
			7375	12627	USP4
			9960	12626	USP3
			84669	19143	USP32

			23326	12621	USP22
			8237	12609	USP11
			57663	18563	USP29
			373509	20079	USP50
			57695	20063	USP37
			83844	13485	USP26
			124739	20072	USP43
CG17919*	40780	CG17919	5037	8630	PEBP1
			157310	28319	PEBP4
			64978	14033	MRPL38
CG6758*	37532	CG6758	54455	29249	FBXO42
			10244	16896	RABEPK
			3054	4839	HCFC1
			8216	6742	LZTR1
			54758	25272	KLHDC4
			29915	24972	HCFC2
			116138	20704	KLHDC3
			126823	28489	KLHDC9
			122773	19836	KLHDC1
			23008	22194	KLHDC10
			23588	20231	KLHDC2
CG6363*	41850	MRG15	10933	16989	MORF4L1
			9643	16849	MORF4L2
			10943	7370	MSL3
			51742	15550	ARID4B
			5926	9885	ARID4A
CG3389*	41774	Cad88C	54825	18231	CDHR2
			64072	13733	CDH23
			5097	8655	PCDH1
			27328	8656	PCDH11X
			92211	14550	CDHR1
			5099	8659	PCDH7
			64881	14257	PCDH20
			83259	15813	PCDH11Y
			5101	8661	PCDH9
			1014	1755	CDH16
			389118	34527	CDHR4
			120114	23112	FAT3
			2195	3595	FAT1
			2196	3596	FAT2
			26167	8690	PCDHB5
			8642	13681	DCHS1
			79633	23109	FAT4
			54798	23111	DCHS2
CG3808*	40074	CG3808	27037	24974	TRMT2A
			79979	25748	TRMT2B
CG31110*/CG42283*	326119	5Ptasel	3632	6076	INPP5A
			2879	4556	GPX4
CG4266*	37411	CG4266	57466	19304	SCAF4
			22828	20959	SCAF8
			4841	7871	NONO
			64783	14959	RBM15
			55269	20320	PSPC1
			6421	10774	SFPQ
			29890	24303	RBM15B
CG16807*	39818	roq	149041	29434	RC3H1
			54542	21461	RC3H2
			378884	21576	NHLRC1
			643596	41912	RNF224
			221687	28522	RNF182
			284023	27571	RNF227
CG10377*	33968	Hrb27C	26528	2683	DAZAP1
			124540	18585	MSI2
			4440	7330	MSI1
			9987	5037	HNRNPDL
			220988	24941	HNRNPA3
			3182	5034	HNRNPAB
			3184	5036	HNRNPD
			3181	5033	HNRNPA2B1
			3178	5031	HNRNPA1
			221662	21539	RBM24
CG13467*/CG42247*	39617	DCX-EMAP	27436	1316	EML4
			2009	3330	EML1

			24139	18035	EML2
			256364	26666	EML3
			51473	18141	DCDC2
			149069	32576	DCDC2B
			728597	32696	DCDC2C
			55779	25631	CFAP44
			161436	18197	EML5
			94137	15946	RP1L1
			400954	35412	EML6
			9201	2700	DCLK1
			6101	10263	RP1
			1641	2714	DCX
CG7855#	41615	timeout	8914	11813	TIMELESS
CG9601#	40994	CG9601	11284	9154	PNKP
			54840	15984	APTX
CG15534#	43613	CG15534	6609	11120	SMPD1
			27293	21416	SMPDL3B
			10924	17389	SMPDL3A
CG10001#	43393	AstA-R2	8811	4133	GALR2
			8484	4134	GALR3
			2587	4132	GALR1
			84634	4510	KISS1R
			53831	4535	GPR84
			56413	19260	LTB4R2
			2837	4468	UTS2R
			1241	6713	LTB4R
			4353	7218	MPO
			4544	7464	MTNR1B
			5995	9990	RGR
			57007	23692	ACKR3
CG12935#	36134	CG12935	79064	28464	TMEM223
CG31048#	43404	spg	1795	2989	DOCK3
			9732	19192	DOCK4
			1793	2987	DOCK1
			80005	23476	DOCK5
			1794	2988	DOCK2
			659	1078	BMPR2
			85440	19190	DOCK7
			55619	23479	DOCK10
			139818	23483	DOCK11
			57572	19189	DOCK6
			81704	19191	DOCK8
			23348	14132	DOCK9
CG1119#	40607	Gnf1	5981	9969	RFC1
			51379	17177	CRLF3
			79915	25752	ATAD5
CG1695#	33046	CG1695	129049	29410	SGSM1
			9905	29026	SGSM2
			729873	19031	TBC1D3
			23061	29097	TBC1D9B
			23232	29082	TBC1D12
			102723859	27071	TBC1D3E
			26083	24509	TBC1D29P
			353149	28745	TBC1D26
			54662	25571	TBC1D13
			9712	16858	USP6NL
			729877	30708	TBC1D3H
			23329	29164	TBC1D30
			254272	26858	TBC1D28
			57533	29246	TBC1D14
			83874	23609	TBC1D10A
			9910	24663	RABGAP1L
			23637	17155	RABGAP1
			23158	21710	TBC1D9
			64786	25694	TBC1D15
			26000	24510	TBC1D10B
			11138	17791	TBC1D8
			414060	24889	TBC1D3C
			23102	29183	TBC1D2B
			54885	24715	TBC1D8B
			4943	8092	TBC1D25
			161514	28536	TBC1D21
			101060389	28944	TBC1D3D

			79774	20310	GRTP1
			125058	28356	TBC1D16
			55357	18026	TBC1D2
			9098	12629	USP6
			79735	25699	TBC1D17
			374403	24702	TBC1D10C
			101060321	29860	TBC1D3G
			101060351	51245	TBC1D3K
			9779	19166	TBC1D5
			102724862	32709	TBC1D3I
			27352	25228	SGSM3
CG4881#	34568	salr	6299	10524	SALL1
			57167	15924	SALL4
			6297	10526	SALL2
			27164	10527	SALL3
			51222	13011	ZNF219
			9745	29025	ZNF536
			51427	12887	ZNF107
			163051	20629	ZNF709
			285971	28501	ZNF775
			7569	13001	ZNF182
			7772	13022	ZNF229
			284459	4928	ZNF875
			92285	30948	ZNF585B
			7769	13019	ZNF226
			26152	15809	ZNF337
			10780	13027	ZNF234
			199704	26305	ZNF585A
			374879	24750	ZNF699
			64763	26166	ZNF574
			7770	13020	ZNF227
			110116772		ZNF765-ZNF761
			7644	13166	ZNF91
			91664	25112	ZNF845
			342892	27994	ZNF850
			100131827	29448	ZNF717
			90987	13045	ZNF251
			163059	20811	ZNF433
			643836	23241	ZFP62
			170960	29425	ZNF721
			10224	20878	ZNF443
			7776	13028	ZNF236
			162962	34333	ZNF836
			90338	12948	ZNF160
			7694	12919	ZNF135
			10795	13061	ZNF268
			9310	12866	ZNF235
CG8781#	35924	tsu	9939	9905	RBM8A
			4691	7667	NCL
CG6873#	32861	CG6873	1073	1875	CFL2
			11034	15750	DSTN
			1072	1874	CFL1
CG3799#/CG42665#	39900	Exn	25791	7807	NGEF
			27237	15515	ARHGEF16
			22899	15590	ARHGEF15
			26084	24490	ARHGEF26
			128272	26604	ARHGEF19
			7984	13209	ARHGEF5
			50650	683	ARHGEF3
			10276	14592	NET1
			9138	681	ARHGEF1
			8997	4814	KALRN
			23370	17090	ARHGEF18
			64283	30322	ARHGEF28
			9826	14580	ARHGEF11
			221472	3664	FGD2
			23365	14193	ARHGEF12
			445328	33846	ARHGEF35
			11214	371	AKAP13
			50618	6184	ITSN2
			440107	33829	PLEKHG7
			57449	29105	PLEKHG5
			55200	25562	PLEKHG6

			89846	16027	FGD3
			121512	19125	FGD4
			9181	682	ARHGEF2
			6453	6183	ITSN1
			2245	3663	FGD1
CG13298#	38720	Sf3b6	51639	30096	SF3B6
CG14966#	38390	CG14966	123207	28443	C15orf40
CG14622#	31075	DAAM	23002	18142	DAAM1
			23500	18143	DAAM2
			1730	2877	DIAPH2
			81624	15480	DIAPH3
			1729	2876	DIAPH1
			392862	18464	GRID2IP
			64423	23791	INF2
			752	1212	FMNL1
			85462	29363	FHDC1
			91010	23698	FMNL3
			114793	18267	FMNL2
			342184	3768	FMN1
			56776	14074	FMN2
CG3869#	31581	Marf	9927	16877	MFN2
			55669	18262	MFN1
			4599	7532	MX1
			1759	2972	DNM1
			26052	29125	DNM3
			4976	8140	OPA1
			10059	2973	DNM1L
			4600	7533	MX2
			1785	2974	DNM2
CG6115#	50459	CG6115	144363	27052	ETFRF1
CG5229#	43928	chm	11143	17016	KAT7
			84148	17933	KAT8
			10524	5275	KAT5
			23522	17582	KAT6B
			7994	13013	KAT6A
			90378	17958	SAMD1
CG6627#	34503	Dnz1	340481	20750	ZDHHC21
			51304	18470	ZDHHC3
			158866	20342	ZDHHC15
			253832	20749	ZDHHC20
			51201	18469	ZDHHC2
			55625	18459	ZDHHC7
			283576	20106	ZDHHC22
			254359	27387	ZDHHC24
			84287	20714	ZDHHC16
			64429	19160	ZDHHC6
			84243	20712	ZDHHC18
			79844	19158	ZDHHC11
			51114	18475	ZDHHC9
			84885	19159	ZDHHC12
			29800	17916	ZDHHC1
			55146	18471	ZDHHC4
			653082	32962	ZDHHC11B
			23390	18412	ZDHHC17
			29801	18474	ZDHHC8
			25921	18472	ZDHHC5
			79683	20341	ZDHHC14
			54503	18413	ZDHHC13
			254887	28654	ZDHHC23
			131540	20713	ZDHHC19
CG3678#	42045	CG3678	9694	28963	EMC2
CG10872#/ CG33128#	326263	CG33128	5222	8887	PGA5
			1510	2530	CTSE
			5972	9958	REN
			9476	13395	NAPSA
			643847	8886	PGA4
			5225	8890	PGC
			643834	8885	PGA3
			1509	2529	CTSD
			25825	934	BACE2
			23621	933	BACE1
			11113	1985	CIT
CG8954#	34804	Smg5	23381	24644	SMG5

			9887	16792	SMG7
			23293	17809	SMG6
CG2887#	31978	CG2887	25822	14887	DNAJB5
			3337	5270	DNAJB1
			11080	14886	DNAJB4
			374407	30718	DNAJB13
			3300	5228	DNAJB2
			79982	25881	DNAJB14
			10049	14888	DNAJB6
			150353	24986	DNAJB7
			165721	23699	DNAJB8
			54788	14891	DNAJB12
			55466	14885	DNAJA4
			80331	16235	DNAJC5
			5611	9439	DNAJC3
			202052	28429	DNAJC18
			120526	26979	DNAJC24
			51726	14889	DNAJB11
			552891	37501	DNAJC25-GNG10
			3301	5229	DNAJA1
			79962	25802	DNAJC22
			23341	29157	DNAJC16
			548645	34187	DNAJC25
			4189	6968	DNAJB9
			54431	24637	DNAJC10
			85479	24138	DNAJC5B
			9093	11808	DNAJA3
			285126	24844	DNAJC5G
			134218	27030	DNAJC21
			55735	25570	DNAJC11
			10294	14884	DNAJA2
			7266	12392	DNAJC7
CG5748#+	37068	Hsf	3297	5224	HSF1
			3298	5225	HSF2
			3299	5227	HSF4
			100506164	29603	HSFX1
			101927685	52398	HSFX4
			124535	26862	HSF5
			86614	18568	HSFY1
			101928917	52395	HSFX3
			100130086	32701	HSFX2
			159119	23950	HSFY2
CG6930#	41423	l(3)neo38	7071	11810	KLF10
			83855	16857	KLF16
			136259	23025	KLF14
			28999	14536	KLF15
			8462	11811	KLF11
			687	1123	KLF9
			6667	11205	SP1
			221527	19066	ZBTB12
			360023	24819	ZBTB41
			6670	11208	SP3
			51043	18668	ZBTB7B
CG11722#	41227	CG11722	29078	21034	NDUFAF4
CG15399#	33472	CG15399	285282	18072	RABL3
CG3225#	33680	CG3225	60625	15861	DHX35
			165545	20410	DQX1
			1659	2749	DHX8
			79665	18018	DHX40
			1665	2738	DHX15
			55760	16717	DHX32
			56919	16718	DHX33
			8449	2739	DHX16
			9785	17211	DHX38
			57647	17210	DHX37
			122402	20122	TDRD9
			54505	15815	DHX29
			64848	24721	YTHDC2
			1660	2750	DHX9
			9704	16719	DHX34
			90957	20086	DHX57
			51538	30246	ZCCHC17
			22907	16716	DHX30

			170506	14410	DHX36
CG17753#	46035	Ccs	9973	1613	CCS
			6647	11179	SOD1
CG4016#	36448	Spt-I	10558	11277	SPTLC1
			55304	16253	SPTLC3
			23464	4188	GCAT
			9517	11278	SPTLC2
			212	397	ALAS2
			211	396	ALAS1
CG31641#	33863	stai	81551	16078	STMN4
			50861	15926	STMN3
			11075	10577	STMN2
			3925	6510	STMN1
			100500808	38911	MIR3917
			401236	44668	STMND1
			56888	20589	KCMF1
CG18679#/CG43795#	5740629	CG43795	57512	23689	GPR158
			440435	31371	GPR179
CG12345#	42249	ChAT	1103	1912	CHAT
			1384	2342	CRAT
CG7066#	38934	Sbp2	79048	30972	SECISBP2
			9728	28997	SECISBP2L
			4809	7819	SNU13
CG10524#/CG42349#	32191	Pkcdelta	5580	9399	PRKCD
			5588	9410	PRKCQ
			5581	9401	PRKCE
			5583	9403	PRKCH
			5578	9393	PRKCA
			5579	9395	PRKCB
			5582	9402	PRKCG
			5585	9405	PKN1
			5586	9406	PKN2
			29941	17999	PKN3
			5584	9404	PRKCI
			5590	9412	PRKCZ
			100533105	48354	C8orf44-SGK3
			207	391	AKT1
			208	392	AKT2
			10110	13900	SGK2
			10000	393	AKT3
			23678	10812	SGK3
			6446	10810	SGK1
			124923	26314	RSKR
CG4288#	42426	MFS9	26503	10933	SLC17A5
			10246	10930	SLC17A2
			10786	10931	SLC17A3
			57084	16703	SLC17A6
			57030	16704	SLC17A7
			246213	20151	SLC17A8
			10050	10932	SLC17A4
			6568	10929	SLC17A1
			63910	16192	SLC17A9
CG2708+	44910	unc-45	146862	14304	UNC45B
			55898	30594	UNC45A
			54970	23700	TTC12
			374659	30522	HDDC3
			54557	23567	SGTB
			6449	10819	SGTA
			10910	16987	SUGT1
			130502	32954	TTC32
			83893	29935	SPATA16
			64427	25759	TTC31
			10953	15746	TOMM34
CG5160+	34015	CG5160	65997	23804	RASL11B
			79785	26213	RERGL
			6016	10023	RIT1
			6014	10017	RIT2
			387496	23802	RASL11A
			85004	15980	RERG
			51285	30289	RASL12
CG7436+	38909	Nmt	9397	7858	NMT2
			4836	7857	NMT1
CG7843+	35539	Ars2	51593	24101	SRRT

CG10281+	40790	TfIIFalpha	2962	4652	GTF2F1
CG2145+	32027	CG2145	8909	14369	ENDOU
			5455	9216	POU3F3
CG15739+	32146	CG15739	57026	30259	PDXP
			283871	8909	PGP
			64077	30042	LHPP
			2631	4179	NIPSNAP2
			8508	7827	NIPSNAP1
			27440	1843	HDHD5
			84064	25364	HDHD2
CG7275+	39669	CG7275	25879	24535	DCAF13
CG9207+	33973	Gas41	8089	24859	YEATS4
			55689	25489	YEATS2
			4300	7136	MLLT3
			4298	7134	MLLT1
CG6921+	42657	bond	64834	14418	ELOVL1
			79993	26292	ELOVL7
			60481	21308	ELOVL5
			6785	14415	ELOVL4
			54898	14416	ELOVL2
			83401	18047	ELOVL3
			79071	15829	ELOVL6
CG16785+	31023	fz3	11211	4039	FZD10
			8326	4047	FZD9
			7855	4043	FZD5
			7976	4041	FZD3
			8324	4045	FZD7
			8321	4038	FZD1
			6423	10777	SFRP2
			6425	10779	SFRP5
			6424	10778	SFRP4
			2487	3959	FRZB
			6422	10776	SFRP1
			8322	4042	FZD4
			8325	4046	FZD8
			8323	4044	FZD6
			6608	11119	SMO
			2535	4040	FZD2
			2171	3560	FABP5
			57727	15909	NCOA5
			100616500	41883	MIR4683
			8532	2333	CPZ
			10699	19012	CORIN
			83552	18121	MFRP
CG31687+	318886	CG31687	8697	1724	CDC23
			16	20	AARS
			57505	21022	AARS2
CG9753+	43583	AdoR	136	264	ADORA2B
			134	262	ADORA1
			135	263	ADORA2A
			140	268	ADORA3
			151306	19680	GPBAR1
CG7709+	42246	Muc91C	4582	7508	MUC1
			100101267	34005	POM121C
			57055	15964	DAZ2
			1297	2217	COL9A1
CG7807+	40398	TfAP-2	7020	11742	TFAP2A
			7022	11744	TFAP2C
			339488	30774	TFAP2E
			7021	11743	TFAP2B
			83741	15581	TFAP2D
CG7085+	33402	sau	64083	15452	GOLPH3
			55204	24882	GOLPH3L
CG31318+/CG43663+	326128	Ada2a	6871	11531	TADA2A
			93624	30781	TADA2B
			5433	9191	POLR2D
CG1129+	40599	CG1129	29925	22932	GMPPB
			29926	22923	GMPPA
			8893	3261	EIF2B5
			8891	3259	EIF2B3
CG6944+	33782	Lam	84823	6638	LMNB2
			4000	6636	LMNA
			4001	6637	LMNB1

			1674	2770	DES
			7431	12692	VIM
			102466806	49998	MIR7108
			3856	6446	KRT8
			3884	6451	KRT33B
			3881	6448	KRT31
			3850	6440	KRT3
			3868	6423	KRT16
			51350	24430	KRT76
			3866	6421	KRT15
			4741	7734	NEFM
			3854	6444	KRT6B
			4747	7739	NEFL
			3880	6436	KRT19
			3872	6427	KRT17
			3852	6442	KRT5
			3855	6445	KRT7
			3883	6450	KRT33A
			3861	6416	KRT14
			4744	7737	NEFH
			220136	26530	CFAP53
			9119	24431	KRT75
			3858	6413	KRT10
			9118	6057	INA
			3853	6443	KRT6A
			3859	6414	KRT12
			2670	4235	GFAP
			3860	6415	KRT13
			3886	6453	KRT35
			3857	6447	KRT9
			100653049		LOC100653049
			160492	26683	LMNTD1
			256329	28561	LMNTD2
CG6589+	34581	spag4	23353	18587	SUN1
			25777	14210	SUN2
			256979	22429	SUN3
			140732	16252	SUN5
			6676	11214	SPAG4
CG8431+	36784	CysRS	833	1493	CARS
			79587	25695	CARS2
CG31321+	318681	CG31321	283537	27501	SLC46A3
			113235	30521	SLC46A1
			57864	16055	SLC46A2
			84641	23376	MFSD14B
			64645	23363	MFSD14A
CG5404+	41901	CG5404	284129	14471	SLC26A11
			116369	14468	SLC26A8
			5172	8818	SLC26A4
			1811	3018	SLC26A3
			65012	14470	SLC26A10
			115111	14467	SLC26A7
			65010	14472	SLC26A6
			115019	14469	SLC26A9
			10861	10993	SLC26A1
			1836	10994	SLC26A2
			375611	9359	SLC26A5
CG5310+	32396	nmdyn-D6	10201	20567	NME6
			51314	16473	NME8
			29922	20461	NME7
			8382	7853	NME5
			347736	21343	NME9
			4830	7849	NME1
			4831	7850	NME2
			4833	7852	NME4
			4832	7851	NME3
CG8189+	39143	ATPsynB	515	840	ATP5PB
			3777	6278	KCNK3
CG17081+	39647	Cep135	9662	29086	CEP135
			80705	14927	TSGA10
CG18812+	59173	Gdap2	54834	18010	GDAP2
			28992	29598	MACROD1
			140733	16126	MACROD2
			9555	4740	H2AFY

			55506	14453	H2AFY2
			54625	29232	PARP14
			165631	26876	PARP15
			83666	24118	PARP9
CG9742+	32636	SNRPG	6637	11163	SNRPG
			100130932	49371	SNRPGP15
			51690	20470	LSM7
			23658	17162	LSM5
CG16938+/CG3278+	35454	Tif-IA	54700	30346	RRN3
			730092	30548	RRN3P1
			653390	37619	RRN3P2
CG7279+	43973	Lip1	8513	6622	LIPF
			643414	23444	LIPK
			3988	6617	LIPA
			340654	23455	LIPM
			643418	23452	LIPN
			142910	21773	LIPJ
			3156	5006	HMGCR
			253152	23758	EPHX4
			84836	28235	ABHD14B
			670	1094	BPHL
			83451	16407	ABHD11
			79575	23759	ABHD8
			4232	7028	MEST
			2053	3402	EPHX2
			57406	21398	ABHD6
			63874	20154	ABHD4
			25864	24538	ABHD14A
			51099	21396	ABHD5
			79852	23760	EPHX3
			253190	29446	SERHL2
			51400	30178	PPME1
			55347	25656	ABHD10
			2052	3401	EPHX1
CG1640+	32292	CG1640	2875	4552	GPT
			84706	18062	GPT2
			84680	23989	ACCS
			883	1564	KYAT1
			390110	34391	ACCSL
			6898	11573	TAT
			56267	33238	KYAT3
CG11136+	37342	Lrt	349667	23053	RTN4RL2
			164312	16208	LRRN4
			221091	33724	LRRN4CL
			54674	17200	LRRN3
			339977	34299	LRRC66
			57611	29286	ISLR2
			3671	6133	ISLR
			23769	3760	FLRT1
			100130733	35155	LRRC70
			23767	3762	FLRT3
			5310	9008	PKD1
			340745	23443	LRIT2
			347902	24073	AMIGO2
CG5599+	32441	CG5599	1629	2698	DBT
			4313	7166	MMP2
			1743	2911	DLST
			8050	21350	PDHX
			1737	2896	DLAT
CG12524+/CG34356+	5740442	bma	55681	19286	SCYL2
CG6340+	32482	CG6340	65117	30559	RSRC2
CG4241+	42429	DPCoAC	284439	28380	SLC25A42
			8034	10986	SLC25A16
			29957	20662	SLC25A24
			114789	20663	SLC25A25
			79085	19375	SLC25A23
			203427	30557	SLC25A43
			284427	28533	SLC25A41
			60386	14409	SLC25A19
CG2917+	37970	Orc4	5000	8490	ORC4
CG6066+	43267	CG6066	79576	29873	NKAP
			222698	21584	NKAPL
CG8849+	33703	mRpL24	79590	14037	MRPL24

			6154	10327	RPL26
			51121	17050	RPL26L1
CG4132+	34957	pkaap	11216	368	AKAP10
CG17419+/CG41099+	3355072	CG41099	51479	20763	ANKFY1
			79722	25681	ANKRD55
			26057	23575	ANKRD17
			338699	26752	ANKRD42
			23243	29024	ANKRD28
			283373	26614	ANKRD52
			404734	33530	ANKHD1-EIF4EBP3
			91526	25259	ANKRD44
			288	494	ANK3
			286	492	ANK1
			287	493	ANK2
			255239	21027	ANKK1
			54101	496	RIPK4
			8737	10019	RIPK1
			4293	6861	MAP3K9
			6885	6859	MAP3K7
			4294	6849	MAP3K10
			4342	7199	MOS
			8767	10020	RIPK2
			53349	13180	ZFYVE1
			55872	18282	PBK
			11035	10021	RIPK3
			120892	18618	LRRK2
			84936	20758	ZFYVE19
			100526835	42952	FPGT-TNNI3K
			25778	29043	DSTYK
			9146	4897	HGS
			84451	29798	MAP3K21
			4296	6850	MAP3K11
			51086	19661	TNNI3K
			197259	26617	MLKL
			79705	18608	LRRK1
			51776	17797	MAP3K20
CG4152+	48782	Mtr4	23517	18734	MTREX
			6499	10898	SKIV2L
			164045	20193	HFM1
			10527	9852	IPO7
			55601	25942	DDX60
			10526	9853	IPO8
			91351	26429	DDX60L
CG9245+	32506	Pis	10423	1769	CDIPT
			54675	16148	CRLS1
CG3759+	34258	Mco1	341208	30477	HEPHL1
			1356	2295	CP
			9843	4866	HEPH
			2157	3546	F8
			2153	3542	F5
			4583	7512	MUC2
CG11010+	39461	Ent3	222962	23097	SLC29A4
			2030	11003	SLC29A1
			55315	23096	SLC29A3
			3177	11004	SLC29A2
CG9958+	3772677	Snapin	23557	17145	SNAPIN
CG4928+	32682	CG4928	54346	12570	UNC93A
			81622	13481	UNC93B1
CG7826+/CG42273+	32771	mnb	1859	3091	DYRK1A
			9149	3092	DYRK1B
			8444	3094	DYRK3
			8798	3095	DYRK4
			8445	3093	DYRK2
			28996	14402	HIPK2
			204851	19006	HIPK1
			10114	4915	HIPK3
			1198	2071	CLK3
			57396	13659	CLK4
			147746	19007	HIPK4
			53938	9262	PPIL3
			1195	2068	CLK1
			1196	2069	CLK2
			8899	17346	PRPF4B

CG17681+	35086	CG17681	389396	21349	GLYATL3
			10249	13734	GLYAT
			92292	30519	GLYATL1
			219970	24178	GLYATL2
			100287520	37865	GLYATL1B
CG6335+	32841	HisRS	3035	4816	HARS
			23438	4817	HARS2
			27102	24921	EIF2AK1
			440275	19687	EIF2AK4
CG10126+	41579	CG10126	133690	28375	CAPSL
			828	1487	CAPS
			84698	16471	CAPS2
			79012	28788	CAMKV
			91807	29826	MYLK3
			139728	13415	PNCK
			5681	9529	PSKH1
			8536	1459	CAMK1
			7204	12303	TRIO
			84033	15719	OBSCN
			814	1464	CAMK4
			57172	14585	CAMK1G
			85481	18997	PSKH2
			57118	19341	CAMK1D
			65975	14568	STK33
			340156	27972	MYLK4
			9262	11396	STK17B
			1613	2676	DAPK3
			9263	11395	STK17A
			23604	2675	DAPK2
			166614	19002	DCLK2
			10290	16901	SPEG
			9201	2700	DCLK1
			151651	26330	EFHB
			1612	2674	DAPK1
			85443	19005	DCLK3
			127933	19683	UHMK1
			85366	16243	MYLK2
CG14905+	42024	CG14905	160762	26669	CCDC63
			93233	26560	CCDC114
CG31291+/CG45105+	41932	CG45105	10806	10671	SDCCAG8
			4741	7734	NEFM
CG31000+	48571	heph	5725	9583	PTBP1
			58155	17662	PTBP2
			9991	10253	PTBP3
			282996	27424	RBM20
			100616459	41868	MIR4745
			27332	17894	ZNF638
			9782	6912	MATR3
			3191	5045	HNRNPL
			92906	25127	HNRNPLL
CG31211+	41443	CG31211	25957	21222	PNISR
			89876	24010	MAATS1
CG2124+	31989	CG2124	60493	25790	FASTKD5
			9238	17443	TBRG4
			79072	28758	FASTKD3
			22868	29160	FASTKD2
			79675	26150	FASTKD1
			10922	24676	FASTK
CG9927+	41699	Art6	3276	5187	PRMT1
			56341	5188	PRMT8
			55170	18241	PRMT6
			10196	30163	PRMT3
			3275	5186	PRMT2
			10498	23393	CARM1
			90826	25099	PRMT9
			134145	27029	ATPSCKMT
			114049	16405	BUD23
			79807	25806	GSTCD
			196410	28276	METTL7B
			65990	14152	ANTKMT
			57604	26725	TRMT9B
			25840	24550	METTL7A
			91801	25189	ALKBH8

			54496	25557	PRMT7
			79133	15899	NDUFAF5
			155368	19068	METTL27
CG7598+	43503	CIA30	51103	18828	NDUFAF1
CG5121+	43079	MED28	80306	24628	MED28
CG3776+	37996	CG3776	79568	26198	MAIP1
CG4482+	34872	mol	90527	26507	DUOXA1
			405753	32698	DUOXA2
CG3035+	31647	cm	10947	570	AP3M2
			26985	569	AP3M1
CG7935+	44747	msk	10527	9852	IPO7
			10526	9853	IPO8
			6499	10898	SKIV2L
			55601	25942	DDX60
			23517	18734	MTREX
			91351	26429	DDX60L
CG13779+	50428	Sem1	7979	10845	SEM1
CG9998+	32602	U2af50	11338	23156	U2AF2
CG11360+	43810	CG11360	51320	28040	MEX3C
			84206	25297	MEX3B
			399664	16734	MEX3D
			92312	33482	MEX3A
CG31704+	318906	CG31704	6691	11245	SPINK2
			84651	24643	SPINK7
			643394	32951	SPINK9
			6690	11244	SPINK1
			408187	33825	SPINK14
			404203	29486	SPINK6
			27290	16646	SPINK4
			646424	33160	SPINK8
			153218	27200	SPINK13
CG32253+/CG11583+	326206	CG11583	55299	24170	BRIX1
CG5085+	42414	Sirt2	22933	10886	SIRT2
			23410	14931	SIRT3
			23411	14929	SIRT1
			23408	14933	SIRT5
			51548	14934	SIRT6
			23409	14932	SIRT4
			51547	14935	SIRT7
CG5335+	37140	CG5335	654346	33874	LGALS9C
			3964	6569	LGALS8
			3965	6570	LGALS9
			284194	24842	LGALS9B
			3958	6563	LGALS3
			85329	15788	LGALS12
			29094	25012	LGALSL
			3960	6565	LGALS4
			402635	4577	GRIFIN
			56891	30054	LGALS14
			1178	2014	CLC
			29124	15449	LGALS13
			148003	40039	LGALS16
			3957	6562	LGALS2
			3956	6561	LGALS1
			3963	6568	LGALS7
			653499	34447	LGALS7B
CG7014+	41807	RpS5b	6193	10426	RPS5
			51081	14499	MRPS7
CG10913+	49803	Spn55B	1992	3311	SERPINB1
			5269	8950	SERPINB6
			5274	8943	SERPINI1
			6317	10569	SERPINB3
			89778	14221	SERPINB11
			5273	8942	SERPINB10
			5272	8955	SERPINB9
			5271	8952	SERPINB8
			6318	10570	SERPINB4
			5275	8944	SERPINB13
			5276	8945	SERPINI2
			5055	8584	SERPINB2
			5270	8951	SERPINE2
			89777	14220	SERPINB12
			462	775	SERPINC1

			5268	8949	SERPINB5
			647174	24774	SERPINE3
			327657	15995	SERPINA9
			5054	8583	SERPINE1
			866	1540	SERPINA6
			3053	4838	SERPIND1
			5267	8948	SERPINA4
			256394	19193	SERPINA11
			6906	11583	SERPINA7
			390502	8985	SERPINA2
			8710	13902	SERPINB7
			284293	23037	HMSD
			145264	18359	SERPINA12
			388007	30909	SERPINA13P
			51156	15996	SERPINA10
			710	1228	SERPING1
			5345	9075	SERPINF2
			5176	8824	SERPINF1
			5104	8723	SERPINA5
			5265	8941	SERPINA1
			183	333	AGT
			12	16	SERPINA3
			871	1546	SERPINH1
CG4202+	31447	Sas10	57050	24477	UTP3
CG10693+	42940	slo	3778	6284	KCNMA1
			157855	18867	KCNU1
CG5553+	44915	DNApol-alpha60	5558	9370	PRIM2
			101930420		LOC101930420
CG33505+	3346176	U3-55K	9136	16829	RRP9
CG10564+	40333	Ac78C	114	239	ADCY8
			111	236	ADCY5
			112	237	ADCY6
			196883	235	ADCY4
			4882	7944	NPR2
			120892	18618	LRRK2
			107	232	ADCY1
			4881	7943	NPR1
			2984	4688	GUCY2C
			23239	20610	PHLPP1
			2977	4684	GUCY1A2
			4883	7945	NPR3
			3000	4689	GUCY2D
			23035	29149	PHLPP2
			108	233	ADCY2
			2983	4687	GUCY1B1
			115	240	ADCY9
			109	234	ADCY3
			55811	21285	ADCY10
			2982	4685	GUCY1A1
			2986	4691	GUCY2F
			113	238	ADCY7
CG8933+	32567	exd	5090	8634	PBX3
			5089	8633	PBX2
			5087	8632	PBX1
			80714	13403	PBX4
			63876	16714	PKNOX2
			7050	11776	TGIF1
			4212	7001	MEIS2
			60436	15764	TGIF2
			90655	18569	TGIF2LY
			56917	29537	MEIS3
			90316	18570	TGIF2LX
			4211	7000	MEIS1
			5316	9022	PKNOX1
CG13849+	42633	Nop56	10528	15911	NOP56
			51602	29926	NOP58
			100302138	35364	MIR1292
			26121	15446	PRPF31
CG4035+	45525	eIF4E1	1977	3287	EIF4E
			253314	33179	EIF4E1B
			317649	31837	EIF4E3
			9470	3293	EIF4E2
CG16884+	34812	Vajk3	57473	29212	ZNF512B

			84450	29380	ZNF512
			199720	18869	GGN
CG30048+	246415	CG30048	168507	18053	PKD1L1
			342372	21716	PKD1L3
			114780	21715	PKD1L2
			125336	26521	LOXHD1
			765	1380	CA6
			10343	9015	PKDREJ
			5310	9008	PKD1
CG10582+	40325	Sin	55718	30347	POLR3E
CG1989+	32295	Yippee	51646	18329	YPEL5
			29799	12845	YPEL1
			219539	18328	YPEL4
			83719	18327	YPEL3
			388403	18326	YPEL2
CG7769+	41611	pic	1642	2717	DDB1
CG4969+	34010	Wnt6	7475	12785	WNT6
			7471	12774	WNT1
			7483	12778	WNT9A
			7480	12775	WNT10B
			7476	12786	WNT7A
			7472	12780	WNT2
			7477	12787	WNT7B
			7481	12776	WNT11
			7478	12788	WNT8A
			7482	12781	WNT2B
			7474	12784	WNT5A
			54361	12783	WNT4
			81029	16265	WNT5B
			80326	13829	WNT10A
			7479	12789	WNT8B
			7473	12782	WNT3
			51384	16267	WNT16
			89780	15983	WNT3A
			7484	12779	WNT9B
CG7176+	44291	Idh	3417	5382	IDH1
			3418	5383	IDH2
CG3158+	41919	spn-E	122402	20122	TDRD9
			54505	15815	DHX29
			64848	24721	YTHDC2
			1660	2750	DHX9
			9704	16719	DHX34
			90957	20086	DHX57
			22907	16716	DHX30
			170506	14410	DHX36
			65124	26149	SOWAHC
			647286	40912	RD3L
			165545	20410	DQX1
			1659	2749	DHX8
			79665	18018	DHX40
			60625	15861	DHX35
			1665	2738	DHX15
			55760	16717	DHX32
			51538	30246	ZCCHC17
			57647	17210	DHX37
			56919	16718	DHX33
			8449	2739	DHX16
			9785	17211	DHX38
CG5911+	42523	ETHR	7201	12299	TRHR
			2693	4267	GHSR
			10316	4518	NMUR1
			56923	16454	NMUR2
CG17075+	33191	CG17075	29800	17916	ZDHHC1
			79844	19158	ZDHHC11
			653082	32962	ZDHHC11B
			131540	20713	ZDHHC19
			23390	18412	ZDHHC17
			84243	20712	ZDHHC18
			84287	20714	ZDHHC16
			29801	18474	ZDHHC8
			25921	18472	ZDHHC5
			158866	20342	ZDHHC15
			79683	20341	ZDHHC14

			51304	18470	ZDHHC3
			340481	20750	ZDHHC21
			283576	20106	ZDHHC22
			51114	18475	ZDHHC9
			84885	19159	ZDHHC12
			253832	20749	ZDHHC20
			51201	18469	ZDHHC2
			64429	19160	ZDHHC6
			54503	18413	ZDHHC13
			254887	28654	ZDHHC23
			55625	18459	ZDHHC7
			254359	27387	ZDHHC24
			55146	18471	ZDHHC4
CG11278+	39485	Syx13	203062	26437	TSNARE1
			23673	11430	STX12
			8417	11442	STX7
			8675	11431	STX16
			55014	11432	STX17
CG9696+	45655	dom	57634	11958	EP400
			10847	16974	SRCAP
			54617	26956	INO80
CG5869+	34963	GMF	9535	4374	GMFG
			2764	4373	GMFB
			930	1633	CD19
CG10033+	44817	for	5592	9414	PRKG1
			5593	9416	PRKG2
			5568	9382	PRKACG
			375775	24768	PNPLA7
			10908	16268	PNPLA6
			5575	9390	PRKAR1B
			5613	9441	PRKX
			5577	9392	PRKAR2B
			140894	16145	CNBD2
			5566	9380	PRKACA
			5576	9391	PRKAR2A
			5567	9381	PRKACB
			5573	9388	PRKAR1A
CG1882+	35733	CG1882	63874	20154	ABHD4
			51099	21396	ABHD5
			79852	23760	EPHX3
			8513	6622	LIPF
			253152	23758	EPHX4
			84836	28235	ABHD14B
			643414	23444	LIPK
			670	1094	BPHL
			83451	16407	ABHD11
			79575	23759	ABHD8
			4232	7028	MEST
			2053	3402	EPHX2
			57406	21398	ABHD6
			3988	6617	LIPA
			25864	24538	ABHD14A
			253190	29446	SERHL2
			643418	23452	LIPN
			340654	23455	LIPM
			51400	30178	PPME1
			142910	21773	LIPJ
			55347	25656	ABHD10
			2052	3401	EPHX1
CG11739+	40552	Sfxn1-3	94081	16085	SFXN1
			81855	16087	SFXN3
			94097	16073	SFXN5
			118980	16086	SFXN2
			119559	16088	SFXN4
CG12298+	44870	sub	10112	9787	KIF20A
			9585	7212	KIF20B
			9493	6392	KIF23
CG11958+	44643	Cnx99A	821	1473	CANX
			1047	2060	CLGN
			811	1455	CALR
CG1139+	38264	CG1139	285641	19659	SLC36A3
			153201	18762	SLC36A2
			206358	18761	SLC36A1

			120103	19660	SLC36A4
			146167	32434	SLC38A8
			145389	19863	SLC38A6
			140679	11018	SLC32A1
			153129	26907	SLC38A9
			81539	13447	SLC38A1
			55238	25582	SLC38A7
			54407	13448	SLC38A2
			55089	14679	SLC38A4
			10991	18044	SLC38A3
			92745	18070	SLC38A5
			151258	26836	SLC38A11
			124565	28237	SLC38A10
CG3329+	39628	Prosbeta2	5695	9544	PSMB7
			5699	9538	PSMB10
			5689	9537	PSMB1
			122706	31963	PSMB11
			5696	9545	PSMB8
			5693	9542	PSMB5
			5687	9535	PSMA6
			5684	9532	PSMA3
			143471	22985	PSMA8
			5688	9536	PSMA7
			5682	9530	PSMA1
			5690	9539	PSMB2
			5685	9533	PSMA4
			5691	9540	PSMB3
			5686	9534	PSMA5
CG2241+	43635	Rpt6R	5705	9552	PSMC5
			5701	9548	PSMC2
			5700	9547	PSMC1
			5706	9553	PSMC6
			5702	9549	PSMC3
			5704	9551	PSMC4
			2710	4289	GK
			54454	29230	ATAD2B
			29028	30123	ATAD2
			23729	1492	SHPK
			11104	6216	KATNA1
			84056	28361	KATNAL1
			55277	25610	FGGY
			256356	28635	GK5
			83473	25387	KATNAL2
			2712	4291	GK2
CG3305+	35411	Lamp1	3916	6499	LAMP1
			3920	6501	LAMP2
			27074	14582	LAMP3
			968	1693	CD68
			24141	16097	LAMP5
2905+/ CG10549+/CG335	35483	Nipped-A	8295	12347	TRRAP
			5289	8974	PIK3C3
			2475	3942	MTOR
			5591	9413	PRKDC
			552900	29488	BOLA2
			5297	8983	PI4KA
			5291	8976	PIK3CB
			5286	8971	PIK3C2A
			5298	8984	PI4KB
			5288	8973	PIK3C2G
			654483	32479	BOLA2B
			107282092	53563	BOLA2-SMG1P6
			5290	8975	PIK3CA
			545	882	ATR
			5287	8972	PIK3C2B
			285590	29242	SH3PXD2B
			5293	8977	PIK3CD
			9644	23664	SH3PXD2A
			5294	8978	PIK3CG
			23049	30045	SMG1
CG6827+	39387	Nrx-IV	26047	13830	CNTNAP2
			8506	8011	CNTNAP1
			85445	18747	CNTNAP4
			79937	13834	CNTNAP3

			129684	18748	CNTNAP5
			728577	32035	CNTNAP3B
			100289279	53878	CNTNAP3C
			9369	8010	NRXN3
			9378	8008	NRXN1
			9379	8009	NRXN2
CG7431+	42136	TyrR	146	280	ADRA1D
			147	278	ADRA1B
			152	283	ADRA2C
			151	282	ADRA2B
			148	277	ADRA1A
			150	281	ADRA2A
			1813	3023	DRD2
			1814	3024	DRD3
			3360	5299	HTR4
			3274	5183	HRH2
			3269	5182	HRH1
CG2918+	31215	CG2918	10525	16931	HYOU1
			10808	16969	HSPH1
			3312	5241	HSPA8
			259217	19022	HSPA12A
			3309	5238	HSPA5
			284525	28664	SLC9C2
			3303	5232	HSPA1A
			339416	24786	ANKRD45
			51182	29526	HSPA14
			3304	5233	HSPA1B
			116835	16193	HSPA12B
			3310	5239	HSPA6
			3305	5234	HSPA1L
			3313	5244	HSPA9
			3308	5237	HSPA4
			6782	11375	HSPA13
			22824	17041	HSPA4L
			3306	5235	HSPA2
CG11546+	46027	kermit	126326	18183	GIPC3
			10755	1226	GIPC1
			54810	18177	GIPC2
			245711	30613	SPDYA
CG5651+	39027	pix	6059	69	ABCE1
CG12275+	43321	RpS10a	6204	10383	RPS10
			93144	15795	RPS10P5
			100529239	49181	RPS10-NUDT3
			5339	9069	PLEC
CG5969+	40269	CG5969	203547	22082	VMA21
CG13391+	34156	AlaRS	16	20	AARS
			57505	21022	AARS2
			8697	1724	CDC23
CG2478+	35325	brun	83696	30832	TRAPPC9
CG1030+	40833	Scr	3202	5106	HOXA5
			3215	5116	HOXB5
			3222	5127	HOXC5
			3233	5138	HOXD4
			3214	5115	HOXB4
			3201	5105	HOXA4
			3221	5126	HOXC4
			3204	5108	HOXA7
			3217	5118	HOXB7
			3232	5137	HOXD3
			4222	7013	MEOX1
			3231	5132	HOXD1
			170825	24959	GSX2
			3224	5129	HOXC8
			3218	5119	HOXB8
			3198	5099	HOXA1
			3212	5113	HOXB2
			3223	5128	HOXC6
			3213	5114	HOXB3
			4223	7014	MEOX2
			2637	4186	GBX2
			2636	4185	GBX1
			3651	6107	PDX1
			3199	5103	HOXA2

			3110	4979	MNX1
			3200	5104	HOXA3
			3216	5117	HOXB6
			3211	5111	HOXB1
			3203	5107	HOXA6
			3234	5139	HOXD8
			219409	20374	GSX1
CG3589+	37966	CG3589	219743	28531	TYSND1
			94031	30406	HTRA3
			5715	9567	PSMD9
			5654	9476	HTRA1
			27429	14348	HTRA2
			203100	26909	HTRA4
CG14511+	43445	CG14511	84912	20584	SLC35B4
CG31289+	42663	Dph5	51611	24270	DPH5
CG6509+	34573	Dlg5	9231	2904	DLG5
			160622	18707	GRASP
			9595	9506	CYTIP
			10083	12597	USH1C
			84433	16393	CARD11
			84708	6657	LNX1
			64398	18669	MPP5
			100529257	48350	SYNJ2BP-COX16
			9351	11076	SLC9A3R2
			29775	16422	CARD10
			3603	5980	IL16
			23037	18486	PDZD2
			9368	11075	SLC9A3R1
			79955	26257	PDZD7
			5174	8821	PDZK1
			1739	2900	DLG1
			23426	18708	GRIP1
			8777	7208	MPDZ
			1741	2902	DLG3
			58538	13680	MPP4
			51678	18167	MPP6
			8573	1497	CASK
			2987	4693	GUK1
			51248	28034	PDZD11
			57120	17643	GOPC
			4354	7219	MPP1
			79092	16446	CARD14
			117583	14446	PARD3B
			1742	2903	DLG4
			222484	20421	LNX2
			143162	28572	FRMPD2
			55333	18955	SYNJ2BP
			25861	16361	WHRN
			260425	29647	MAGI3
			10207	28881	PATJ
			392862	18464	GRID2IP
			143098	26542	MPP7
			136332	21964	LRGUK
			4355	7220	MPP2
			4356	7221	MPP3
			1740	2901	DLG2
			79849	19891	PDZD3
			56288	16051	PARD3
CG5751+	39015	TrpA1	8989	497	TRPA1
			286	492	ANK1
			287	493	ANK2
			288	494	ANK3
			65124	26149	SOWAHC
			347454	32960	SOWAHD
			654463	28065	FER1L6
			26509	3656	MYOF
			8291	3097	DYSF
			9381	8515	OTOF
CG1903+/CG44436+	32273	sno	55206	22973	SBNO1
			22904	29158	SBNO2
			102466877	50174	MIR8072
CG10315+	37706	eIF2Bdelta	8890	3260	EIF2B4
			8892	3258	EIF2B2

			1967	3257	EIF2B1
CG3843+	41811	RpL10Aa	4736	10299	RPL10A
			65008	14275	MRPL1
CG7162+	40403	MED1	5469	9234	MED1
CG4960+	43115	CG4960	7905	30077	REEP5
			92840	30078	REEP6
			221035	23711	REEP3
			51308	17975	REEP2
			80346	26176	REEP4
			65055	25786	REEP1
CG3849+	39864	Lasp	3927	6513	LASP1
			10529	16932	NEBL
			4703	7720	NEB
			28988	2696	DBNL
			4892	7988	NRAP
CG4521+	32637	mthl1	30817	3337	ADGRE2
			221188	19010	ADGRG5
			9289	4512	ADGRG1
			266977	18990	ADGRF1
			347088	18651	ADGRD2
			222487	13728	ADGRG3
			10149	4516	ADGRG2
			57211	13841	ADGRG6
			165082	18989	ADGRF3
			2015	3336	ADGRE1
			221393	19011	ADGRF4
			283383	19893	ADGRD1
			22859	20973	ADGRL1
			84873	19241	ADGRG7
			976	1711	ADGRE5
			221395	19030	ADGRF5
			139378	18992	ADGRG4
			64123	20822	ADGRL4
			222611	18991	ADGRF2
			23266	18582	ADGRL2
			23284	20974	ADGRL3
			84658	23647	ADGRE3
CG3499+	37636	YME1L	10730	12843	YME1L1
			6687	11237	SPG7
			10939	315	AFG3L2
			617	1020	BCS1L
CG17293+	34153	Wdr82	80335	28826	WDR82
CG12031+	38073	MED14	9282	2370	MED14
CG6146+	32458	Top1	7150	11986	TOP1
			116447	29787	TOP1MT
CG7757+	40172	Prp3	9129	17348	PRPF3
			286187	33732	PPP1R42
CG12727+/CG44328+	32303	Neto	81831	14644	NETO2
			81832	13823	NETO1
CG7742+	33750	CG7742	55296	25624	TBC1D19
CG4843+	41853	Tm2	7170	12012	TPM3
			7168	12010	TPM1
			7169	12011	TPM2
			7171	12013	TPM4
			402643	39167	TPM3P4
CG6835+	32775	Gss1	2937	4624	GSS
CG9344+	37372	CG9344	11157	17017	LSM6
			6636	11162	SNRPF
			84316	28212	NAA38
			6632	11158	SNRPD1
			23658	17162	LSM5
			6628	11153	SNRPB
			57819	13940	LSM2
			6635	11161	SNRPE
			6634	11160	SNRPD3
			6633	11159	SNRPD2
			84967	17562	LSM10
			6638	11164	SNRPN
CG12283+	34688	kek1	441381	28947	LRRC24
			221091	33724	LRRN4CL
			54674	17200	LRRN3
			339977	34299	LRRC66
			164312	16208	LRRN4

			57611	29286	ISLR2
			3671	6133	ISLR
			57463	20824	AMIGO1
			386724	24075	AMIGO3
			347902	24073	AMIGO2
			339398	31814	LINGO4
			349667	23053	RTN4RL2
			57689	29317	LRRC4C
			645191	21206	LINGO3
			64101	15586	LRRC4
			158038	21207	LINGO2
			84894	21205	LINGO1
			57622	29290	LRFN1
			146760	21329	RTN4RL1
			65078	18601	RTN4R
			94030	25042	LRRC4B
CG12325+	36144	CG12325	102724159		LOC102724159
			5822	9711	PWP2
CG8222+	34127	Pvr	3791	6307	KDR
			2324	3767	FLT4
			2321	3763	FLT1
			5156	8803	PDGFRA
			5159	8804	PDGFRB
			3815	6342	KIT
			1436	2433	CSF1R
			2322	3765	FLT3
			8085	7133	KMT2D
			79368	14875	FCRL2
			125931	24879	CEACAM20
			933	1643	CD22
			6614	11127	SIGLEC1
			7010	11724	TEK
			2264	3691	FGFR4
			5979	9967	RET
			5157	8805	PDGFRL
			2260	3688	FGFR1
			2261	3690	FGFR3
			55359	18889	STYK1
			2263	3689	FGFR2
			7075	11809	TIE1
			53834	3693	FGFRL1
CG4357+	39410	Ncc69	6558	10911	SLC12A2
			6557	10910	SLC12A1
			6559	10912	SLC12A3
			10723	10915	SLC12A7
			9990	10914	SLC12A6
			6560	10913	SLC12A4
			57468	13818	SLC12A5
			9056	11065	SLC7A7
			57709	29326	SLC7A14
			6542	11060	SLC7A2
			56996	17435	SLC12A9
			9057	11064	SLC7A6
			6541	11057	SLC7A1
			23657	11059	SLC7A11
			84561	15595	SLC12A8
			11136	11067	SLC7A9
			8140	11063	SLC7A5
			157724	23092	SLC7A13
			56301	11058	SLC7A10
			6545	11062	SLC7A4
			23428	11066	SLC7A8
			84889	11061	SLC7A3
CG4180+	49424	CIAPIN1	57019	28050	CIAPIN1
CG9961+	33459	CG9961	5232	8898	PGK2
			5230	8896	PGK1
CG6534+	42547	slou	54729	24975	NKX1-1
			390010	31652	NKX1-2
			4222	7013	MEOX1
			4223	7014	MEOX2
			137814	32940	NKX2-6
			85474	15525	LBX2
			27287	13639	VENTX

			3196	5057	TLX2
			4869	7910	NPM1
			8538	956	BARX2
			120237	33185	DBX1
			3195	5056	TLX1
			343472	954	BARHL2
			56751	953	BARHL1
			3142	4978	HLX
			440097	33186	DBX2
			30012	13532	TLX3
			10660	16960	LBX1
			56033	955	BARX1
CG9619+	40102	Gbs-76A	5506	9291	PPP1R3A
			5509	9294	PPP1R3D
			79660	14942	PPP1R3B
			5507	9293	PPP1R3C
			90673	14943	PPP1R3E
			648791	14945	PPP1R3G
			89801	14944	PPP1R3F
			7253	12373	TSHR
			57594	20164	HOMEZ
CG5179+	37586	Cdk9	1025	1780	CDK9
			8621	1733	CDK13
			51755	24224	CDK12
			100616250	41595	MIR3960
			8558	1770	CDK10
			984	1729	CDK11B
			728642	1730	CDK11A
CG7772+	32776	CG7772	51537	26945	MTFP1
CG3431+	39102	Uch-L5	51377	19678	UCHL5
			8314	950	BAP1
CG4165+	31458	Usp16-45	85015	20080	USP45
			10600	12614	USP16
			7375	12627	USP4
			10869	12617	USP19
			57478	20060	USP31
			84669	19143	USP32
			10868	12619	USP20
			23032	20059	USP33
			8237	12609	USP11
			9098	12629	USP6
			9958	12613	USP15
			124739	20072	USP43
CG30000+	35995	GstT1	2953	4642	GSTT2
			2952	4641	GSTT1
			653689	33437	GSTT2B
			25774	26930	GSTT4
			100652871		LOC100652871
			54332	15968	GDAP1
			53405	13517	CLIC5
			54102	2065	CLIC6
			78997	4213	GDAP1L1
			9446	13312	GSTO1
			1193	2063	CLIC2
			9022	2064	CLIC3
			25932	13518	CLIC4
			119391	23064	GSTO2
			1192	2062	CLIC1
			2954	4643	GSTZ1
			7407	12651	VARS
			4141	6898	MARS
			1937	3213	EEF1G
			9521	3212	EEF1E1
CG7292+	41798	Rrp6	5394	9138	EXOSC10
CG4438+	34257	CG4438	11333	14634	PDAP1
CG12318+/CG33121+	326261	Spn28Db	5276	8945	SERPINI2
			5274	8943	SERPINI1
			5270	8951	SERPINE2
			647174	24774	SERPINE3
			5054	8583	SERPINE1
			1992	3311	SERPINB1
			6318	10570	SERPINB4
			3053	4838	SERPIND1

			5267	8948	SERPINA4
			462	775	SERPINC1
			327657	15995	SERPINA9
			866	1540	SERPINA6
			6317	10569	SERPINB3
			5269	8950	SERPINB6
			256394	19193	SERPINA11
			145264	18359	SERPINA12
			388007	30909	SERPINA13P
			51156	15996	SERPINA10
			6906	11583	SERPINA7
			710	1228	SERPING1
			5345	9075	SERPINF2
			5176	8824	SERPINF1
			5104	8723	SERPINA5
			5265	8941	SERPINA1
			183	333	AGT
			12	16	SERPINA3
			390502	8985	SERPINA2
			5272	8955	SERPINB9
			5273	8942	SERPINB10
			89777	14220	SERPINB12
			5055	8584	SERPINB2
			8710	13902	SERPINB7
			89778	14221	SERPINB11
			871	1546	SERPINH1
			284293	23037	HMSD
			5275	8944	SERPINB13
			5268	8949	SERPINB5
			5271	8952	SERPINB8
CG7636+	39253	mRpL2	51069	14056	MRPL2
			6132	10368	RPL8
CG16812+	34722	CG16812	126526	26723	C19orf47
CG8727+	40162	cyc	406	701	ARNTL
			56938	18984	ARNTL2
			9915	16876	ARNT2
			405	700	ARNT
			8863	8847	PER3
			8202	7670	NCOA3
			4862	7895	NPAS2
			8648	7668	NCOA1
			9575	2082	CLOCK
			10499	7669	NCOA2
CG2578+/CG42338+	32183	Ten-a	55714	29944	TENM3
			10178	8117	TENM1
			57451	29943	TENM2
			26011	29945	TENM4
			11197	18081	WIF1
			63923	22942	TNN
			7143	11953	TNR
			3371	5318	TNC
CG17664+	37737	Eglp2	361	637	AQP4
			358	633	AQP1
			4284	7103	MIP
			362	638	AQP5
			366	643	AQP9
			359	634	AQP2
			363	639	AQP6
			343	642	AQP8
			360	636	AQP3
			89872	16029	AQP10
			364	640	AQP7
			100509620		LOC100509620
			6755	11334	SSTR5
			2539	4057	G6PD
			7201	12299	TRHR
CG10898+	41384	CG10898	79873	26194	NUDT18
			11162	8053	NUDT6
CG3876+	33258	PGAP2	27315	17893	PGAP2
			80157	26133	CWH43
CG7899+	48445	Acph-1	53	123	ACP2
			55	125	ACPP

			93650	14376	ACP4
			51205	29609	ACP6
			9562	7102	MINPP1
CG7222+	36138	CG7222	51029	24264	DESI2
			27351	24577	DESI1
CG1578+	32135	CG1578	89978	30543	DPH6
			10247	16897	RIDA
CG1433+	40684	Atu	123169	30401	LEO1
CG11454+	33175	CG11454	10179	9904	RBM7
			54033	9897	RBM11
			10262	10771	SF3B4
CG5018+	39774	l(3)72Dn	84916	1983	UTP4
CG17949+	326273	His2B:CG17949	255626	18730	HIST1H2BA
			128312	20514	HIST3H2BB
			8348	4758	HIST1H2BO
			8970	4761	HIST1H2BJ
			3018	4751	HIST1H2BB
			8341	4749	HIST1H2BN
			85236	13954	HIST1H2BK
			8349	4760	HIST2H2BE
			8340	4748	HIST1H2BL
			8347	4757	HIST1H2BC
			440689	24700	HIST2H2BF
			8344	4753	HIST1H2BE
			8339	4746	HIST1H2BG
			8342	4750	HIST1H2BM
			8346	4756	HIST1H2BI
			8345	4755	HIST1H2BH
			3017	4747	HIST1H2BD
			114483833		LOC114483833
			8343	4752	HIST1H2BF
			158983	27252	H2BFWT
			286436	27867	H2BFM
			102724334		LOC102724334
			54145	4762	H2BFS
CG5735+/CG43782+	39018	orb2	132864	21745	CPEB2
			80315	21747	CPEB4
			22849	21746	CPEB3
			55852	30884	TEX2
			64506	21744	CPEB1
CG13926+	38192	CG13926	51501	26938	HIKESHI
CG8877+	36304	Prp8	10594	17340	PRPF8
CG31657+/CG33526+	33270	PNUTS	5514	9284	PPP1R10
CG11201+	33946	TTLL3B	164714	34000	TTLL8
			26140	24483	TTLL3
			100526693	38830	ARPC4-TTLL3
			150465	21586	TTL
			164395	16118	TTLL9
			23093	19963	TTLL5
			25809	1312	TTLL1
			254173	26693	TTLL10
			284076	26664	TTLL6
			448834	31823	KPRP
			83887	21211	TTLL2
CG11861+/CG42616+	34896	Cul3	8452	2553	CUL3
			8451	2554	CUL4A
			8450	2555	CUL4B
			8454	2551	CUL1
			8065	2556	CUL5
			8453	2552	CUL2
			143384	23727	CACUL1
CG31201+	318623	GluRIIE	2898	4580	GRIK2
			2897	4579	GRIK1
			2900	4582	GRIK4
			2899	4581	GRIK3
			2901	4583	GRIK5
			2894	4575	GRID1
			2895	4576	GRID2
			116443	16767	GRIN3A
			2891	4572	GRIA2
			2892	4573	GRIA3
			2893	4574	GRIA4
			2904	4586	GRIN2B

			2890	4571	GRIA1
			2905	4587	GRIN2C
			2906	4588	GRIN2D
			2903	4585	GRIN2A
			116444	16768	GRIN3B
			5168	3357	ENPP2
CG33931+	3772007	Rpp20	10248	19949	POP7
			29780	14653	PARVB
			64098	14654	PARVG
			55742	14652	PARVA
			94107	28217	TMEM203
CG11105+/CG44422+	32063	CG44422	80333	30083	KCNIP4
			30818	15523	KCNIP3
			30820	15521	KCNIP1
			30819	15522	KCNIP2
			7447	12722	VSNL1
			51440	18212	HPCAL4
			23413	3953	NCS1
			3241	5145	HPCAL1
			644096	33867	SDHAF1
			4925	8044	NUCB2
			2979	4679	GUCA1B
			3208	5144	HPCA
			83988	7655	NCALD
			84669	19143	USP32
			79645	25678	EFCAB1
			2978	4678	GUCA1A
			9626	4680	GUCA1C
			5957	9937	RCVRN
CG5394+	42834	GluProRS	2058	3418	EPRS
			5956	9936	OPN1LW
			57505	21022	AARS2
			124454	29419	EARS2
			116832	17094	RPL39L
			6170	10350	RPL39
			5859	9751	QARS
			25973	30563	PARS2
CG5353+	45784	ThrRS	6897	11572	TARS
			123283	24728	TARSL2
			80222	30740	TARS2
			54148	14027	MRPL39
CG3071+	31213	CG3071	84135	25758	UTP15
			7090	11839	TLE3
			112840	20489	WDR89
CG8091+	39173	Dronc	835	1503	CASP2
			23581	1502	CASP14
			842	1511	CASP9
			837	1505	CASP4
			838	1506	CASP5
			100506742	19004	CASP12
			834	1499	CASP1
			59082	28861	CARD18
			839	1507	CASP6
			114769	33701	CARD16
			8837	1876	CFLAR
			440068	33827	CARD17
			841	1509	CASP8
			653519	31984	GPR89A
			51463	13840	GPR89B
			260434	30261	PYDC1
			29108	16608	PYCARD
			8682	8822	PEA15
			836	1504	CASP3
			197350	27290	CASP16P
			22900	17057	CARD8
			840	1508	CASP7
			843	1500	CASP10
CG1271+	38364	CG1271	256356	28635	GK5
			2710	4289	GK
			2712	4291	GK2
			54454	29230	ATAD2B
			29028	30123	ATAD2
			23729	1492	SHPK

			11104	6216	KATNA1
			84056	28361	KATNAL1
			55277	25610	FGGY
			5701	9548	PSMC2
			5705	9552	PSMC5
			83473	25387	KATNAL2
			5700	9547	PSMC1
CG7650+	39694	CG7650	5082	8770	PDCL
			5132	8759	PDC
			132954	29524	PDCL2
CG6852+	40053	Grx1	51022	16065	GLRX2
			2745	4330	GLRX
			114112	20667	TXNRD3
			7296	12437	TXNRD1
CG6364+	42894	Uck	7371	12562	UCK2
			83549	14859	UCK1
			54963	15938	UCKL1
			139596	28334	UPRT
			100500832	38963	MIR3658
			54981	26057	NMRK1
			3728	6207	JUP
			1499	2514	CTNNB1
			27231	17871	NMRK2
			85300	779	ATCAY
CG10726+	35287	barr	23397	1112	NCAPH
CG5582+	39981	Cln3	1201	2074	CLN3
CG7039+	31841	Arfrp1	10139	662	ARFRP1
			84100	13210	ARL6
			80117	22974	ARL14
			1584	2591	CYP11B1
			400	692	ARL1
			402	693	ARL2
			10499	7669	NCOA2
			200894	25419	ARL13B
CG7234+	33789	GluRIIB	2898	4580	GRIK2
			2897	4579	GRIK1
			2900	4582	GRIK4
			2899	4581	GRIK3
			2894	4575	GRID1
			2895	4576	GRID2
			2901	4583	GRIK5
			116443	16767	GRIN3A
			2891	4572	GRIA2
			2892	4573	GRIA3
			2893	4574	GRIA4
			2904	4586	GRIN2B
			2890	4571	GRIA1
			2905	4587	GRIN2C
			2906	4588	GRIN2D
			2903	4585	GRIN2A
			116444	16768	GRIN3B
			5168	3357	ENPP2
CG10037+	38752	vvl	5454	9215	POU3F2
			5456	9217	POU3F4
			5455	9216	POU3F3
			5453	9214	POU3F1
			134187	26367	POU5F2
			5449	9210	POU1F1
			5460	9221	POU5F1
			5462	9223	POU5F1B
			5457	9218	POU4F1
			5459	9220	POU4F3
			5458	9219	POU4F2
			347475	37286	CCDC160
			5463	9224	POU6F1
			11281	21694	POU6F2
			5451	9212	POU2F1
			5452	9213	POU2F2
			25833	19864	POU2F3
			3204	5108	HOXA7
			3217	5118	HOXB7
			4009	6653	LMX1A
			4010	6654	LMX1B

			139324	26411	HDX
			54535	13930	CCHCR1
CG14206+	32953	RpS10b	6204	10383	RPS10
			93144	15795	RPS10P5
			100529239	49181	RPS10-NUDT3
			5339	9069	PLEC
CG15772+	31498	CG15772	221895	28917	JAZF1
CG10811+	43839	eIF4G1	1981	3296	EIF4G1
			8672	3298	EIF4G3
			1982	3297	EIF4G2
			10605	16945	PAIP1
CG1412+	33048	RhoGAP19D	57636	29293	ARHGAP23
			57584	23725	ARHGAP21
			64333	14130	ARHGAP9
			201176	31813	ARHGAP27
			94134	16348	ARHGAP12
			55843	21030	ARHGAP15
			613	1014	BCR
			9743	17399	ARHGAP32
			115703	23085	ARHGAP33
			57514	29216	ARHGAP31
CG13387+	34167	emb	7514	12825	XPO1
			57510	17675	XPO5
			23214	19733	XPO6
CG6707+	39168	CG6707	90809	19299	PIP4P1
			55529	25452	PIP4P2
CG7788+	43514	Drice	840	1508	CASP7
			836	1504	CASP3
			839	1507	CASP6
			835	1503	CASP2
			4868	7908	NPHS1
			8682	8822	PEA15
			59082	28861	CARD18
			197350	27290	CASP16P
			842	1511	CASP9
			114769	33701	CARD16
			837	1505	CASP4
			838	1506	CASP5
			440068	33827	CARD17
			8837	1876	CFLAR
			22900	17057	CARD8
			23581	1502	CASP14
			841	1509	CASP8
			834	1499	CASP1
			843	1500	CASP10
CG9924+/CG12537+	41704	rdx	8405	11254	SPOP
			339745	27934	SPOPL
			284697	21019	BTBD8
CG4751+	34551	CG4751	84954	25934	MPND
			6599	11104	SMARCC1
			6601	11105	SMARCC2
			57559	24105	STAMBPL1
			114803	29401	MYSM1
			10617	16950	STAMBP
			10987	2240	COPS5
			10213	16889	PSMD14
			5713	9565	PSMD7
			10980	21749	COPS6
			79184	24185	BRCC3
CG12891+	36109	whd	1374	2328	CPT1A
			1375	2329	CPT1B
			126129	18540	CPT1C
			1120	1938	CHKB
			54677	2366	CROT
			1376	2330	CPT2
			1103	1912	CHAT
			386593	41998	CHKB-CPT1B
			4057	6720	LTF
CG7480+	48775	Pgant35A	63917	19875	GALNT11
			168391	21725	GALNTL5
			100528030	42957	POC1B-GALNT4
			57452	23233	GALNT16
			11226	4128	GALNT6

			79695	19877	GALNT12
			11227	4127	GALNT5
			114805	23242	GALNT13
			51809	4129	GALNT7
			79623	22946	GALNT14
			2589	4123	GALNT1
			2590	4124	GALNT2
			117248	21531	GALNT15
			5159	8804	PDGFRB
			64409	16347	GALNT17
			2591	4125	GALNT3
			50614	4131	GALNT9
			442117	33844	GALNTL6
			26290	4130	GALNT8
			8693	4126	GALNT4
			55568	19873	GALNT10
			374378	30488	GALNT18
CG4780+	38614	Membrin	9570	4431	GOSR2
CG33193+	252554	sav	60485	17795	SAV1
			9223	946	MAGI1
			9863	18957	MAGI2
			260425	29647	MAGI3
			79917	30006	MAGIX
CG9867+	33424	Eogt	285203	28526	EOGT
			84892	25902	POMGNT2
CG11877+	43438	Atg14	22863	19962	ATG14
CG2901+	31338	CG2901	9213	12827	XPR1
CG11299+	37755	Sesn	143686	23060	SESN3
			27244	21595	SESN1
			83667	20746	SESN2
CG8258+	35882	CCT8	10694	1623	CCT8
			150160	15553	CCT8L2
			155100	32153	CCT8L1P
			22948	1618	CCT5
			7203	1616	CCT3
			908	1620	CCT6A
			10693	1621	CCT6B
			10575	1617	CCT4
CG5163+	42822	TfIIA-S	2958	4647	GTF2A2
CG1064+	40657	Snr1	6598	11103	SMARCB1
CG9802+	32627	SMC3	9126	2468	SMC3
			27127	11112	SMC1B
			160857	26478	CCDC122
			10970	16991	CKAP4
			550631	33854	CCDC157
			23137	20465	SMC5
			8243	11111	SMC1A
			79677	20466	SMC6
			10592	14011	SMC2
			10051	14013	SMC4
CG6226+	41860	Fkbp39	2280	3711	FKBP1A
			2281	3712	FKBP1B
			2286	3718	FKBP2
			51661	3723	FKBP7
			23770	3724	FKBP8
			2289	3721	FKBP5
			60681	18169	FKBP10
			283237	28432	TTC9C
			11328	3725	FKBP9
			23307	23397	FKBP15
			8468	3722	FKBP6
			2288	3720	FKBP4
			2287	3719	FKBP3
			55033	18625	FKBP14
			51303	18624	FKBP11
CG10192+	42819	eIF4G2	8672	3298	EIF4G3
			1981	3296	EIF4G1
			1982	3297	EIF4G2
			10605	16945	PAIP1
CG10546+	38651	Cralbp	157807	23139	CLVS1
			134829	23046	CLVS2
			6017	10024	RLBP1
			79183	16114	TTPAL

			7274	12404	TTPA
			284904	20627	SEC14L4
			6397	10698	SEC14L1
			730005	40047	SEC14L6
			9717	29032	SEC14L5
			266629	18655	SEC14L3
			23541	10699	SEC14L2
CG10716+/CG33100+	326255	eIF4EHP	9470	3293	EIF4E2
			253314	33179	EIF4E1B
			317649	31837	EIF4E3
			1977	3287	EIF4E
CG13349+	36545	Rpn13	11047	15759	ADRM1
CG1616+	35679	dpa	4173	6947	MCM4
			4175	6949	MCM6
			4174	6948	MCM5
			84515	16147	MCM8
			4171	6944	MCM2
			4176	6950	MCM7
			254394	21484	MCM9
			4172	6945	MCM3
			157777	26368	MCMDC2
CG1316+	38526	CG1316	129831	24468	RBM45
CG1718+	33103	ABCA	21	33	ABCA3
			19	29	ABCA1
			26154	14637	ABCA12
			10351	38	ABCA8
			23460	36	ABCA6
			10350	39	ABCA9
			10349	30	ABCA10
			154664	14638	ABCA13
			10347	37	ABCA7
			23461	35	ABCA5
			24	34	ABCA4
			20	32	ABCA2
			2271	3700	FH
			259	453	AMBP
			5265	8941	SERPINA1
			64137	13884	ABCG4
			9429	74	ABCG2
			64240	13886	ABCG5
			64241	13887	ABCG8
			9619	73	ABCG1
CG5913+	43132	CG5913	25940	24520	FAM98A
			283742	26773	FAM98B
			147965	27119	FAM98C
CG10975+	39443	Ptp69D	5788	9666	PTPRC
			5786	9664	PTPRA
			5791	9669	PTPRE
			5792	9670	PTPRF
			374462	9679	PTPRQ
			5789	9668	PTPRD
			10076	9683	PTPRU
			5797	9675	PTPRM
			11122	9682	PTPRT
			5802	9681	PTPRS
			5796	9674	PTPRK
CG9426+	34719	CG9426	3652	6108	IPP
			9817	23177	KEAP1
			55975	15646	KLHL7
			3126	4952	HLA-DRB4
			51088	6356	KLHL5
			27252	25056	KLHL20
			64410	25732	KLHL25
			10625	16951	IVNS1ABP
			56062	6355	KLHL4
			57626	6352	KLHL1
			23276	29120	KLHL18
			54813	19741	KLHL28
			59349	19360	KLHL12
			57563	18644	KLHL8
CG11989+	39175	vnc	8260	18704	NAA10
			84779	28125	NAA11
			9027	18069	NAT8

			80218	29533	NAA50
			339983	26742	NAT8L
			51126	15908	NAA20
			122830	19844	NAA30
			79903	25875	NAA60
			57325	15904	KAT14
CG5994+	38982	Nelf-E	7936	13974	NELFE
			100302242	33925	MIR1236
			54715	18222	RBFOX1
CG14396+	43875	Ret	5979	9967	RET
			2264	3691	FGFR4
			2260	3688	FGFR1
			2261	3690	FGFR3
			2263	3689	FGFR2
			7010	11724	TEK
			3791	6307	KDR
			5157	8805	PDGFRL
			2322	3765	FLT3
			5156	8803	PDGFRA
			55359	18889	STYK1
			2324	3767	FLT4
			2321	3763	FLT1
			7075	11809	TIE1
			3815	6342	KIT
			53834	3693	FGFRL1
			5159	8804	PDGFRB
			1436	2433	CSF1R
CG11184+	37792	Upf3	65109	20439	UPF3B
			65110	20332	UPF3A
CG5499+	43229	His2Av	94239	20664	H2AFV
			3015	4741	H2AFZ
			8336	4735	HIST1H2AM
			723790	29668	HIST2H2AA4
			474381	18298	H2AFB2
			83740	14455	H2AFB3
			55766	14456	H2AFJ
			85235	13671	HIST1H2AH
			8969	4737	HIST1H2AG
			317772	20508	HIST2H2AB
			8329	4725	HIST1H2AI
			3013	4729	HIST1H2AD
			8330	4726	HIST1H2AK
			474382	22516	H2AFB1
			8334	4733	HIST1H2AC
			3012	4724	HIST1H2AE
			3014	4739	H2AFX
			9555	4740	H2AFY
			221613	18729	HIST1H2AA
			55506	14453	H2AFY2
			8332	4730	HIST1H2AL
			8338	4738	HIST2H2AC
			8335	4734	HIST1H2AB
			8331	4727	HIST1H2AJ
			92815	20507	HIST3H2A
CG3058+	33645	Dim1	10907	30551	TXNL4A
			54957	26041	TXNL4B
CG8841+	36336	CG8841	283987	15736	HID1
CG3011+	31524	Shmt	6470	10850	SHMT1
			6472	10852	SHMT2
			102466733	50183	MIR6778
CG1676+	33043	cactin	58509	29938	CACTIN
			91862	30525	MARVELD3
CG10984+	39446	CG10984	23253	29135	ANKRD12
			29123	21316	ANKRD11
CG5405+	42843	KrT95D	23241	23794	PACS2
			55690	30032	PACS1
CG11899+	46391	CG11899	29968	19129	PSAT1
CG31809+	318954	CG31809	83693	16475	HSDL1
			51144	18646	HSD17B12
			3293	5212	HSD17B3
CG10657+	39423	CG10657	157807	23139	CLVS1
			134829	23046	CLVS2
			6017	10024	RLBP1

			79183	16114	TTPAL
			7274	12404	TTPA
			6397	10698	SEC14L1
			730005	40047	SEC14L6
			284904	20627	SEC14L4
			9717	29032	SEC14L5
			266629	18655	SEC14L3
			23541	10699	SEC14L2
CG4090+	42080	Mur89F	27159	17432	CHIA
			5016	8524	OVGP1
			1118	1936	CHIT1
			1486	2496	CTBS
			1116	1932	CHI3L1
CG8384+	43162	gro	7091	11840	TLE4
			7090	11839	TLE3
			7088	11837	TLE1
			7089	11838	TLE2
			79816	30788	TLE6
			166	307	TLE5
			102723796	53648	TLE7
CG2503+	40593	atms	54623	25459	PAF1
CG10776+	44096	wit	659	1078	BMPR2
			92	173	ACVR2A
			269	465	AMHR2
			93	174	ACVR2B
			23347	29090	SMCHD1
			1113	1929	CHGA
			51360	15455	MBTPS2
			7048	11773	TGFBR2
CG7791+	35511	CG7791	4285	7104	MIPEP
			7064	11793	THOP1
			57486	16058	NLN
			341640	25396	FREM2
CG8786+	40144	CG8786	81847	21336	RNF146
			26472	9057	PPP1R14B
CG4735+	45360	shu	8468	3722	FKBP6
			2280	3711	FKBP1A
			11328	3725	FKBP9
			23307	23397	FKBP15
			2281	3712	FKBP1B
			23770	3724	FKBP8
			51661	3723	FKBP7
			2289	3721	FKBP5
			2286	3718	FKBP2
			2288	3720	FKBP4
			2287	3719	FKBP3
			55033	18625	FKBP14
			51303	18624	FKBP11
			60681	18169	FKBP10
CG8151+	36598	Tfb1	2965	4655	GTF2H1
CG7623+	42115	sll	347734	16872	SLC35B2
			10237	20798	SLC35B1
			100616124	41594	MIR4647
			222553	21483	SLC35F1
			113829	20753	SLC35A4
			7355	11022	SLC35A2
			51000	21601	SLC35B3
			23443	11023	SLC35A3
			159371	26607	SLC35G1
			54733	23615	SLC35F2
			54978	26055	SLC35F6
			55032	20792	SLC35A5
			51006	17117	SLC35C2
			10559	11021	SLC35A1
			80255	23617	SLC35F5
CG11907+	33207	Ent1	2030	11003	SLC29A1
			55315	23096	SLC29A3
			3177	11004	SLC29A2
			2120	3495	ETV6
			222962	23097	SLC29A4
CG3644+	45827	bic	91408	30547	BTF3L4
			689	1125	BTF3
CG32602+	32384	Muc12Ea	4582	7508	MUC1

			374897	24950	SBSN
			5544	9339	PRB3
			5545	9340	PRB4
			23145	21998	SSPO
			140453	16800	MUC17
			100288332	41980	NPIPA5
			4588	7517	MUC6
			101059938	41982	NPIPA7
			4583	7512	MUC2
			642799	41979	NPIPA2
			9284	7909	NPIPA1
			101059953	41983	NPIPA8
			642778	41978	NPIPA3
			94025	15582	MUC16
			4585	7514	MUC4
			283463	14362	MUC19
			113146	20125	AHNAK2
			727897	7516	MUC5B
			7450	12726	VWF
			340990	8516	OTOG
CG10374+	42810	Lsd-1	10226	16893	PLIN3
			123	248	PLIN2
			440503	33196	PLIN5
			5346	9076	PLIN1
CG16901+	41666	sqd	3182	5034	HNRNPAB
			3184	5036	HNRNPD
			9987	5037	HNRNPDL
			124540	18585	MSI2
			4440	7330	MSI1
			26528	2683	DAZAP1
			221662	21539	RBM24
CG12929+	35987	CG12929	56063	28837	TMEM234
CG10961+	31746	Traf6	7189	12036	TRAF6
			7185	12031	TRAF1
			10193	18401	RNF41
			7186	12032	TRAF2
			7187	12033	TRAF3
			7188	12035	TRAF5
			9618	12034	TRAF4
			146310	23235	RNF151
			23024	17704	PDZRN3
			84231	20456	TRAF7
			84708	6657	LNX1
			29951	30552	PDZRN4
CG1740+	33078	Ntf-2	10204	13722	NUTF2
CG5640+	34377	Utx	7403	12637	KDM6A
			7404	12638	UTY
			23135	29012	KDM6B
			83857	24099	TMTC1
			439996	23442	IFIT1B
			79836	21152	LONRF3
			10765	18039	KDM5B
			160418	26899	TMTC3
			5927	9886	KDM5A
			585	969	BBS4
			84899	25904	TMTC4
			506	830	ATP5F1B
			158248	26536	TTC16
			3437	5411	IFIT3
			161582	21493	DNAAF4
			160335	25440	TMTC2
			6674	11212	SPAG1
			3433	5409	IFIT2
			164118	32348	TTC24
			63943	13949	FKBPL
			130502	32954	TTC32
			164832	24788	LONRF2
			24138	13328	IFIT5
			8473	8127	OGT
			3434	5407	IFIT1
			8242	11114	KDM5C
			83538	25280	TTC25
			10953	15746	TOMM34

			3720	6196	JARID2
CG7926+	43565	Axn	8312	903	AXIN1
			8313	904	AXIN2
			5999	10000	RGS4
			6004	9997	RGS16
			10287	13735	RGS19
			8601	14600	RGS20
			6003	9995	RGS13
			5997	9998	RGS2
			6000	10003	RGS7
			5996	9991	RGS1
			431704	26839	RGS21
			8787	10004	RGS9
			26575	14088	RGS17
			6002	9994	RGS12
			64407	14261	RGS18
			392862	18464	GRID2IP
			5998	9999	RGS3
			8786	9993	RGS11
			6001	9992	RGS10
			9628	10002	RGS6
			8490	10001	RGS5
			10636	9996	RGS14
			85397	16810	RGS8
CG5186+	37121	slim	23008	22194	KLHDC10
			126823	28489	KLHDC9
			122773	19836	KLHDC1
			54455	29249	FBXO42
			10244	16896	RABEPK
			23588	20231	KLHDC2
CG7257+	39351	Rpt4R	5706	9553	PSMC6
			5702	9549	PSMC3
			5704	9551	PSMC4
			5705	9552	PSMC5
			5700	9547	PSMC1
			5701	9548	PSMC2
CG13628+	42942	Rpb10	5441	9199	POLR2L
CG3881+	34282	GlcAT-S	26229	923	B3GAT3
			135152	922	B3GAT2
			27087	921	B3GAT1
CG12951+	41110	CG12951	3816	6357	KLK1
			25818	6366	KLK5
			43847	6362	KLK14
			5653	6367	KLK6
			11202	6369	KLK8
			3817	6363	KLK2
			26085	6361	KLK13
			354	6364	KLK3
			5650	6368	KLK7
			339105	34407	PRSS53
			146547	26906	PRSS36
			55554	20453	KLK15
			11012	6359	KLK11
			5655	6358	KLK10
			43849	6360	KLK12
			345062	24635	PRSS48
			284366	6370	KLK9
			9622	6365	KLK4
			6768	11344	ST14
			344805	30846	TMPRSS7
			80975	14908	TMPRSS5
			28983	24465	TMPRSS11E
			164656	16517	TMPRSS6
			100288960	37323	PRSS43P
			360200	30079	TMPRSS9
			5652	9491	PRSS8
			5646	9486	PRSS3
			64063	14368	PRSS22
			25823	14134	TPSG1
			154754	43788	PRSS3P2
			260429	30405	PRSS33
			5645	9483	PRSS2
			5644	9475	PRSS1

			360226	30715	PRSS41
			10942	9485	PRSS21
			23430	14118	TPSD1
			83886	15475	PRSS27
			7177	12019	TPSAB1
			8858	9460	PROZ
			1511	2532	CTSG
			1675	2771	CFD
			400668	31397	PRSS57
CG18419+/CG33298+	2768929	CG33298	57205	13549	ATP10D
			23120	13543	ATP10B
			57194	13542	ATP10A
			10396	13531	ATP8A1
			23200	13553	ATP11B
			5205	3706	ATP8B1
			79895	13536	ATP8B4
			286410	13554	ATP11C
			148229	13535	ATP8B3
			23250	13552	ATP11A
			57198	13534	ATP8B2
			51761	13533	ATP8A2
			10079	13540	ATP9A
			374868	13541	ATP9B
			489	813	ATP2A3
			9914	29103	ATP2C2
			495	819	ATP4A
			344905	31789	ATP13A5
			488	812	ATP2A2
			79572	24113	ATP13A3
			477	800	ATP1A2
			490	814	ATP2B1
			57130	24215	ATP13A1
			492	816	ATP2B3
			480	14073	ATP1A4
			27032	13211	ATP2C1
			491	815	ATP2B2
			487	811	ATP2A1
			23400	30213	ATP13A2
			479	13816	ATP12A
			476	799	ATP1A1
			493	817	ATP2B4
			84239	25422	ATP13A4
			478	801	ATP1A3
CG5844+	41533	CG5844	55862	21489	ECHDC1
			55268	23408	ECHDC2
			124359	23030	CDYL2
			9425	1811	CDYL
			9085	1809	CDY1
			9426	1810	CDY2A
			203611	23921	CDY2B
			253175	23920	CDY1B
			549	890	AUH
			1962	3247	EHHADH
			3030	4801	HADHA
			1892	3151	ECHS1
			10455	14601	ECI2
			26275	4908	HIBCH
			1632	2703	ECI1
CG4599+	34984	Tpr2	7266	12392	DNAJC7
			5611	9439	DNAJC3
			285126	24844	DNAJC5G
			134218	27030	DNAJC21
			84277	16410	DNAJC30
			11080	14886	DNAJB4
			55466	14885	DNAJA4
			80331	16235	DNAJC5
			3300	5228	DNAJB2
			202052	28429	DNAJC18
			374407	30718	DNAJB13
			120526	26979	DNAJC24
			51726	14889	DNAJB11
			552891	37501	DNAJC25-GNG10
			79982	25881	DNAJB14

			3301	5229	DNAJA1
			3337	5270	DNAJB1
			79962	25802	DNAJC22
			23341	29157	DNAJC16
			548645	34187	DNAJC25
			4189	6968	DNAJB9
			54431	24637	DNAJC10
			85479	24138	DNAJC5B
			10049	14888	DNAJB6
			9093	11808	DNAJA3
			165721	23699	DNAJB8
			150353	24986	DNAJB7
			25822	14887	DNAJB5
			55735	25570	DNAJC11
			10294	14884	DNAJA2
			54788	14891	DNAJB12
CG4086+	39856	Su(P)	80142	17822	PTGES2
CG5677+	42885	Spase22-23	60559	26212	SPCS3
CG2076+	32041	CG2076	27069	17281	GHITM
CG10662+/CG43720+	35277	sick	89797	15997	NAV2
			89795	15998	NAV3
			89796	15989	NAV1
CG2272+	44111	slpr	4293	6861	MAP3K9
			4294	6849	MAP3K10
			4296	6850	MAP3K11
			84451	29798	MAP3K21
			8767	10020	RIPK2
			8737	10019	RIPK1
			6885	6859	MAP3K7
			9175	6852	MAP3K13
			7786	6851	MAP3K12
			1956	3236	EGFR
			4342	7199	MOS
			255239	21027	ANKK1
			55872	18282	PBK
			120892	18618	LRRK2
			11035	10021	RIPK3
			54101	496	RIPK4
			100526835	42952	FPGT-TNNI3K
			25778	29043	DSTYK
			51086	19661	TNNI3K
			197259	26617	MLKL
			79705	18608	LRRK1
			51776	17797	MAP3K20
CG32179+	326198	Krn	3084	7997	NRG1
			9542	7998	NRG2
CG9100+	33988	Rab30	27314	9770	RAB30
			376267	20150	RAB15
			401409	19982	RAB19
			5861	9758	RAB1A
			37	92	ACADVL
			81876	18370	RAB1B
CG1911+	43491	Cap-D2	9918	24305	NCAPD2
CG7398+	38721	Tnpo	3842	6401	TNPO1
			30000	19998	TNPO2
CG2253+	31724	Upf2	26019	17854	UPF2
CG7026+	41806	VhaPPA1-2	533	861	ATP6V0B
			516	841	ATP5MC1
			527	855	ATP6V0C
			517	842	ATP5MC2
			518	843	ATP5MC3
CG4001+	36060	Pfk	5213	8877	PFKM
			5211	8876	PFKL
			5214	8878	PFKP
CG10778+	31708	CG10778	79947	20603	DHDDS
			116150	21042	NUS1
CG11282+	39493	caps	10446	16914	LRRN2
			57633	20980	LRRN1
			100130733	35155	LRRC70
			54674	17200	LRRN3
			116844	29480	LRG1
			375387	24613	NRROS
			158038	21207	LINGO2

			1594	2606	CYP27B1
			23769	3760	FLRT1
			23767	3762	FLRT3
			105378803	25255	LRRC53
			347730	19408	LRRTM1
CG2321+	43471	CG2321	54980	26056	C2orf42
CG17083+	42755	CG17083	160762	26669	CCDC63
			93233	26560	CCDC114
CG1542+	43691	CG1542	10969	15531	EBNA1BP2
			102465439	50239	MIR6733
CG9836+	41059	IscU	23479	29882	ISCU
CG15804+	38226	Dhc62B	201625	2943	DNAH12
			55567	2949	DNAH3
			56171	18661	DNAH7
			1769	2952	DNAH8
			1768	2951	DNAH6
			8701	2942	DNAH11
			196385	2941	DNAH10
			8632	2946	DNAH17
			146754	2948	DNAH2
			1767	2950	DNAH5
			25981	2940	DNAH1
			1770	2953	DNAH9
			127602	2945	DNAH14
			1778	2961	DYNC1H1
			79659	2962	DYNC2H1
			144132	26532	DNHD1
CG18549+	41538	CG18549	79157	25458	MFSD11
CG15744+	2768909	CG15744	25960	17849	ADGRA2
			166647	13839	ADGRA3
			84435	13838	ADGRA1
			139378	18992	ADGRG4
CG1965+	40842	CG1965	94104	13579	PAXBP1
			6936	1317	GCFC2
CG3733+	33505	Chd1	1106	1917	CHD2
			1105	1915	CHD1
			100507217	48626	LINC01578
			55636	20626	CHD7
			80205	25701	CHD9
			84181	19057	CHD6
			57680	20153	CHD8
			124773	26990	C17orf64
CG3297+	39625	mnd	9056	11065	SLC7A7
			8140	11063	SLC7A5
			9057	11064	SLC7A6
			23428	11066	SLC7A8
			23657	11059	SLC7A11
			56301	11058	SLC7A10
			11136	11067	SLC7A9
			157724	23092	SLC7A13
			57709	29326	SLC7A14
			6542	11060	SLC7A2
			6541	11057	SLC7A1
			6545	11062	SLC7A4
			84889	11061	SLC7A3
			81893	29458	SLC7A5P1
			387254	24951	SLC7A5P2
			10723	10915	SLC12A7
			6559	10912	SLC12A3
			9990	10914	SLC12A6
			6560	10913	SLC12A4
			56996	17435	SLC12A9
			84561	15595	SLC12A8
			6557	10910	SLC12A1
			57468	13818	SLC12A5
			6558	10911	SLC12A2
CG15816+/CG42684+	32754	raskol	9462	9874	RASAL2
			153090	17294	DAB2IP
			8831	11497	SYNGAP1
			64926	26129	RASAL3
			8437	9873	RASAL1
			5921	9871	RASA1
			100847012	43532	MIR5004

			5922	9872	RASA2
			10156	23181	RASA4
			100271927	35202	RASA4B
			22821	20331	RASA3
CG4364+	34287	CG4364	23481	8848	PES1
CG7034+	42499	Sec15	23233	17085	EXOC6B
			54536	23196	EXOC6
CG6443+	34477	CG6443	51507	15890	RTF2
CG12139+/CG42611+	8674055	mgl	4036	6694	LRP2
			53353	6693	LRP1B
			4035	6692	LRP1
			4038	6696	LRP4
			388633	32069	LDLRAD1
			3949	6547	LDLR
			7436	12698	VLDLR
			1950	3229	EGF
			4041	6697	LRP5
			91355	25323	LRP5L
			51293	16692	CD320
			9993	2845	DGCR2
			4040	6698	LRP6
			6653	11185	SORL1
			26020	14553	LRP10
			143458	27046	LDLRAD3
			4037	6695	LRP3
			7804	6700	LRP8
			29967	31708	LRP12
CG14034+	33751	CG14034	5406	9155	PNLIP
			5407	9156	PNLIPRP1
			119548	23492	PNLIPRP3
			149998	18821	LIPI
			5408	9157	PNLIPRP2
			200879	18483	LIPH
			51365	17661	PLA1A
			4023	6677	LPL
			9388	6623	LIPG
			3990	6619	LIPC
CG8887+	40133	ash1	55870	19088	ASH1L
			26040	15573	SETBP1
			7468	12766	NSD2
			64324	14234	NSD1
			29072	18420	SETD2
			54904	12767	NSD3
			8085	7133	KMT2D
			58508	13726	KMT2C
			51105	24280	PHF20L1
			23067	29187	SETD1B
			55904	18541	KMT2E
			9739	29010	SETD1A
			11083	2680	DIDO1
			51230	16098	PHF20
			55209	25566	SETD5
			6392	10683	SDHD
			79813	24650	EHMT1
			2145	3526	EZH1
			693140	32811	MIR555
			83852	20263	SETDB2
			9757	15840	KMT2B
			4297	7132	KMT2A
			9869	10761	SETDB1
CG15666+	37439	BBS9	27241	30000	BBS9
CG31551+	318795	CG31551	7062	11791	TCHH
			4744	7737	NEFH
CG31256+	42087	Brf	2972	11551	BRF1
			55290	17298	BRF2
			2959	4648	GTF2B
CG4738+	34549	Nup160	23279	18017	NUP160
CG31522+	40567	CG31522	79993	26292	ELOVL7
			64834	14418	ELOVL1
			6785	14415	ELOVL4
			54898	14416	ELOVL2
			60481	21308	ELOVL5
			102466723	50219	MIR6734

			79071	15829	ELOVL6
			83401	18047	ELOVL3
CG6603+	39557	Hsc70Cb	3308	5237	HSPA4
			10808	16969	HSPH1
			22824	17041	HSPA4L
			3312	5241	HSPA8
			3303	5232	HSPA1A
			3310	5239	HSPA6
			3304	5233	HSPA1B
			3305	5234	HSPA1L
			259217	19022	HSPA12A
			3309	5238	HSPA5
			10525	16931	HYOU1
			284525	28664	SLC9C2
			339416	24786	ANKRD45
			51182	29526	HSPA14
			116835	16193	HSPA12B
			3313	5244	HSPA9
			6782	11375	HSPA13
			3306	5235	HSPA2
CG5676+	34368	CG5676	139341	28746	FUNDC1
			65991	24925	FUNDC2
CG11641+/CG42698+	35813	pdm3	5463	9224	POU6F1
			11281	21694	POU6F2
			54535	13930	CCHCR1
			5454	9215	POU3F2
			134187	26367	POU5F2
			5456	9217	POU3F4
			5453	9214	POU3F1
			5449	9210	POU1F1
			5451	9212	POU2F1
			5457	9218	POU4F1
			5460	9221	POU5F1
			5459	9220	POU4F3
			5462	9223	POU5F1B
			5452	9213	POU2F2
			25833	19864	POU2F3
			5455	9216	POU3F3
			5458	9219	POU4F2
CG10837+	3355041	eIF4B	1975	3285	EIF4B
			7458	12741	EIF4H
			3178	5031	HNRNPA1
			54952	30813	TRNAU1AP
			3182	5034	HNRNPAB
			144983	27067	HNRNPA1L2
			22913	15921	RALY
			649330	51235	HNRNPCL3
			29896	16645	TRA2A
			1153	1982	CIRBP
			3183	5035	HNRNPC
			135295	21220	SRSF12
			10949	5030	HNRNPA0
			1618	2685	DAZL
			66037	14273	BOLL
			220988	24941	HNRNPA3
			3181	5033	HNRNPA2B1
			440563	48813	HNRNPCL2
			85437	29620	ZCRB1
			23029	28965	RBM34
			138046	27036	RALYL
			6434	10781	TRA2B
			3184	5036	HNRNPD
			5935	9900	RBM3
			81892	20495	SLIRP
			9987	5037	HNRNPDL
			101060301	51333	HNRNPCL4
			10772	16713	SRSF10
CG8975+	36280	RnrS	6241	10452	RRM2
			50484	17296	RRM2B
CG3339+	43295	CG3339	1770	2953	DNAH9
			8701	2942	DNAH11
			8632	2946	DNAH17
			196385	2941	DNAH10

			146754	2948	DNAH2
			127602	2945	DNAH14
			201625	2943	DNAH12
			1769	2952	DNAH8
			55567	2949	DNAH3
			25981	2940	DNAH1
			56171	18661	DNAH7
			1768	2951	DNAH6
			1767	2950	DNAH5
			144132	26532	DNHD1
			1778	2961	DYNC1H1
			79659	2962	DYNC2H1
			81839	15512	VANGL1
			114548	16400	NLRP3
CG11870+/CG43143+	41256	Nuak1	9891	14311	NUAK1
			81788	29558	NUAK2
			3898	6472	LAD1
			102724428	52389	SIK1B
			84446	18994	BRSK1
			30811	13326	HUNK
			5562	9376	PRKAA1
			150094	11142	SIK1
			83983	30410	TSSK6
			9024	11405	BRSK2
			81629	15473	TSSK3
CG2779+/CG32656+	32174	Muc11A	55911	24087	APOBR
			1277	2197	COL1A1
			1278	2198	COL1A2
			4582	7508	MUC1
			5544	9339	PRB3
			5545	9340	PRB4
			144455	23820	E2F7
			1297	2217	COL9A1
			79733	24727	E2F8
			2312	3748	FLG
CG13425+	43862	HnRNP-K	3190	5044	HNRNPK
			57060	8652	PCBP4
			54039	8651	PCBP3
			5094	8648	PCBP2
			10643	28868	IGF2BP3
			407043	31638	MIR7-1
CG6475+	42538	Ugt49B2	7365	12544	UGT2B10
			7366	12546	UGT2B15
			7367	12547	UGT2B17
			10720	12545	UGT2B11
			54658	12530	UGT1A1
			54490	13479	UGT2B28
			54659	12535	UGT1A3
			7363	12553	UGT2B4
			79799	28528	UGT2A3
			7364	12554	UGT2B7
			7368	12555	UGT8
			54578	12538	UGT1A6
			574537	28183	UGT2A2
			54657	12536	UGT1A4
			54575	12531	UGT1A10
			54577	12539	UGT1A7
			54579	12537	UGT1A5
			54600	12541	UGT1A9
			54576	12540	UGT1A8
			133688	26625	UGT3A1
			167127	27266	UGT3A2
			10941	12542	UGT2A1
CG32202+	326199	CG32202	29844	13630	TFPT
			7343	12511	UBTF
			7019	11741	TFAM
			3146	4983	HMGB1
			642623	14533	UBTFL1
			84969	16095	TOX2
			10362	5002	HMG20B
			3148	5000	HMGB2
			9760	18988	TOX
			10363	5001	HMG20A

			27324	11972	TOX3
			3149	5004	HMGB3
CG9938+	32316	Ndc80	10403	16909	NDC80
CG3923+	47141	ebo	23214	19733	XPO6
			7514	12825	XPO1
			57510	17675	XPO5
CG5692+	53569	pins	29899	29501	GPSM2
			26086	17858	GPSM1
			23331	29179	TTC28
			126006	30209	PCP2
CG5596+	43323	Mlc1	4637	7587	MYL6
			4635	7585	MYL4
			140465	29823	MYL6B
			4632	7582	MYL1
			4634	7584	MYL3
			56344	13714	CABP5
			163688	24193	CALML6
CG14286+	42280	CG14286	65265	26104	C8orf33
CG5323+	37137	CG5323	84908	25911	FAM136A
CG8108+	39161	CG8108	25792	16744	CIZ1
CG9177+	32566	eIF5	1983	3299	EIF5
			8894	3266	EIF2S2
CG17743+	43819	pho	7528	12856	YY1
			404281	31684	YY2
			132625	30949	ZFP42
			6299	10524	SALL1
			195828	18320	ZNF367
			27164	10527	SALL3
			102466730	49994	MIR6764
			148254	28382	ZNF555
			91120	28857	ZNF682
			340252	26897	ZNF680
			84146	29222	ZNF644
			84671	16447	ZNF347
			6667	11205	SP1
			163255	25331	ZNF540
			125919	25281	ZNF543
CG9973+/CG43444+	38347	Tet	200424	28313	TET3
			80312	29484	TET1
			54790	25941	TET2
			55870	19088	ASH1L
CG9633+	40972	RpA-70	6117	10289	RPA1
			254528	28569	MEIOB
CG8351+	41054	CCT7	10574	1622	CCT7
			10576	1615	CCT2
			6950	11655	TCP1
			22948	1618	CCT5
			908	1620	CCT6A
			7203	1616	CCT3
			79738	26291	BBS10
			154807	21492	VKORC1L1
			3329	5261	HSPD1
			8195	7108	MKKS
			10693	1621	CCT6B
			10575	1617	CCT4
CG3714+	33626	Naprt	93100	30450	NAPRT
			10135	30092	NAMPT
CG3542+	33513	CG3542	25766	25031	PRPF40B
			55660	16463	PRPF40A
			51322	17327	WAC
CG14210+	32958	CG14210	79080	28359	CCDC86
CG12005+	40626	Mms19	64210	13824	MMS19
CG4389+	34276	Mtpalpha	3030	4801	HADHA
			1962	3247	EHHADH
			124359	23030	CDYL2
			549	890	AUH
			55268	23408	ECHDC2
			9425	1811	CDYL
			1892	3151	ECHS1
			10455	14601	ECI2
			26275	4908	HIBCH
			1632	2703	ECI1
			55862	21489	ECHDC1

CG7293+	39332	Klp68D	9371	6320	KIF3B
			3797	6321	KIF3C
			11127	6319	KIF3A
			3833	6389	KIFC1
			57576	19167	KIF17
			221458	21202	KIF6
			56992	17273	KIF15
			64147	16666	KIF9
			113220	21495	KIF12
			26153	20226	KIF26A
			55083	25484	KIF26B
CG10920+	31688	CG10920	23788	17587	MTCH2
			23787	17586	MTCH1
CG10165+	35242	CG10165	11068	30253	CYB561D2
			284613	26804	CYB561D1
			57592	29277	ZNF687
			55205	30940	ZNF532
CG4062+	45783	ValRS	7407	12651	VARS
			57176	21642	VARS2
CG12085+	38173	hfp	22827	17042	PUF60
CG6349+	42553	DNApol-alpha180	5422	9173	POLA1
			5980	9968	REV3L
			5426	9177	POLE
			5424	9175	POLD1
CG7929+	43567	ocn	29085	30033	PHPT1
CG7665+	42133	Lgr1	3973	6585	LHCGR
			2492	3969	FSHR
			7253	12373	TSHR
			8549	4504	LGR5
			55366	13299	LGR4
			59350	19718	RXFP1
			122042	17318	RXFP2
			59352	19719	LGR6
CG6545+	42542	lbe	10660	16960	LBX1
			85474	15525	LBX2
			3217	5118	HOXB7
			3225	5130	HOXC9
			3235	5140	HOXD9
			3222	5127	HOXC5
			3205	5109	HOXA9
			3219	5120	HOXB9
			3226	5122	HOXC10
			3232	5137	HOXD3
			3213	5114	HOXB3
			3200	5104	HOXA3
			54729	24975	NKX1-1
			27287	13639	VENTX
			3196	5057	TLX2
			4869	7910	NPM1
			8538	956	BARX2
			120237	33185	DBX1
			3195	5056	TLX1
			343472	954	BARHL2
			56751	953	BARHL1
			390010	31652	NKX1-2
			3142	4978	HLX
			440097	33186	DBX2
			30012	13532	TLX3
			56033	955	BARX1
CG5528+	40245	Toll-9	81793	15634	TLR10
			10333	16711	TLR6
			7096	11847	TLR1
			7097	11848	TLR2
			7099	11850	TLR4
			7100	11851	TLR5
			4064	6726	CD180
			51284	15631	TLR7
			7098	11849	TLR3
			54106	15633	TLR9
			51311	15632	TLR8
			2811	4439	GP1BA
CG7686+	36146	LTV1	84946	21173	LTV1
CG5684+	39366	Pop2	29883	14101	CNOT7

			9337	9207	CNOT8
CG30390+	37429	Sgf29	112869	25156	SGF29
			613038		LOC613038
			388242		LOC388242
			7010	11724	TEK
CG3820+	46091	Nup214	8021	8064	NUP214
			94026	13973	POM121L2
			100288540	34004	POM121B
			23742	1190	NPAP1
			9883	19702	POM121
			285877	25369	POM121L12
			100101267	34005	POM121C
CG12812+	41231	Fancl	55120	20748	FANCL
CG1378+	43656	tll	7101	7973	NR2E1
			10002	7974	NR2E3
CG14077+	40066	CG14077	1337	2277	COX6A1
			1339	2279	COX6A2
			285849	35239	COX6A1P2
CG13077+	35252	CG13077	11068	30253	CYB561D2
			284613	26804	CYB561D1
CG3931+	37731	Rrp4	23404	17097	EXOSC2
			51010	17944	EXOSC3
CG5950+/CG33162+	47283	SrpRbeta	58477	24085	SRPRB
CG12630+	44272	tio	10194	10669	TSHZ1
			128553	13010	TSHZ2
			57616	30700	TSHZ3
CG1571+	31725	CG1571	64446	18744	DNAI2
			1781	2964	DYNC1I2
			1780	2963	DYNC1I1
			55112	21862	WDR60
			89891	28296	WDR34
			27019	2954	DNAI1
			126820	30711	WDR63
CG9198+	32473	shtd	64682	19988	ANAPC1
			102724642		LOC102724642
			107985931		LOC107985931
			730268		LOC730268
			402096		LOC402096
CG13431+	37323	Mgat1	4245	7044	MGAT1
			55624	19139	POMGNT1
CG7067+	38029	NitFhit	4817	7828	NIT1
			2272	3701	FHIT
			56954	29878	NIT2
			8875	12706	VNN2
			3094	4912	HINT1
			84681	18344	HINT2
			8876	12705	VNN1
			51733	16297	UPB1
			135114	18468	HINT3
			686	1122	BTD
CG12050+	35374	l(2)05287	84128	25725	WDR75
			317	576	APAF1
CG4079+	34293	Taf11	6882	11544	TAF11
			391742	53845	TAF11L2
			102723526	53085	LINC02218
CG9480+/CG44244+	37419	Gyg	2992	4699	GYG1
			8908	4700	GYG2
CG8086+	34131	CG8086	284451	26841	ODF3L2
			113746	19905	ODF3
			440836	34388	ODF3B
			161753	28735	ODF3L1
			441476	37285	STPG3
			23636	8066	NUP62
			4928	8068	NUP98
			9818	20261	NUP58
			1038	1798	CDR1
			105378193		LOC105378193
			9972	8062	NUP153
			285555	28712	STPG2
CG6369+	42994	Smg6	23293	17809	SMG6
			9887	16792	SMG7
			54823	16785	SWT1
			23381	24644	SMG5

CG6375+	42595	pit	8886	2741	DDX18
			54606	18193	DDX56
			57062	13266	DDX24
			64794	16715	DDX31
			57696	20085	DDX55
			317781	20082	DDX51
			1653	2734	DDX1
			10269	12877	ZMPSTE24
			146212	24753	KCTD19
CG12238+	32965	e(y)3	55274	18250	PHF10
			8193	20225	DPF1
			23522	17582	KAT6B
			7994	13013	KAT6A
			8110	17427	DPF3
			5977	9964	DPF2
CG15749+	32291	dmrt11E	10655	2935	DMRT2
			63946	13911	DMRTC2
			63947	13910	DMRTC1
			63948	13913	DMRTB1
			63950	13908	DMRTA2
			63951	13826	DMRTA1
			1761	2934	DMRT1
			58524	13909	DMRT3
			728656	31686	DMRTC1B
			644041	40037	C18orf63
CG5788+	37035	Ubc10	7332	12488	UBE2L3
			171222	13477	UBE2L5
			9246	12490	UBE2L6
			7323	12476	UBE2D3
			7325	12478	UBE2E2
			57448	13516	BIRC6
			55284	25616	UBE2W
			7319	12472	UBE2A
			65264	25847	UBE2Z
			7329	12485	UBE2I
			3093	4914	UBE2K
			7324	12477	UBE2E1
			63893	29554	UBE2O
			997	1734	CDC34
			29089	25009	UBE2T
			148581	28559	UBE2U
			51465	17598	UBE2J1
			7322	12475	UBE2D2
			51619	21647	UBE2D4
			7320	12473	UBE2B
			7326	12482	UBE2G1
			10477	12479	UBE2E3
			27338	17895	UBE2S
			7321	12474	UBE2D1
			54926	19907	UBE2R2
			11065	15937	UBE2C
			7334	12492	UBE2N
CG3358+	35604	CG3358	83940	24220	TATDN1
			9797	28988	TATDN2
			102466200	50135	MIR6844
			128387	27010	TATDN3
CG7516+	34839	l(2)34Fd	79954	25862	NOL10
CG7052+	34044	Tep2	135228	21685	CD109
			144568	23336	A2ML1
			5858	9750	PZP
			2	7	A2M
			727	1331	C5
			721	1324	C4B
			718	1318	C3
			720	1323	C4A
			27151	23228	CPAMD8
			388503	34414	C3P1
			408186		OVOS
			144203		OVOS2
			110384692		LOC110384692
			100293534	42398	C4B_2
			100287171	24361	WASHC1
CG32376+	318002	CG32376	339105	34407	PRSS53

			146547	26906	PRSS36
			3003	4711	GZMK
			23430	14118	TPSD1
			7177	12019	TPSAB1
			25823	14134	TPSG1
			64499	14120	TPSB2
			1215	2097	CMA1
			400668	31397	PRSS57
			5644	9475	PRSS1
			5646	9486	PRSS3
CG5374+	42649	CCT1	6950	11655	TCP1
			10576	1615	CCT2
			10574	1622	CCT7
			22948	1618	CCT5
			908	1620	CCT6A
			7203	1616	CCT3
			79738	26291	BBS10
			154807	21492	VKORC1L1
			3329	5261	HSPD1
			8195	7108	MKKS
			10693	1621	CCT6B
			10575	1617	CCT4
CG5546+	39987	MED19	219541	29600	MED19
CG9155+	38153	Myo61F	4641	7597	MYO1C
			283446	13879	MYO1H
			4643	7599	MYO1E
			4640	7595	MYO1A
			4642	7598	MYO1D
			64005	13880	MYO1G
			4430	7596	MYO1B
			4542	7600	MYO1F
CG7281+	41801	CycC	892	1581	CCNC
			8812	1596	CCNK
			905	1600	CCNT2
			902	1594	CCNH
			904	1599	CCNT1
			92002	28434	CCNQ
			57018	20569	CCNL1
			81669	20570	CCNL2
CG33051+	39941	CG33051	84265	28466	POLR3GL
			10622	30075	POLR3G
CG6343+	42591	ND-42	4705	7684	NDUFA10
			1716	2858	DGUOK
			1633	2704	DCK
			7084	11831	TK2
CG7376+	38715	CG7376	257218	19336	SHPRH
CG7128+	32792	Taf8	129685	17300	TAF8
			83860	17303	TAF3
CG10687+	35194	AsnRS	4677	7643	NARS
			79731	26274	NARS2
			81894	23472	SLC25A28
			51312	29786	SLC25A37
			1615	2678	DARS
CG10645+	38610	lama	196463	27283	PLBD2
			79887	26215	PLBD1
CG10719+	35197	brat	10612	10064	TRIM3
			23321	15974	TRIM2
			387921	33751	NHLRC3
			378884	21576	NHLRC1
			7706	12932	TRIM25
			131405	32669	TRIM71
			388591	32947	RNF207
			727800	25420	RNF208
			80263	19018	TRIM45
			22954	16380	TRIM32
			220441	26811	RNF152
			81844	19028	TRIM56
CG6620+	34504	aurB	6795	11391	AURKC
			9212	11390	AURKB
			6790	11393	AURKA
			11040	8987	PIM2
CG4649+	41313	Sodh-2	6652	11184	SORD
CG31015+	43640	PH4alphaPV	283208	30135	P4HA3

			5033	8546	P4HA1
			8974	8547	P4HA2
			54681	28858	P4HTM
CG9004+	38303	CG9004	64434	13244	NOM1
CG6772+/CG43756+	34038	Slob	54899	23326	PXK
CG12752+	37769	Nxt1	29107	15913	NXT1
			55916	18151	NXT2
CG10808+	36533	Syngr	9145	11498	SYNGR1
			9143	11501	SYNGR3
			9144	11499	SYNGR2
			23546	11502	SYNGR4
CG13778+	33991	Mnn1	4221	7010	MEN1
CG7564+	39956	CG7564	55692	6723	LUC7L
			51631	21608	LUC7L2
			100996928	44671	FMC1-LUC7L2
			51747	24309	LUC7L3
CG9705+	39875	CG9705	23589	17150	CARHSP1
			27254	30359	CSDC2
			4904	8014	YBX1
			389421	32207	LIN28B
			8531	2428	YBX3
			51087	17948	YBX2
			79727	15986	LIN28A
CG32374+	38848	CG32374	339105	34407	PRSS53
			146547	26906	PRSS36
			400668	31397	PRSS57
			5644	9475	PRSS1
			5646	9486	PRSS3
CG6249+	34548	Csl4	51013	17286	EXOSC1
CG9049+/CG32592+	32429	hiw	23077	23386	MYCBP2
CG9124+	45682	eIF3h	8667	3273	EIF3H
CG16837+	37904	CG16837	83657	15467	DYNLRB2
			83658	15468	DYNLRB1
CG9200+	33977	Atac1	26009	24523	ZZZ3
			27000	13192	DNAJC2
			64215	20090	DNAJC1
CG7070+	42620	PyK	5315	9021	PKM
			5313	9020	PKLR
CG14230+	32984	CG14230	55035	23387	NOL8
			6430	10787	SRSF5
CG5440+	33318	CG5440	10477	12479	UBE2E3
			7325	12478	UBE2E2
			7324	12477	UBE2E1
			7323	12476	UBE2D3
			7322	12475	UBE2D2
			51619	21647	UBE2D4
			7321	12474	UBE2D1
			57448	13516	BIRC6
			55284	25616	UBE2W
			7332	12488	UBE2L3
			7319	12472	UBE2A
			65264	25847	UBE2Z
			7329	12485	UBE2I
			3093	4914	UBE2K
			63893	29554	UBE2O
			9246	12490	UBE2L6
			997	1734	CDC34
			29089	25009	UBE2T
			148581	28559	UBE2U
			51465	17598	UBE2J1
			7320	12473	UBE2B
			7326	12482	UBE2G1
			27338	17895	UBE2S
			54926	19907	UBE2R2
			11065	15937	UBE2C
			7334	12492	UBE2N
CG15481+	34721	Ski6	54512	18189	EXOSC4
			102465510	50022	MIR6847
			118460	19055	EXOSC6
			56915	24662	EXOSC5
CG4602+	34312	Srp54	140890	17882	SREK1
			9295	10782	SRSF11
CG7861+	35532	Tbce	6905	11582	TBCE

			219899	28115	TBCEL
CG5383+	42616	PSR	23210	19355	JMJD6
CG9452+	40119	CG9452	53	123	ACP2
			55	125	ACPP
			93650	14376	ACP4
			51205	29609	ACP6
CG10230+	42802	Rpn9	5719	9558	PSMD13
CG3069+	33468	Taf10b	6881	11543	TAF10
CG18578+	53510	Ugt302C1	10720	12545	UGT2B11
			54658	12530	UGT1A1
			7363	12553	UGT2B4
			7366	12546	UGT2B15
			54490	13479	UGT2B28
			54659	12535	UGT1A3
			7367	12547	UGT2B17
			79799	28528	UGT2A3
			7364	12554	UGT2B7
			7365	12544	UGT2B10
			7368	12555	UGT8
			574537	28183	UGT2A2
			54657	12536	UGT1A4
			54575	12531	UGT1A10
			54577	12539	UGT1A7
			54579	12537	UGT1A5
			54600	12541	UGT1A9
			54578	12538	UGT1A6
			54576	12540	UGT1A8
			133688	26625	UGT3A1
			167127	27266	UGT3A2
			10941	12542	UGT2A1
CG11985+	50007	Sf3b5	83443	21083	SF3B5
CG10308+	38428	CycJ	79616	25876	CCNJL
			54619	23434	CCNJ
			8900	1577	CCNA1
			79935	25805	CNTD2
			10309	18576	CCNO
			890	1578	CCNA2
			9134	1590	CCNE2
			898	1589	CCNE1
			85417	18709	CCNB3
			9133	1580	CCNB2
			6520	11026	SLC3A2
			4041	6697	LRP5
			645121	33869	CCNI2
			10983	1595	CCNI
			900	1592	CCNG1
			899	1591	CCNF
			891	1579	CCNB1
			901	1593	CCNG2
CG1789+	31812	CG1789	51118	24329	UTP11
CG8695+	35826	Mal-A3	6519	11025	SLC3A1
			6520	11026	SLC3A2
			276	474	AMY1A
			278	476	AMY1C
			280	478	AMY2B
			277	475	AMY1B
			279	477	AMY2A
CG2854+	31219	CG2854	285343	25241	TCAIM
CG10098+	40851	CG10098	79634	30382	SCRN3
			90507	30381	SCRN2
			9805	22192	SCRN1
			10109	705	ARPC2
CG30327+/CG44249+	19834761	CG44249	55599	18666	RNPC3
			55285	25617	RBM41
			90459	23994	ERI1
			112479	30541	ERI2
CG9995+	43392	htt	3064	4851	HTT
CG4448+	42750	wda	27097	17304	TAF5L
			6877	11539	TAF5
			80349	30300	WDR61
			79269	23686	DCAF10
			256764	26790	WDR72
			7011	11726	TEP1

			23335	13490	WDR7
			317	576	APAF1
			151525	26697	WDSUB1
CG9527+	33898	CG9527	8310	121	ACOX3
			55289	25621	ACOXL
			35	90	ACADS
			33	88	ACADL
			36	91	ACADSB
			28976	21497	ACAD9
			51	119	ACOX1
			34	89	ACADM
			8309	120	ACOX2
			2639	4189	GCDH
			27034	87	ACAD8
			37	92	ACADVL
			3712	6186	IVD
CG3022+	33248	GABA-B-R3	9568	4507	GABBR2
			165829	20844	GPR156
			2550	4070	GABBR1
CG9288+	41689	CG9288	54942	1364	ABITRAM
CG9191+	38135	Klp61F	3832	6388	KIF11
			11127	6319	KIF3A
CG8657+	36408	Dgkepsilon	8526	2852	DGKE
			1609	2856	DGKQ
			1607	2850	DGKB
			139189	32395	DGKK
			1608	2853	DGKG
			1606	2849	DGKA
CG8107+	39165	CalpB	10753	1486	CAPN9
			824	1479	CAPN2
			388743	1485	CAPN8
			825	1480	CAPN3
			823	1476	CAPN1
			11131	1478	CAPN11
			147968	13249	CAPN12
			92291	16663	CAPN13
			440854	16664	CAPN14
			11132	1477	CAPN10
			726	1482	CAPN5
			6650	11182	CAPN15
			23473	1484	CAPN7
			8842	9454	PROM1
			25801	15990	GCA
			553115	30009	PEF1
			10016	8765	PDCD6
			6717	11292	SRI
			84290	16371	CAPNS2
			827	1483	CAPN6
			79747	21212	ADGB
CG6258+	34550	RfC38	5983	9971	RFC3
			5984	9972	RFC4
			5985	9973	RFC5
			5982	9970	RFC2
			5884	9807	RAD17
CG14709+	41387	Mrp4	10257	55	ABCC4
			1080	1884	CFTR
			8714	54	ABCC3
			94160	14640	ABCC12
			85320	14639	ABCC11
			89845	52	ABCC10
			1244	53	ABCC2
			6833	59	ABCC8
			10060	60	ABCC9
			368	57	ABCC6
			4363	51	ABCC1
			10057	56	ABCC5
			383	663	ARG1
			340273	46	ABCB5
			8647	42	ABCB11
			6890	43	TAP1
			23456	41	ABCB10
			5244	45	ABCB4
			6891	44	TAP2

			11194	49	ABCB8
CG11276+	39484	RpS4	6191	10424	RPS4X
			6192	10425	RPS4Y1
			140032	18501	RPS4Y2
CG4005+	37851	yki	10413	16262	YAP1
			25937	24042	WWTR1
			51008	24268	ASCC1
			8522	4169	GAS7
			9320	12306	TRIP12
			25831	20157	HECTD1
			54477	30036	PLEKHA5
			79654	26117	HECTD3
			57520	29853	HECW2
			51191	24368	HERC5
			23327	7728	NEDD4L
			55008	26072	HERC6
			51366	16806	UBR5
			4734	7727	NEDD4
			143279	26736	HECTD2
			11060	16804	WWP2
			8916	4876	HERC3
			9531	939	BAG3
			7337	12496	UBE3A
			10075	30892	HUWE1
			11059	17004	WWP1
			26091	24521	HERC4
			89910	13478	UBE3B
			80014	24148	WWC2
			9690	16803	UBE3C
			55841	29237	WWC3
			23072	22195	HECW1
			83737	13890	ITCH
			144100	27049	PLEKHA7
			23286	29435	WWC1
			64750	16809	SMURF2
			260425	29647	MAGI3
			79917	30006	MAGIX
			9223	946	MAGI1
			9870	20363	AREL1
			9863	18957	MAGI2
			57154	16807	SMURF1
			57531	21033	HACE1
CG7989+	36831	wcd	51096	24274	UTP18
			151525	26697	WDSUB1
CG4907+	42686	CG4907	23556	8967	PIGN
			22875	3359	ENPP4
			5167	3356	ENPP1
			133121	23409	ENPP6
			59084	13717	ENPP5
			54872	25985	PIGG
			339221	23764	ENPP7
			84720	23215	PIGO
			5168	3357	ENPP2
			5169	3358	ENPP3
CG4247+	41838	mRpS10	55173	14502	MRPS10
			6224	10405	RPS20
CG1404+	44072	Ran	5901	9846	RAN
CG5742+	37072	CG5742	81573	25374	ANKRD13C
			88455	21268	ANKRD13A
			338692	27880	ANKRD13D
			124930	26363	ANKRD13B
CG14690+	41285	tomboy20	9804	20947	TOMM20
			387990	33752	TOMM20L
CG32708+	318161	CG32708	29777	17369	ABT1
CG10578+	38643	DnaJ-1	25822	14887	DNAJB5
			11080	14886	DNAJB4
			3337	5270	DNAJB1
			374407	30718	DNAJB13
			3300	5228	DNAJB2
			79982	25881	DNAJB14
			10049	14888	DNAJB6
			150353	24986	DNAJB7
			165721	23699	DNAJB8

			54788	14891	DNAJB12
			55466	14885	DNAJA4
			80331	16235	DNAJC5
			5611	9439	DNAJC3
			202052	28429	DNAJC18
			120526	26979	DNAJC24
			51726	14889	DNAJB11
			552891	37501	DNAJC25-GNG10
			3301	5229	DNAJA1
			79962	25802	DNAJC22
			23341	29157	DNAJC16
			548645	34187	DNAJC25
			4189	6968	DNAJB9
			54431	24637	DNAJC10
			85479	24138	DNAJC5B
			9093	11808	DNAJA3
			285126	24844	DNAJC5G
			134218	27030	DNAJC21
			55735	25570	DNAJC11
			10294	14884	DNAJA2
			7266	12392	DNAJC7
CG9899+	37676	CG9899	9646	16850	CTR9
			79809	25660	TTC21B
CG11804+	35971	ced-6	51454	18649	GULP1
			26119	18640	LDLRAP1
			26060	24035	APPL1
			55198	18242	APPL2
CG16804+/CG33671+	3772247	Mvk	4598	7530	MVK
CG3229+/CG33123+	326262	LeuRS	51520	6512	LARS
			23395	17095	LARS2
CG5367+	34401	CG5367	1515	2538	CTSV
			1514	2537	CTSL
			1520	2545	CTSS
			1075	2528	CTSC
			1513	2536	CTSK
			8722	2531	CTSF
			1521	2546	CTSW
			5170	8816	PDPK1
			2697	4274	GJA1
			23031	19036	MAST3
			27283	14599	TINAG
			1519	2542	CTSO
			1508	2527	CTSB
			1522	2547	CTSZ
			1512	2535	CTSH
CG31531+/CG43427+	40583	smash	22998	29191	LIMCH1
			4008	6646	LMO7
			8994	6612	LIMD1
			54751	24686	FBLIM1
			2275	3704	FHL3
			3987	6616	LIMS1
			96626	30047	LIMS3
			7205	12311	TRIP6
			55679	16084	LIMS2
			8796	10573	SCEL
			26136	14620	TES
			7739	12976	ZNF185
			2274	3703	FHL2
			29995	6633	LMCD1
			144165	17019	PRICKLE1
			7791	13200	ZYX
			4007	6645	PRICKLE3
			29964	16805	PRICKLE4
			100288695	39941	LIMS4
			166336	20340	PRICKLE2
			84962	20250	AJUBA
			126374	20964	WTIP
			2273	3702	FHL1
			9457	17371	FHL5
CG5021+	39025	CG5021	780776	20398	TVP23A
			51030	20399	TVP23B
			100533496	42961	TVP23C-CDRT4
			201158	30453	TVP23C

			284040	14383	CDRT4
CG31155+	261631	Rpb7	5436	9194	POLR2G
			171568	30349	POLR3H
CG7860+	32488	CG7860	80150	16448	ASRGL1
			55617	15859	TASP1
			175	318	AGA
CG11395+	36937	Gbp2	340562	27992	SATL1
			84074	25326	QRICH2
			112483	23160	SAT2
			6303	10540	SAT1
CG5429+	42850	Atg6	8678	1034	BECN1
			441925	38606	BECN2
CG10797+/CG32498+	31309	dnc	5142	8781	PDE4B
			5144	8783	PDE4D
			5143	8782	PDE4C
			5141	8780	PDE4A
			5152	8795	PDE9A
			5151	8793	PDE8A
			8622	8794	PDE8B
			729966		LOC729966
			8654	8784	PDE5A
			27115	8792	PDE7B
			5138	8777	PDE2A
			50940	8773	PDE11A
			5146	8787	PDE6C
			5145	8785	PDE6A
			10846	8772	PDE10A
			5150	8791	PDE7A
			5158	8786	PDE6B
CG6582+	35053	cass	8539	594	API5
CG6701+	36550	CG6701	4343	7200	MOV10
			54456	7201	MOV10L1
			23064	445	SETX
			9931	16878	HELZ
			54967	26047	CT55
			1763	2939	DNA2
			85441	30021	HELZ2
			5976	9962	UPF1
			55345	25654	ZGRF1
			3508	5542	IGHMBP2
			57169	29271	ZNFX1
CG12959+/CG43729+	5740318	Stacl	246329	28423	STAC3
			6769	11353	STAC
			342667	23990	STAC2
CG1627+/CG42276+	32233	Pde9	5152	8795	PDE9A
			5141	8780	PDE4A
			5142	8781	PDE4B
			5143	8782	PDE4C
			5144	8783	PDE4D
			50940	8773	PDE11A
			5151	8793	PDE8A
			8622	8794	PDE8B
			8654	8784	PDE5A
			27115	8792	PDE7B
			5138	8777	PDE2A
			5146	8787	PDE6C
			5145	8785	PDE6A
			10846	8772	PDE10A
			5150	8791	PDE7A
			5158	8786	PDE6B
			5153	8775	PDE1B
			10842	16973	PPP1R17
			5140	8779	PDE3B
			5139	8778	PDE3A
			5136	8774	PDE1A
			729966		LOC729966
CG15776+/CG42265+	7354434	OtopLc	92736	19657	OTOP2
			133060	19656	OTOP1
			347741	19658	OTOP3
CG17835+	36239	inv	2019	3342	EN1
			2020	3343	EN2
			105371346	51815	CPHXL
			80712	14865	ESX1

			727940	33519	RHOXF2B
			84528	30011	RHOXF2
			3204	5108	HOXA7
			3233	5138	HOXD4
			3217	5118	HOXB7
			3231	5132	HOXD1
			170825	24959	GSX2
			3224	5129	HOXC8
			3218	5119	HOXB8
			3212	5113	HOXB2
			3223	5128	HOXC6
			4223	7014	MEOX2
			2637	4186	GBX2
			3214	5115	HOXB4
			2636	4185	GBX1
			3651	6107	PDX1
			3201	5105	HOXA4
			3110	4979	MNX1
			3216	5117	HOXB6
			3211	5111	HOXB1
			219409	20374	GSX1
			3232	5137	HOXD3
			4222	7013	MEOX1
			3198	5099	HOXA1
			3215	5116	HOXB5
			3213	5114	HOXB3
			3222	5127	HOXC5
			3199	5103	HOXA2
			3202	5106	HOXA5
			3200	5104	HOXA3
			3221	5126	HOXC4
			3203	5107	HOXA6
			3234	5139	HOXD8
CG5753+	37065	stau	27067	11371	STAU2
			6780	11370	STAU1
			6895	11569	TARBP2
			23217	29189	ZFR2
			8575	9438	PRKRA
CG33786+&	3772640	CG33786	79693	28905	YRDC
CG15143+	35062	CG15143	89876	24010	MAATS1
CG17935+	40886	Mst84Dd	na	na	na
CG9271+	34758	Vm34Ca	na	na	na

Supplementary Table 4: Paralogous human genes of the fly modifiers ataxin-3 genes identified by Zhang, according to DIOPT.

FlyBase Gene ID	Fly Gene ID	Fly gene symbol	Human Gene ID	HGNC ID	Human gene symbol
CG10578	38643	DnaJ-1	25822	14887	DNAJB5
			11080	14886	DNAJB4
			3337	5270	DNAJB1
			374407	30718	DNAJB13
			3300	5228	DNAJB2
			79982	25881	DNAJB14
			10049	14888	DNAJB6
			150353	24986	DNAJB7
			165721	23699	DNAJB8
			54788	14891	DNAJB12
			55466	14885	DNAJA4
			80331	16235	DNAJC5
			5611	9439	DNAJC3
			202052	28429	DNAJC18
			120526	26979	DNAJC24
			51726	14889	DNAJB11
			552891	37501	DNAJC25-GNG10
			3301	5229	DNAJA1
			79962	25802	DNAJC22
			23341	29157	DNAJC16
			548645	34187	DNAJC25
			4189	6968	DNAJB9
			54431	24637	DNAJC10
			85479	24138	DNAJC5B
			9093	11808	DNAJA3
			285126	24844	DNAJC5G
			134218	27030	DNAJC21
			55735	25570	DNAJC11
			10294	14884	DNAJA2
			7266	12392	DNAJC7
CG2720	33202	Stip1	10963	11387	STIP1
			54970	23700	TTC12
			10953	15746	TOMM34
			10910	16987	SUGT1
			23331	29179	TTC28
			64427	25759	TTC31
CG8542	36583	Hsc70-5	3313	5244	HSPA9
			3312	5241	HSPA8
			3309	5238	HSPA5
			3304	5233	HSPA1B
			3310	5239	HSPA6
			3305	5234	HSPA1L
			3306	5235	HSPA2
			6782	11375	HSPA13
			3303	5232	HSPA1A
			137814	32940	NKX2-6
			10808	16969	HSPH1
			259217	19022	HSPA12A
			10525	16931	HYOU1
			284525	28664	SLC9C2
			339416	24786	ANKRD45
			51182	29526	HSPA14
			116835	16193	HSPA12B
			3308	5237	HSPA4
			22824	17041	HSPA4L
CG6603	39557	Hsc70Cb	3308	5237	HSPA4
			10808	16969	HSPH1
			22824	17041	HSPA4L
			3312	5241	HSPA8
			3303	5232	HSPA1A
			3310	5239	HSPA6
			3304	5233	HSPA1B

			3305	5234	HSPA1L
			259217	19022	HSPA12A
			3309	5238	HSPA5
			10525	16931	HYOU1
			284525	28664	SLC9C2
			339416	24786	ANKRD45
			51182	29526	HSPA14
			116835	16193	HSPA12B
			3313	5244	HSPA9
			6782	11375	HSPA13
			3306	5235	HSPA2
CG5748	37068	Hsf	3297	5224	HSF1
			3298	5225	HSF2
			3299	5227	HSF4
			100506164	29603	HSFX1
			101927685	52398	HSFX4
			124535	26862	HSF5
			86614	18568	HSFY1
			101928917	52395	HSFX3
			100130086	32701	HSFX2
			159119	23950	HSFY2
CG1242	38389	Hsp83	3326	5258	HSP90AB1
			3320	5253	HSP90AA1
			7184	12028	HSP90B1
			3327	5259	HSP90AB3P
			391634	32537	HSP90AB2P
			664618	32538	HSP90AB4P
			3323	5255	HSP90AA4P
			730211	32535	HSP90AA5P
			10131	16264	TRAP1
			3324	5256	HSP90AA2P
CG4147	32133	Hsc70-3	3309	5238	HSPA5
			3312	5241	HSPA8
			3304	5233	HSPA1B
			3310	5239	HSPA6
			3305	5234	HSPA1L
			3306	5235	HSPA2
			3313	5244	HSPA9
			3303	5232	HSPA1A
			6782	11375	HSPA13
			137814	32940	NKX2-6
			10808	16969	HSPH1
			259217	19022	HSPA12A
			10525	16931	HYOU1
			284525	28664	SLC9C2
			339416	24786	ANKRD45
			51182	29526	HSPA14
			116835	16193	HSPA12B
			3308	5237	HSPA4
			22824	17041	HSPA4L
CG4264	41840	Hsc70-4	3312	5241	HSPA8
			3304	5233	HSPA1B
			3306	5235	HSPA2
			3305	5234	HSPA1L
			3310	5239	HSPA6
			3303	5232	HSPA1A
			3309	5238	HSPA5
			3313	5244	HSPA9
			3311	5240	HSPA7
			6782	11375	HSPA13
			137814	32940	NKX2-6
			10808	16969	HSPH1
			259217	19022	HSPA12A
			10525	16931	HYOU1
			284525	28664	SLC9C2
			339416	24786	ANKRD45

			51182	29526	HSPA14
			116835	16193	HSPA12B
			3308	5237	HSPA4
			22824	17041	HSPA4L
CG5374	42649	CCT1	6950	11655	TCP1
			10576	1615	CCT2
			10574	1622	CCT7
			22948	1618	CCT5
			908	1620	CCT6A
			7203	1616	CCT3
			79738	26291	BBS10
			154807	21492	VKORC1L1
			3329	5261	HSPD1
			8195	7108	MKKS
			10693	1621	CCT6B
			10575	1617	CCT4
CG11027	43823	Arf102F	378	655	ARF4
			381	658	ARF5
			375	652	ARF1
			377	654	ARF3
			382	659	ARF6
			100506084	32387	ARL17B
			2239	4452	GPC4
			400	692	ARL1
			373	660	TRIM23
			10123	698	ARL4C
			221079	23052	ARL5B
			84100	13210	ARL6
			80117	22974	ARL14
			132946	23592	ARL9
			10124	695	ARL4A
			115761	24046	ARL11
			390790	31111	ARL5C
			379	656	ARL4D
			26225	696	ARL5A
CG5166	41883	Atx2	11273	31326	ATXN2L
			6311	10555	ATXN2
CG9277	37238	betaTub56D	10383	20771	TUBB4B
			10382	20774	TUBB4A
			203068	20778	TUBB
			347733	30829	TUBB2B
			7280	12412	TUBB2A
			84617	20776	TUBB6
			10381	20772	TUBB3
			81027	16257	TUBB1
			347688	20773	TUBB8
			260334	24983	TUBB8B
			7846	20766	TUBA1A
			56604	12413	TUBB7P
			51175	20775	TUBE1
			84790	20768	TUBA1C
			112714	20765	TUBA3E
			10376	18809	TUBA1B
			7278	12408	TUBA3C
			51174	16811	TUBD1
			51807	12410	TUBA8
			7283	12417	TUBG1
			79861	23534	TUBAL3
			27175	12419	TUBG2
			113457	24071	TUBA3D
			7277	12407	TUBA4A
CG1059	40581	Karybeta3	3843	6402	IPO5
			26953	9851	RANBP6
			79711	19426	IPO4
CG9191	38135	Klp61F	3832	6388	KIF11
			11127	6319	KIF3A

CG6743	34481	Nup107	57122	29914	NUP107
CG11856	43041	Nup358	5903	9848	RANBP2
			653489	32416	RGPD3
			400966	32414	RGPD1
			285190	32417	RGPD4
			729857	32415	RGPD2
			727851	9849	RGPD8
			729540	32419	RGPD6
			5902	9847	RANBP1
			84220	32418	RGPD5
			9648	23218	GCC2
CG6251	36830	Nup62	23636	8066	NUP62
			54830	25960	NUP62CL
			4928	8068	NUP98
			9818	20261	NUP58
			282973	23523	JAKMIP3
CG10198	42816	Nup98-96	4928	8068	NUP98
			23636	8066	NUP62
			9818	20261	NUP58
			57727	15909	NCOA5
CG3320	42524	Rab1	5861	9758	RAB1A
			81876	18370	RAB1B
			441400	23683	RAB1C
			401409	19982	RAB19
			376267	20150	RAB15
			37	92	ACADVL
			27314	9770	RAB30
			5865	9778	RAB3B
			51762	30273	RAB8B
			5872	9762	RAB13
			9545	9779	RAB3D
			10890	9759	RAB10
			4218	7007	RAB8A
			5864	9777	RAB3A
			115827	30269	RAB3C
			83452	16075	RAB33B
			55684	24703	RABL6
			339122	19983	RAB43
			9363	9773	RAB33A
CG5771	42501	Rab11	8766	9760	RAB11A
			9230	9761	RAB11B
			57111	18238	RAB25
			11159	9799	RABL2A
			11158	9800	RABL2B
CG1250	40694	Sec23	10484	10701	SEC23A
			10483	10702	SEC23B
CG9539	33905	Sec61alpha	55176	17702	SEC61A2
			29927	18276	SEC61A1
CG10541	38653	Tektin-C	83659	15534	TEKT1
			146279	26554	TEKT5
			150483	31012	TEKT4
			64518	14293	TEKT3
			27285	11725	TEKT2
CG2275	36057	Jra	3725	6204	JUN
			3727	6206	JUND
			3726	6205	JUNB
			1386	784	ATF2
			11016	792	ATF7
CG12437	44851	raw	6041	10050	RNASEL
CG14217	32948	Tao	57551	29259	TAOK1
			51347	18133	TAOK3
			9344	16835	TAOK2
CG7392	34096	Cka	29966	15720	STRN3
			6801	11424	STRN
			29888	15721	STRN4
			128025	26570	WDR64

CG12244	32257	lic	5608	6846	MAP2K6
			5606	6843	MAP2K3
			6416	6844	MAP2K4
			5604	6840	MAP2K1
			5605	6842	MAP2K2
			646643	34416	SBK2
			5607	6845	MAP2K5
			5609	6847	MAP2K7
			27347	17717	STK39
			100996792		LOC100996792
			10746	6854	MAP3K2
			4215	6855	MAP3K3
			4216	6856	MAP3K4
			4750	7744	NEK1
CG32743	31625	nonC	23049	30045	SMG1
			107984138		LOC107984138
			2475	3942	MTOR
			5591	9413	PRKDC
			5289	8974	PIK3C3
			552900	29488	BOLA2
			5297	8983	PI4KA
			5291	8976	PIK3CB
			5286	8971	PIK3C2A
			8295	12347	TRRAP
			5298	8984	PI4KB
			5288	8973	PIK3C2G
			654483	32479	BOLA2B
			107282092	53563	BOLA2-SMG1P6
			5290	8975	PIK3CA
			545	882	ATR
			5287	8972	PIK3C2B
			5293	8977	PIK3CD
			285590	29242	SH3PXD2B
			9644	23664	SH3PXD2A
			5294	8978	PIK3CG
CG8954	34804	Smg5	23381	24644	SMG5
			9887	16792	SMG7
			23293	17809	SMG6
CG1559	32153	Upf1	5976	9962	UPF1
			85441	30021	HELZ2
			55345	25654	ZGRF1
			23064	445	SETX
			9931	16878	HELZ
			54967	26047	CT55
			1763	2939	DNA2
			3508	5542	IGHMBP2
			54456	7201	MOV10L1
			57169	29271	ZNFX1
			4343	7200	MOV10
CG2253	31724	Upf2	26019	17854	UPF2
CG14981	38459	mge	56993	18002	TOMM22
CG31196	42186	14-3-3epsilon	7531	12851	YWHAE
			7534	12855	YWHAZ
			7529	12849	YWHAB
			10971	12854	YWHAQ
			7533	12853	YWHAH
			2810	10773	SFN
			7532	12852	YWHAG
CG9984	32607	TH1	51497	15934	NELFCD
CG7838	35522	BubR1	699	1148	BUB1
			701	1149	BUB1B
			55806	5172	HR
CG7581	43490	Bub3	9184	1151	BUB3
			8480	9828	RAE1
CG1676	33043	cactin	58509	29938	CACTIN
			91862	30525	MARVELD3

CG1098	40710	Madm	29959	7993	NRBP1
			340371	19339	NRBP2
			102466748	49956	MIR6845
			65125	14540	WNK1
			65266	14544	WNK4
			65267	14543	WNK3
			25778	29043	DSTYK
CG12306	40232	polo	5347	9077	PLK1
			10769	19699	PLK2
			1263	2154	PLK3
			126520	27001	PLK5
			10733	11397	PLK4
			2317	3755	FLNB
CG16944	32007	sesB	291	10990	SLC25A4
			292	10991	SLC25A5
			293	10992	SLC25A6
			83447	25319	SLC25A31
			3458	5438	IFNG
CG1906	43481	alph	5494	9275	PPM1A
			5495	9276	PPM1B
			147699	26845	PPM1N
			9647	19388	PPM1F
			5496	9278	PPM1G
			22843	19322	PPM1E
			57546	30263	PDP2
			151649	28406	PP2D1
			333926	20785	PPM1J
			132160	26506	PPM1M
			57460	18583	PPM1H
			151742	16381	PPM1L
			54704	9279	PDP1
			8493	9277	PPM1D
			10454	18157	TAB1
			160760	30695	PPTC7
			152926	25415	PPM1K
			80895	15566	ILKAP
CG11621	39329	Pi3K68D	5286	8971	PIK3C2A
			5287	8972	PIK3C2B
			5288	8973	PIK3C2G
			5291	8976	PIK3CB
			5290	8975	PIK3CA
			5293	8977	PIK3CD
			5294	8978	PIK3CG
			5289	8974	PIK3C3
			2475	3942	MTOR
			5591	9413	PRKDC
			552900	29488	BOLA2
			5297	8983	PI4KA
			8295	12347	TRRAP
			5298	8984	PI4KB
			654483	32479	BOLA2B
			107282092	53563	BOLA2-SMG1P6
			545	882	ATR
			285590	29242	SH3PXD2B
			9644	23664	SH3PXD2A
			23049	30045	SMG1
CG13570	43958	spag	79657	26151	RPAP3
			10953	15746	TOMM34
CG17520	48448	CkIIalpha	1457	2457	CSNK2A1
			1459	2459	CSNK2A2
			283106	2458	CSNK2A3
			3636	6080	INPPL1
CG15224	32132	CkIIbeta	1460	2460	CSNK2B
			58496	13931	LY6G5B
CG5092	47396	Tor	2475	3942	MTOR
			5591	9413	PRKDC

			23049	30045	SMG1
			3123	4948	HLA-DRB1
			472	795	ATM
			107984138		LOC107984138
			5289	8974	PIK3C3
			552900	29488	BOLA2
			5297	8983	PI4KA
			5291	8976	PIK3CB
			5286	8971	PIK3C2A
			8295	12347	TRRAP
			5298	8984	PI4KB
			5288	8973	PIK3C2G
			654483	32479	BOLA2B
			107282092	53563	BOLA2-SMG1P6
			5290	8975	PIK3CA
			545	882	ATR
			5287	8972	PIK3C2B
			285590	29242	SH3PXD2B
			5293	8977	PIK3CD
			9644	23664	SH3PXD2A
			5294	8978	PIK3CG
CG1972	43506	IntS11	54973	26052	INTS11
			102465435	50171	MIR6727
			51692	2326	CPSF3
			64421	17642	DCLRE1C
			64858	17641	DCLRE1B
			53981	2325	CPSF2
			9937	17660	DCLRE1A
			55756	25592	INTS9
CG32721	31681	NELF-B	25920	24324	NELFB
CG5222	39763	IntS9	55756	25592	INTS9
			64421	17642	DCLRE1C
			64858	17641	DCLRE1B
			51692	2326	CPSF3
			53981	2325	CPSF2
			9937	17660	DCLRE1A
			54973	26052	INTS11
CG5874	42520	Nelf-A	7469	12768	NELFA
			100126332	33689	MIR943
CG5994	38982	Nelf-E	7936	13974	NELFE
			100302242	33925	MIR1236
			54715	18222	RBFOX1
CG4001	36060	Pfk	5213	8877	PFKM
			5211	8876	PFKL
			5214	8878	PFKP
CG9412	47998	rin	10146	30292	G3BP1
			9908	30291	G3BP2
			23082	30025	PPRC1
			10891	9237	PPARGC1A
CG6058	43183	Ald1	230	418	ALDOC
			226	414	ALDOA
			229	417	ALDOB
			112694756		LOC112694756
			2867	4501	FFAR2
CG11583	326206	CG11583	55299	24170	BRIX1
CG1420	43427	Slu7	10569	16939	SLU7
CG1957	43426	Cpsf100	53981	2325	CPSF2
			64421	17642	DCLRE1C
			64858	17641	DCLRE1B
			51692	2326	CPSF3
			9937	17660	DCLRE1A
			54973	26052	INTS11
			55756	25592	INTS9
CG3605	33514	Sf3b2	10992	10769	SF3B2
CG5274	40257	CG5274	79034	21702	C7orf26
CG6197	36514	fand	56949	14089	XAB2

			63897	24076	HEATR6
CG6905	38062	Cdc5	988	1743	CDC5L
			4602	7545	MYB
			6566	10922	SLC16A1
			4603	7547	MYBL1
			9988	14603	DMTF1
			7270	12397	TTF1
			6621	11137	SNAPC4
			4605	7548	MYBL2
CG8241	36561	pea	1659	2749	DHX8
			1665	2738	DHX15
			8449	2739	DHX16
			9785	17211	DHX38
			165545	20410	DQX1
			79665	18018	DHX40
			60625	15861	DHX35
			55760	16717	DHX32
			56919	16718	DHX33
			57647	17210	DHX37
			122402	20122	TDRD9
			54505	15815	DHX29
			64848	24721	YTHDC2
			1660	2750	DHX9
			9704	16719	DHX34
			90957	20086	DHX57
			51538	30246	ZCCHC17
			22907	16716	DHX30
			170506	14410	DHX36
CG3193	31208	crn	51340	15762	CRNKL1
CG4878	36981	eIF3b	8662	3280	EIF3B
			83939	3254	EIF2A
CG8430	36782	Got1	2805	4432	GOT1
			137362	28487	GOT1L1
			2806	4433	GOT2
CG7269	33781	Hel25E	7919	13917	DDX39B
			10212	17821	DDX39A
CG10367	42803	Hmgcr	3156	5006	HMGCR
CG4152	48782	Mtr4	23517	18734	MTREX
			6499	10898	SKIV2L
			164045	20193	HFM1
			10527	9852	IPO7
			55601	25942	DDX60
			10526	9853	IPO8
			91351	26429	DDX60L
CG12396	44391	Nnp-1	23076	23818	RRP1B
			8568	18785	RRP1
CG3127	33461	Pgk	5230	8896	PGK1
			5232	8898	PGK2
CG7070	42620	PyK	5315	9021	PKM
			5313	9020	PKLR
CG8882	33710	eIF3i	8668	3272	EIF3I
CG8276	35552	bin3	56257	20247	MEPCE
			144233	27050	BCDIN3D
CG13399	3772329	Chrac-14	54107	13546	POLE3
			4801	7805	NFYB
CG6694	38968	ZC3H3	23144	28972	ZC3H3
			642843	33632	CPSF4L
			376940	24762	ZC3H6
			84524	30941	ZC3H8
			10898	2327	CPSF4
			23211	17808	ZC3H4
CG4654	36461	Dp	7029	11751	TFDP2
			7027	11749	TFDP1
			51270	24603	TFDP3
CG6474	32762	e(y)1	6880	11542	TAF9
			51616	17306	TAF9B

CG4903	36986	MESR4	51147	19423	ING4
			84289	19421	ING5
			3621	6062	ING1
			3622	6063	ING2
			54556	14587	ING3
			51157	29473	ZNF580
			220929	21029	ZNF438
			63976	14000	PRDM16
			2122	3498	MECOM
			83860	17303	TAF3
CG33554	35483	Nipped-A	8295	12347	TRRAP
			5289	8974	PIK3C3
			2475	3942	MTOR
			5591	9413	PRKDC
			552900	29488	BOLA2
			5297	8983	PI4KA
			5291	8976	PIK3CB
			5286	8971	PIK3C2A
			5298	8984	PI4KB
			5288	8973	PIK3C2G
			654483	32479	BOLA2B
			107282092	53563	BOLA2-SMG1P6
			5290	8975	PIK3CA
			545	882	ATR
			5287	8972	PIK3C2B
			285590	29242	SH3PXD2B
			5293	8977	PIK3CD
			9644	23664	SH3PXD2A
			5294	8978	PIK3CG
			23049	30045	SMG1
CG42277	40879	rn	149076	18079	ZNF362
			170958	29423	ZNF525
			7629	13149	ZNF76
			146050	26673	ZSCAN29
			7745	12983	ZKSCAN8
			26048	23716	ZNF500
			7753	12994	ZNF202
			342357	25677	ZKSCAN2
			285268	24787	ZNF621
			390963	33265	ZNF818P
			55769	13158	ZNF83
			9753	13172	ZSCAN12
			55892	14955	MYNN
			54925	20812	ZSCAN32
			57336	13502	ZNF287
			342945	4929	ZSCAN22
			80108	26138	ZFP2
			105379427	13143	ZNF73P
			7626	13145	ZNF75D
			79692	23640	ZNF322
			360023	24819	ZBTB41
			169834	27271	ZNF883
			147947	25393	ZNF542P
			729944	13148	ZNF75CP
			7741	12978	ZSCAN26
			374899	34032	ZNF829
			7716	12949	VEZF1
			4150	6914	MAZ
			171017	11955	ZNF384
			195828	18320	ZNF367
			342892	27994	ZNF850
CG7471	38565	HDAC1	3065	4852	HDAC1
			3066	4853	HDAC2
			8841	4854	HDAC3
			55869	13315	HDAC8
			9759	14063	HDAC4

			51564	14067	HDAC7
			79885	19086	HDAC11
			83933	18128	HDAC10
			10013	14064	HDAC6
			10014	14068	HDAC5
			9734	14065	HDAC9
CG8815	36382	Sin3A	25942	19353	SIN3A
			23309	19354	SIN3B
CG4817	37767	Ssrp	6749	11327	SSRP1
			93349	25105	SP140L
CG5444	39765	Taf4	6875	11538	TAF4B
			6874	11537	TAF4
CG7752	40351	pzg	56980	13995	PRDM10
			152485	27193	ZNF827
			146542	30489	ZNF688
			7738	12975	ZNF184
			7637	13159	ZNF84
			51427	12887	ZNF107
			92595	28200	ZNF764
			79788	25885	ZNF665
			7652	13175	ZNF99
			7757	12999	ZNF208
			7644	13166	ZNF91
			8427	13076	ZNF282
			55900	13848	ZNF302
			139735	12865	ZFP92
			197407	13114	ZNF48
			115509	25173	ZNF689
			65988	28350	ZNF747
			90338	12948	ZNF160
			84671	16447	ZNF347
			100287226	32464	ZNF729
			162968	23714	ZNF497
			146540	26496	ZNF785
			339318	12971	ZNF181
CG11989	39175	vnc	8260	18704	NAA10
			84779	28125	NAA11
			9027	18069	NAT8
			80218	29533	NAA50
			339983	26742	NAT8L
			51126	15908	NAA20
			122830	19844	NAA30
			79903	25875	NAA60
			57325	15904	KAT14
CG5942	39744	brm	6595	11098	SMARCA2
			6597	11100	SMARCA4
CG8817	33496	lilli	27125	17869	AFF4
			2334	3776	AFF2
			3899	6473	AFF3
			4299	7135	AFF1
			473	9965	RERE
CG18740	41942	mor	6601	11105	SMARCC2
			6599	11104	SMARCC1
			114803	29401	MYSM1
			84954	25934	MPND
CG16983	31016	SkpA	6500	10899	SKP1
CG1782	35998	Uba1	7317	12469	UBA1
			7318	12471	UBA7
			55236	25581	UBA6
			10055	30660	SAE1
			27304	15765	MOCS3
			10054	30661	UBA2
			9039	12470	UBA3
			79876	23230	UBA5
			10533	16935	ATG7
			8883	621	NAE1

CG12276	41532	Aos1	10055	30660	SAE1
			8883	621	NAE1
			27304	15765	MOCS3
			7317	12469	UBA1
			10054	30661	UBA2
			9039	12470	UBA3
			7318	12471	UBA7
			79876	23230	UBA5
			10533	16935	ATG7
			55236	25581	UBA6
CG42641	35176	Rpn3	5709	9560	PSMD3
CG5519	37123	Prp19	27339	17896	PRPF19
CG8392	46058	Prosbeta1	5694	9543	PSMB6
			5698	9546	PSMB9
			5699	9538	PSMB10
CG3018	33226	lwr	7329	12485	UBE2I
			7323	12476	UBE2D3
			7325	12478	UBE2E2
			57448	13516	BIRC6
			55284	25616	UBE2W
			7332	12488	UBE2L3
			7319	12472	UBE2A
			65264	25847	UBE2Z
			3093	4914	UBE2K
			63893	29554	UBE2O
			7324	12477	UBE2E1
			9246	12490	UBE2L6
			997	1734	CDC34
			29089	25009	UBE2T
			148581	28559	UBE2U
			51465	17598	UBE2J1
			7322	12475	UBE2D2
			51619	21647	UBE2D4
			7320	12473	UBE2B
			7326	12482	UBE2G1
			10477	12479	UBE2E3
			27338	17895	UBE2S
			7321	12474	UBE2D1
			54926	19907	UBE2R2
			11065	15937	UBE2C
			7334	12492	UBE2N
CG7619	40388	Rpn10	5710	9561	PSMD4
			266971	23733	PIPSL
CG10938	36951	Prosalpha5	5686	9534	PSMA5
			5684	9532	PSMA3
			143471	22985	PSMA8
			5682	9530	PSMA1
			5685	9533	PSMA4
			5687	9535	PSMA6
			5688	9536	PSMA7
			5683	9531	PSMA2
			5689	9537	PSMB1
			5693	9542	PSMB5
			5695	9544	PSMB7
			5691	9540	PSMB3
			5699	9538	PSMB10
			5696	9545	PSMB8
			122706	31963	PSMB11
			5690	9539	PSMB2
CG7762	40174	Rpn1	5708	9559	PSMD2
CG4494	33981	smt3	6612	11124	SUMO3
			6613	11125	SUMO2
			387082	21181	SUMO4
			7341	12502	SUMO1
			7327	12483	UBE2G2
			84901	25906	NFATC2IP

CG10370	42805	Rpt5	5702	9549	PSMC3
			5706	9553	PSMC6
			5704	9551	PSMC4
			5705	9552	PSMC5
			5700	9547	PSMC1
			5701	9548	PSMC2
CG9712	39881	TSG101	7251	15971	TSG101
			55293	30866	UEVLD
CG7528	44496	Uba2	10054	30661	UBA2
			9039	12470	UBA3
			27304	15765	MOCS3
			7317	12469	UBA1
			7318	12471	UBA7
			79876	23230	UBA5
			10533	16935	ATG7
			10055	30660	SAE1
			55236	25581	UBA6
			8883	621	NAE1
CG15319	43856	nej	2033	3373	EP300
			1387	2348	CREBBP
			100302237	35359	MIR1281
			57634	11958	EP400
			23476	13575	BRD4
			8019	1104	BRD3
			8850	8638	KAT2B
			2648	4201	KAT2A
			11176	962	BAZ2A
			2186	3581	BPTF
			55193	30064	PBRM1
			11177	960	BAZ1A
			10902	19874	BRD8
			29994	963	BAZ2B
			6046	1103	BRD2
			676	1105	BRDT
			9031	961	BAZ1B
CG16908	41189	CG16908	9675	29029	TTI1
CG17153	39375	ssp	345222	33741	MSANTD1
			4792	7797	NFKBIA
CG43707	33601	CG43707	84687	9298	PPP1R9B
			54477	30036	PLEKHA5
			10256	19700	CNKSR1
			55607	14946	PPP1R9A
			160622	18707	GRASP
			9595	9506	CYTIP
			10083	12597	USH1C
			51248	28034	PDZD11
			57120	17643	GOPC
			117583	14446	PARD3B
			84708	6657	LNX1
			222484	20421	LNX2
			143162	28572	FRMPD2
			55333	18955	SYNJ2BP
			25861	16361	WHRN
			100529257	48350	SYNJ2BP-COX16
			9351	11076	SLC9A3R2
			10207	28881	PATJ
			9231	2904	DLG5
			3603	5980	IL16
			23037	18486	PDZD2
			392862	18464	GRID2IP
			9368	11075	SLC9A3R1
			79955	26257	PDZD7
			5174	8821	PDZK1
			23426	18708	GRIP1
			8777	7208	MPDZ
			79849	19891	PDZD3

			56288	16051	PARD3
CG3363	37874	ocm	50945	11600	TBX22
			6911	11605	TBX6
			6913	11594	TBX15
			57057	11598	TBX20
			9096	11595	TBX18
			6910	11604	TBX5
			347853	11593	TBX10
			6909	11597	TBX2
			9496	11603	TBX4
			23269	14010	MGA
			9095	11596	TBX19
			6862	11515	TBXT
			8320	3372	EOMES
			6899	11592	TBX1
			6926	11602	TBX3
			30009	11599	TBX21
			10716	11590	TBR1
CG5859	36886	IntS8	55656	26048	INTS8
CG8211	32745	IntS2	57508	29241	INTS2
CG9591	41674	omd	80789	29352	INTS5
CG18176	39141	defl	25896	24484	INTS7
CG12113	31793	IntS4	92105	25048	INTS4
			644619	22351	INTS4P2
			101929322		LOC101929322
			285905	21925	INTS4P1
CG10080	37462	mahj	9730	30911	DCAF1
CG18398	35155	Tango6	79613	25749	TANGO6
CG30349	35885	CG30349	23160	28945	WDR43
CG31111	318595	CG31111	84897	29551	TBRG1
			8085	7133	KMT2D
			58508	13726	KMT2C
CG4738	34549	Nup160	23279	18017	NUP160
CG9300	40128	CG9300	25926	24557	NOL11
CG9667	40960	CG9667	100534599	42969	ISY1-RAB43
			57461	29201	ISY1
			339122	19983	RAB43
CG9775	40576	CG9775	26097	24511	CHTOP
CG1796	32168	Tango4	5356	9089	PLRG1
CG7357	42145	Odj	85460	29365	ZNF518B
			3104	4930	ZBTB48
			147807	28322	ZNF524
			163087	18609	ZNF383
			63934	28854	ZNF667
			79891	26279	ZNF671
			389114	31930	ZNF662
			286075	27815	ZNF707
			7988	13004	ZNF212
			1877	3121	E4F1
			7552	13128	ZNF711
			149076	18079	ZNF362
			140467	16838	ZNF358
			51545	25017	ZNF581
			55657	26049	ZNF692
			4150	6914	MAZ
			285349	26720	ZNF660
			284390	27614	ZNF763
			63978	14001	PRDM14
			100507290	38705	ZNF865
			8328	4238	GFI1B
			147741	26484	ZNF560
			23528	13075	ZNF281
			7554	13154	ZNF8
CG4294	37579	CG4294	na	na	na
CG10712	40508	Chro	na	na	na
CG1957	43426	Cpsf100	53981	2325	CPSF2

64421	17642	DCLRE1C
64858	17641	DCLRE1B
51692	2326	CPSF3
9937	17660	DCLRE1A
54973	26052	INTS11
55756	25592	INTS9

Supplementary Table 5: Paralogous human genes of the fly modifiers ataxin-3 genes identified by Bilen and Bonine according to DIOPT. * are reported in Vobfeldt ; # are reported in Zhang. & represent the genes where gene name were used to search human orthologs

FlyBase Gene ID	Fly Gene ID	Fly gene symbol	Human Gene ID	HGNC ID	Human gene symbol
CG5436	42852	Hsp68	3304	5233	HSPA1B
			3312	5241	HSPA8
			3310	5239	HSPA6
			3305	5234	HSPA1L
			3306	5235	HSPA2
			3303	5232	HSPA1A
			3309	5238	HSPA5
			3313	5244	HSPA9
			6782	11375	HSPA13
			3311	5240	HSPA7
			137814	32940	NKX2-6
			10808	16969	HSPH1
			259217	19022	HSPA12A
			10525	16931	HYOU1
			284525	28664	SLC9C2
			339416	24786	ANKRD45
			51182	29526	HSPA14
			116835	16193	HSPA12B
			3308	5237	HSPA4
			22824	17041	HSPA4L
CG8448	36797	mrj	3300	5228	DNAJB2
			10049	14888	DNAJB6
			150353	24986	DNAJB7
			165721	23699	DNAJB8
			414061	32397	DNAJB3
			11080	14886	DNAJB4
			55466	14885	DNAJA4
			80331	16235	DNAJC5
			5611	9439	DNAJC3
			202052	28429	DNAJC18
			374407	30718	DNAJB13
			120526	26979	DNAJC24
			51726	14889	DNAJB11
			552891	37501	DNAJC25-GNG10
			79982	25881	DNAJB14
			3301	5229	DNAJA1
			3337	5270	DNAJB1
			79962	25802	DNAJC22
			23341	29157	DNAJC16
			548645	34187	DNAJC25
			4189	6968	DNAJB9
			54431	24637	DNAJC10
			85479	24138	DNAJC5B
			9093	11808	DNAJA3
			285126	24844	DNAJC5G
			134218	27030	DNAJC21
			25822	14887	DNAJB5
			55735	25570	DNAJC11
			10294	14884	DNAJA2
			54788	14891	DNAJB12
			7266	12392	DNAJC7
CG14207	32955	CG14207	1409	2388	CRYAA
			3315	5246	HSPB1
			1410	2389	CRYAB
			102724652	51901	CRYAA2
			3316	5247	HSPB2
			26353	30171	HSPB8
			8988	5248	HSPB3
			126393	26511	HSPB6
			94086	30589	HSPB9
			27129	5249	HSPB7

			100528019	41996	HSPB2-C11orf52
CG5486	38644	Usp47	55031	20076	USP47
			11274	12616	USP18
			57646	12625	USP28
			29761	12624	USP25
			373856	20070	USP41
			7874	12630	USP7
			55230	20069	USP40
			23358	12623	USP24
			84196	18533	USP48
			8239	12632	USP9X
			9736	20066	USP34
CG8209	38888	CG8209	51035	18402	UBXN1
			23190	14860	UBXN4
CG10372	35129	Faf2	23197	24666	FAF2
			7993	30307	UBXN8
			11124	3578	FAF1
CG11033	41090	Kdm2	22992	13606	KDM2A
			84678	13610	KDM2B
			54620	25300	FBXL19
			5253	8920	PHF2
			102465665	50006	MIR7107
			26231	13605	LRRC29
			146330	14150	FBXL16
			23133	20672	PHF8
			162517	28565	FBXO39
			79176	28155	FBXL15
			26235	13601	FBXL4
			80853	22224	KDM7A
			64839	13615	FBXL17
			26233	13603	FBXL6
			283807	27537	FBXL22
			222235	21658	FBXL13
			144699	28624	FBXL14
			23194	13604	FBXL7
			26224	13599	FBXL3
			54850	13611	FBXL12
			196394	27281	AMN1
CG11172	32321	NFAT	10725	7774	NFAT5
			4775	7777	NFATC3
			4773	7776	NFATC2
			4776	7778	NFATC4
			4772	7775	NFATC1
CG11371	33161	dbr	na	na	na
CG1624/CG42396	44653	wech	131405	32669	TRIM71
			10612	10064	TRIM3
			23321	15974	TRIM2
			378884	21576	NHLRC1
			388591	32947	RNF207
			727800	25420	RNF208
			80263	19018	TRIM45
			22954	16380	TRIM32
			387921	33751	NHLRC3
			220441	26811	RNF152
			81844	19028	TRIM56
CG1691	32009	Imp	10644	28867	IGF2BP2
			10643	28868	IGF2BP3
			10642	28866	IGF2BP1
			100500888	38893	MIR3940
			57060	8652	PCBP4
			54039	8651	PCBP3
			8939	4005	FUBP3
			4857	7886	NOVA1
			5093	8647	PCBP1
			5094	8648	PCBP2
			8880	4004	FUBP1

CG5009	37028	CG5009	51	119	ACOX1
			8309	120	ACOX2
			10267	9843	RAMP1
			35	90	ACADS
			33	88	ACADL
			36	91	ACADSB
			28976	21497	ACAD9
			34	89	ACADM
			2639	4189	GCDH
			27034	87	ACAD8
			37	92	ACADVL
			55289	25621	ACOXL
			8310	121	ACOX3
			3712	6186	IVD
CG10578* #	38643	DnaJ-1	25822	14887	DNAJB5
			11080	14886	DNAJB4
			3337	5270	DNAJB1
			374407	30718	DNAJB13
			3300	5228	DNAJB2
			79982	25881	DNAJB14
			10049	14888	DNAJB6
			150353	24986	DNAJB7
			165721	23699	DNAJB8
			54788	14891	DNAJB12
			55466	14885	DNAJA4
			80331	16235	DNAJC5
			5611	9439	DNAJC3
			202052	28429	DNAJC18
			120526	26979	DNAJC24
			51726	14889	DNAJB11
			552891	37501	DNAJC25-GNG10
			3301	5229	DNAJA1
			79962	25802	DNAJC22
			23341	29157	DNAJC16
			548645	34187	DNAJC25
			4189	6968	DNAJB9
			54431	24637	DNAJC10
			85479	24138	DNAJC5B
			9093	11808	DNAJA3
			285126	24844	DNAJC5G
			134218	27030	DNAJC21
			55735	25570	DNAJC11
			10294	14884	DNAJA2
			7266	12392	DNAJC7
CG13387*	34167	emb	7514	12825	XPO1
			57510	17675	XPO5
			23214	19733	XPO6
CG4599*	34984	Tpr2	7266	12392	DNAJC7
			5611	9439	DNAJC3
			285126	24844	DNAJC5G
			134218	27030	DNAJC21
			84277	16410	DNAJC30
			11080	14886	DNAJB4
			55466	14885	DNAJA4
			80331	16235	DNAJC5
			3300	5228	DNAJB2
			202052	28429	DNAJC18
			374407	30718	DNAJB13
			120526	26979	DNAJC24
			51726	14889	DNAJB11
			552891	37501	DNAJC25-GNG10
			79982	25881	DNAJB14
			3301	5229	DNAJA1
			3337	5270	DNAJB1
			79962	25802	DNAJC22
			23341	29157	DNAJC16

			548645	34187	DNAJC25
			4189	6968	DNAJB9
			54431	24637	DNAJC10
			85479	24138	DNAJC5B
			10049	14888	DNAJB6
			9093	11808	DNAJA3
			165721	23699	DNAJB8
			150353	24986	DNAJB7
			25822	14887	DNAJB5
			55735	25570	DNAJC11
			10294	14884	DNAJA2
			54788	14891	DNAJB12
CG8815#	36382	Sin3A	25942	19353	SIN3A
			23309	19354	SIN3B
CG11700&	31564	CG11700	7314	12463	UBB
			6233	10417	RPS27A
			7311	12458	UBA52
			7316	12468	UBC
			8266	12505	UBL4A
			50613	12510	UBQLN3
			56893	1237	UBQLN4
			164153	32309	UBL4B
			8638	8090	OASL
			29978	12509	UBQLN2
			9636	4053	ISG15
			29979	12508	UBQLN1
			5886	9812	RAD23A
			4738	7732	NEDD8
			10537	18795	UBD
			5887	9813	RAD23B
			93550	23504	ZFAND4
			84993	28221	UBL7
			100528064	39551	NEDD8-MDP1
			2197	3597	FAU
			143630	28294	UBQLNL
CG43782*&	39018	orb2	132864	21745	CPEB2
			80315	21747	CPEB4
			22849	21746	CPEB3
			55852	30884	TEX2
			64506	21744	CPEB1

Supplementary Table 6. Level 2 ataxin-3 interactors that interact with level 1 ataxin-3 interactors

Gene ID	UniprotID	Protein	Number of ataxin-3 L1 interactors
7316	P0CG48	UBC	134
7157	P04637	P53	52
5071	O60260	PRKN	40
7341	P63165	SUMO1	39
7415	P55072	TERA	39
351	P05067	A4	37
3312	P11142	HSP7C	36
3308	P34932	HSP74	33
4738	Q15843	NEDD8	33
7189	Q9Y4K3	TRAF6	32
3320	P07900	HS90A	30
57154	Q9HCE7	SMUF1	28
10013	Q9UBN7	HDAC6	27
5886	P54725	RD23A	26
10273	Q9UNE7	CHIP	26
7314	P0CG47	UBB	25
1026	P38936	CDN1A	24
3303	P0DMV8	HS71A	24
4214	Q13233	M3K1	24
7846	Q71U36	TBA1A	24
1387	Q92793	CBP	22
5710	P55036	PSMD4	22
8878	Q13501	SQSTM	22
203068	P07437	TBB5	22
2130	Q01844	EWS	21
2932	P49841	GSK3B	21
5705	P62195	PRS8	21
7334	P61088	UBE2N (UBC13)	21
9531	O95817	BAG3	21
3301	P31689	DNJA1	20
4792	P25963	IKBA	20
6195	Q15418	KS6A1	20
7317	P22314	UBA1	19
2033	Q09472	EP300	18
292	P05141	ADT2	16
6389	P31040	SDHA	16
8841	O15379	HDAC3	16
29979	Q9UMX0	UBQL1	16
4697	O00483	NDUA4	15
5887	P54727	RD23B	15
7332	P68036	UB2L3	15
2547	P12956	XRCC6	14
10059	O00429	DNM1L	14
47	P53396	ACLY	13
821	P27824	CALX	13
1019	P11802	CDK4	13
5371	P29590	PML	13

9611	O75376	NCOR1	13
83737	Q96J02	ITCH	13
267	Q9UKV5	AMFR	12
1460	P67870	CSK2B	12
7335	Q13404	UB2V1	12
9656	Q14676	MDC1	12
10277	O95155	UBE4B	12
10808	Q92598	HS105	12
1385	P16220	CREB1	11
3300	P25686	DNJB2	11
8975	Q92995	UBP13	11
57159	Q9BYV2	TRI54	11
78990	Q96DC9	OTUB2	11
84676	Q969Q1	TRI63	11
387522	I3L0A0	PEDS1	11
5250	Q00325	MPCP	10
8850	Q92831	KAT2B	10
27338	Q16763	UBE2S	10
598	Q07817	B2CL1	9
836	P42574	CASP3	9
3105	P04439	1A03	9
5713	P51665	PSMD7	9
6128	Q02878	RPL6	9
6175	P05388	RLA0	9
7326	P62253	UBE2G1	9
84447	Q86TM6	SYVN1	9
293	P12236	ADT3	8
9463	Q9NRD5	PICK1	8
10892	Q9UDY8	MALT1	8
310	P20073	ANXA7	7
6390	P21912	SDHB	7
7083	P04183	KITH	7
83932	Q9H040	SPRTN	7
396	P52565	GDIR1	6
871	P50454	SERPH	6
1785	P50570	DYN2	6
11284	Q96T60	PNKP	6
54708	Q9NX47	MARH5	6
83892	Q9H3F6	BACD3	6
84675	Q9BYV6	TRI55	6
5631	P60891	PRPS1	5
6576	P53007	TXTP	5
9524	Q9NZ01	TECR	5
10212	O00148	DX39A	5
22824	O95757	HS74L	5
23295	O60291	MGRN1	5
23647	P53365	ARFP2	5
64219	Q8NG27	PJA1	5
112724	Q8NBN7	RDH13	5
337867	Q8NBM4	UBAC2	5

493856	Q8N5K1	CISD2	5
824	P17655	CAN2	4
834	P29466	CASP1	4
1468	Q9UBX3	DIC	4
9894	Q9Y4R8	TELO2	4
57472	Q9ULM6	CNOT6	4
84263	Q6YN16	HSDL2	4
117584	Q8WZ73	RFFL	4
3420	O43837	IDH3B	3
4303	P98177	FOXO4	3
4702	P51970	NDUA8	3
6520	P08195	4F2	3
6566	P53985	MOT1	3
6717	P30626	SRI	3
8569	Q9BUB5	MKNK1	3
9001	P54257	HAP1	3
9274	Q8WUZ0	BCL7C	3
23011	Q9UL25	RAB21	3
51773	Q96T23	RSF1	3
54499	Q9UM00	TMCO1	3
79751	Q9H936	GHC1	3
79888	Q8NF37	PCAT1	3
90550	Q8NE86	MCU	3
121536	Q6ZN18	AEBP2	3
41	P78348	ASIC1	2
391	P84095	RHOG	2
6383	P34741	SDC2	2
10797	P13995	MTDC	2
51115	Q96DB5	RMD1	2
51170	Q8NBQ5	DHB11	2
56052	Q9BT22	ALG1	2
56159	Q8IYF3	TEX11	2
65260	Q96BR5	COA7	2
80262	Q9BSU1	CP070	2
81929	Q96EE3	SEH1	2
84722	Q6PGN9	PSRC1	2
92667	Q9BQP7	MGME1	2
119559	Q6P4A7	SFXN4	2
100287932	O14925	TIM23	2
8443	O15228	GNPAT	1
10999	Q6P1M0	S27A4	1
23597	Q9Y305	ACOT9	1
27146	Q9ULE4	F184B	1
57662	Q9P1Y5	CAMP3	1
84986	Q14CB8	RHG19	1
91942	Q8N183	NDUF2	1
200205	Q5T440	CAF17	1

Supplementary Table 7: Identification of the *Drosophila* selected UniProt sequences (all common with human).

Protein Name	Gene name	FlyBase Gene ID	Gene ID	UniProt ID
Ribonuclease P protein subunit p20	Rpp20	CG33931	3772007	Q2MGL3
Serpin 28Db	Spn28Db	CG33121	326261	Q9VLV3
LD31163p	ssp	CG17153	39375	Q9VTT3
ADP,ATP carrier protein	sesB	CG16944	32007	Q26365
Casein kinase II subunit beta	CkIIbeta	CG15224	32132	P08182
GEO10511p1	tomboy20	CG14690	41285	Q9VGX9
Ubiquitin carboxyl-terminal hydrolase Usp2	Usp2	CG14619	33132	Q8IQ27
Bromodomain containing 8	Brd8	CG14514	43460	Q9VAM5
Activator of SUMO 1	Aos1	CG12276	41532	Q7KSM5
Calnexin 99A, isoform A	Cnx99A	CG11958	44643	Q9VAL7
Sideroflexin-1-3	Sfxn1-3	CG11739	40552	Q9VN13
Uncharacterized protein	Ubi-p5E5	CG11700	31564	R9PY16
GH01161p	Traf6	CG10961	31746	Q9W3I9
SD11922p	Spn55B	CG10913	49803	Q7JV69
DnaJ protein homolog 1	DnaJ-1	CG10578	38643	Q24133
FI07206p	PNKP	CG9601	40994	Q9VHS0
Pickpocket 14	ppk14	CG9501	33887	Q9VME8
Tubulin beta-1 chain	betaTub56D	CG9277	37238	Q24560
HECT and RLD domain containing E3 ubiquitin ligase 4, isoform C	Herc4	CG9153	38151	E8NHA2
DnaJ-like-2, isoform A	Droj2	CG8863	41646	Q9VFV9
Maltase A3	Mal-A3	CG8695	35826	P07192
Mrj, isoform E	mrj	CG8448	36797	A8DYF7
Calpain-B	CalpB	CG8107	39165	Q9VT65
Caspase Dronc	Dronc	CG8091	39173	Q9XYF4
Caspase	Drice	CG7788	43514	O01382
26S proteasome non-ATPase regulatory subunit 4	Rpn10	CG7619	40388	P55035
SUMO-activating enzyme subunit	Uba2	CG7528	44496	Q7KUA4
Histone deacetylase HDAC1	HDAC1	CG7471	38565	Q94517
ATP-dependent RNA helicase WM6	Hel25E	CG7269	33781	Q27268
Cell division cycle 5, isoform A	Cdc5	CG6905	38062	Q9W0R0
Hsc70Cb, isoform G	Hsc70Cb	CG6603	39557	M9MSL3
Ubiquitin-conjugating enzyme E2-18 kDa	Ubc10	CG5788	37035	Q7K738
Uncharacterized protein, isoform B	Dmel\CG5440	CG5440	33318	Q9VQ00
MPN domain-containing protein CG4751	CG4751	CG4751	34551	Q9VKJ1
Tetratricopeptide repeat protein 2	Tpr2	CG4599	34984	Q9V3W1
Small ubiquitin-related modifier	smt3	CG4494	33981	O97102
RE58623p	Spt-I	CG4016	36448	Q6NR46
Transcriptional coactivator yorkie	yki	CG4005	37851	Q45VV3
Transmembrane GTPase Marf	Marf	CG3869	31581	Q7YU24
Dorsal interacting protein 4	lwr	CG3018	33226	Q7KNM2
AT19485p	Dmel\CG2887	CG2887	31978	Q9W2U5
Regulatory particle triple-A ATPase 6-related	Rpt6R	CG2241	43635	Q9VA54
Ubiquitin-activating enzyme E1	Uba1	CG1782	35998	Q8T0L3
Heat shock protein 83	Hsp83	CG1242	38389	P02828
Histone acetyltransferase	nej	CG15319	43856	M9MS40

Supplementary Table 8: Identification of JosD1 network. * represent the proteins common with ataxin-3 network.

Protein	Gene Symbol	Genes ID	UniProt ID
Microtubule-associated tumor suppressor candidate 2	MTUS2	23281	Q5JR59
Keratin-associated protein 9-3	KRTAP9-3	83900	Q9BYQ3
Zinc finger protein RFP	TRIM27	5987	P14373
Keratin-associated protein 5-9	KRTAP5-9	3846	P26371
Keratin, type I cytoskeletal 40	KRT40	125115	Q6A162
Ubiquitin carboxyl-terminal hydrolase 15	USP15	9958	Q9Y4E8
Keratin-associated protein 10-4	KRTAP10-4	386672	P60372
E3 ubiquitin-protein ligase TRIM63*	TRIM63	84676	Q969Q1
E3 ubiquitin-protein ligase Praja-1*	PJA1	64219	Q8NG27
Calmodulin-1	CALM1	801	P0DP23
Mitochondrial import inner membrane translocase subunit Tim8 A	TIMM8A	1678	O60220
Keratin, type I cytoskeletal 27	KRT27	342574	Q7Z3Y8
Fibulin-2	FBLN2	2199	P98095
Keratin-associated protein 10-3	KRTAP10-3	386682	P60369
E3 ubiquitin-protein ligase TRIM23	TRIM23	373	P36406
Calmodulin-3	CALM3	808	P0DP25
Ubiquitin carboxyl-terminal hydrolase 28	USP28	57646	Q96RU2
Keratin, type II cuticular Hb6	KRT86	3892	O43790
Ubiquitin carboxyl-terminal hydrolase 21*	USP21	27005	Q9UK80
Calmodulin-2	CALM2	805	P0DP24
Protein-glutamine gamma-glutamyltransferase K	TGM1	7051	P22735
Tripartite motif containing protein 54*	TRIM54	57159	Q9BYV2
Caspase recruitment domain-containing protein 10	CARD10	29775	Q9BWT7
Keratin-associated protein 9-2	KRTAP9-2	83899	Q9BYQ4
TNF receptor-associated factor 1	TRAF1	7185	Q13077
Keratin-associated protein 1-1	KRTAP1-1	81851	Q07627
MyoD family inhibitor	MDFI	4188	Q99750
Probable E3 ubiquitin-protein ligase MID2	MID2	11043	Q9UJV3
ELAV-like protein 1	ELAVL1	1994	Q15717
E3 ubiquitin-protein ligase LNX	LNX1	84708	Q8TBB1
Polyubiquitin-C*	UBC	7316	P0CG48
E3 ubiquitin-protein ligase CHIP*	STUB1	10273	Q9UNE7
Keratin, type I cuticular Ha1	KRT31	3881	Q15323
Cysteine-rich tail protein 1	CYSRT1	375791	A8MQ03
Keratin-associated protein 10-8	KRTAP10-8	386681	P60410
Eukaryotic translation initiation factor 3 subunit F	EIF3F	8665	O00303
Keratin-associated protein 12-3	KRTAP12-3	386683	P60328
ADAMTS-like protein 4	ADAMTSL4	54507	Q6UY14
Notch homolog 2 N-terminal-like protein A	NOTCH2NLA	388677	Q7Z3S9

Supplementary Table 9: Identification of JosD2 network. * represent the proteins common with ataxin-3 network.

Protein	Gene Symbol	Genes ID	UniProt ID
Transmembrane O-methyltransferase	LRTOMT	220074	Q8WZ04
COMM domain-containing protein 3	COMMD3	23412	Q9UBI1
Trafficking protein particle complex subunit 2	TRAPPC2	6399	P0DI81
Adenosylhomocysteinase 3	AHCYL2	23382	Q96HN2
NADH dehydrogenase [ubiquinone] 1 alpha subcomplex subunit 8*	NDUFA8	4702	P51970
Probable global transcription activator SNF2L2	SMARCA2	6595	P51531
CKLF-like MARVEL transmembrane domain-containing protein 5	CMTM5	116173	Q96DZ9
Phospholipase A2, membrane associated	PLA2G2A	5320	P14555
E3 ubiquitin-protein ligase CHIP*	STUB1	10273	Q9UNE7
Small proline-rich protein 3	SPRR3	6707	Q9UBC9
S-adenosylhomocysteine hydrolase-like protein 1	AHCYL1	10768	O43865
Peroxisomal leader peptide-processing protease	TYSND1	219743	Q2T9J0
Polyubiquitin-C*	UBC	7316	P0CG48
Protein YIF1A	YIF1A	10897	O95070
Hemoglobin subunit beta	HBB	3043	P68871
Mast cell-expressed membrane protein 1	MCEMP1	199675	Q8IX19
Dual specificity phosphatase 28	DUSP28	285193	Q4G0W2

Supplementary Table 10: Identification of interactors more prone to interact with WT or EXP ataxin3. The polyQ tract were excluded from comparations. * represent the proteins common with *Drosophila,* & represent proteins that interact at an equal amount with WT and EXP ataxin3, and bold represent proteins that interact more with EXP form.

Protein Name	Gene name	Gene ID	Total		JD		C-terminal tail	
			WT	EXP	WT	EXP	WT	EXP
Heat shock cognate 71 kDa protein*	HSPA8	3312	85	82	57	47	28	35
Heat shock protein HSP 90-alpha *	HSP90AA1	3320	77	66	37	20	40	46
Serpin H1*	**SERPINH1**	**871**	61	66	50	45	11	21
DnaJ homolog subfamily B member 2*	**DNAJB2**	**3300**	65	66	39	38	26	28
4F2 cell-surface antigen heavy chain*	SLC3A2	6520	64	57	47	47	17	10
Histone deacetylase 6*	**HDAC6**	**10013**	59	74	47	40	12	34
Caspase 3*	CASP3	836	74	66	52	42	22	24
ADP/ATP translocase 2*	**SLC25A5**	**292**	66	71	33	32	33	39
ADP/ATP translocase 3*&	SLC25A6	293	65	65	38	42	27	23
ATP-dependent RNA helicase DDX39A*&	DDX39A	10212	57	57	30	30	27	27
Monocarboxylate transporter 1*	SLC16A1	6566	100	88	59	51	41	37
Sideroflexin 4*	**SFXN4**	**119559**	77	93	60	44	17	49
2-amino-3-ketobutyrate coenzyme A ligase*	GCAT	23464	78	77	56	49	22	28
BAG family molecular chaperone regulator 3*	BAG3	9531	71	63	29	34	42	29
Ubiquitin carboxyl-terminal hydrolase 21*	USP21	27005	84	64	55	47	29	17
Polynucleotide kinase 3´-phosphatase*&	PNKP	11284	66	66	47	40	19	26
Calnexin*	CANX	821	88	69	66	44	22	25
Alpha-parvin*	PARVA	55742	77	75	29	50	48	25
TOMM20-like protein 1*	**TOMM20L**	**387990**	66	70	53	51	13	19
Sorcin*	SRI	6717	57	52	43	28	14	24
Tubulin alpha-1A chain*	TUBA1A	7846	61	54	46	32	15	22
26S proteasome non-ATPase regulatory subunit 4*	PSMD4	5710	62	51	45	30	17	21
Small ubiquitin like modifier 1*	SUMO1	7341	52	51	36	33	16	18
Ubiquilin 1*	**UBQLN1**	**29979**	87	93	67	37	20	56
Ubiquitin-conjugating enzyme E2 L3*	UBE2L3	7332	59	54	45	35	14	19
Ubiquitin-conjugating enzyme E2 G1*	UBE2G1	7326	57	56	42	31	15	25
Ubiquitin-conjugating enzyme E2 S*	UBE2S	27338	70	69	37	44	33	25
Ubiquitin-conjugating enzyme E2 N*	**UBE2N**	**7334**	55	56	44	32	11	24
Polyubiquitin-B*	**UBB**	**7314**	58	68	49	47	9	21
Polyubiquitin-C*	**UBC**	**7316**	73	85	50	26	23	59
RAD23 homolog A, nucleotide excision repair*	**RAD23A**	**5886**	68	69	56	16	12	53
NEDD8 ubiquitin like modifier*	**NEDD8**	**4738**	52	54	39	36	13	18
DNA-dependent metalloprotease SPRTN	SPRTN	83932	76	69	13	48	63	21
Ubiquitin carboxyl-terminal hydrolase 13	USP13	8975	63	59	44	46	19	13
Ubiquitin thioesterase OTUB2	**OTUB2**	**78990**	55	56	38	33	17	23
E3 ubiquitin-protein ligase AMFR	**AMFR**	**267**	72	83	54	51	18	32
E3 ubiquitin-protein ligase CHIP	**STUB1**	**10273**	66	70	48	47	18	23
E3 ubiquitin-protein ligase rififylin	RFFL	117584	66	61	52	42	14	19
Cyclin dependent kinase inhibitor 1	**CDKN1A**	**1026**	63	64	26	32	37	32
Protein PML	**PML**	**5371**	71	72	42	46	29	26
Glycogen synthase kinase 3 beta	GSK3B	2932	61	60	53	41	8	19
Rho GDP-dissociation inhibitor 1	**ARHGDIA**	**396**	50	60	38	39	12	21
Tripartite motif containing protein 55	TRIM55	84675	59	58	29	33	30	25
Thymidine kinase 1	**TK1**	**7083**	53	57	43	35	10	22
RNA-binding protein EWS	EWSR1	2130	71	70	24	38	47	32
Annexin A7	**ANXA7**	**310**	52	56	34	33	18	23
HLA class I histocompatibility antigen, A alpha chain	**HLA-A**	**3105**	57	69	52	45	5	24
MAPK interacting serine/threonine kinase 1	MKNK1	8569	72	66	51	41	21	25
B-cell CLL/lymphoma 7 protein family member C	**BCL7C**	**9274**	52	73	47	55	5	18
Calcium load-activated calcium channel	TMCO1	54499	75	61	55	38	20	23
Phagosome assembly factor 1 &	PHAF1	80262	73	73	61	46	12	27
NADH dehydrogenase [ubiquinone] 1 alpha subcomplex assembly factor 2	NDUFAF2	91942	73	65	54	41	19	24
Zinc finger protein AEBP2	**AEBP2**	**121536**	79	81	50	49	29	32
Dead end protein homolog 1&	DND1	373863	74	74	43	48	31	26
Plasmanylethanolamine desaturase	PEDS1	387522	71	69	62	43	9	26
Ubiquitin-conjugating enzyme E2 variant 1	**UBE2V1**	**7335**	62	73	45	32	17	41
Mitochondrial import inner membrane translocase subunit Tim23	TIMM23	100287932	63	60	46	37	17	23
Succinate dehydrogenase [ubiquinone] iron-sulfur subunit	**SDHB**	**6390**	52	55	32	44	20	11
Cytochrome c oxidase assembly factor 7	**COA7**	**65260**	70	73	56	43	14	30
Cytochrome c oxidase subunit NDUFA4	NDUFA4	4697	66	63	41	37	25	26
ATP-citrate synthase	ACLY	47	76	69	44	34	32	35
Cyclin dependent kinase 4	**CDK4**	**1019**	62	77	57	30	5	47
Hydroxysteroid dehydrogenase-like protein 2&	HSDL2	84263	68	68	19	49	49	19
Retinol dehydrogenase 13	RDH13	112724	65	60	52	38	13	22
Rho-related GTP-binding protein RhoG	RHOG	391	57	54	39	38	18	16
Acyl-coenzyme A thioesterase 9	**ACOT9**	**23597**	73	89	52	55	21	34
Long-chain fatty acid transport protein 4	SLC27A4	10999	90	80	12	43	78	37
Tricarboxylate transport protein	**SLC25A1**	**6576**	73	76	68	29	5	47
Nucleoporin SEH1&	SEH1L	81929	65	65	49	48	16	17
Mitochondrial dicarboxylate carrier	**SLC25A10**	**1468**	71	88	51	41	20	47
Bifunctional methylenetetrahydrofolate dehydrogenase/cyclohydrolase	MTHFD2	10797	64	60	42	32	22	28
Phosphate carrier protein	SLC25A3	5250	72	68	38	49	34	19
Ubiquitin-associated domain-containing protein 2	UBAC2	337867	65	64	50	39	15	25
Mitochondrial genome maintenance exonuclease 1	**MGME1**	**92667**	54	76	29	39	25	37
Very-long-chain enoyl-CoA reductase	**TECR**	**9524**	56	71	43	34	13	37
Arfaptin-2	ARFIP2	23647	70	60	50	35	20	25
UPF0598 protein C8orf82	**C8orf82**	**414919**	60	61	57	40	3	21
Lysophosphatidylcholine acyltransferase 1	LPCAT1	79888	94	80	56	24	38	56
Isocitrate dehydrogenase [NAD] subunit beta	IDH3B	3420	74	70	59	52	15	18
Chitobiosyldiphosphodolichol beta-mannosyltransferase	**ALG1**	**56052**	52	71	35	34	17	37
60S acidic ribosomal protein P0	**RPLP0**	**6175**	59	86	45	45	14	41
E3 ubiquitin-protein ligase MARCHF5	MARCHF5	54708	58	55	21	35	37	20
Ras-related protein Rab-21	RAB21	23011	72	61	53	34	19	27
NADH dehydrogenase [ubiquinone] 1 alpha subcomplex subunit 8	**NDUFA8**	**4702**	68	71	35	34	33	37

CDGSH iron-sulfur domain-containing protein 2	**CISD2**	**493856**	47	50	32	27	15	23
Estradiol 17-beta-dehydrogenase 11	**HSD17B11**	**51170**	69	76	49	35	20	41